

## RADIOBIOLOGICAL AND CLINICAL BASES OF PARTICLE THERAPY (REVIEW)

André WAMBERSIE

Université Catholique de Louvain, Unité de Radiothérapie, Neutron- et Curiothérapie, Cliniques Universitaires St-Luc  
1200, Bruxelles (Belgium)

### Introduction

Application of new types of ionizing radiations is today one of the most promising approaches for improving the efficiency of radiotherapy. However, there are still controversies concerning the conclusions which can be drawn from the available clinical results with fast neutrons, and thus concerning the future of high-LET radiation in cancer therapy. This in turn raises controversies about the priority level which should be given to rather large and costly investments, such as those implied in heavy-particle therapy programs.

When discussing the place of non-conventional ionizing radiations, one has to distinguish :

- particle beams which only improve the physical selectivity of the irradiation, i.e. the dose distribution (e.g. proton beams or helium ion beams);
- high-LET radiations which produce different types of biological effects, and which aim at improving the differential effect between tumour and normal tissues (e.g. : fast neutrons);
- the two approaches can be combined and one could seek after a high physical selectivity with high-LET radiation (e.g.: heavy ions).

### Improvement of the physical selectivity with proton and helium ion beams

Historically, the major improvement in the efficiency of radiation therapy was the replacement of conventional X-rays (200 kV X-rays) by high-energy photons or electrons. The clinical benefit was rapidly evident for all, or for the majority of the patients. This illustrates the importance of the physical selectivity in radiation therapy.

We are now close to make a further step : the introduction of proton beams. The characteristics of the proton beams make them superior to high-energy photons from the point of view of the physical selectivity. On the other hand, no advantage has to be expected from the biological point of view : for the high energy required to the protons in external irradiation, we stay in the field of low-LET radiations. For the present discussion, we can assume that helium ion beams are similar to proton beams.

The clinical benefit of proton beams has been demonstrated for several well selected tumour types or sites for which a physical selectivity is essential. The best example is the uveal melanoma, which has been treated since 1974 by proton beams at the Harvard cyclotron [ 1 ].

The high physical selectivity of the proton (and helium ion) beams can be exploited for other localisations : radioresistant tumours close to critical organs such as chordomas or chondrosarcomas of the base of the skull, paraspinal tumours, and meningiomas (Suit in [ 18 ]; Castro in [ 19 ]).

There is an increasing number of projects which aim at treating with protons many other tumour types, and larger proportions of patients. One of the most impressive is the Loma Linda project at Los Angeles. Once all treatment rooms will be fully operational, the centre is expected to have a capacity of 1 000 new proton beam patients per year [ 14 ]. This kind of project really aims at systematically substituting proton to photon beams; it raises at least 3 types of problems :

- 1) to what extent will the clinical benefit justify the increased cost and efforts involved;
- 2) such program will imply, in a more or less near future, a redefinition of the radiotherapy network, and a progressive replacement of several small photon therapy units (or departments) by huge proton therapy facilities;
- 3) finally, the benefit of the high physical selectivity of the proton beams will be fully exploited only to the extent that the accuracy in patient-beam positioning and in dosimetry would reach the same level as with photons. The proton beam generators should also be as reliable as the modern linear accelerators.

It is at present the task of the teams who have access to high-energy cyclotrons to provide a clear, and quick, response to that problem. It would be indeed a significant improvement to be able to deliver high-doses (60-70 Gy) to bronchus or oesophagus tumours, or to treat a Hodgkin patient, with a (nearly) full sparing of the spinal cord.

### The differential effect and the potential advantage of fast neutrons and high-LET radiations

#### 1. Radiobiological data

Historically, fast neutrons were introduced in therapy because of the existence of hypoxic cells and the reduction in OER when increasing LET. However, high-LET radiations exhibit other differences in their biological properties, when compared to low-LET radiations:

- a reduction in the differences in radiosensitivity from cell line to cell line (i.e. "intrinsic radiosensitivity") [ 2 ]. On the other hand, Fertl et al. [ 7 ], comparing the responses of 6 cell lines to X-rays and neutrons, observed a modification in their relative radiosensitivities (i.e. a given cell line more resistant to X-rays could be more sensitive to neutrons another cell line).
- a reduction in the differences in radiosensitivity related to the position of the cell in the mitotic cycle [ 5 ].
- less repair phenomena (in general), and as a consequence less difference between the responses of the cell populations to fractionated irradiation.

From the above arguments, it can be concluded that all cell populations, in all conditions, tend to respond in a more similar way when exposed to neutrons compared to photons. From that point of view, a reduction in OER can be considered as a particular aspect of a more general phenomenon, i.e. a reduced difference in radiosensitivity between cell populations [ 17 ].

Two practical consequences can be derived from the above radiobiological considerations :

1. The importance of patient selection. An absence of (or a wrong) selection of the patients could worsen the clinical results and lead to erroneous conclusions about the value of fast neutrons. This could maybe explain a least some of the reported discrepancies in clinical results.
2. The need for a high physical selectivity with high-LET radiations, which proceeds from the reduced differences in radiosensitivity. When large differences in radiosensitivity are observed between the cancer and normal cell populations, a poor physical selectivity is of limited consequence. In typical cases, such as seminomas or lymphomas, the dose prescribed to

the target volume is below the tolerance dose, and irradiation of a few additional  $\text{cm}^3$  of normal tissue would be of little clinical importance (in chemotherapy, there is obviously no physical selectivity at all, and the potential therapeutic gain depends only on a biological selectivity). By contrast, when the differences in radiosensitivity are reduced with very high-LET radiation, the therapeutic efficiency mainly rests on a high level of physical selectivity; sparing a few  $\text{cm}^3$  of normal tissues then becomes of real importance.

In addition, with low-LET radiations, where repair phenomena play an important role, differences in repair capacity between the normal and cancer cell populations can be exploited by selecting appropriate fractionation regimen. This possibility is reduced with high-LET radiations since repair phenomena are in general smaller. Consequently, from a radiobiological point of view, high-LET radiations then appear to be a treatment modality with limited possibility of enhancing an eventual differential effect by selecting the optimum fraction sizes.

## 2. Clinical data

Fast neutrons therapy is applied today routinely in more than 17 centres throughout the world [ 13 ]. Locally extended salivary gland tumours are the first type of tumours for which the superiority of fast neutrons was recognized. A survey of the results of the non-randomized clinical studies as well as the results of the RTOG/MRC prospective randomized trial overwhelmingly support the contention that fast neutrons offer a significant advance in the treatment of inoperable and unresectable primary or recurrent malignant salivary gland tumours [ 8 ] [ 15 ].

Remarkably good results have also been reported with neutron therapy for locally extended tumours of the paranasal sinuses. In the series treated at the Hammersmith Hospital, 86 % (37/43) of the patients showed complete remission and relief of symptoms was noticed in all cases [ 6 ]. The value of fast neutrons, for tumours in the head and neck area, is questioned [ 9 ].

For soft tissue sarcomas, the results reported from the different centres indicate an overall local control rate after neutron therapy of 53 % for inoperable tumours, which is higher than the 38 % control rate currently observed after low-LET radiation for similar patients series. For primary bone tumours and differentiated chondrosarcomas, better results have also been observed after neutron therapy compared to the current photon therapy results ( reviewed in [ 10 ] and [ 19 ]).

Prostatic adenocarcinomas, having in general a long doubling time, should be a good indication for neutron therapy taking into account the available radiobiological data [ 3 ]. Excellent results were achieved in Hamburg, Louvain-la-Neuve and Chiba [ 11 ] [ 15 ]. The most convincing data are the result of a randomized trial, initiated by the RTOG, on locally advanced (C,D1) adenocarcinomas of the prostatic gland [ 12 ]. The local control rate was 77 % for patients treated with mixed schedule (55 patients) and only 31 % for patients receiving photons alone (36 patients) ( $P < 0.01$ ). Actuarial survival rates at 8 years ("determinantal" survivals, i.e. adjusted by exclusion of intercurrent deaths) were 82 % and 54 % respectively ( $P=0.02$ ). The RTOG is now performing another randomized trial comparing neutrons only to conventional photon treatment.

The value of fast neutrons has been assessed in other tumour types or sites but no definitive conclusions can be drawn yet; some of the results are promising [ 13 ] [ 15 ]. In fact, the general conclusion which emerges from the review of the clinical results is in agreement with what could be expected from the radiobiological data : replacement of X-rays by neutrons - or more generally of low-LET by high-LET radiation - brings a benefit for some types of tumours and, on the contrary, a loss for other tumours. The tumours for which fast neutrons were found to be superior to conventional X-rays are, in general, slowly growing and well differentiated.

In contrast, negative results have been obtained for brain tumours [ 13 ].

As far as the proportion of patients, suitable for neutron therapy is concerned, figures ranging from 10 to 20 % have been suggested. They correspond to the percentages of radiotherapy patients for which neutrons were shown to be superior than conventional X-rays. These percentages are probably at the lower limit since they were often obtained with low energy cyclotrons and poor physical selectivity. It is likely that with high-energy, hospital based modern cyclotrons, neutron therapy will be found to be useful for a larger proportion of patients. In addition, neutrons could extend the field of the indications of radiation therapy by allowing to envisage the treatment of groups of tumours "traditionally" considered to be radioresistant (e.g. adenocarcinomas).

## The rationale for heavy ion therapy

The heavy-ions combine the advantage of a high physical selectivity with the potential advantage of high-LET radiation for the treatment of some tumour types. As far as the physical selectivity is concerned, heavy ions are similar to protons or helium ions. Heavy ion beams have even a smaller penumbra, but it is questionable whether this could be of clinical relevance. More important is the fact that, with heavy ions, the higher RBE at the level of the spread out Bragg peak further improves the advantage of the dose distribution. As far as the high-LET advantage is concerned, the LET at the level of the spread out Bragg peak depends on the type of particle, and on the width of the spread out Bragg peak. These factors then also influence the RBE, OER, etc...

From the radiotherapy point of view, the use of heavy ion beams is justified by 3 sets of arguments [ 16 ] :

- 1) the radiobiological and clinical data indicating that, for the treatment of some tumours types and/or sites, high-LET radiations could be superior to low-LET radiations;
- 2) the fact that a high physical selectivity is even more important with high- than with low-LET radiations, due to a general reduction in the difference of radiosensitivity between cell populations ;
- 3) the encouraging results reported from Berkeley, which are an additional argument, although they were obtained on a limited, selected, group of patients [ 4 ] .

Only a few heavy-ion therapy facilities are planned in the world : the facility at the NIRS in Japan which is under construction, the LIBRA project in the USA, and in Europe the GSI project in Darmstadt-FRG and the EULIMA project. Due to their high cost and complexity, an international cooperation is necessary in

order to ensure the appropriate patient recruitment and a rapid exchange or information. Patient recruitment should aim in principle :

- at selecting for heavy ions tumour types or sites for which there is evidence that better results could normally be expected than with conventional treatments;
- at initiating randomized trials designed to answer specific questions of great relevance in radiobiology and/or therapy.

#### References

- 1 M. AUSTIN-SEYMOUR, MURIE, J. MUZENRIDER, C. WILLETT, M. GOITEIN, L. VERHEY, R. GENTRY, P. McNULTY, A. KOEHLER, H. SUIT Considerations in Fractionated Proton Radiation Therapy: Clinical Potential and Results. *Radiotherapy and Oncology*, 1989, **17**, 29-35.
- 2 G. W. BARENSEN, J.J. BROERSE.  
Differences in radiosensitivity of cells from various types of experimental tumors in relation to the RBE of 15 MeV neutrons. *International Journal Radiation Oncology, Biology, Physics*, **3**, 211-214, 1977.
- 3 BATTERMANN, J.J.  
Clinical application of fast neutrons, the Amsterdam experience. Thesis, University of Amsterdam (The Netherlands), 1981.
- 4 J.R. CASTRO, G. GADEMANN, J.M. COLLIER, D. LINSTAD, S.PITLUCK, K. WOODRUFF, G.GAUGER, D. CHAR, Ph. GUTIN, Th L. PHILLIPS, W. CHU, Sh. HENDERSON  
Strahlentherapie mit schweren Teilchen am Lawrence Berkeley Laboratory der Universität von Kalifornien, *Strahlentherapie und Onkologie* **163**, 1987, 9-16.
- 5 J.D. CHAPMAN  
Biophysical Models of Mammalian Cell Inactivation by Radiation. In R.E. Meyn and H.R. Withers (Eds). *Radiation Biology in Cancer Research*, Raven Press, New-York, 21-32, 1988.
- 6 ERRINGTON, R.D.  
Advanced carcinoma of the paranasal sinuses treated with 7.5 MeV fast neutrons. *Bull. Cancer (Paris)*, **73**, 569-576, 1986.
- 7 B.FERTIL, P.J. DESCHAVANNE, J. GUEULETTE, A. POSSOZ, A. WAMBERSIE, and E.P. MALAISE  
In vitro radiosensitivity of six human cell lines. II. Relation to the RBE of 50-MeV neutrons. *Radiation Research*, **90**, 526-537, 1982.
- 8 GRIFFIN, B.R., LARAMORE, G.E., RUSSELL, K.J. GRIFFIN, T.W. AND EENMAA, J.  
Fast neutron radiotherapy for advanced malignant salivary gland tumors. *Radiotherapy and Oncology*, **12**, 105-111, 1988.
- 9 GRIFFIN, T.W., PAJAK, T.F., MAHOR, M.H., LARAMORE, G.E., HENDRICKSON, F.R., PARKER, R.G., THOMAS, F.J., DAVIS, L.W.  
Mixed neutron/photon irradiation of unresectable squamous cell carcinomas of the head and neck: the final report of a randomized cooperative trial. *Int. J. Radiation Oncology Biol. Phys.* **17**, 959-965, 1989.
- 10 LARAMORE, G.E., GRIFFETH, J.T., BOESPFLUG, M., PELTON, J.G., GRIFFIN, T.W., GRIFFIN B.R., RUSSELL, K.J., AND KOH, W.  
Fast neutron radiotherapy for sarcomas of soft tissue, bone, and cartilage; in press.
- 11 RICHARD, F., RENARD, L., WAMBERSIE, A.  
Current results of neutron therapy at the UCL, for soft tissue sarcomas and prostatic adenocarcinomas. *Bull. Cancer (Paris)*, 1986 **73**, 562-568.
- 12 RUSSELL, K.J., LARAMORE G.E., KRALL, J.M., THOMAS, F.J. MAOR M.H., HENDRICKSON F.R., KRIEGER, J.N., AND GRIFFIN T.W.  
Eight years experience with neutron radiotherapy in the treatment of stages C and D prostate cancer: Updated results of the RTOG 7704 randomized clinical trial. *The Prostate* **11**: 183-193, 1987.
- 13 SCHMITT, G, WAMBERSIE, A.  
Review of the clinical results of fast neutron therapy. *Radiotherapy and Oncology*, 1990, **17**, 47-56.
- 14 J.M. SLATER and D.W. MILLER  
Loma Linda University Proton Therapy facility. In G. Kraft and U. Grundinger (Ed.). *Third workshop on heavy charged particles in biology and medicine*, GSI - Darmstadt, Report 87-11, ISSN 0171-4546, 1987, KO K-2.
- 15 TSUNEMOTO, H., MORITA, S., SATHO, S., HINO, Y., YUL YOO, S.  
Present status of fast neutron therapy in Asian countries. *Strahlentherapie und Onkologie*, 1989, **165**, 330-336.
- 16 A. WAMBERSIE  
The future of High-LET radiation in cancer therapy. Justification of the heavy-ion therapy programmes. pp.15-40 in K. OKAMOTO (Ed), *Atomic and Molecular Data For Radiotherapy*, International Nuclear Data Committee , International Atomic Energy Agency, Vienna, INDC (NDS) - 217/GZ, 1989.
- 17 A. WAMBERSIE, G.W. BARENSEN, N. BRETEAU,  
Overview and prospects of the application of fast neutrons in cancer therapy. *European Journal of Radiation Oncology*, **5**, 248-264, 1984.
- 18 Proceedings of the International Workshop on Particle Therapy; Annual Meeting of the EORTC Heavy Particulate Therapy Group, October 28-29, 1988, University of Essen, Fed. Rep. of Germany; *Strahlentherapie und Onkologie*, **166**, 1989.
- 19 Proceedings of the EULIMA Workshop on the Potential Value of Light Ion Beam Therapy (P. Chauvel and A. Wambersie, Ed.); Centre Antoine-Lacassagne, Nice-France, November, 3-5, 1988. Publication n° EUR 12165 EN of the Commission of the European Communities, c ECSC-EEC-EAEC, Brussels-Luxembourg, 1989 and CAL Edition (526 pages).

HIGH ENERGY MEDICAL ACCELERATORS

P. MANDRILLON

Laboratoire du Cyclotron, Centre Antoine Lacassagne  
227 Avenue de la Lanterne, 06200 Nice, France

**Abstract :** The treatment of tumours with charged particles, ranging from protons to "light ions" (Carbon, Oxygen, Neon), has many advantages, but up to now has been little used because of the absence of facilities. After the successful pioneering work carried out with accelerators built for physics research, machines dedicated to this new radiotherapy are planned or already in construction. These high energy medical accelerators are presented in this paper.

**Introduction**

It was Robert Wilson in 1946 at Harvard [1] who realised that protons of a given energy travel in almost straight lines, all with roughly equal range and that this property could lead to a new radiotherapeutic tool for targeting deep seated tumours while preserving the surrounding healthy tissues. Almost 45 years later, the first hospital based dedicated proton accelerator is preparing to treat 1000 patients per year. This machine which is installed at the Loma Linda University Medical Center, was designed and fabricated at Fermilab, where Robert Wilson was director from 1967 to 1978. In this sense a loop has been completed.

The use of charged particles has three major advantages over the photon or electron beams which are used for conventional radiotherapy :

- first, a physical selectivity : in contrast to x-rays and electrons the beam does not spread sideways inside the body and has a very well defined range (cf Fig 1 and Fig 2) for a given energy. This is true for protons and even better for heavier ions.

- secondly, the so called Bragg curve : the ionization increases as the particles slows down giving a greater dose at depth than on the surface. Fig 2 shows the relative dose as a function of depth in tissue for different types of classical radiation compared to a light ion (Neon)

- thirdly, heavier ions ranging from Carbon up to Argon, produce a high ionization density, known in the trade as high LET. The so called RBE (Relative Biological Efficiency [2]) increases and the OER (Oxygen Enhancement Ratio [2] decreases). This latter effect is a serious limiting factor in radiotherapy of large tumours which are poorly vascularised and whose cells are less oxygenated and therefore less sensitive to radiations. These two factors which magnify the effect of the Bragg peak are shown on Fig 3 which presents typical variations of RBE and OER and characteristic LET bands for several charged particle beams. Hence a modification of quality of the radiation received by the patient becomes possible.

These biological and physical advantages of high-energy charged particle beams in cancer therapy have been established over a number of years in a series of biomedical experiments and clinical trials carried out in institutions whose accelerators were designed for nuclear physics research : Berkeley and Harvard in the United States, Uppsala in Sweden, Dubna and Moscow in the USSR, Tsukuba and Chiba in Japan, PSI in Switzerland. The total number of patients treated in 35 years is about 9000 throughout the world.

Following these good results, physicians are now asking for dedicated facilities which include not only a specific accelerator but also sophisticated beam delivery systems in order to treat a large number of patients. Several projects, both for protons and light ions, in the United States, Japan and plans in Europe will be discussed in this paper.

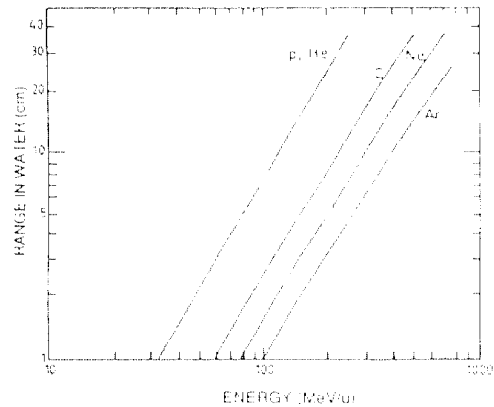


Fig 1 : Range of ions in water as a function of kinetic energy

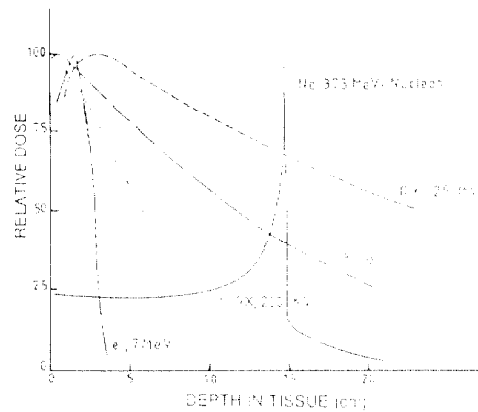


Fig 2 : Depth dose distribution for different radiation

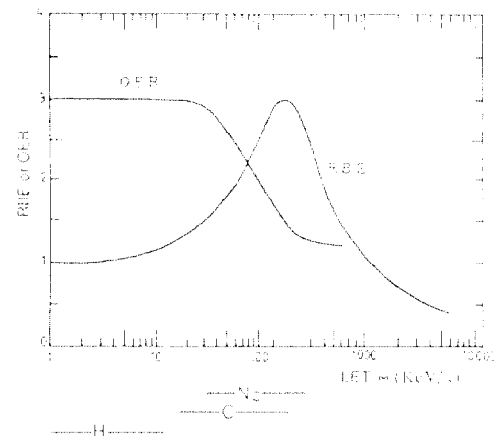


Fig 3 : RBE and OER as a function of LET for several ions



### Medical constraints

The main requirements for a new radiotherapy facility are as follows :

1- Installed in a large hospital in order to get an adequate supply of medical and scientific staff for developing high technical level diagnosis and treatment systems.

2- Accelerator highly reliable and easy to operate.

3- Beam delivery system permitting to scan the beam over the tumour volume.

4- Avoiding to move the patient, i.e. possibility to use different directions for the beam : horizontal and vertical beams, either above or below the couch. An isocentric gantry is suitable if the maximum beam rigidity makes this requirement realistic (possible for protons, massive for ions...).

5- Maximum range in tissues : 25 cm. This fixes the maximum energy for the beam ; 200 MeV for protons and several hundred MeV per nucleon for the ions.

6- Maximum dose rate at the tumour : 5 Gray/minute in a 2 litre volume. This fixes the beam intensity (cf. Table 3)

7- Maximum irradiated field :  $30 \times 30 \text{ cm}^2$ .

8- Possibility to check the treatment plans by PET verification of the irradiated volume.

### The accelerator

Imposing a range in tissue of 25 cm, the maximum kinetic energy and magnetic rigidity of proton and fully stripped ion beams are given in Table 1. From these figures it is clear that the proton machines and light ions machines will be quite different in size and cost. Two kinds of accelerators are feasible and the choice is not simple because these machines lie in the overlap of large isochronous cyclotrons and small synchrotrons.

Table 1

	Protons	Carbon	Oxygen	Neon
Energy (MeV/nucleon)	200	380	430	520
Bp (T.m.)	2,15	6,16	6,62	7,42

### Isochronous cyclotrons

A fixed frequency isochronous cyclotron, giving a fixed energy for accelerating ions at a given harmonic number of the radiofrequency, is certainly the simplest accelerator to operate. A simple Programmable Logic Controller is enough to tune and control such an accelerator.

### Neutrontherapy machines

This simplicity and the ability to accelerate large intensity has made the medium energy cyclotron the working horse of high energy fast neutron therapy programmes. Fast neutrons are classified as high LET particles because of the high ionization density of the recoil protons giving biological advantages over the conventional radiations for radioresistant tumours with the drawback of poor localisation. In order to get the required flux, a proton beam is accelerated up to 50-65 MeV onto a thick beryllium target. A high intensity is requested (15 microamps) and therefore several isochronous cyclotrons have been designed for neutrontherapy. Fig 4 shows the 65 MeV proton isochronous cyclotron designed and installed in Nice. Use has been made of  $\text{H}^-$  acceleration to facilitate the extraction system, avoiding a cumbersome, power consuming and difficult to construct extraction channel [3]. A compact superconducting cyclotron (K100) rotating around the patient has been constructed by H.G. Blosser [4] and is being installed in the Harper Hospital in Detroit (USA). The 40 MeV deuteron maximum energy orbit of this cyclotron has a radius of only 30 cm.

### Iontherapy machines

For the higher energies requested for protons and light ions therapy, the design of the machine becomes more difficult. For protons the use of superconducting coils for the magnetic field is an open question and recently two interesting designs have been proposed : IBA [5] has chosen a high field design (2.15 Tesla on the extraction radius) produced by conventional coils (cf. Fig. 5) and a compact superconducting synchrocyclotron has been proposed by H. G. Blosser [6](cf Fig 6).

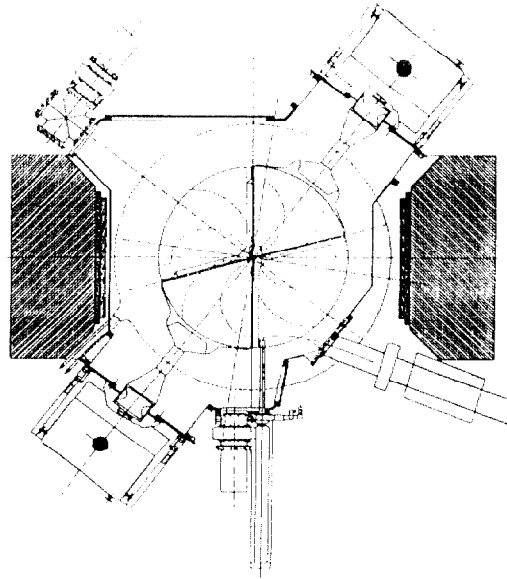


Fig 4 : Median plane view of the 65 MeV  $\text{H}^-$  MEDICYC cyclotron installed in Nice

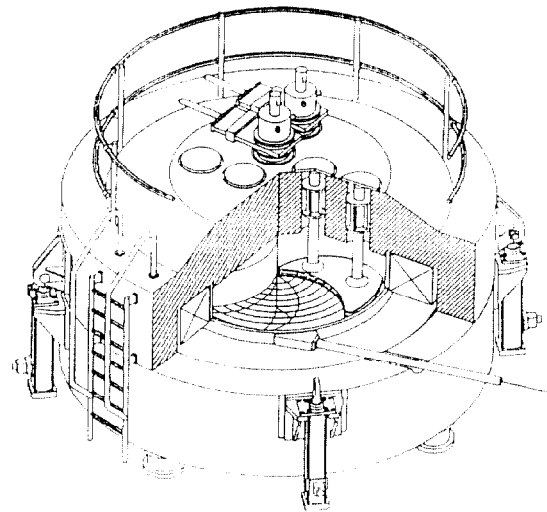


Fig 5 : The "CYCLONE 230" proposed by IBA

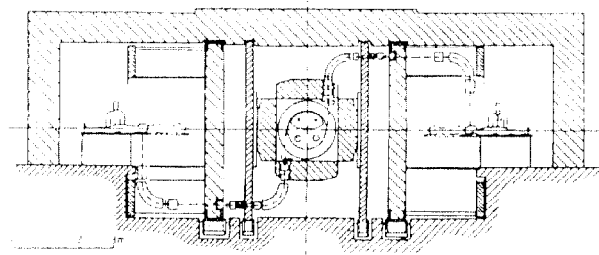


Fig 6 : 250 MeV Superconducting Synchrocyclotron proposed by H.G. Blosser, rotating around the patient.

Nevertheless for light ion acceleration the high magnetic field required is in favor of a superconducting solution.

Preliminary studies of the EULIMA project [7] concentrated on a superconducting separated-sector cyclotron accelerating fully stripped light ions axially injected from a high voltage platform located on the vertical axis of the machine. The magnet consists of four tightly spiraled sectors spanning 35° that are driven into saturation by a common cylindrical superconducting coil. The accelerating system comprises of two spiraled cavities located inside the vacuum chamber. The layout of the machine is shown in Fig 7 and the major parameters are given in Table 2.

Table 2

Particle frequency	17.4 Mhz
Max. energy fully stripped light ions	430 MeV/nucleon
Number of magnet sectors	4
Iron weight per sector	155 tons
Sector gap	50 mm
Sector angular width	35°
Average sector spiral	30°/m
Sector height	4.80 m
Sector maximum radius	2.20 m
Coil internal radius	2.31 m
Coil external radius	2.61 m
Coil current density	2850 A/cm <sup>2</sup>
Number of RF cavities	2
RF frequency	69.6 Mhz
RF harmonic number	4
RF peak voltage at extraction	250 kV
RF peak voltage at injection	125 kV

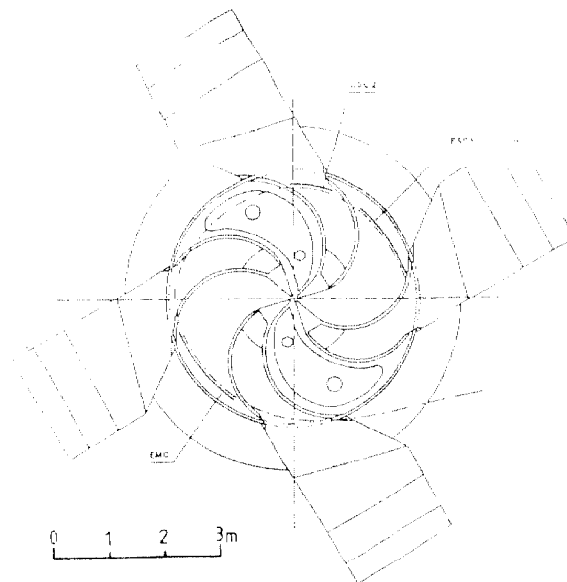


Fig 7: Top view of the EULIMA superconducting cyclotron

Details of this machine are described in several papers presented at this conference [8].

The common feature of all these high energy cyclotrons is the fixed energy. Hence scanning of the beam in depth is necessary to reduce the energy by using a degrader. Extensive calculations of the effect on the beam quality of such systems are then necessary to assess the performances of such systems [9].

Synchrotrons

The Table 3 presents for the same particles as Table 2, the required minimum current to give 5 Gray over a volume 20 x 20 x 5 cm<sup>3</sup> for different ions in one minute.

Table 3

	Proton	Carbon	Oxygen	Neon
Intensity (pps)	$2 \times 10^{10}$	$10^9$	$7 \times 10^8$	$5 \times 10^8$

These intensities are of course within the reach of a classical synchrotron and several projects have been proposed.

Protontherapy machines

Fig 8 presents the first high energy medical facility based in a large hospital located on the Loma Linda University campus in southern California. This facility houses a proton synchrotron giving a variable energy from 70 Mev up to 250 MeV. Three treatment rooms with isocentric gantries and one room with a fixed horizontal beam are presently being installed [10].

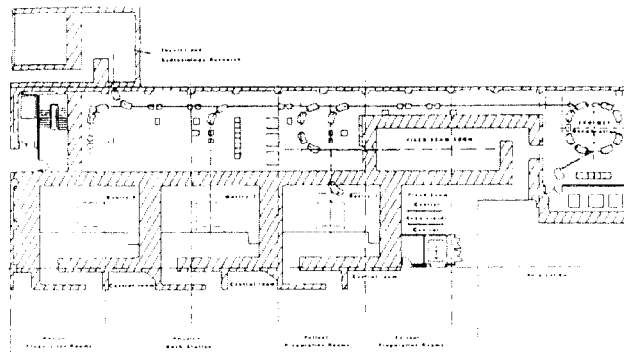


Fig 8 The Loma Linda facility

The zero gradient synchrotron has eight 45 degree dipole magnets arranged to have four straight sections providing space for injection, acceleration and extraction systems. The 30 KeV proton beam from the duoplasmatron system is injected into a 2 MeV-RFQ operating at 425 Mhz. A debuncher reduces the momentum spread from 1 % to 0.3 % at injection. Acceleration to 250 MeV is made via simple ferrite loaded RF cavity operating on the first harmonic. The beam is extracted from the synchrotron by using half-integral resonance. The cycle time is 2,4 or 8 seconds and the extraction time is variable from 0.4 sec to 10 sec. The design intensity is 10<sup>11</sup> protons/sec. This design is a result of a collaboration between the Loma Linda University Medical Centre, the Fermi National Laboratory and the Science Applications International Corporation (SAIC) Company.

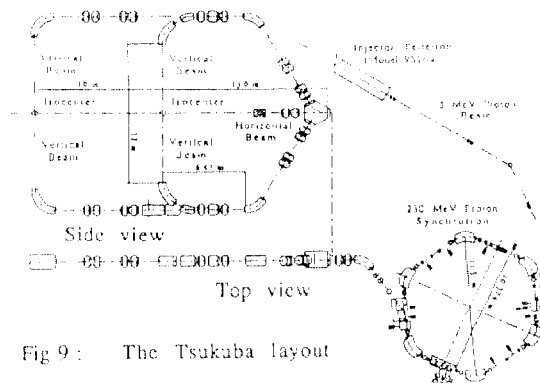


Fig 9: The Tsukuba layout

Following the pioneering work at the Particle Radiation Medical Science Centre (PARMS) of the University of Tsukuba which started to treat patients with a 250 MeV proton beam provided from the degraded beam of the 500 Mev booster synchrotron of KEK, a dedicated 230 MeV proton facility [11] will be build next to the conventional radiotherapy department at the University Hospital. Fig 9 shows the proposed facility which has two treatment rooms, the first will be equipped with three beams : one horizontal beam and two vertical beams for upper and lower directions. The second room with two vertical beams in opposite directions. The synchrotron is a 6 superperiods machine accelerating 5 MeV protons from an injection up to 230 MeV in 0.5 sec. The main parameters of this machine are summarized in Table 4.

Table 4

Energy range	5 - 230 MeV
Circumference	34.9 m
Structure	DOFB
6 Bending magnets	$B_{max}=1.5$ T
12 Q-poles magnets	$G_{max}=6.0$ T/m
Ion source	Multicusp $H^+$
Injection energy	5 MeV Tandem
Acceleration	$f=0.88 - 5.11$ Mhz $V=450-300$ Volts
Ejection spill	up to 1 s, half-integer resonance slow ejection

Light ions therapy machines

Following the stimulative results of the BEVALAC research and clinical trials with ions [12], the HIMAC project proceeds along a 10 year strategy for cancer treatment launched in Japan in 1983. The National Institute of Radiological Sciences (NIRS) in Chiba started in 1987 the construction of a facility for radiotherapy with ions up to Ar. Based on a two ring large synchrotron, the completion of the facility is foreseen for 1993 and will be the first ion-therapy facility in the world [13]. Three irradiation rooms will be constructed : one, equipped with a horizontal and vertical beams, and two rooms with a single beam direction (horizontal and vertical). Extra rooms will be available for radiobiology, secondary beams experiments and general purpose research. The main parameters of this accelerators complex are given in Table 5.

Table 5

Energy range	100-800 MeV/n
Average diameter	41 m
Structure	FODO
12 Bending magnets	$B_{max}=1.5$ T
24 Q-poles magnets	$G_{max}=7.0$ T/m
Ion source	PIG + ECR
Injection energy	6 MeV/n Alvarez linac
Acceleration	$f=1.0 - 7.5$ Mhz $V=6KV$
Ejection spill	0.4 s, 1/3 integer resonance slow ejection

Following similar ideas of other light-ion radiotherapy facilities, a synchrotron solution has been also studied for EULIMA. The beam energy interval from 100 to 450 MeV/n was considered, corresponding to the magnetic rigidity of 6.8 Tm, which is very similar to LEAR at CERN. The circumference of the EULIMA synchrotron is estimated at about 60 m, and the machine could be designed in a form of a ring or a racetrack, depending on the site conditions and the design of insertion devices. In Table 6, the preliminary parameters of this design are given, and its possible layout is depicted in Fig 12.

Table 6

Energy range	100-450 MeV/n
Circumference	60 m
Structure	FODO
8 Bending magnets	$B_{max}=1.2$ T
18 Q-poles magnets	$G_{max}=10.$ T/m
Ion source	ECR
Injection energy	2-5 MeV/n (RFQ or linac)
Acceleration	$f=0.5 - 4$ Mhz $V=10$ KV
Ejection spill	0.5 - 1 s, 1/3 integer resonance ultra slow ejection

This basic design could be refined to include better monitoring of the extracted beam, and beam storage and cooling facility with a higher repetition rate injector. Hence, modulation of the beam intensity and programming of dose across the irradiation volume, as well as storage of radioactive beams could become possible.

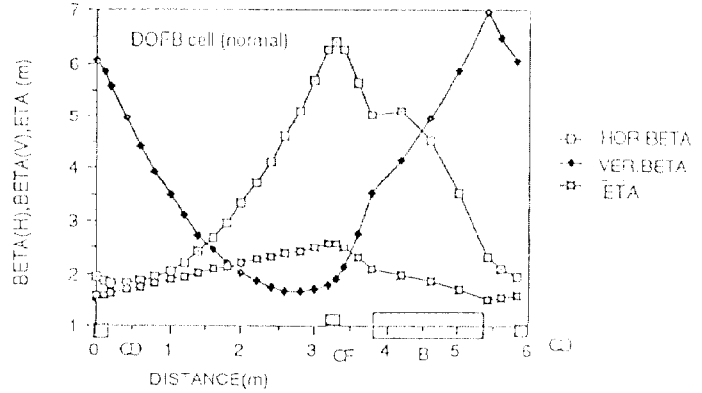


Fig 10 :  $\beta$  an  $\eta$  functions in the unit cell of the 230 MeV Tsukuba proton synchrotron

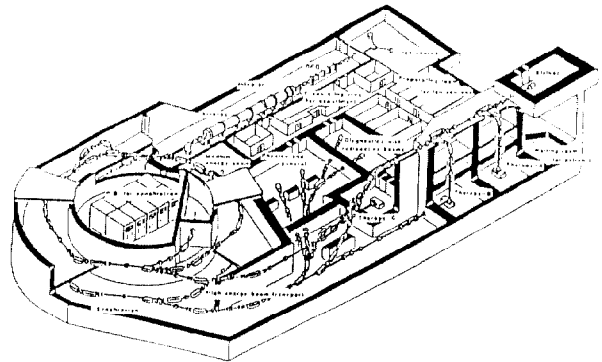


Fig 11 : Bird-eye-view of the HIMAC facility in construction in Chiba

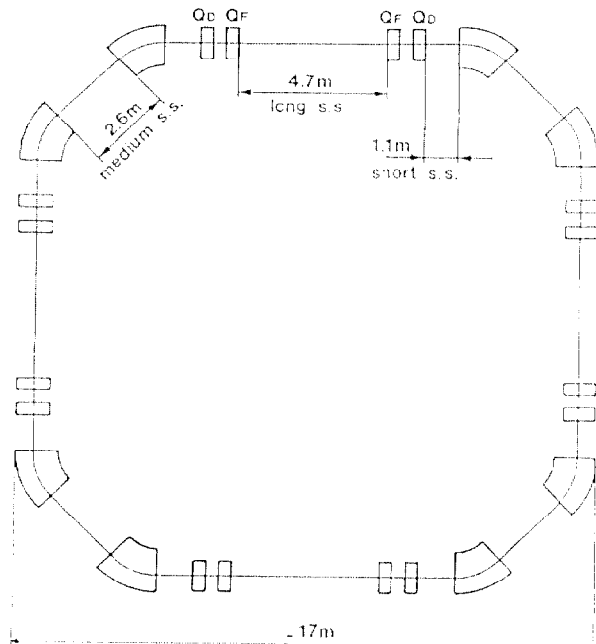


Fig 12 : An arrangement of EULIMA synchrotron lattice

Emphasis has been put on dedicated full time facilities to medical treatment but significant part time therapy programs are also planned at GSI in Darmstadt using the SIS synchrotron which accelerates light ions up to 2 GeV/nucleon. In order to use this accelerator complex in an efficient way for radiotherapy, it is proposed [14] to add a dedicated injector for light ions (3 MeV/nucleon) and to install a separated area for patient treatment.

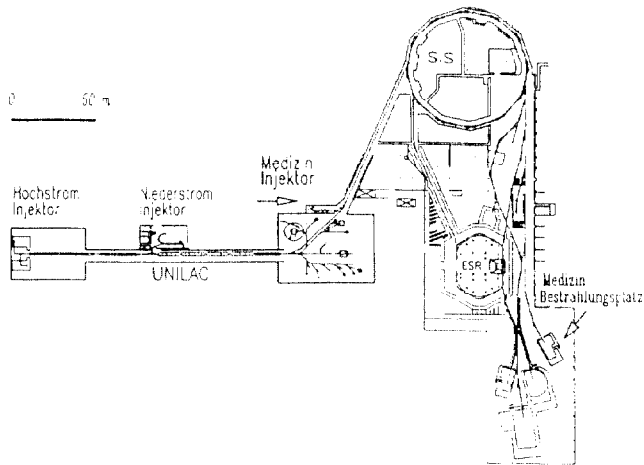


Fig 13 : GSI accelerator complex with the medical injector and the radiotherapy facility

It is very well known that the radiotherapy with light ions was started in LBL using the BEVALAC part time (1/3 therapy, 2/3 physics) and they now have 15 years of experience on which to base the next step which will be a dedicated medical accelerator to replace the Bevatron when it shuts down in the mid 1990's [15]. The design parameters of this machine are presented in Table 7.

Table 7

Range	30 cm
Beams	From proton to neon
Intensities	$5 \times 10^{11}$ /sec for proton, helium $4 \times 10^9$ /sec for carbon, neon

Fig 14 shows the proposed layout which uses as much of the present BEVALAC infrastructure as possible, hence a large circumference (120 m) synchrotron.

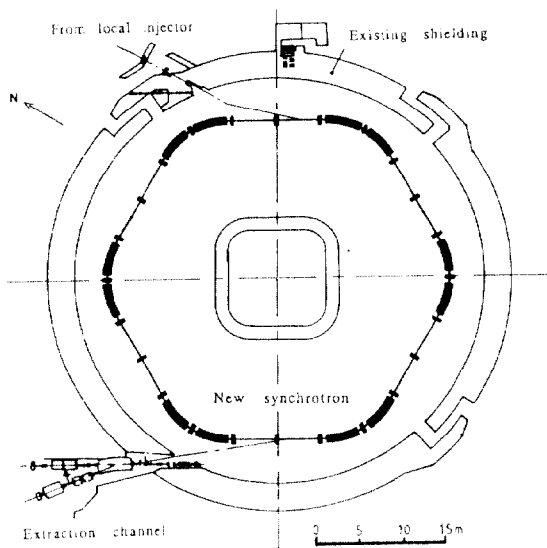


Fig 14 : The proposed LBL Heavy Medical Accelerator to replace the Bevatron

Synchrotron versus Cyclotron

I have presented designs for cyclotrons and synchrotrons but it is difficult to choose between the two because the energy requested by the physicians is high for a cyclotron and somewhat low for a synchrotron : the cyclotron needs a large magnet which requires a superconducting coil, particularly for light ions. On the other hand with a small synchrotron it is hard to reach the desired intensity due to space charge limitation at injection, particularly for protons. The cyclotron gives a continuous beam of fixed energy with plenty of intensity to spare ; the synchrotron beam is pulsed, variable energy. All these characteristics have implications for the beam delivery system and treatment planning [9]. Some important features that may influence the final choice of the facility are presented in Table 8.

Table 8

	Cyclotron	Synchrotron
Energy variation	degrader	machine adjustable
Beam Intensity	High (CW mode)	Low (Pulsed mode)
Injection energy	0.01-0.1 MeV/n	1-5 MeV/n
Typical diameter		
ions	8 m	18 m
protons	3 m	6 m
Operation	simple PLC control	computer controls
Beam delivery system	Raster and Pixel	Raster

Conclusion

The development of sophisticated diagnosis methods (CT-scans, MRI, PET cameras), together with the high level of accelerator technology are now in favor of the development of new radiotherapeutic tools using protons and ions. In the next five years the Loma Linda proton facility will have treated a large number of patients and the HIMAC accelerator complex will start treatment with high LET particles, new medical experience with this type of radiations will be available. Several other projects both for protons and ions will probably be funded. Hence the applications of accelerators in radiotherapy will continue to be a major spin-off of high energy research technology outside big science, and a challenge for accelerator engineering.

References

- [1] R. Wilson, Radiological use of fast protons.: 47, 487-491, 1946.
- [2] M. R. Raju, Heavy particle Radiotherapy, Academic Press (1980).
- [3] P. Mandrillon et al, Commissioning and implementation of the MEDICYC Cyclotron Programme, 12th Int. Conf. Cyclotrons and their Applications , Berlin, May, 1989.
- [4] H. Blosser et al, 1988 Annual Report of the National Superconducting Cyclotron Laboratory, Michigan State University p. 107.
- [5] Y. Jongen et al, Preliminary design of a reduced cost proton therapy facility using a compact, high field isochronous cyclotron, paper presented at the XIII PTCOG meeting, Loma Linda May 1990.
- [6] H. Blosser, Present and Future Superconducting Cyclotrons, BAPS 32 (1987)171, Particle Accelerator Conf., Washington DC, 1987.
- [7] P. Mandrillon et al, Proceedings of the EULIMA Workshop on the Potential Value of light ion therapy, Nice, 1988, EUR 12165EN.
- [8] P. Mandrillon et al, Progress of the feasibility studies of the European Light Ion Medical Accelerator. Proceedings of this Conference.
- [9] F. Farley, Ch. Carli EULIMA beam delivery. Proceedings of this Conference.
- [10] J. Slater, The Loma Linda facility, Proceedings of this conference.
- [11] S. Fukumoto et al, Tsukuba Medical Proton Synchrotron KEK-89-168, Dec. 1989.
- [12] J. Castro, Review of medical treatment with particle beams, Proceedings of this conference.
- [13] Y. Hirao, HIMAC project at NIRS-Japan, Proceedings of this conference.
- [14] K. Blasche et al, The GSI project : biomedical and radiobiological activities at GSI, Proceedings of the EULIMA Workshop on the Potential Value of light ion therapy, Nice, 1988, EUR 12165EN.
- [15] J. Staples, The LBL Heavy Ion Biomedical Accelerator, Paper presented to the spring meeting of the American Physical Society, April 1990.

**DOSE SPECIFICATION FOR REPORTING A THERAPEUTIC IRRADIATION.  
SPECIFIC PROBLEMS ENCOUNTERED IN FAST NEUTRON BEAM THERAPY**

A. Wambersie <sup>1</sup>, H.G. Menzel <sup>2</sup>, B.J. Mijnheer <sup>3</sup>, G.R.H. Sealy <sup>4</sup>

1. Université Catholique de Louvain, Cliniques Universitaires St-Luc, 1200-Brussels, Belgium.
2. Commission of the European Communities, Radiation Protection Programme, 1049-Brussels, Belgium
3. Antoni van Leeuwenhoekhuis, 1066 CX Amsterdam, The Netherlands
4. MRCRO, Clatterbridge Hospital, Merseyside, L63 4JY, United Kingdom.

Recommendations for reporting external radiotherapy with photons and electrons were published by the ICRU in 1978 [6]. These recommendations are being updated [14]. They are applicable to a large extent to fast neutron therapy. However, with neutrons, an additional problem is raised by the need for specifying the radiation quality. As a matter of fact, with the low LET radiations currently used in radiation therapy (i.e. cobalt-60  $\gamma$  rays, photon and electron beams from a few MeV up to about 50 MeV), the RBE does not vary with energy neither differs between photons and electrons significantly in clinical terms. Therefore, the absorbed dose (and the time factors) are generally sufficient to predict the radiobiological and clinical effects.

In contrast, with the fast neutron beams currently used in therapy, the RBE of the neutrons, relative to cobalt-60  $\gamma$  rays, is significantly different from unity and varies with neutron energy. It depends on dose, biological system and criterion, dose rate, environmental conditions (such as oxygenation), etc. From a practical point of view, this raises three types of problems:

- the comparison of a neutron beam of a given energy with a neutron beam of a different energy;
- the comparison of a given neutron beam with photons;
- potential change of neutron energy spectra within the patient.

### 1. Comparison between neutron beams of different energy spectra

As the biological effectiveness of a given neutron beam depends on energy, any exchange of clinical information from one neutron therapy centre to another one requires to take account of the difference in radiation quality. Ideally, a single conversion factor between the two neutron energy spectra and related RBE values could be used.

RBE determinations were performed using different biological systems and criteria and involving most of the neutron beams actually used for clinical applications. The results of systematic RBE determinations as a function of neutron energy, as well as those of intercomparisons performed at different neutron therapy centres have been recently reviewed [1][3].

It is desirable and seems reasonable to use a single conversion factor to take into account the RBE differences between any two neutron beams, provided that the differences between the two energy spectra are not too large. This is fulfilled if only the high-energy neutron beams recently introduced in therapy are compared. The conversion factor could be called Clinical Neutron Intercomparison Factor (CNIF) [13]. The use of the CNIF concept should be restricted to the field of neutron therapy, when comparing or transferring clinical information from one centre to another one.

One of the remaining problems is the single parameter specification of the neutron energy spectrum. Since the spectra of the neutron beams produced by protons and deuterons on beryllium (and by the (d,T) generators) are different in shape, the indication of the energy of the incident particles is not adequate. On the other hand, it is not always possible to measure the entire neutron energy spectrum; the "mean" neutron energy is then difficult to evaluate. As a practical approach, the penetration of the beam, measured in well defined conditions, can be proposed as a first indication of the neutron beam quality (e.g. half value thickness, or HVT, derived from depth dose measurements, in a water phantom, for a 10 x 10 cm<sup>2</sup> field size, and normalized for an

infinite SSD). The measurements should be made e.g. between 5 and 15 cm or between 10 and 20 cm in depth depending on the beam energy and on the clinical situation. This information is easy to obtain and depth dose curves are, in any case, required for the therapeutic applications.

An alternative approach is based on the measurement of microdosimetric spectra with small tissue equivalent proportional counters. These spectra provide a particular description of the secondary radiation components resulting from neutron interactions and are closely related to the LET spectra of these secondary charged particles at least for the neutron energies of relevance in therapy. As the biological properties of neutrons are directly correlated to the types and energy spectra of the secondary radiation, it appears to be consequent to base the derivation of an adequate biological weighting or conversion factor on measured microdosimetric spectra.

In addition to this fundamental consideration, the microdosimetric approach has a number of practical advantages. The measurements can be made within phantoms and free in air under irradiation conditions identical to those used in actual therapy, clinical dosimetry and possibly related radiation biology. The measured spectra implicitly take into account the influence of any irradiation parameters such as field size, target thickness and beam filtration on radiation quality. The measured spectra include both the neutron and the photon components. The achievable precision in the measurements is as good as for any method in clinical neutron dosimetry. It appears feasible that simplified measuring procedures using dedicated microelectronics, similar to those achieved for radiation protection, can be developed enabling routine application of this method.

The microdosimetric spectra themselves are very complex and there is the necessity to evaluate a single radiation quality parameter from these spectra. Recently, an approach has been suggested [8][11][15][16] based on a systematic microdosimetric measurement intercomparison at all European centres under the auspices of the "Heavy Particle Therapy Group" of the EORTC (European Organization for Research on Treatment of Cancer) and systematic biological intercomparisons [1], at most of these centres. By using the microdosimetric spectra and the RBE ratio determined for the same neutron beams, an empirical weighting function was derived applying a suitable numerical unfolding procedure. It was shown that this procedure can be used to evaluate a single parameter specification for radiation quality which provides estimates for RBE ratios for any two neutron therapy beams with an accuracy at a level as required in therapy (better than 3.5% [9]). This statement is restricted to the range of neutron energies relevant to neutron therapy and, at present, to the biological systems and endpoints used in the analysis [10][11]. More systematic biological data on early and late effects are urgently required.

The proposed microdosimetric approach fulfills the requirements for clinical applications, in particular, with regard to the achievable accuracy. In fact, the accuracy achievable in individual radiobiological experiments in general, and at absorbed dose levels corresponding to the current doses per fraction in particular, is low if compared to the accuracy requirements in clinical neutron dosimetry. Systematic combined microdosimetric and radiobiological analysis provides constraints and thus improves the confidence in RBE ratios. If

reliable biological weighting functions are established only microdosimetric measurements are required which are much less time consuming and less expensive than full scale radiobiological experiments.

## 2. Comparison between neutron and photon beams

In several situations in neutron therapy there is a need to convert the neutron absorbed doses into the "equivalent" photon absorbed doses, e.g.:

- when defining the neutron therapy arm equivalent to the photon control arm during the preparation of a therapeutic protocol (using the clinical experience accumulated with photons);
- when combining neutron and photon absorbed doses in mixed schedule irradiation.

The conversion factor should be, in principle, the RBE of neutrons relative to photons, but the difficulty arises from the fact that the RBE varies within large intervals with the dose per fraction and the biological effect or system. Therefore, it would be an oversimplification to use a single conversion factor to take into account the RBE differences between neutrons and photons. However, in some clinical situations, a single conversion factor has to be selected and thus the concept of Clinical Neutron Potency Factor (CNPF) was introduced [ 13 ]. The CNPF can be defined as an "average" or "overall" RBE of a given neutron beam (relative to photons) for undesirable late effects in normal tissues, and for a standard fractionation scheme (i.e. 2 Gy per fraction for photons). The expression "clinical RBE" has been used by some authors for the same concept.

Similarly as the CNIF concept, the use of the CNPF should be restricted to clinical neutron therapy since both are probably of very limited radiobiological significance. The CNIF concept assumes in particular the same RBE value for all the late effects in normal tissues (which possibly is related to connective tissue injury). This assumption seems reasonable in practice provided that its limitations are kept in mind (and if the late tolerance of the central nervous system, for which a higher RBE has been observed, is excluded).

The CNPF, as defined above, can be deduced from radiobiological experiments. However, in clinical practice, the neutron dose to be prescribed cannot be simply obtained by dividing the photon dose which would be delivered in a similar situation by the CNPF. Firstly, a correction has to be applied when the adopted fractionation schemes, for photons and neutrons, are different from the reference fractionation scheme (see below :  $\gamma C_{fr}$  and  $n C_{fr}$ ). Secondly, when prescribing the neutron dose, the therapist has to take into account the difference in physical selectivity between the photon and neutron irradiations, which could influence, to a large extent, the clinical tolerance especially with "low-energy" cyclotrons (see below :  $g_n/\gamma$ ). With the introduction of high-energy cyclotrons, this factor will come closer and closer to unity. The beam penetrations are improving and beam arrangements will be chosen to be more and more similar for neutrons and photons.

Another approach would consist in defining the CNPF as the ratio of the total doses in the planning volume, which could be tolerated with photons and neutrons, respectively. For example, if for a given tumour type and site, the clinically "tolerable" dose with photon irradiation is 70 Gy and with neutron irradiation is 25 Gy, the CNPF would be 2.8.

This second approach implies some clinical judgement and experience, and it does not imply as above the same RBE value for the late tolerance of all normal tissues since this factor is included in the "general clinical" tolerance. However, this second approach has a great disadvantage due to the fact that the

clinical tolerance strongly depends on the physical dose distribution (especially with low energy cyclotrons, e.g. skin ulcerations, subcutaneous fibrosis, etc.). The CNPF would then vary, even in a given centre, with the tumour depth and localization, the size of the target volume and also the beam arrangement. This would make any intercomparison and exchange of information between centres very difficult. The second approach to define the CNPF can therefore not be followed.

The CNPF values for different centres are, of course, correlated with the corresponding CNIF value. For example, if centres 1 and 2 are compared, one has :

$$\frac{(\text{CNPF}_1)}{(\text{CNPF}_2)} = \text{CNIF}_{1/2}$$

The use of the CNPF concept is illustrated as follows for two practical situations :

### a) Preparation of a new therapeutic protocol comparing neutrons to photons

The ratio of the prescribed doses at the planning volume in the photon and neutron arms, is given by the expression :

$$\frac{D_\gamma}{D_n} = (\text{CNPF}) \times \gamma C_{fr} \times n C_{fr} \times g_n/\gamma$$

where :

- (CNPF) has been defined above;
- $\gamma C_{fr}$  is the efficiency of the actual fractionation scheme for photons relative to the reference (2 Gy per fraction) fractionation scheme ( $\gamma C_{fr}$  will not be discussed here, nor the use of the NSD concept to evaluate  $\gamma C_{fr}$ ). It can be assumed that  $\gamma C_{fr}$  is similar for most of the late effects;
- $n C_{fr}$  has the similar meaning as  $\gamma C_{fr}$ , but for neutrons. Its value is probably close to unity in many situations;
- $g_n/\gamma$  takes into account the differences in the irradiation geometry or physical selectivity for neutrons and photons, and their influence on the late clinical tolerance.

### b) Computation and display of the dose distribution in mixed (neutrons + photons) schedule irradiation

In mixed schedule irradiations, at some point of the treatment planning procedures, combination of photon and neutron doses (or isodoses) becomes necessary, in order to check if the chosen beam arrangement and beam weighting adequately covers the planning volume, as well as to identify the normal tissues at risk.

Simple addition of the neutron and photon doses is meaningless and a biological weighting factor has to be introduced : the CNPF can also be used for that purpose, and the neutron doses multiplied by the CNPF have to be added to the photon doses [ 12 ].

However, for safety, in a second step, the photon "equivalent" dose to the normal tissues at risk should be evaluated using the RBE values actually measured for these tissues and for the planned doses per fraction. The photon "equivalent" doses calculated in this way should then be compared to the accepted photon schedules. This is particularly true when irradiation involves the CNS taking into account the risk of late damage.

## Discussion and conclusion

An important goal to achieve for improved exchange of clinical information is that the therapeutic irradiations be reported in a uniform way in the different neutron therapy centres.

Therefore, simple relevant quantities, which can be directly and easily measured, should be recommended for reporting. The first quantity actually measured is the total absorbed dose, and some consensus and uniformity has been achieved and guaranteed through existing protocols for the measurement of this quantity [ 7 ].

An additional problem, specific to neutron therapy, is due to the fact that the radiation quality has to be specified. As a matter of fact, the neutron energy significantly influences the biological effect.

Microdosimetry appears at present to be the most promising approach to describe the radiation quality, at the point of interest, in a complete and relevant way. Specification of the neutron and gamma components only today appears to be a poor and insufficient description of the radiation quality.

For reporting a therapeutic irradiation with fast neutron beams, following recommendations can be proposed :

- 1) the description of the tumour, target and planning volume(s), in the same way as recommended for photon therapy;
- 2) the specification of the absorbed dose at the "ICRU point", as well as the maximum and the minimum dose within the planning volume, as recommended also for photon therapy. Absorbed dose at other clinically relevant points (within the target volume or in normal tissues) could be added when required by the clinical situations;
- 3) the fractionation and overall time (more generally, a complete description of the dose/time relationship) as recommended for photon therapy;
- 4) in addition to what is recommended for photon therapy, the quality of the neutron beam has to be specified using the following parameters :
  - energy of the incident particles and nuclear reaction;
  - HVT determined in well defined reference conditions;
  - microdosimetric characteristics of the beams, as complete as possible, at several relevant points.
- 5) to facilitate the interpretation of the protocols, the adopted CNPF (and eventually CNIF) has to be added.

Lastly, it is, in principle, possible to derive from the above quantities several weighted quantities, such as, for example, the "effective dose"[ 2 ] [ 4 ] [ 5 ] [ 15 ]. They can be used, and be helpful, for several types of clinical studies. However, these derived quantities, which always imply some biological weighting factors (and thus assumptions) can be used in addition too, but should not replace the more straightforward quantities recommended above for reporting.

## References

1. M. BEAUDUIN, J. GUEULETTE, V. GREGOIRE, B.M. DE COSTER, S. VYNCKIER, A. WAMBERSIE  
Radiobiological comparison of fast neutron beams used in therapy. Survey of the published data.  
*Strahlentherapie und Onkologie*, **166**, 18-21, 1990.
2. M.C. CATTERALL AND D.K. BEWLEY  
Fast neutrons in the treatment of cancer.  
Academic Press, 1979.
3. P. CHAUVEL, A. WAMBERSIE (Ed.)  
Proceedings of the EULIMA Workshop on the Potential Value of Light Ion Beam Therapy, Centre Antoine-Lacassagne, Nice-France, November, 3-5, 1988. Publication n° EUR 12165 EN of the Commission of the European Communities, c ECSC-EEC-EAEC, Brussels-Luxembourg, 1989 and CAL Edition.
4. S.B. FIELD and M.C. JOINER  
Expression of dose in neutron therapy.  
*Radiother. and Oncol.*, **17**: 73-79, 1990.
5. E. HALL  
Specification of dose in neutron therapy  
*Radiother. and Oncol.* **17**, 264-266, 1990.
6. INTERNATIONAL COMMISSION ON RADIATION UNITS AND MEASUREMENTS  
Dose Specification for Reporting External Beam Therapy with Photons and Electrons.  
ICRU Report 29 (1978)  
ICRU Publications 7910 Woodmont avenue, Suite 1016, BETHESDA, Maryland 20814, USA.
7. INTERNATIONAL COMMISSION ON RADIATION UNITS AND MEASUREMENTS  
Clinical Neutron Dosimetry. Part I: Determination of Absorbed Dose in a Patient Treated by External Beams of Fast Neutrons. ICRU Report 45 (1989)  
ICRU Publications 7910 Woodmont avenue, Suite 1016, BETHESDA, Maryland 20814, USA.
8. H.G. MENZEL, P. PIHET and A. WAMBERSIE  
Microdosimetric specification of radiation quality in neutron radiation therapy.  
*International Journal of Radiation Biology*, 1990, **57**, 865-883.
9. B.J. MIJNHEER, J.J. BATTERMANN and A. WAMBERSIE What degree of accuracy is required and can be delivered in photon and neutron therapy ?  
*Radiother. and Oncol.* **8**, 237-252, 1987.
10. P. PIHET  
Etude microdosimétrique de faisceaux de neutrons de haute énergie. Applications dosimétriques et radiobiologiques, Thesis (Louvain-la-Neuve: Université Catholique de Louvain).
11. P. PIHET, H.G. MENZEL, R. SCHMIDT, M. BEAUDUIN and A. WAMBERSIE.  
Biological weighting function for RBE specification of neutron therapy beams. Intercomparison of 9 European therapy centres Proceedings of the 10th Symposium on Microdosimetry, Rome, 1989. *Radiation Protection Dosimetry* (in press).
12. A. WAMBERSIE  
Specific problems in neutron treatment planning in comparison with photon treatment planning, in G. Burger, A. Breit and J.J. Broerse (Eds.), *Treatment planning for external beam therapy with neutrons*, Urban and Schwarzenberg. München-Wien-Baltimore, Supplement to *Strahlentherapie*, **77**, pp. 24-35, 1981.
13. A. WAMBERSIE and J.J. BATTERMANN  
Practical problems related to RBE in neutrontherapy. In K.H. Kärcher, H.D. Kogelnik and T. Szepesi (Eds), *Progress in Radio-Oncology III*, ICRO (International Club for Radio-Oncology), Vienna, Austria, pp. 155-162, 1987.
14. A. WAMBERSIE, T. LANDBERG, K.A. JOHANSSON, J. DOBBS, J.P. GERARD AND I. SENTENAC  
Dose Prescription and Specification in External Radiotherapy : Evaluation of ICRU Report 29 and New Trends. *ICRU NEWS*, 1989, **2**, 25-27.  
International Commission on Radiation Units and Measurements (ICRU) 7910 Woodmont avenue, BETHESDA, MD 20814-3095, USA.
15. A. WAMBERSIE and B.J. MIJNHEER  
"Expression of Dose in Neutron Therapy"  
*Radiotherapy and Oncology*, **17**, 261-263, 1990.
16. WAMBERSIE, A. PIHET, P. and MENZEL, H.G.  
The role of microdosimetry in radiotherapy. Proceedings of the 10th Symposium on Microdosimetry, Rome, 1989. *Radiation Protection Dosimetry* (in press).

## CHARACTERISTICS OF A 62MEV PROTON THERAPY BEAM

D.E. Bonnett, A. Kacperek and M.A. Sheen  
MRC Cyclotron Unit, Clatterbridge Hospital, Bebington,  
Wirral, Merseyside, L63 4JY, U.K.

This paper describes the 62MeV proton therapy beam at the MRC Cyclotron Unit at the Clatterbridge Hospital. The characteristics of the beam are reported in terms of range, beam penumbra, the variation in output with field area, and beam shaping.

### Introduction

The 62MeV proton beam produced by the Scanditronix MC60 cyclotron at the Clatterbridge Hospital has been used in the treatment of eye tumours (ocular melanoma) since June 1989, and to date a total of 73 patients have been treated. The beam line is shown in figure 1 and consists of a double scattering foil system incorporating a central stopper, parallel plate ionisation chambers, range shifter and beam modulator together with anti-scatter collimators. The scattering foil system is used to provide uniform beam profiles over an area of 30mm in diameter. The foils are made of tungsten and are separated by a distance of 300mm. The first foil is 0.017mm thick and the second 0.027mm thick and the central stopper has a 3.05mm radius. These parameters were calculated using the method described by Gottschalk (1986). The overall length of the beam line is 1.8m and the distance from the final collimator to the isocentre is 70mm. Both range shifters and beam modulators are constructed from Perspex (Lucite). The range shifters define the maximum penetration of the beam for a given patient treatment. The modulators are stepped vanes which rotate in the beam to produce a uniform dose distribution across the target volume from the proton Bragg peak (Koehler et al 1975).

The purpose of this paper is to report the characteristics of this beam line in terms of range, beam penumbra, the variation of output with field area and beam shaping.

### Range

The beam line was designed to minimise energy losses in order to treat all possible sites within the eye. The advantage of this system over a single foil system is illustrated in table 1. The distance of the double foil system is measured from the first foil to the point of measurement. In the case of the single foil this distance was increased until the flatness of the two beam lines was comparable. The depth of penetration is measured to the distal 90% isodose line using a small silicon photo-diode (type BPW34). It can be seen that the double foil system gives an extra 1.4mm of range compared with the single foil. The maximum beam range required so far has been 28.7mm of eye tissue compared with a final measured maximum range for the beam line of  $30.4 \pm 0.2$ mm. The maximum required range is in good agreement with the value of 28.6mm (eye tissue) for 99% of the patients treated at the Harvard cyclotron (Goitein et al 1983).

### Beam Penumbra

In order to achieve maximum range the modulator and range shifter were placed 600mm from the final collimator to maximise the length of the beam line in vacuum. Measurements of beam penumbra have been made in a water phantom using a small diode (BAS11) and a three dimensional scanner. For the current position the penumbra measured between 90% and 10% isodose lines varied from  $2.3 \pm 0.1$ mm to  $3.6 \pm 0.1$ mm as the effective thickness of Perspex (i.e. thickness of range shifter +  $\frac{1}{2}$  thickness of modulator) was increased from 7.5 to 23.8mm. If, however, the modulator and range shifter were placed further upstream, that is just after the scattering foils then the penumbra was virtually independent of the thickness of Perspex and measured  $1.9 \pm 0.2$ mm. In order to achieve this position the amount of beam line in vacuum was shortened and consequently the maximum range was reduced to  $29.7 \pm 0.2$ mm. This would still be adequate to treat all patients seen to date. The improvement in penumbra can easily be understood in terms of geometrical considerations. An improved penumbra would reduce the required safety margin. This latter quantity is calculated as the 90% - 50% penumbra + 1.5mm to allow for microscopic spread of disease and positioning error.

### Variation in Output with Field Area

The treatment of ocular melanoma incorporates the use of irregular shaped collimators, each milled from a design produced by the planning program (Goitein & Miller 1983). Calibration of the beam is normally carried out using a 25mm diameter collimator and a 0.1cc thimble ionisation chamber (Far West Technology type IC-18). The variation in output with field size was investigated using a small diode and a selection of patient collimators. The output was normalised to the 25mm collimator and the results shown in figure 2 both for a modulated and unmodulated (full energy) beam. The modulated beam is the normal condition and the variation with field area is <1% for a representative range of patient collimators, therefore no output corrections are made to the chamber calibration. A much larger variation was seen in the case of the unmodulated beam indicating that the scattering out of the beam is much more dominant in this case.

### Beam Shaping

The planning program incorporates the facility for shaping the beam with the use of aluminium wedges. These are placed 40mm downstream from the collimator to minimise perturbations of the beam relative to the target volume (Egger private communication). Figure 3 shows a set of isodose curves measured in a water phantom for a wedge with a nominal angle of 25° in eye tissue and compares with a measured angle of 22°.



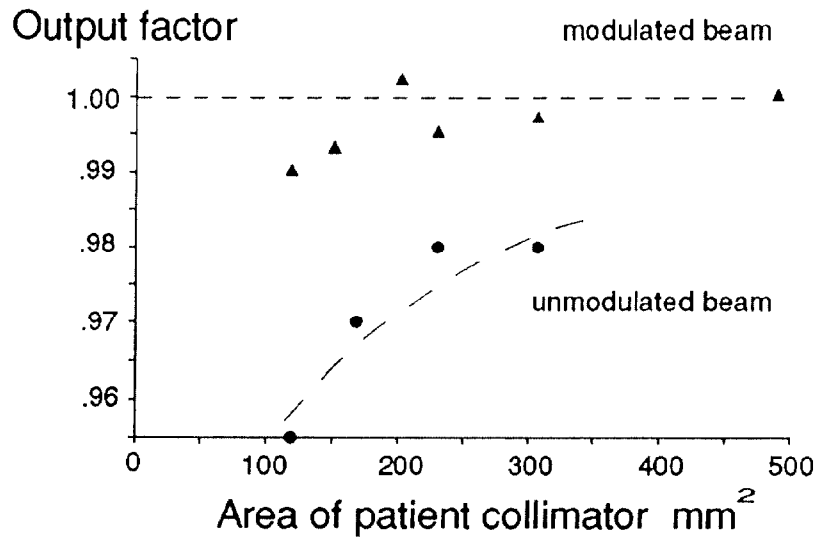


Figure 2: The variation of output in terms of dose with respect to collimator area ( modulated beam, unmodulated beam)

### ISODOSES OF A WEDGED FIELD

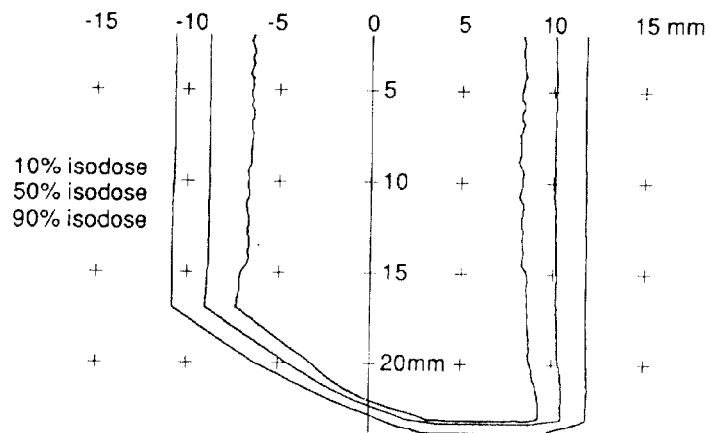


Figure 3: The isodose dsitriution for a field half covered by an aluminium wedge giving an effective wedge anle of 22° in eye tissue

Conclusions

The current beam line design has been able to treat all cases of coular melanoma that have been presented to date. Improvements in the penumbra can be made with an acceptable loss of penetration. It has also been shown that there is a negligible variation of output with field area and that shaping of the beam can be adequately achieved by the use of aluminium wedges.

References

M. Goitein and T. Miller, "Planning proton therapy of the eye", Medical Physics, vol. 10, pp. 275-283, May/June 1983.

M. Goitein, R. Gentry and A.M. Koehler, "Energy of Proton Accelerator Necessary for Treatment of Choroidal Melanomas", Int. J. Radiation Oncology Biol. Phys., vol. 9, pp. 259-260, 1983.

B. Gottschalk, "Double-scattering system with optimum dose uniformity in proton radiotherapy". Harvard Cyclotron Laboratory technical note PTAB/1/86, 1986.

A.M. Koehler, R.J. Schneider and J.M. Sisterson, "Range Modulators for Protons and Heavy Ions", Nuclear Instruments and Methods, vol. 131, pp. 437-440, 1975.

Table 1

A comparison of single and double tungsten foil scattering systems for a 62 MeV proton beam

Condition	Distance (mm)	Flatness (90%/50%)	Depth in Eye Tissue (mm)
No foil	--	--	31.0 ±0.4
Single W foil (0.15mm)	2200	93±1	29.3 ±0.4
Double W foil (0.044mm)	1500	94±1	30.7 ±0.4

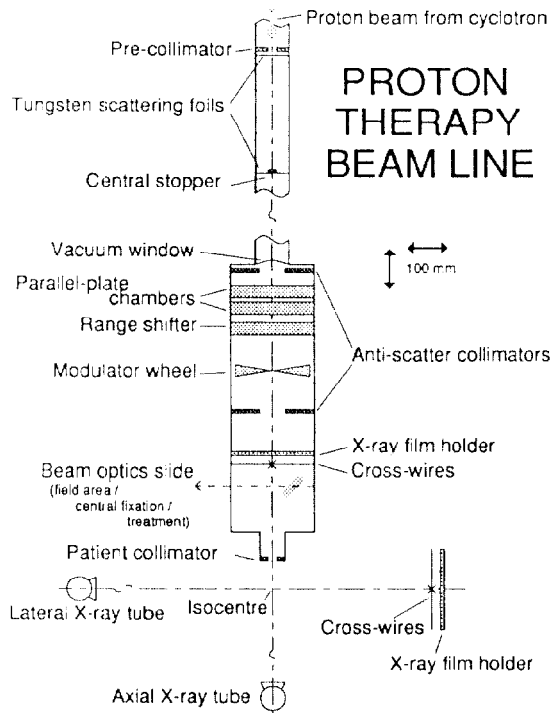


Figure 1: The proton therapy beam line at Clatterbridge

## AVERAGE IONIZATION ENERGY, $w$ , FOR 65 MEV PROTONS IN NITROGEN

J.M. Denis, I. Slypen, I. Tilquin, J.-P. Meulders  
 Université Catholique de Louvain, Institut de Physique Nucléaire,  
 Chemin du Cyclotron, 2, B-1348 Louvain-la-Neuve, Belgium

**Abstract :** An important parameter for the dosimetry of fast proton beam used in radiotherapeutic applications is  $w_p$ , the average energy required to produce an ion pair in gas. This paper presents preliminary results obtained in nitrogen with the 65 MeV proton beam of Louvain-la-Neuve's cyclotron. The experimental method and the first results are presented and discussed.

### Introduction

An increasing number of radiotherapeutic facilities use proton beams with energies ranging from the 60-85 MeV region (ocular melanoma - superficial tumors) up to the 150-200 MeV region (treatment of deep lying tumors). An accurate dosimetry with ionization chambers requires the knowledge of the  $w$  value for different gases, the average energy needed to produce an ion pair. At present, almost no value exists between a few MeV and 150 MeV (Table 1). A measurement of  $w$  in nitrogen has been initiated at the Louvain-la-Neuve's cyclotron and preliminary results obtained at 65 MeV are reported.

**Table 1 :** Experimental values for  $w_p$  in nitrogen ( $E_p > 1$  MeV).

Proton energy (MeV)	w or W	W value (eV/ion pair)	Authors
1,83	W	$36.68 \pm 0.34$	Larson [1]
2,51	W	$35.2 \pm 0.17$	Thomas and Burke [2]
3,6	w	$36.6 \pm 0.7$	Parks et al. [3]
150	w	$36.3 \pm 0.8$	Petti et al. [4]
340	w	33.6	Bakker and Segrè [5]

### Experimental method

The layout of the experiment is shown on Figure 1 and is similar to the one described in ref. 4. The proton beam goes through a long ionization chamber where the total charge is recorded. The differential  $w$  value is expressed by :

$$w(E_i) = N_p \frac{e}{Q} \frac{\ell}{L} \Delta E.$$

where :  $N_p$  : the number of protons passing through the chamber

$\frac{Q}{e}$  : the total number of ion pairs produced in the gas

$\frac{\ell}{L}$  : the ratio of the length of the collecting electrode to the total length of the gas volume in the chamber

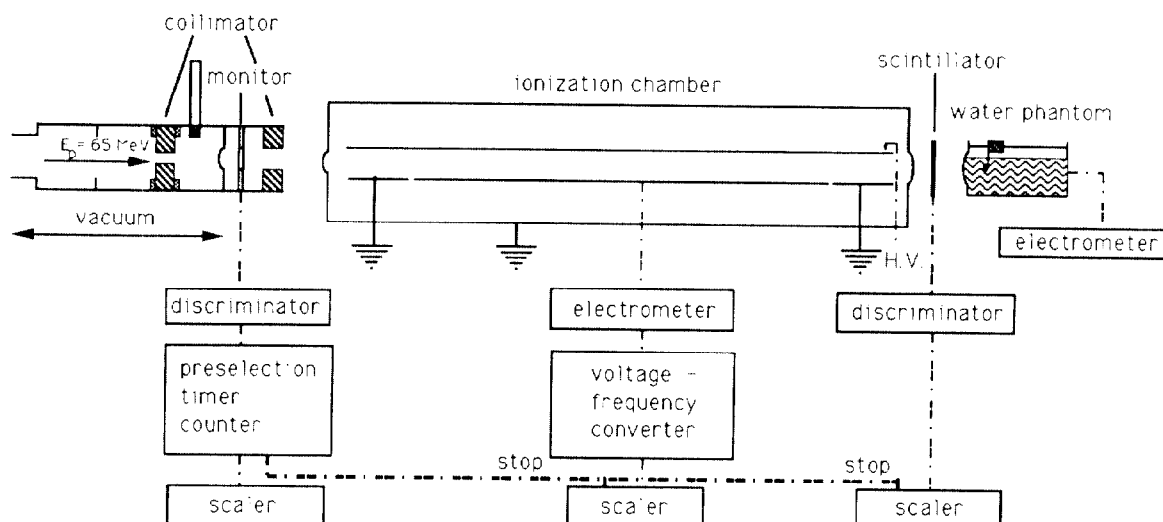
$\Delta E$  : the energy loss of the transmitted protons.

### Measurement of Q

The charge  $Q$  produced by the protons traversing the gas volume is collected by a parallel plate ionization chamber situated in a cylindrical gas cell (23 cm in diameter and 117.5 cm in length). The effective collecting area is 84 cm x 9 cm and the plate separation is 6 cm. The collecting plate is surrounded by a grounded guard ring ; its length, 12 cm, has been calculated with a computer code ELENS, which draws equipotential lines for different chamber configurations.

The proton beam is focused in a 2 mm diameter collimator, followed by a 10 mm collimator. After optimization of the beam conditions with a graphite Faraday cup, put in the position of the ionization chamber, the beam is reduced to a few fA ( $10^{-15}$  A). Beam intensity and collected current are recorded with a Keithley 617 electrometer. Under those conditions, an excellent saturation curve can be measured and an amplification of 25000 of the initial electric charges is obtained at a pressure of 1 atm nitrogen.

figure 1 : General layout of the experiment



### Measurement of $N_p$

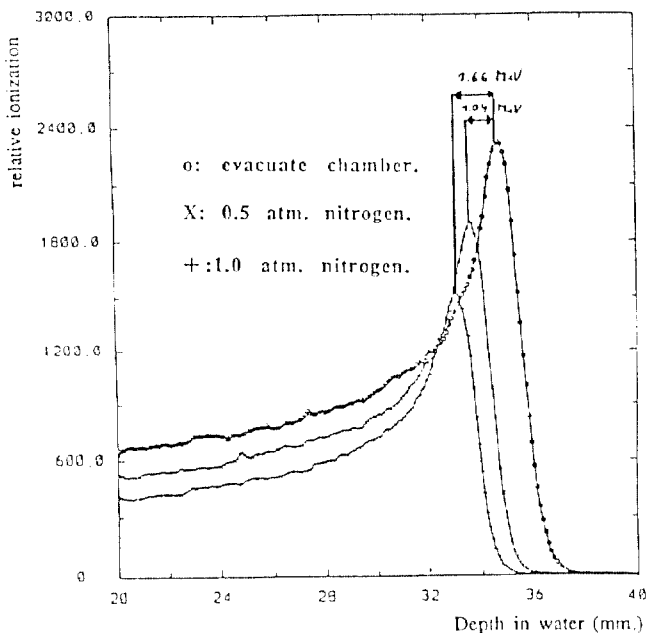
The exact knowledge of the protons number passing through the chamber is crucial in this experiment : the protons entering the chamber should travel through all the length of the chamber. With this respect, great care has been paid to avoid material in the beam axis, which could be responsible for multiple scattering. Only two mylar foils (125  $\mu\text{m}$  thick) are located in front of the ionization chamber. The proton number  $N_p$  is recorded by a 4 mm thick NE 102 plastic scintillator placed at the end of the chamber. The monitor of the experiment is a U-shaped NE 102 scintillator, situated between the first and the second collimator.

The transmission of the protons has been regularly checked by putting the 4 mm NE 102 detector in front and at the back of the ionization chamber : more than 99 % are obtained for gas pressures ranging from 0.5 atm to 2 atm.

### Measurement of $\Delta E$

The energy loss of the protons,  $\Delta E$ , is determined by recoil of the Bragg peak measured by a semi-conductor immersed in a water phantom ( $10 \times 10 \times 20 \text{ cm}^3$ ). The detector is a Si crystal ( $3.5 \times 3.5 \times 0.5 \text{ mm}^3$ ) located at a depth of 60  $\mu\text{m}$  from the front of the detector embedded in an epoxy resin. The Figure 2 shows the recoil of the Bragg peak at different gas pressure. A precision of 2 % in the  $\Delta E$  measurement can be obtained. As an alternative method, a NaI detector can be used. The protons produce a narrow peak with a FWHM of 1.5 %.

figure 2 : measurements of the energy loss ( $\Delta E$ ) in nitrogen gas



### Results

The results obtained in two separate runs are given in Table 2. The good reproducibility of the experimental method is proved by a comparison of the  $w$  values. A Monte-Carlo code is in progress for the correction of the  $\delta$  rays losses. This correction is based on the procedure proposed by Lauleinen and Bichsel<sup>[6]</sup>. Moreover, it is assumed that knock-on processes contribute for half of the total energy losses (Attix<sup>[7]</sup>). On the other hand, the correction for lack of compensation at the entrance and the exit of the collecting volume must be evaluated and will be checked by experiment.

Table 2 :  $w$  values in  $\text{N}_2$  and air.\*

Pressure (atm.)	$w$ (uncorrected) (eV/ion pair)	
$\text{N}_2$	0.5	$39.06 \pm 1.01$ $39.01 \pm 1.07$
	1.	$37.99 \pm 0.67$ $38.31 \pm 0.85$
	1.5	$37.86 \pm 0.69$ $37.90 \pm 0.76$
	2.	$37.74 \pm 1.29$
	Air	1.

The value of  $w$  in air at 1 atm is also shown in Table 2.

The ratio  $\frac{w_p(\text{N}_2)}{w_p(\text{air})} = 1.031$  is in agreement with the result obtained at 70 MeV by Hiraoka and al.<sup>[8]</sup>. These measurements will be expanded to other gases and to other energies.

\* Note added in proof

The corrected  $w$  values presented at the oral contribution need further confirmation.

### References

- [1] H. Larson, Phys. Rev. **112** (1958) 1927
- [2] D. Thomas, M. Burke, Phys. Med. Biol. **31** (1986) 1129
- [3] J. Parks, G. Hurst, T. Stewart, H. Weidner, J. Chem. Phys. **12** (1972) 5467
- [4] P.L. Petti, L. Verhey, R. Wilson, Phys. Med. Biol. **31** (1986) 1129
- [5] C. Bakker, E. Segrè, Phys. Rev. **81** (1951) 489
- [6] N. Lauleinen, H. Bichsel, Nucl. Instr. and Meth. **104** (1972) 531
- [7] F.H. Attix, Radiological Physics and Radiation Dosimetry, Ed. John Wiley (1986)
- [8] T. Hiraoka, K. Kawashima, K. Hoshima, Phys. Med. Biol. **33**, Suppl. 1 (1988) 131

# Microdosimetric Measurements on the Clatterbridge Proton Therapy Beam

A.C.A. Aro<sup>1</sup>, D. Bonnet<sup>2</sup>, V. Cosgrove<sup>1</sup>,  
S. Green<sup>1</sup>, A. Kacperek<sup>2</sup>, M.C.Scott<sup>1</sup>,  
and G.C. Taylor<sup>1</sup>.

<sup>1</sup> School of Physics and Space Research,  
University of Birmingham, England.

<sup>2</sup> Douglas Cyclotron Centre,  
Clatterbridge Hospital, England.

## Abstract

The interpretation of RBE studies relating to proton, neutron and ion beams can be aided by a knowledge of the distribution in LET (or lineal energy) of the incident and recoil particles. In order to provide such information for the Clatterbridge proton therapy beam, a programme of microdosimetric measurements is currently under way. Preliminary measurements using a commercial single-wire proportional counter have been followed by the design and use of a planar microdosimetric detector. Details of the planar detector design are presented here, together with some measurements made with it, and comparisons with equivalent measurements made with a silicon diode dosimeter.

## 1 Introduction

It is well known that charged particles exhibit a dose with depth profile which sharply rises towards the end of the particle track. It is also of course possible to focus charged particle beams, and these factors, together with the steep slope of the distal edge, combine to allow a much more localised dose to be delivered than is possible with neutrons. For these reasons protons have been exploited for therapy purposes at many centres<sup>1</sup>.

At Clatterbridge, proton therapy began last year using the 62 MeV proton beam and concentrating, because of the relatively low penetration of the beam, on tumors of the eye. To this date 73 patients have been treated at this centre and a randomised trial of this form of treatment against others is about to begin.

Microdosimetry has been applied to charged particle beams by many other groups<sup>(2-5)</sup>, generally using "wall-less" detectors<sup>6</sup>. These detectors are almost always spherical, a fact which derives from the need for an isotropic response to particles incident in any direction and is typical of neutron microdosimetry applications. For proton therapy the incident beam is unidirectional and hence we feel that for certain types of measurements a planar detector is more appropriate. This will be primarily for beams which are narrower than the detector entrance window, as discussed below.

## 2 Initial Measurements.

An initial set of measurements was performed with a standard Far West Technology LET SW $\frac{1}{2}$  filled to 2 $\mu$ m pressure with methane based tissue-equivalent gas. These were designed to give us an introduction to the general area of proton microdosimetry and revealed a few problems.

The first of these was the simple one of detector positioning which is important for narrow beams crossing a spherical cavity, and the second related to the level of noise in the detector which was too high to allow adequate measurement of the full energy (62MeV) beam.

We were particularly interested in the shape of the  $y.d(y)$

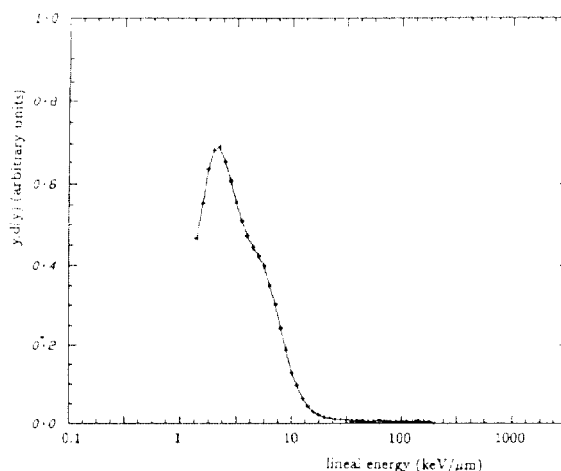


Figure 1: A preliminary measurement of the Clatterbridge beam with the spherical counter.

curves above the proton edge. Events here must originate in proton reactions with the detector wall materials. Figure 1 shows a typical  $y.d(y)$  distribution for a depth equivalent to about 15mm of perspex measured with the Far West detector. Even with this walled counter there are not significant numbers of events above the proton edge, from which we conclude that the proton energy at Clatterbridge is too low to produce the sort of high LET events seen in experiments on the Harvard (160MeV) proton beam<sup>7</sup>. This observation does not however preclude the presence of events below the proton edge (140 keV/ $\mu$ m) which are due to particles other than primary protons. These will mostly consist of delta rays and scattered protons produced in the wall, the impact of which are difficult to assess without further measurements.

In conclusion to this section we note that our preliminary experiments gave no reason to suggest that a wall-less counter design was necessary for the work that we intended to do on the Clatterbridge beam.

## 3 Detector Design and Testing

The general outline of our detector is shown in figure 2. It consists of five 25 $\mu$ m parallel wires 5mm apart to give a total active width of roughly 20mm. The outer pair of wires act as guards to delimit the collecting region with the central wire acting as an anode. It was originally thought that multiple anodes would be required to give a uniform collection efficiency across the full active region and hence the inclusion of an extra pair of wires. This seems not to be the case although further experiments to test the detector are under way.

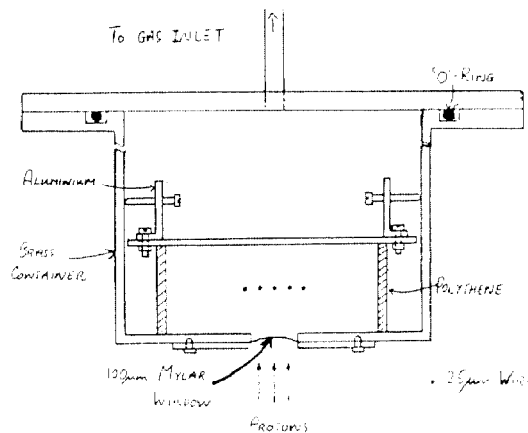


Figure 2: A schematic of the planar detector construction.

The variation in collection efficiency across the detector face was tested at Clatterbridge using a 2mm collimated beam at 3 lateral positions across the detector, and the results are shown in table 1. Normalisation is taken from the integrated beam current falling on the beam central stopper. The  $d(y)$  distributions measured at each lateral displacement were identical.

Lateral Displacement (mm)	Relative dose recorded (arbitrary units)
0	$23.77 \pm 0.5$
2	$25.19 \pm 0.5$
4	$24.67 \pm 0.5$

Table 1: Detector uniformity measurement

The maximum collimator diameter used so far in our therapy beam measurements is 5mm and so the primary beam always crosses the detector near its centre and distortions in the detector response due to non-uniform collection will be minimised.

A comparison of the performance of our detector with the commercial one, is shown in figure 3 for a 2mm collimator size. In both cases, these were obtained with +900V on the central anode and used methane based TEG at a pressure of 70mbar for the planar detector and 160mbar for the spherical, to simulate  $2\mu\text{m}$  of tissue. Measurements were made simultaneously at two amplifier gain settings and combined off-line to give the data presented here. Throughout this paper, different "depths" in perspex are simulated with a perspex wheel which has steps to give variable thicknesses on rotation.

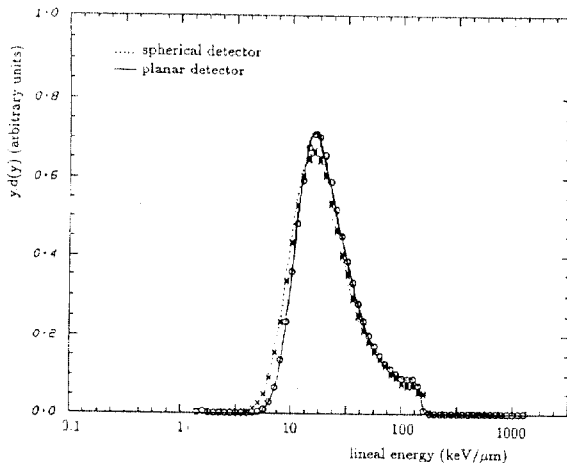


Figure 3: Comparison of the  $y.d(y)$  distributions measured at the Bragg peak with two detectors.

The measurements shown in figure 3 were made on the Bragg peak (see below) and are quite similar. The differences between these two curves are believed to be due to differences in the detector characteristics (primarily resolution), rather than different numbers of wall events in each case.

## 4 Therapy Beam Measurements

### 4.1 Relative Dose Measurements

As an integral check of our detector performance we have constructed depth/dose profiles for different collimator sizes to compare with those obtained with the Clatterbridge silicon diode dosimeter. This is a 4mm by 4mm by  $50\mu\text{m}$  Farnell BPW34 silicon diode used for dosimetry purposes in the way reported in the literature<sup>8</sup>. Normalisation is once again taken from the beam central stopper integrated current. A comparison of the two detectors for a collimator diameter of 2mm is shown in figure 4. When correction is made for the layer of material which overlays the diode, the peak and distal edge fall at approximately the same depth for both detectors to within

0.1mm. According to the literature<sup>9</sup> the depth at 90% of the distal edge corresponds to 0.996 of the usually quoted range value for the energy concerned. This gives a range of the Clatterbridge beam in perspex of 27.33mm which agrees well with standard tables.<sup>10</sup>

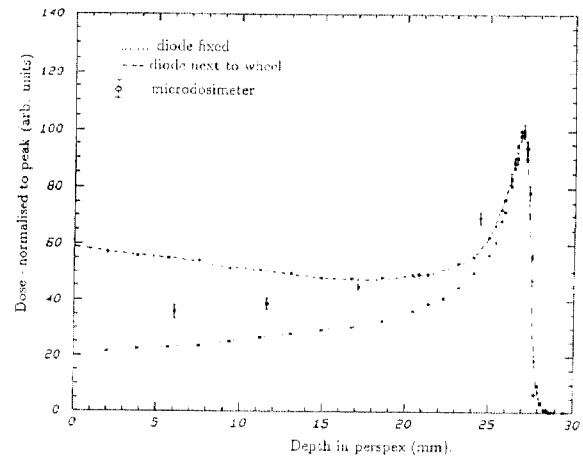


Figure 4: Dose with depth curve for a 2mm collimator diameter as measured with a silicon diode and the planar microdosimetric detector.

This observation has been verified by further measurements with a parallel plate ionisation chamber similar to the one described in reference 11.

The difference in the plateau height in figure 4 is, we believe, explained by the presence of proton scattering in the collimator or the modulating perspex wheel. The diode is much smaller than our microdosimeter, being roughly 4mm by 4mm and hence it would detect a smaller scattered component. This was tested by repeating the diode experiment with it positioned close to the rotating wheel rather than (as above) at a fixed distance from the collimator. A different profile again is obtained as shown by the dashed line in figure 4 and we conclude from these experiments that there is a diverging scattered proton component emerging from the collimator/wheel and that each detector detects an amount which varies with the solid angle that it subtends at the collimator.

We have noted with both microdosimeter and diode measurements, a change in the peak to plateau ratio with collimator size. The trends that we observe are in agreement with calculations reported in the literature<sup>12</sup> although the absolute

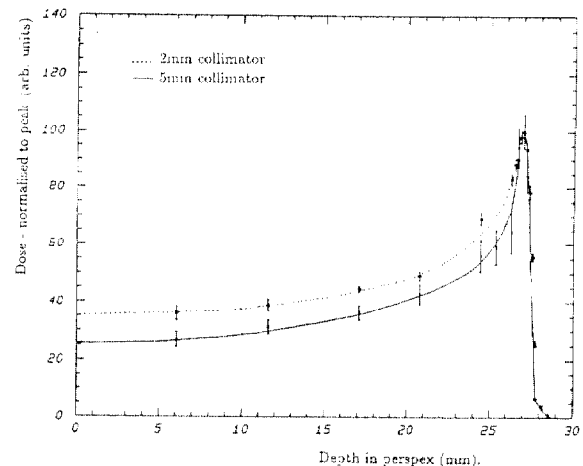


Figure 5: Dose with depth curve measured with the planar microdosimetric detector for 2 and 5mm collimator diameters.

differences seen by us are much smaller than those reported in reference 12. Figure 5 shows our results for 2 and 5 mm diameter collimators. The differences between our measurements and the published data are probably due to differences in the basic parameters describing each situation. Clearly the detector size and position modelled will be important, as will such beam parameters as energy spread and angular divergence. At present we are developing a Monte Carlo code with which we shall repeat the sort of calculations reported in reference 12, using parameters relating to our experiments and the Clatterbridge beam transport system.

## 4.2 $y_d(y)$ Measurements

Initial measurements have concentrated on small collimator diameters because of the need to avoid high count-rates in the detector. The  $y_d(y)$  distributions obtained for a 2mm diameter collimator at four different depths in perspex are shown in figure 6. These curves show clearly the reduced noise-level in the planar detector (measurements go down to  $0.3\text{keV}/\mu\text{m}$ ). Table 2 shows the change in  $\bar{y}_f$  and  $\bar{y}_d$ <sup>13</sup> with depth in a perspex phantom for different positions. The quoted errors consider only statistical counting uncertainties.

As expected, the most rapid changes in  $\bar{y}_d$  occur in the last few mm of the proton tracks. Also in table 2 is the  $\bar{y}_d$  value for a <sup>22</sup>Na gamma source, measured with a standard spherical neutron microdosimeter at a simulated diameter of  $2\mu\text{m}$ . This can be taken as typical of fast gamma spectra such as <sup>60</sup>Co and it can be seen that the  $\bar{y}_d$  for the Clatterbridge proton beam

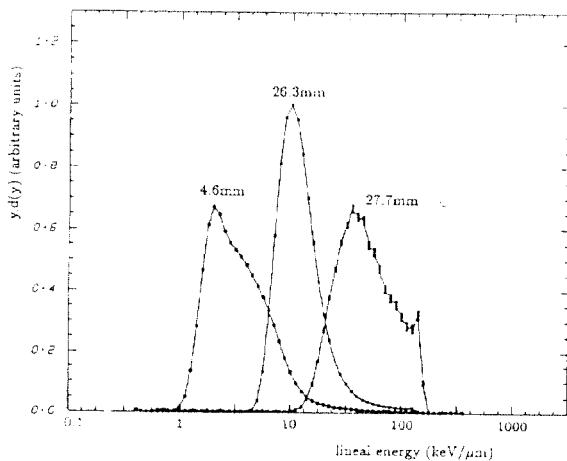


Figure 6:  $y_d(y)$  distributions at three depths in perspex measured with the planar microdosimetric detector.

Position (approx.)	Depth in Perspex (mm)	$\bar{y}_f$ (keV/ $\mu\text{m}$ )	$\bar{y}_d$ (keV/ $\mu\text{m}$ )
PLATEAU	4.58	$2.27 \pm 0.002$	$4.75 \pm 0.02$
PLATEAU	19.82	$3.89 \pm 0.003$	$5.79 \pm 0.01$
PROXIMAL	26.29	$10.80 \pm 0.01$	$14.41 \pm 0.03$
PEAK	27.03	$17.76 \pm 0.02$	$26.21 \pm 0.05$
50% DISTAL	27.35	$25.67 \pm 0.04$	$38.65 \pm 0.1$
5% DISTAL	27.70	$29.1 \pm 0.2$	$53.2 \pm 0.5$
<sup>22</sup> Na	-	$0.53 \pm 0.001$	$1.92 \pm 0.01$

Table 2: Dose parameters

ranges from a value which is roughly twice that for fast gammas, to a value which is roughly 25 times.

It should be expected that, as reported in the literature<sup>14</sup>, this change in  $y_d$  will be accompanied by a change in RBE with depth in phantom.

## 5 Summary and Conclusions

We have built and tested a planar microdosimetric counter for measurements on the Clatterbridge proton therapy beam. The detector has been used to measure depth/dose profiles that are consistent with those measured with the Clatterbridge silicon diode. The  $y_d(y)$  spectra measured at different depths in perspex show clearly the wide range of linear energies that can be produced with this sort of beam, and provides exciting possibilities for radiobiological studies using this beam.

It is worth noting that the experiments that we have performed so far have used collimation to give proton beams which are much smaller in diameter than the detectors used. This was done primarily to reduce the count-rate in the detector, but with the beam passing through the cavity it means that delta-ray events are not detected separately from proton events. We cannot therefore use our measurements so far to infer the real  $d(y)$  distribution that will be seen in bulk tissue from this beam; however, experiments to investigate delta-ray effects are planned.

## 6 References

- Sisterson, J.M. - "Clinical Use of Proton and Ion beams from a World-Wide perspective". *Nucl. Inst. Meth. in Phys. Res.* B40/41 (1989) 1350-1353.
- Zaider, M., Dicello, J.F., Brenner, D.J., Takai, M. and Raju, M.R. - "Microdosimetry of Range-Modulated Beams of Heavy Ions". *Rad. Res.* 87 (1981) 511-520.
- Klianga, P., Colvett, R.D., Goodman, L.J. and Lam, Y.M. - "Microdosimetry of 400 MeV/AMU <sup>12</sup>C and 450 MeV/AMU <sup>40</sup>Ar Beams". *Proc. 6th Symp. Microdosimetry* (1978) 1173-1183.
- Glass, W.A. and Roesch, W.C. - "Measurement of Ionization Distributions in Tissue Equivalent Gas". *Rad. Res.* 49 (1972) 477-494.
- Glass, W.A. and Braby, L.A. - "A Wall-Less Detector for Measuring Energy Deposition Spectra". *Rad. Res.* 39 (1969) 230-240.
- Rodgers, R.C., Dicello, J.F. and Gross, W. - "The Biophysical Properties of 3.9 GeV Nitrogen Ions (II Microdosimetry)". *Rad. Res.* 54 (1973) 12-23.
- Klianga, P.J., Colvett, R.D., Lam, Y.M. and Rossi, H.H. - "The Relative Biological Effectiveness of 100 MeV Protons (I Microdosimetry)". *Int. J. Radiat. Onc. Biol. Phys.* Vol 4 (1978) 1001-1008.
- Koehler, A. - "Dosimetry of proton beams using small silicon diodes". *Rad. Res. Suppl.* Vol 7 (1967) 51-63.
- Goitein, M., Gentry, R. and Koehler, A. - "Energy of proton accelerator necessary for treatment of choroidal melanomas". *Int. J. Radiat. Onc. Biol. Phys.* Vol 9 (1983) 259-260.
- Janni, J.F. - "Proton Range-Energy Tables from 1 keV to 10 GeV". *Atomic and Nuclear Data tables* Vol 27 Nos 2/3 (1982)
- Knoll, G.F. - "Radiation Detection and Measurement". Second edition. John Wiley and Sons (1989).
- Preston and Koehler, A. - "The effects of scattering on small proton beams". *Harvard University Internal report* (1968).
- ICRU Report 36 - "Microdosimetry" International Commission on Radiation Units and Measurements (1983).
- Bettega, D. and Tallone Lombardi, L. "Physical and Radiobiological Parameters of Proton Beams up to 31 MeV". *Il Nuovo Cimento* Vol 2D No. 3 (1983) 907-916.

TISSUE-EQUIVALENT CALORIMETER DEVELOPPED AT LMRI  
FOR THE MEASUREMENT OF ABSORBED DOSE.

J.Daures, J.P.Simoen, A.Ostrowsky.  
LMRI CEN SACLAY BP 21 91190 GIF SUR YVETTE FRANCE.

### Abstract

A Tissue-Equivalent calorimeter, made of Shonka A150 plastic has been constructed. The measurements in neutron beams from cyclotrons have shown that the total absorbed dose to A150 can be determined with an uncertainty (one standard deviation) close to 0.6 %, instead of more than 1.5 % for ionization chambers.

Former experiments with a similar calorimeter in heavy charged particle beams have proven the feasibility and the great interest of such a measurement.

At request, our laboratory is capable to perform in-situ absorbed dose measurement with this standard calorimeter, in medical neutron or heavy charged particle beams, thus enabling the calibration of the user's reference dosimeter.

### Introduction

The calorimetric method is very attractive because it is the more direct way to reach the absorbed dose, the reference quantity of interest in radiotherapy.

The absorbed dose [1] is defined as the quotient of  $dE$  by  $dm$ , where  $dE$  is the mean energy imparted by ionizing radiation to matter of mass  $m$ .

$$D = \frac{dE}{dm} \quad (1)$$

The special name for the unit of absorbed dose is gray ( Gy ) and :

$$1 \text{ Gy} = 1 \text{ Jkg}^{-1}$$

The calorimeter measures directly the energy converted into heat under irradiation, and before construction, the mass of the sensitive element is accurately measured.

Unfortunately the Tissue-Equivalent material used, the A150 plastic, presents a heat defect, because part of the energy is not converted into heat but employed in endoenergetic chemical reactions. It depends then upon a calorific yield  $r_{cal}$ .

Fortunately this dimensionless calorific yield is close to 1 (0.96). It was measured for several particles and energies with a standard deviation of 0.5 % [2].

On the other hand, ionometry involves secondary processes which require the knowledge of the average energy expended to produce an ion pair. Moreover ionization chambers are not homogeneous and stopping power ratios are needed. With a calorimeter the sensitive element is identical to the surrounding medium and so stopping power corrections are avoided.

In table 1 the uncertainties for one standard deviation are given.

Standard deviation of absorbed dose to A150 / %		
	Neutrons	Heavy Charged-Particles
Calorimetry	0.6	0.6
Ionometry	>1.5	>2.1

Table 1 : Calorimetric and ionometric uncertainties.

The standard deviation for calorimetry is relative to our instrument. The main uncertainty is due to the calorific yield.

For ionometry the standard deviation is derived from the European [3] or US protocols [2].

The standard deviation for calorimetry is much lower than for ionometry and justifies technical efforts.

### Principle

The sensitive element, the core, of mass  $m$ , is thermally insulated from the surrounding by means of vacuum gaps. So the mean absorbed dose is related to the heat quantity  $Q$  by the simple equation:

$$\bar{D} = \frac{Q}{m} \cdot \frac{1}{r_{cal}} \quad (2)$$

Where  $Q$  depends on the temperature increase  $\Delta T$  by the relation:

$$Q = m \cdot c_p \cdot \Delta T \quad (3)$$



But because of too high uncertainties on the specific heat  $c_p$  and on the correction for residual heat transfers, a relative method is employed for the heat measurement.

This method consists in an electrical calibration of the calorimeter. By Joule effect a known calorific energy  $Q_{ec}$  is dissipated in the core, giving a reading  $R_{ec}$  proportional to the thermistor resistance variation, thus to the temperature rise.

The electrical calibration factor is given by the following equation:

$$F_{ec} = \frac{Q_{ec}}{R_{ec}} \quad (4)$$

So that for each reading  $R$  resulting from irradiation, the calorific energy is determined by :

$$Q = F_{ec} \cdot R \quad (5)$$

The mean absorbed dose in the core is therefore in practice given by the equation :

$$\bar{D} = \frac{F_{ec} \cdot R}{m} \cdot \frac{1}{r_{cal}} \quad (6)$$

For obtaining the quantity of interest, which is the absorbed dose  $D$  at the reference point in the homogeneous medium, corrections for vacuum gaps, impurities and absorbed dose gradients must be applied, i.e.:

$$D = \bar{D} \cdot k_v \cdot k_i \cdot k_g \quad (7)$$

Due to careful design and construction of the calorimeter, these corrections are only of some per mil.

But calorimetry is a delicate technique. Its sensitivity is less than one millikelvin per gray. The thermal stability during electrical calibration or irradiation has to be kept at the level of ten microkelvins.

Nevertheless, in radiotherapy beams, dose rates are sufficiently high to allow measurements with a repeatability close to one per mil.

#### The LMRI calorimeter

A schematic presentation of our new TE-standard calorimeter is shown in figure 1. One can see the three main parts, thermally insulated one from another and from the surrounding medium:

- the central core, which is the sensitive element, ( $\phi=16\text{mm}$ ,  $t=3\text{mm}$ ),
- the jacket, whose temperature is maintained very close to the core's one by a feed-back thermal control,
- the shield, which is regulated at a constant temperature.

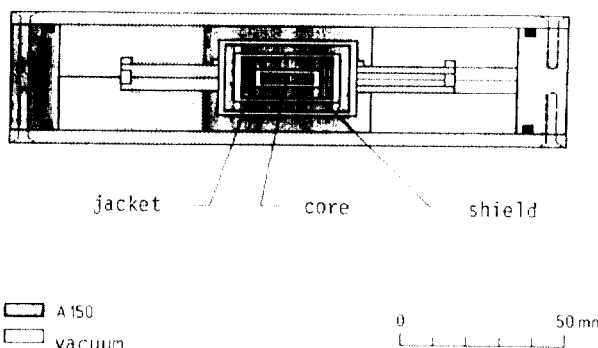


Figure 1 : The LMRI TE calorimeter

Twenty-six thermistors of very small mass ( around 0.5 mg ) are embeded in the calorimeter. They are used for heat measurement and for dissipation of heat during electrical calibration and for thermal regulation.

The main device of the associated measuring chain is a Wheatstone bridge. What is actually plotted is the bridge dc voltage, as a function of time. The reading  $L$  is, in fact, the relative variation of the thermistor resistance.

A typical plot of a calorimetric run is given in figure 2 .

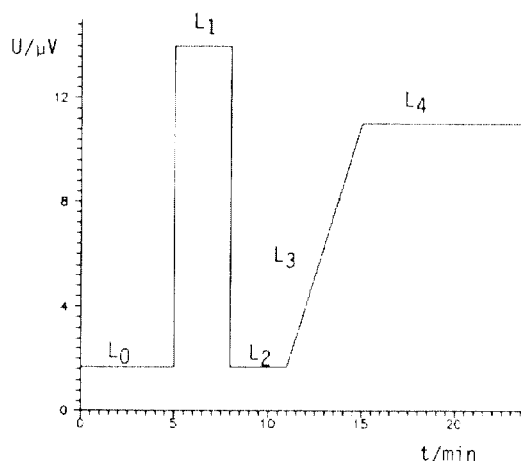


Figure 2 : plot of a calorimetric run

From the slopes  $L_0$ ,  $L_1$ ,  $L_2$ , the ohm-volt calibration of the bridge is obtained. From the slopes  $L_2$ ,  $L_3$ ,  $L_4$ , the reading  $R_{ec}$  or  $R$  is determined.

The absorbed dose is then calculated from equations 4-7

### Applications

This calorimeter constitutes the French National Standard for absorbed dose measurements in neutron beams. Several measurements have been performed in cyclotron neutron beams with standard deviations close to 0.6 % [4,5,6].

This standard instrument is well suited for measurements in protons or heavy charged-particle beams [2], with the same level of accuracy. So, as for neutrons, it permits:

- direct calibrations of therapy dosimeters in user's beams,
- determination of the product of the mean energy expended in the gas per ion pair formed, by the wall-to-gas stopping power ratio.

### References

- [1] ICRU report 33, "Radiation Quantities and Units," April 1980.
- [2] AAPM Report 16, "Protocol for Heavy Charged-Particle Therapy Beam Dosimetry," April 1986.
- [3] B. J. Mijnheer, p. Wootton, J. R. Williams, J. Eenmaa, C. J. Parnell, "Uniformity in Dosimetry Protocols for Therapeutic Applications of Fast Neutron Beams," *Med. Phys.* vol. 14, pp. 1020-1026, Nov/Dec 1987.
- [4] J. Caumes, A. Ostrowsky, K. Steinschaden, M. Mancaux, M. Cance, J. P. Simoen, R. Sabattier, N. Breteau, "Direct Calibration of Ionization Chambers with a TE Calorimeter at the Orléans Cyclotron Neutron Facility," *Strahlentherapie*, vol.160, pp. 127-128, 1984.
- [5] J. Caumes, A. Ostrowsky, K. Steinschaden, M. Mancaux, M. Cance, J. P. Simoen, "Calorimètre Equivalent-Tissu pour l'Etalonnage Direct des Chambres d'Ionisation dans les Faisceaux de Neutrons," in Proceedings of the fifth symposium on neutron dosimetry EUR 9762 EN, pp. 1215-1226, 1984.
- [6] H. J. Brede, D. Schlegel-Bickmann, G. Dietze, J. Daures-Caumes, A. Ostrowsky, "Determination of Absorbed Dose Within an A150 plastic Phantom for a d(13.35 MeV)+Be Neutron Source," *Phys. Med. Biol.*, vol. 33, pp. 413-426, 1988.

ELEMENTAL SYNTHESIS OF REAL TISSUE MICRODOSIMETRIC RESPONSES TO HIGH ENERGY NEUTRONS: PRINCIPLES AND LIMITATIONS

M.C. Scott, A. de Aro, S. Green, G.C. Taylor

Medical Physics Group, School of Physics and Space Research, University of Birmingham, Birmingham B15 2TT, U.K.

Abstract

The factors which could limit the elemental synthesis of real tissue microdosimetric responses are discussed and a determination of the response due to oxygen from 15.5 MeV neutrons is described.

Introduction

Neutron microdosimetric measurements attempt to reproduce the charged particle energy deposition in a small volume of tissue (typically 1-2  $\mu\text{m}$ ) by sampling that obtained in a much larger gas-filled cavity surrounded by tissue equivalent material. Unfortunately, however, it is not possible to synthesize a wall material having the same proportions of the major elements (C,H,N and O) as real tissue, the latter containing significantly more oxygen, and proportionately less carbon, than, for example, the widely used "tissue equivalent" A150 plastic. Since the cross sections for neutron induced charged particle production vary strongly both with neutron energy (particularly above 15 MeV or so) and the elemental isotopes concerned, the microdosimetric response of real tissue differs significantly from that of tissue equivalent materials. These differences at 15 MeV were shown by Caswell and Coyne [1] to be  $\sim 15\%$  in integral quantities like  $y_D$  (the dose averaged lineal energy deposition), but at energies of interest in current neutron therapy (up to 65 MeV or so) data uncertainties make estimation of the resulting microdosimetric differences between real and simulated tissue very difficult to quantify.

In order to overcome this problem we proposed [2] that the microdosimetric distributions be determined on an elemental basis, eg. for C, H, O and N separately, so that the response for any particular tissue type could be 'synthesised', i.e. constructed from that of its constituent elements. In order to do so we proposed to construct counters differing only in the element of interest, and hence to find the response for that element by a difference technique. Thus, the response of hydrogen alone would be determined from counters made of polythene ( $\text{CH}_2$ ) and carbon; an example of the microdosimetric response of such detectors to the p(62)Be Clatterbridge beam and the resulting hydrogen-only spectrum is shown in Fig. 1.

In this paper we consider in more detail the principles and limitations of the technique proposed.

Underlying principles

For the elemental synthesis approach to give an exact prediction of the real tissue response the shape of the microdosimetric response due to each element has to be identical both in the detectors involved in its determination and in real tissue, that is, the shape of the elemental response must be independent of the matrix in which it is incorporated. The subtraction or synthesis procedures can then be performed using simple scaling factors for differences in, for example, elemental density. There are three factors which determine whether or not this criterion is satisfied, namely

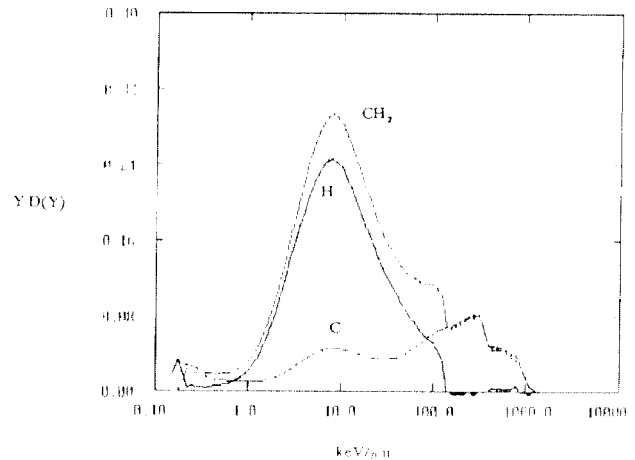


Fig. 1 Response of  $\text{CH}_2$  and C counters to the p(62) Be neutron beam at Clatterbridge, and the resulting microdosimetric response for H only.

- differences between the neutron spectrum incident in real tissue and in the different detectors involved,
- differences in charged particle stopping powers for the matrices involved, and
- microdosimetric events produced by the filling gas.

We shall present a preliminary examination of the importance of each in turn.

(a) Neutron spectrum perturbation

When a neutron beam is incident on any body the resulting spatial dependence of the neutron spectrum in the body depends on the neutron scattering and absorption properties of the constituent elements and their distribution. If we then introduce a local inhomogeneity into the body the neutron spectrum will be perturbed, both in the inhomogeneity and in the surrounding medium. The magnitude and spatial extent of this perturbation depends upon how much the neutron interaction properties of the inhomogeneity differ from those of the surrounding medium. At the same time, we note that it will be the neutron spectrum in the immediate vicinity of the detector cavity which will determine the response to heavy ion, alpha particle and low energy proton events, whereas the high energy proton component will be generated through a much larger volume of the detector. Thus, the spatial dependence of the neutron flux within the counter could be important.

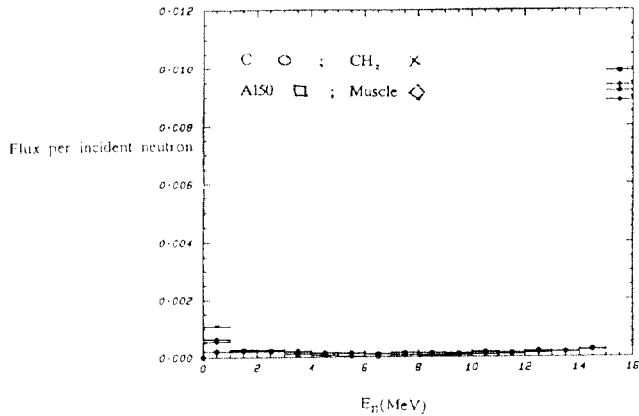


Fig. 2. Calculated neutron flux at a central cavity (per source neutron incident) in a detector having 3 cm thick walls of different materials.

In order to estimate the importance of this detector perturbation we used the Monte Carlo code MCNP [3] to calculate the neutron flux in a central cavity in polythene, carbon and A150 plastic counters having 3cm thick walls and irradiated with 15.5 MeV neutrons. These spectra are shown in Fig. 2, where they are compared with that in muscle. From this we see that there are differences  $\sim 10\%$  in the 15.5 MeV neutron flux per incident neutron at the cavity. At the low energy end the differences are larger; however, calculations using narrower energy intervals show that this difference is in very low energy neutrons ( $< 100$  keV). The differences calculated using NESTLES [4] in microdosimetric response for polythene (which showed the largest effect) is shown in Fig. 3, where we see that the shapes of the alpha particle and heavy ion components (arising from high energy neutrons) are identical, but that there are differences in the proton response. In Fig. 4 we see the corresponding figure for carbon where the differences are negligible. Note that if measurements are made in a body phantom (normally containing water as a tissue equivalent medium) then the polythene will give the least perturbation and carbon the most.

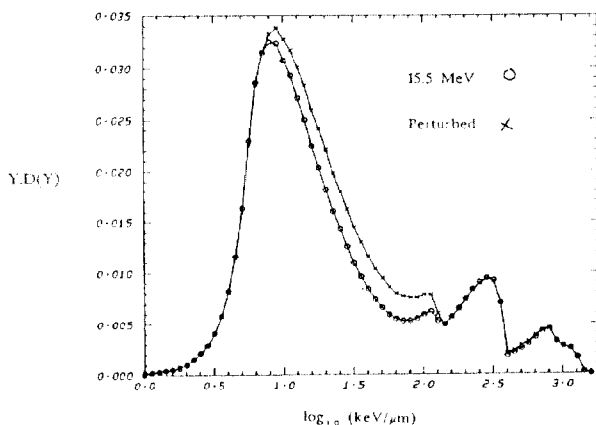


Fig. 3. Calculated microdosimetric response of a  $\text{CH}_2$  detector exposed to 15.5 MeV neutrons with and without perturbation.

Overall, these differences will limit the accuracy of the synthesis approach, but the magnitude of the limitation remains to be determined for in-phantom measurements, i.e. those of most relevance to neutron therapy.

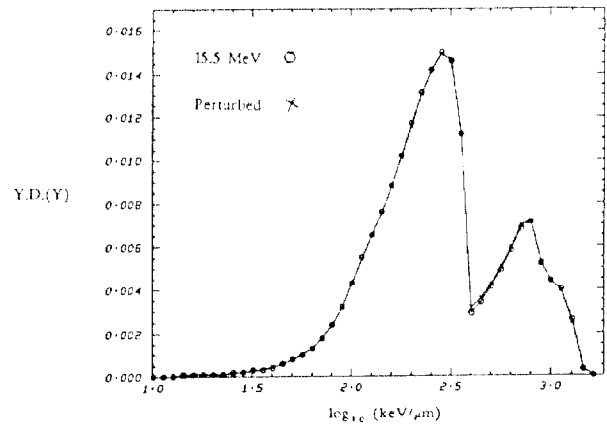


Fig. 4. Calculated microdosimetric responses of a carbon detector exposed to 15.5 MeV neutrons with and without perturbation.

### (b) Stopping power effects

The shape of the microdosimetric response from a given element will be affected by the energy dependence of the stopping power for each of the charged particle types involved. Thus, in order for the elemental synthesis approach to work the stopping powers of the different media involved have to have the same shape, noting that differences in magnitude can be accommodated using a linear scaling factor. The energy dependence of the ratios of the stopping powers for protons and alpha particles in polythene and carbon are shown in Fig. 5 where we see that the ratios are constant above a few MeV, and that the maximum difference ( $\sim 15\%$ ) occurs around the Bragg peak energies. Within the limitations imposed at low energies it is therefore possible to scale spectra for stopping power differences, as has been done when measuring elemental kerma factors [5].

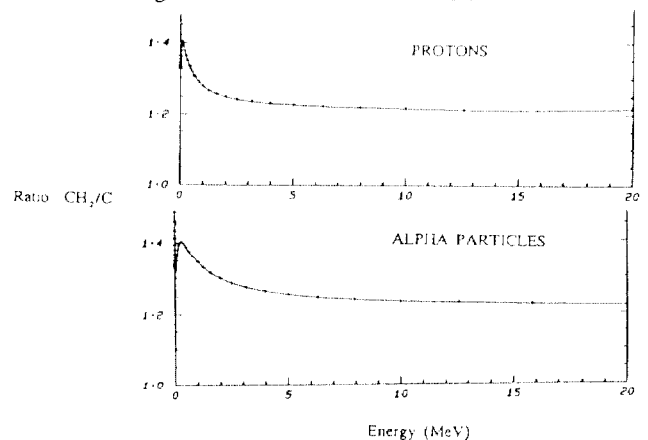


Fig. 5. Energy dependent stopping power ratios for protons and alpha particles in  $\text{CH}_2$  and C.

### (c) Gas events

Our own Monte Carlo code [6] has been used to calculate the gas events in different counters, an example of which is shown in Fig. 6, where we see that events produced in the filling gas contribute to the microdosimetric response above  $100 \text{ keV } \mu\text{m}^{-1}$  or so, and contribute typically 20% of the events. However, the fractions clearly depend on the gas, the gas pressure and on the wall materials. A combination of computation and experiment will be used to correct for this. Because the proportion of gas events is generally small, errors arising from these corrections should also be small, and less than other uncertainties [7].

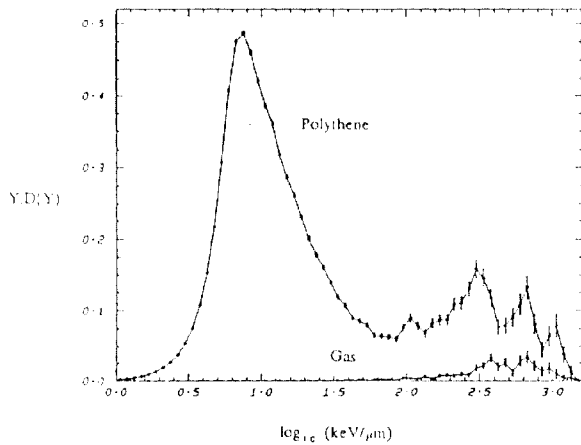


Fig. 6. Monte Carlo calculation of the microdosimetric response of a  $\text{CH}_4$  filled ( $2\mu\text{m}$ ) polythene counter exposed to 15.5 MeV neutrons

#### Experimental determination of the microdosimetric response of oxygen at 15.5 MeV

We have already noted the use of  $\text{CH}_2$  and carbon counters to determine the elemental microdosimetric response of hydrogen (see Fig. 1).

Using the pencil grid technique described elsewhere to provide a conducting cathode [2] we have built a cylindrical, 14 cm thick walled  $\text{Al}_2\text{O}_3$  counter with a central, spherical, cavity, and used this in conjunction with a 16 mm walled Al counter to determine the response of oxygen alone to 15.5 MeV neutrons. The spectrum from each detector is shown in Fig. 7 whilst the resulting oxygen-only response is shown in Fig. 8, where it is compared to that for a carbon counter. Interestingly we see that the shapes of the carbon and oxygen responses are similar.

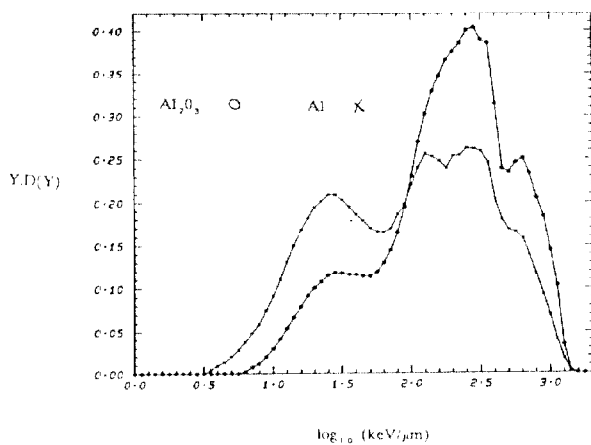


Fig. 7.  $Y.D.(Y)$  spectrum for Al and  $\text{Al}_2\text{O}_3$  microdosimeters exposed to 15.5 MeV neutrons.

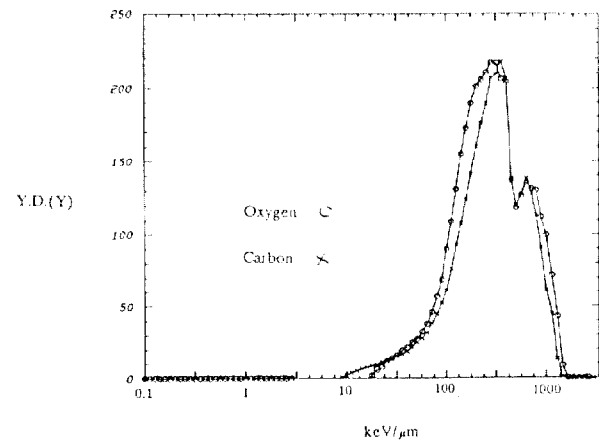


Fig. 8. Microdosimetric response of oxygen and carbon to 15.5 MeV neutrons.

#### Conclusions

We have examined the factors which affect the accuracy of our proposed elemental synthesis approach for determining real tissue microdosimetric responses. Of these, detector perturbation is likely to provide the greatest uncertainty. However, how the resulting uncertainties compare to with arising from the use of tissue equivalent plastic remains to be determined, the first step being to examine the importance of detector perturbation in in-phantom measurements, i.e. the measurement of greatest clinical interest.

#### Acknowledgements

The support of the Brazilian Government (CNPq) for A.C.A. de Aro, and the Clatterbridge Cancer Research Trust for the whole programme, is gratefully acknowledged, as is the interest and encouragement of the clinical, research and technical staff of the Clatterbridge cyclotron.

#### References

- [1] R.S. Caswell, J.J. Coyne, "Energy deposition spectra for neutrons based on recent cross section evaluators", Proc. Sixth Symp. Microdosimetry (1978) p1139.
- [2] S. Green, A.C.A. Aro, G.C. Taylor, M.C. Scott, "The development of microdosimetric detectors for investigating LET distribution in different body tissues" 1990 (in press).
- [3] "MCNP - a general purpose Monte Carlo code for neutron and photon transport" LA-7396-M (Rev) Los Alamos Monte Carlo Group, LA National Laboratory (1981).
- [4] A.A. Edwards, J.A. Dennis "NESLES - a computer program which calculates charged particle spectra in materials irradiated by neutrons", NRPB, M-43 (1979).
- [5] P.M. DeLuca, H.H. Barschall, Y. Sun, R.C. Haight, "Kerma factors of oxygen, aluminium, and silicon for 15 to 20 MeV neutrons", Rad. Prot. Dos. **23** (1988) 27-30.
- [6] G.C. Taylor "The prediction and measurement of microdosimetric spectra relating to neutron cancer therapy" Ph.D. thesis, University of Birmingham (1990).
- [7] G. Bühler, H.G. Menzel, H. Schuhmacher, G. Dietze, S. Guldbakke "Neutron kerma factors for magnesium and aluminium measured with low pressure proportional counters" Phys. Med. Biol. **31** (1986) 601-611.

# VERIFICATION OF NEUTRON DOSE DISTRIBUTION OBTAINED BY IRREGULAR SHAPED FIELDS AND MOVING BEAM THERAPY

K.H. Höver, B.M. Hesse, B. Rhein, W.J. Lorenz  
Deutsches Krebsforschungszentrum 6900 Heidelberg

## Abstract

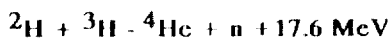
Monoenergetic 14 MeV d-t neutrons beams as used in the German Cancer Research Center suffer from some severe disadvantages, which would not be accepted in modern x-ray equipment. To overcome some of these shortcomings we improved the dose distribution by:

1. *weighted moving beam therapy*
2. *irregular shaped field sizes*
3. *multiple arc therapy*

Measurements of relative dose distributions for these techniques have been performed by the so called "Transfer Method". This is a combination of activating large aluminium foils and contact radiography.

## Introduction

The neutron therapy facility in use for radiation treatment at the German Cancer Research Center in Heidelberg is based on a high power d-t closed system neutron generator. Monoenergetic 14.1 MeV neutrons are produced by the exothermic deuteron-triton fusion reaction:



There is some evidence from clinical and radiobiological results that criteria like

- dose distribution per se
- ratio of treatment to target volume
- homogeneity of dose over the target volume

are more important in therapy with neutrons than with photons. Furtheron the size of the treatment volume seems to be a critical issue. It has been the aim of our investigations to improve the potential of our 14 MeV d-t neutron generator by more elaborate treatment techniques. From the above mentioned techniques, WMBT is now routinely used. In opposite to this irregular shaped fields and small field sizes for multiple arc therapy are in the experimental phase.

## Dosimetry

The use of calibrated A-150 plastic tissue equivalent (TE) ionization chambers with TE gas filling is recommended as dose measuring instrument by the neutron therapy groups. With these relative large tissue equivalent ionization chambers normally used in neutron dosimetry it is often not possible to measure dose distributions obtained by sophisticated treatment techniques. In photon therapy film densitometry often is used to overcome these difficulties. In neutron fields films cannot be used directly due to the high sensitivity to photons. However if neutron spectra and cross sections are known, then the fluence can be measured from the disintegration rate of radioisotopes originating from a neutron induced reaction and from this the Kerma can be calculated. For the determination of relative dose distribution we activated plates of aluminium and measured the activity distribution by contact radiography with low dose films. If pure aluminium is irradiated with fast neutrons the following reactions take place:

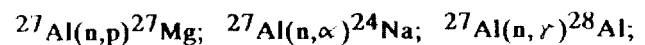


Table 1 shows some of the calculated quantities, beside the cross-sections also the correction factors relative to A-150 are given in the table. Al-28 has a half life of 2,3 minutes, so that after an appropriate waiting time there is no significant activity.

Depth	${}^{27}\text{Al}(n,\alpha){}^{24}\text{Na}$		${}^{27}\text{Al}(n,p){}^{27}\text{Mg}$	
	$\sigma$ [ $10^{-27} \text{ cm}^2$ ]	Correction Factors	$\sigma$ [ $10^{-27} \text{ cm}^2$ ]	Correction Factors
5 cm	90.2	1.0	61.2	1.0
10 cm	85.9	0.97	60.6	1.0
20 cm	81.3	0.94	59.7	1.01
Off Axis	55.0	0.80	47.2	1.03

**Weighted moving beam therapy(WMBT)**

Essentially "WMBT" is based on controlling the gantry position and the angular speed of the gantry continuously to deliver a prescribed dose per angle and to correct for unstable output. This technique presents both, the opportunity to fit the treated volume closely to the tumor volume and to realize a more homogeneous dose over the target volume. As a consequence the use of WMBT allows a higher dose to be concentrated in the target volume, while sparing the surrounding normal tissue. Figure 1 shows the measured dose distribution in a phantom obtained by WMBT.

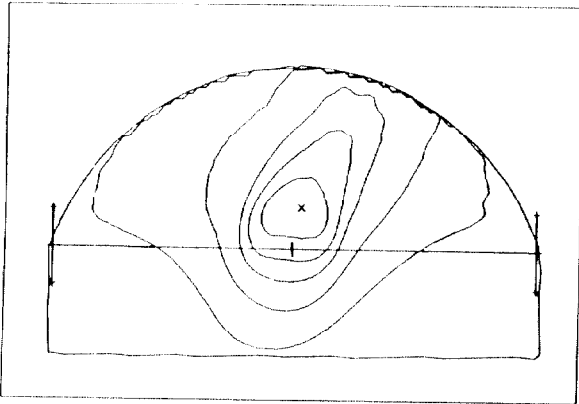


fig. 1 WMBT  
 Isodoses: 90; 80; 50; 30; 20 %  
 Arc: -90° to 90°  
 Weighted-Angle: +20° to +40°  
 Weighting-Factor: 2

"WMBT" is used routinely at our 14 MeV d-t therapy facility to treat patients with recurrent colorectal cancer (see figure 2)

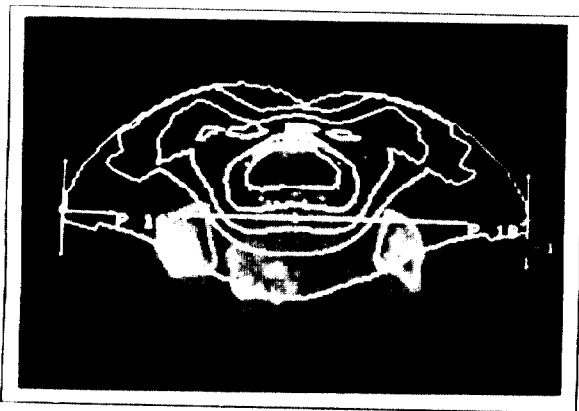


fig.2 showing isodose contours for "WMBT" irradiation of a recurrent colorectal adenocarcinoma

**Irregular shaped field sizes**

The differences between the response of whole tumors and parts of normal organs are reduced with high LET-radiation, so there is an increased need to achieve a high target to non target dose ratio. The technique of irradiation with irregular fields is becoming increasingly important.

We use shielding blocks from tungsten to reduce the dose in organs of risk and to match the dose distribution to the target volume. A thickness of 10 cm tungsten is need, to reduce the dose due to leakage neutrons to less than 20%. to investigate this technique in general we used a manual multi-leaf collimator wich enables us to do irregular field shaping in a more complex way. Figures 3 and 4 show neutron dose distributions obtained by secondary shielding with the multi leafed tungsten collimator. Measurements have been performed by the transfer method in a water phantom.

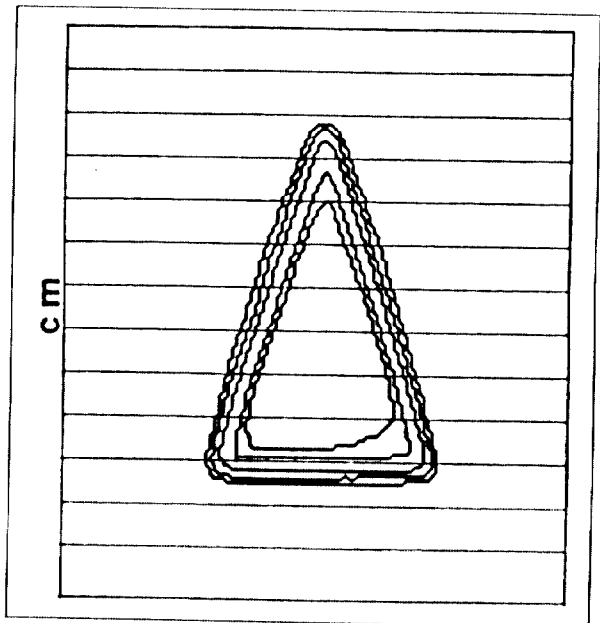


fig. 3 Isodoses: 90; 80; 50; 30; 20 %  
 TSD = 100 cm  
 Depth = 0 cm  
 P80-20 = 6 mm

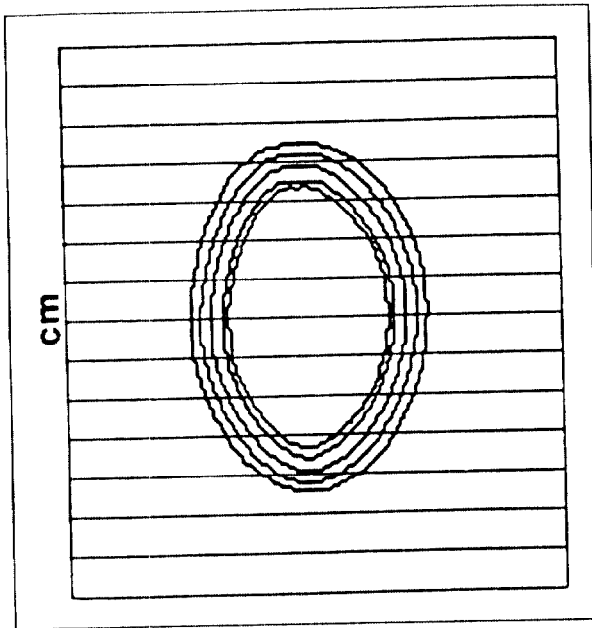


fig. 4 Isodoses: 90; 80; 50; 30; 20 %  
 TSD = 100 cm  
 Depth = 0 cm  
 $P_{80-20} = 6,5$  mm

### Multiple-arc therapy

Multiple non coplanar arc irradiation is a well known method for single high dose treatment in the brain (radiosurgery). It was our aim to investigate whether from the dose distributional point of view this technique can also be used for neutrons. For our investigations we used 24cm thick tungsten inserts with circular field sizes of 10mm to 35mm. Dose measurements have been performed in a tissue equivalent head phantom. The figures 5,6 and 7 show dose distributions in the axial, frontal and saggital cross-sections obtained by a number of 9 semicircular irradiations (arc = 160 degree), each followed by a movement of the treatment table of 22,5 degree.

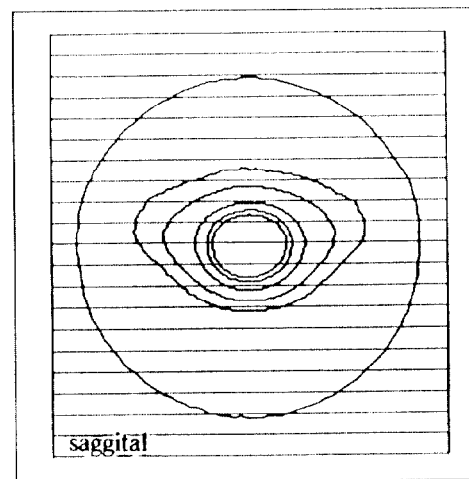
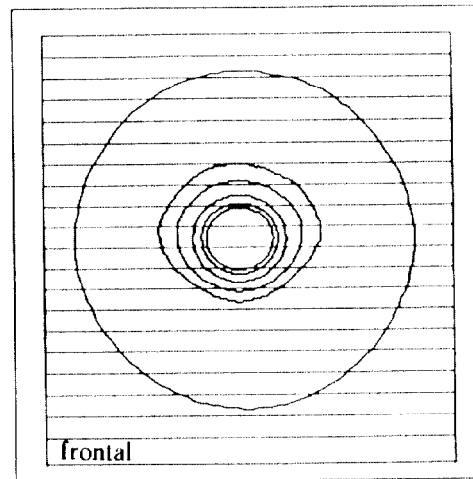
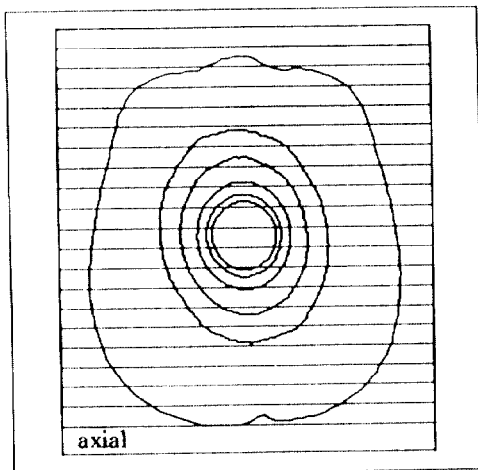


fig.5,6,7 Isodoses: 80; 70; 50; 30; 20 %  
 field size: 25 mm  
 arc: 160 degree  
 number of arcs: 9

### Conclusion

Due to radiobiological properties there is an increased need to improve physical selectivity when using high LET-radiations. The techniques presented allow the therapists to increase the ratio of target absorbed dose to non target dose. This will in certain cases probably reduce the complication rate. The obtained complex dose distribution can easily be measured by the Transefer method.

### References

1. M. Catterall, R.D. Errington, D.K. Bewley, F. Paice, S. Blake, "Observation of thirteen years fast neutron therapy" J. Eur. Radiother., p.5 1984.
2. K.H. Höver, W.J. Lorenz, H. Scharfenberg, W. Schlegel, "Treatment planning for external beam therapy with neutrons, Urban & Schwarzenber, München-Wien-Baltimore, pp 111-122, 1981



**Sensitivity of cultured human carcinoma cells to very high LET particle irradiation : no correlation to low LET radioresponse.**

M.Flente, M.Scholz<sup>2</sup>, M.Wannenmacher

Dept. of Radiology, Univ. of Heidelberg, and Sect. of Radiobiology GSI, Darmstadt<sup>2</sup>, FRG

Response to Low-LET irradiation is determined by a complex interaction of primary lesions (presumably DNA-strand breaks) and repair/misrepair-processes (8). This leads to the typical shouldered dose response in mammalian cells systems, which can be well described by a linear quadratic term. Different cell lines vary especially in their shoulder characteristics, which is thought to reflect differing capacities in accumulating (and repairing) sublethal damage (2). Recovery is decreasing with increasing LET (1), as the number of direct effects and unreparable lesions gets larger.

In the biological pilot phase of the heavy ion clinical project at Heidelberg/ Darmstadt we started experiments comparing sensitivity parameters of established in vitro cell lines for Low-LET <sup>60</sup>Co-rays and 13.4 MeV Argon particles of the Unilac at the GSI in Darmstadt.

## MATERIALS AND METHODS

The **human tumor cell lines** (caski, mri-186, hela : cervix-carcinoma lines, tx-i : lung, widr : colon; Courtesy Tumorbank German Cancer Research Foundation) are mainly recently established and of low passage number. T-1 (human kidney) and V-79 (hamster fibroblasts) are in regular passage at the GSI. Plating efficiency ranged between about 11% (MRI-186) and 80% (V79) in monolayer culture. The cell cycle time (BcUrd-Method) is between 11 (V-79) and 26 (MRI-186) hours.

Cells are cultured in 50 ml cell culture flasks (Falcon) in MEM Dulbecco Medium (Biochrom), FCS 15% and Glutamin (Serva)

at a CO<sub>2</sub> concentration of 5.5%.

Irradiation was carried out at a <sup>60</sup>Co-Gammatron (240 cGy/min)

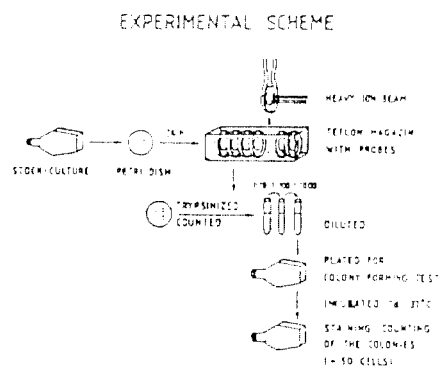
and at the UNILAC for heavy particle experiments at ambient temperature. The setup for heavy particle irradiation has been described before (6).

**Cell survival measurements:** For particle irradiation cells are trypsinized and centerplated in petri dishes 24 hr before treatment at a concentration of 10<sup>5</sup> cells per dish to guarantee homogeneity. For exposure to the particle beam, the samples are stored in a magazine and lifted mechanically for a controlled time into the beam path. Dose is monitored on line. After exposure, the cells are harvested by trypsinization, counted and diluted and plated in triplicate into Falcon-TC-flasks according to expected survival to give a colony number of about 50 to 100 colonies / flask. Cells are incubated

for 10 to 12 days to allow for progression delay at higher doses and colonies are stained with cristaviolet. Aggregates of more than 50 cells are scored as colonies. Survival curves are fitted using exponential least square regression. (Fig. 1)

A more simple procedure can be used for <sup>60</sup>Co-irradiation. The cells are plated in triplicate into TC-flasks at appropriate cell numbers 12 to 24 hours before treatment. At the time of treatment a point 0 control is fixed for multiplicity correction.

After 10 to 12 days colonies are counted. Survival curves are fitted using the linear quadratic algorithm.



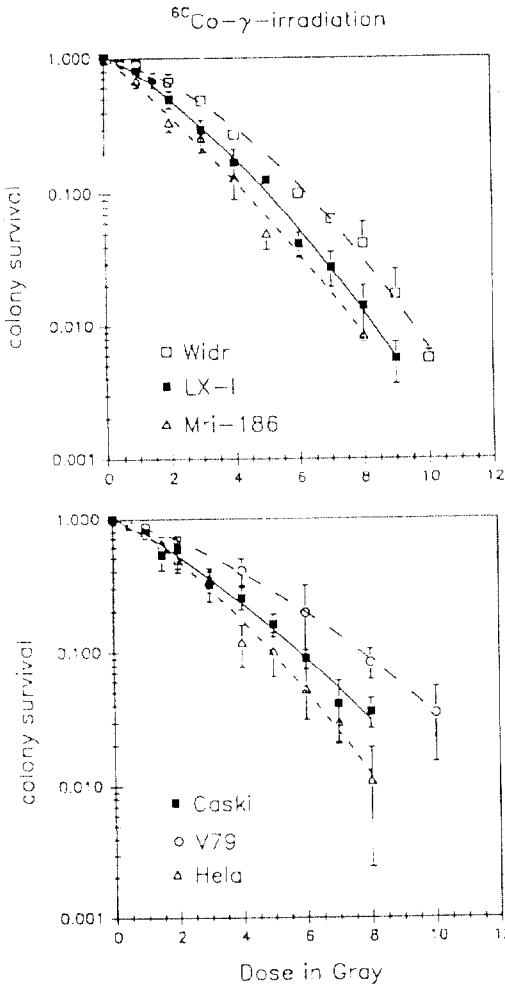
**DNA-ploidy :** cells are removed from petridishes by EDTA/ Trypsin. Trypsin action is stopped with FCS 15%. Cells are fixed with ethanol 70% at 4<sup>0</sup> C for 30 min. Single cell suspensions are prepared by drawing through 27g needles.

Analysis of **DNA-Distributions** is done using DNA-staining by RNase/ Propidium Iodide (60ug/ml) and a FACScan (Becton Dickinson) or Hoechst 33258 and a PHYWE ICP 22.

Relative DNA content (DNA-index) of the respective G<sub>1</sub>-peaks was determined in comparison to peripheral human blood lymphocytes for the human lines and mouse spleen cells for V-79 cells.

## Results

Fig.2a + b shows the typical shouldered dose response of the different cell-lines to Low-LET <sup>60</sup>Co irradiation. Considerable differences are observed. For a single dose exposure survival at 2 Gy ranges between 0.73 (V-79) and 0.42 (MRI-186). Linear quadratic fitting gives alpha/beta Quotients between 22.4 (MRI-186) and 5.8 Gy (WiDr). D<sub>37</sub> varies between 1.47 (MRI-186) and 2.05 Gy (Caski). These data are consistent for human carcinomas cell lines (3).



Inactivation cross section (Argon) <-> survival at 2 Gy (<sup>60</sup>Co)  
 R-value : 0.48

Inactivation cross section (Argon) <-> D<sub>37</sub> (<sup>60</sup>Co)  
 R-value : 0.02

Inactivation cross section (Argon) <-> /β quotient (<sup>60</sup>Co)  
 R-value : 0.23

Inactivation cross section (Argon) <-> DNA-index (Flowcytometry)  
 R-value : 0.98

Irradiation of these cell-lines with Argon (13.4 MeV particles) give a purely linear logarithmic dose response relationship for clonogenic survival at fluences between 0.5 to 7 x 10<sup>6</sup> particles /cm<sup>2</sup>. At the energy used this means exposure of the cell monolayer to the Bragg peak of the particle path at an LET of around 950 keV/ and a statistical probability of one hit/nucleus at a fluency of about 0.5 to 1.3 x 10<sup>6</sup> /cm<sup>2</sup>. Dose is given as particle fluence per area to allow better for the rather discrete dose deposition of heavy particles with a linear correlation between fluence and absorbed volume dose measured in Gray. Sensitivity is expressed in cross sections . Cross sections are derived from the D<sub>37</sub> and measure the probability for a certain biological effect, for instance inactivation of clonogenicity. They are given as an area and can be related to a target size.

Dose response curves after argon irradiation for three cell lines are shown in Fig.3. Also with high LET-particle irradiation differences in sensitivity are seen between the cell lines studied. Variation in cross sections ranged between 50 (least sensitive, V-79) and 90 μ<sup>2</sup> (T-1) To compare Low- and High-LET sensitivity of the cell lines regression analysis was done. There was no convincing relationship between sensitivity to Argon 13.4 MeV and parameters of the low-LET dose response curve.

However a close correlation between sensitivity to argon irradiation and relative DNA-content of the cell-lines was observed. With increasing DNA- content (ploidy) there was an increase in sensitivity to heavy particle irradiation.

### **Discussion**

The cell-lines used show a considerable variation in sensitivity to low-Let irradiation and thereby represent the range regularly observed in radiobiology (3). The differences in dose response are attributed to differences in repair capacity (9).

Also with Argon irradiation considerable differences in sensitivity were seen between the cell lines with a maximal dose modification factor for inactivation cross section of 1.9 between the least and most sensitive lines. Clearly this does not relate to repair, as the dose response for heavy particles is purely linear logarithmic for all lines implying no detectable impact of repair. This is supported by studies on split dose recovery (4).

Correspondingly, there was no correlation between Low-LET and High-LET sensitivity.

However, we could establish a close positive correlation of sensitivity to Argon ions with DNA-Index. DNA-Index is the relative measure of stemline DNA-content and ploidy, respectively.

This is in contrast to Low-LET response, where an increase in ploidy confers a decrease in radiosensitivity. This was explained by an increase in gene copies, which could compensate circumscribed chromosomal damage (5,7). The contrary findings for heavy particle irradiation stress the importance of geometric parameters. The dose distribution is highly inhomogeneous under a microdosimetric view due to the "grainy" nature of particles, however the inactivation probability of the traverse of a single particle through a cell nucleus is between 0.5 and 1 considering Poisson statistics and the nuclear size distribution of the cell population. This makes target area (reflected in DNA-index) the major parameter of influence for sensitivity to heavy particles in the energy range studied up to now at the Unilac. Further studies using the high beam of SIS will establish whether this phenomenon holds true also in for higher energies and lower LET's. This certainly would be of interest in clinical treatment of aneuploid tumors.

### **References :**

- [1] **Barendsen GW :**  
Response of cultured cells, tumors and normal tissues to radiations of different linear energy transfer.  
*Cur.Topics Radiat.Res.Q.* (1968) 4, 293-355
- [2] **Elkind MM; Sutton H :**  
Radiation response of mammalian cells grown in culture.  
*Radiat.Res.* (1960) 13: 556-593
- [3] **Fertil B; Malaise E :**  
Inherent cellular radiosensitivity as a basic concept for human tumor radiosensitivity.  
*Int.J.Radiat.Oncol.Biol.Phys.* (1981) 7: 621-629
- [4] **M.Flentje, J.Bühler, M.Scholz, M.Wannenmacher**  
Split dose potentiation after heavy particle irradiation in a human squamous carcinoma cell-line.  
*Proceedings of the Intern. Heavy Particle workshop. at the PSI.(Paul-Scherrer Institut Villigen) 18-20.9.89*  
Ed.: H. Blattmann in press 8/90
- [5] **Hamilton L :**  
A comparison of the X-ray sensitivity of haploid and diploid zygotes of *Xenopus laevis*.  
*Radiat.Res.* (1967) 30 : 248-260
- [6] **Kraft G :**  
Radiobiological effects of very heavy ions : Inactivation, induction of chromosomal aberration and strand breaks.  
*Nuclear Science Applications* (1987) 3, 1-28
- [7] **Radford IR, Hodgson GS :**  
Effect of ploidy on the response of V79 cells to ionizing radiation.  
*Int.J.Radiat.Biol.* (1987) 51: 765-778
- [8] **Tobias CA, Blakeley EA, Ngo FQH**  
The repair-misrepair model of cell survival.  
in : Pirucello M, Tobias CA: *Biological and Medical research with accelerated heavy ions at the Bevalac 1977-1980.*  
LBL-11220 UC-48 (1980= S.137-146
- [9] **Weichselbaum RR, Dahlberg W, Little JB Ervin TJ, Miller D, Hellman S, Reinwald JG :**  
Cellular X-ray repair parameters of early passage squamous cell carcinoma lines derived from patients with known responses to radiotherapy.  
*Br.J.Cancer* (1988) 48: 235-242

**PATTERNS OF CELL DEATH AND ABORTIVE COLONY FORMATION IN TWO PRIMATE CELL LINES IRRADIATED WITH NEUTRONS,  $\gamma$  RAYS AND THEIR COMBINATIONS.**

By John Calkins\*, Mohammed Kunhi\*, Nazma Hannan\* and William Greer\*\*

\*Department of Biomedical Physics and \*\*Department of Biomedical Statistics and Scientific Computing, King Faisal Specialist Hospital and Research Centre, P.O. Box 3354, Riyadh 11211, Saudi Arabia.

**ABSTRACT**

The ability of gamma irradiation to reduce the lethality of selected doses of neutron exposures has been reported in a previous publication [1]. There are alternative explanations of how the reactivation of neutron killed cells may be achieved. If gamma irradiation recruits non-dividing cells into the population at risk then combinations of neutron and gamma exposures could improve the apparent survival over neutron exposures alone. Analysis of the patterns of abortive colony formation in unirradiated populations and with various combinations of neutron and gamma irradiations suggest that the gamma action is through an improved repair of neutron killed cells in accord with the previously proposed damage-induced-repair (T repair).

**INTRODUCTION**

While some mammalian cell lines produce a colony of cells for almost each single cell plated, this is the exception rather than the rule. Cells given radiation doses which prevent indefinite reproductive survival often divide a few times before ceasing division [2] and thus form what are termed "abortive colonies". The incidence of abortive colonies with various number of cells per clone has been investigated in both irradiated and control cells. It has been observed that certain radiation doses lead to more surviving colonies than were observed with unirradiated control cells [3]. The number and nature of abortive colonies following irradiation with neutrons, gamma rays and combinations which lead to the "reactivation" of non-colony forming cells has also been observed [1].

**METHODS**

Culture, irradiation and assay

The details of culture, irradiation, and counting of surviving colonies were as described in Calkins et al [1]. In brief, we studied two primate cell lines, Vero a monkey line and I 407 a human line. Log phase cells were trypsinized for seeding the experimental flasks, irradiated (with fast neutrons or Co  $\gamma$  rays) in suspension and plated at 1000 cells per T75 flask with 3 replicate flasks at all radiation doses and 6 flasks for unirradiation controls. The cultures had been in continuous logarithmic growth for many months before the experiment and the plating efficiency (PE) was relatively stable.

For colony forming ability, using a dissecting microscope, one observer scores an entire experiment for survival (clone of > 50 cells), marking each colony as it is counted. Then, for abortive colony assay, also using a dissecting microscope, the flasks previously classified for colony formation are counted for abortive colonies by different individuals. The minicolonies are counted by cell number marking each minicolony by color code as it is counted. In many cases it is evident that the plated cell and its progeny underwent a precise number of divisions producing colonies of 2,4,8 etc. cells, but more often it is evident that daughter cells may undergo slightly variable numbers of divisions producing minicolonies of 14-24 cells rather than precisely 16 cells. Clones have been classified by number of divisions; considering the variability of division in daughter cells in abortive colonies the groupings indicated in Table 1 have been made.

Table 1

Cells per Clone	1	2-3	4-6	7-12	13-24	25-29	>50
Average	0	1	2	3	4	5	>5 = survivors
Divisions							

Analysis and Data Presentation

In all cases, dilutions of cell suspensions were made to supply 1000 cells per flask. Statistical fluctuation will occasionally produce more than 1000 clones per flask which leads to a negative number of "missing" clones which is difficult to represent. Two presentations were used: 1) linear scale bar graphs of the numbers of clones in each category and 2) logarithmic scale bar graphs of the number of clones in each category which provides a "spectrum" of the clone distribution. While it is much easier to see that a small gamma ray exposure has increased the average survival and reduced the number of missing clones in the linear plot, the logarithmic plot provide a clearer view of the behaviour of each of the abortive colony categories which is the central focus of this paper.

**RESULTS**

Unirradiated Control Cell Responses

The two lines we have investigated differ regarding abortive colonies in control cultures. The Vero line control flasks shows minicolonies which added to the surviving colonies usually equal  $\approx$  950 cells, with only about 5% missing. The observations are compatible with no lysis of plated cells: the 5% unaccounted clones could have been confluent single cells or minicolonies (too close to other colonies to be resolved) plus variations in the number of cells inoculated.

In the I-407 line there were relatively few abortive clones at the standard time for scoring the flasks. Most of the non-surviving I 407 cells had evidently lysed prior to scoring and only a small percent < 10% of the non-surviving unirradiated cells formed persisting abortive colonies at the time of scoring while the Vero cells plated were essentially all accounted for in survivors and minicolonies.

$\gamma$  irradiated cell response

In the Vero line (data not shown) doses up to the "step" level increase survival, increase slightly the number of clones in most of the various categories of abortive division and, reduce the "missing" category. Progressing to doses above the step, survival falls steadily with increasing dose and the missing category rising correspondingly. Only at 5-6 Gy is there a progressive reduction of the 4 and 5 division abortive colonies while the 0-3 groups still contain more clones than the unirradiated control flasks. The gamma response of the cell I 407 line is shown in two panels (Fig. 1), the first showing doses up to the "step" [3] and the second panel illustrates the effect of doses above the "steps". The I 407 line (Fig. 1) shows the same trends as the Vero line. Survival and abortive colonies increase up to the step dose level; above the step, survival falls and the missing cells rise but abortive colonies in the 0-3 category increase with dose. Only the highest dose (6.9 Gy) reduces the 5 division category from the step value. Even at the highest doses there are many more abortive colonies in all categories than in the unirradiated controls.

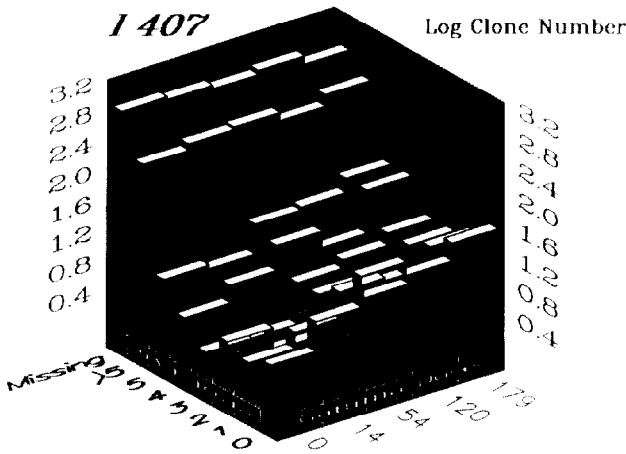


FIG. 1. THE LOGARITHM OF THE NUMBER OF CLONES OF I 407 AS A FUNCTION OF AVERAGE NUMBER OF DIVISIONS AND GAMMA DOSE IN cGy. RESPONSE DOSES UP TO THE "STEPS" (179 cGy) ARE PLOTTED IN THE UPPER PANNEL, DOSE ABOVE THE "STEP" IN THE LOWER PANNEL.

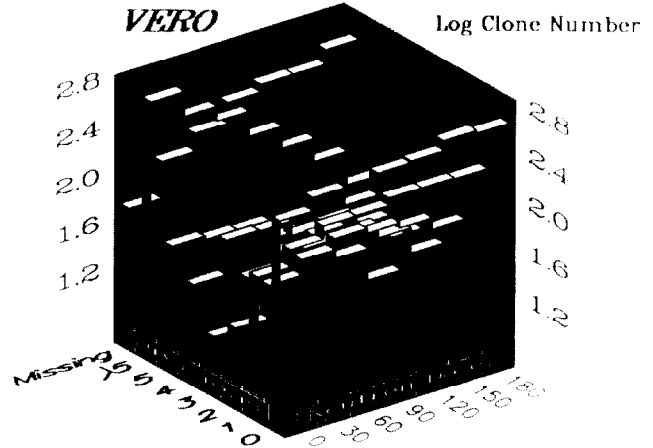
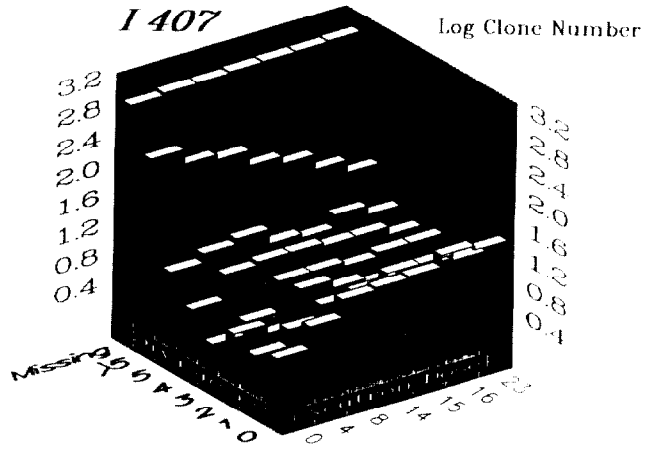
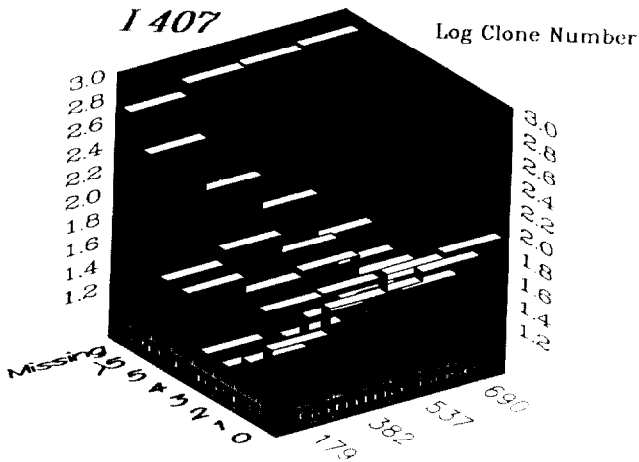


FIG. 2. THE LOGARITHM OF THE CLONES AS A FUNCTION OF AVERAGE NUMBER OF DIVISIONS AND NEUTRON DOSE IN cGy FOR THE TWO CELL LINES.



Neutron Response

The effects of neutron irradiation on abortive colony formation (Fig 2) differs somewhat in the two cell lines; it is also quite distinct from the patterns observed after the low LET ( $\gamma$ ) exposure. In both lines there is no distinct transition in response such as was noted at the "step" in the  $\gamma$  response.

The Vero line shows a simple progression of response; a decrease in survivors and large clones is compensated by increases in missing and small clones. Clones in the 5 division category and survivors (>5) show a progressive reduction with dose; clones in the 2-4 categories rise in numbers at low doses but then progressively fall with increasing dose; the missing, 0, and 1 division categories increase progressively with dose. The I 407 response to neutrons is similar to the Vero for survivors and for the missing 0 and 1 division categories (survivors falling compensated by progressive increases in the missing 0 and 1 categories). Exposure to neutron doses from 0.6-1.8 Gy causes a small increase in clones in categories 2-5 over control levels, an increase which remains approximately constant regardless of dose.

Response to Neutron -  $\gamma$  Combinations

Gamma reactivation of neutron killed Vero cells (data not shown) is evident in these experiments and in many other experiments not reported here; however combinations of neutron plus gamma exposures do not improve survival in all combinations. Cells treated with neutron doses of 0.3 Gy are in general the most likely to be reactivated; cells exposed to neutron doses of 0.6 Gy are more likely to show enhanced killing with added  $\gamma$  exposure. At neutron doses where survival was improved (0.3 and 1.8 Gy N) the number of abortive colonies tended to be increased; when neutron and gamma combinations reduced survival (1.2 Gy N) the overall number of abortive colonies was reduced.

In the I 407 line small gamma doses were more uniformly effective in improving the survival in neutron exposed cultures (Figure 3). In all cases the addition of gamma to neutron exposure increased the abortive colonies over the numbers seen with neutron alone (data not shown). Aside from the relative effectiveness, the trend of the response to neutron-gamma combinations was much the same in the two cell lines.

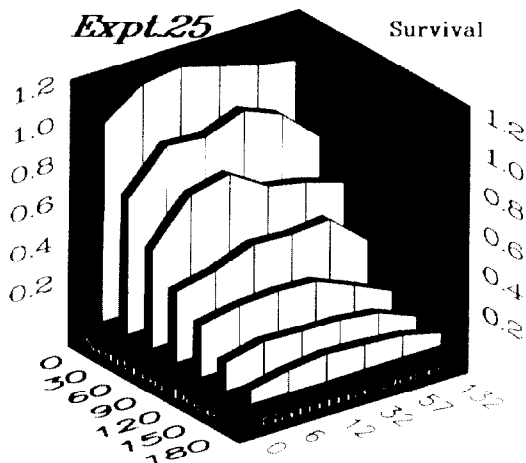


FIG. 3. THE SURVIVING FRACTION (RELATIVE TO UNIRRADIATED CONTROL CULTURES) AS A FUNCTION OF COMBINED NEUTRON AND GAMMA DOSES IN cGy FROM A TYPICAL I 407 EXPERIMENT.

#### DISCUSSION

It is evident that the responses of these two cell lines are very complex. The cell lines differ in significant details of response even in unirradiated control cultures with non-surviving Vero clones tending to form minicolonies while I 407 showing early lysis of non-survivors. However, there are clear similarities of responses to radiation in the two lines. In both lines certain  $\gamma$  doses can increase the survival of unirradiated cells. This improvement in survival comes at the net expense of what would seem to be the least viable cells, i.e., those that lyse before scoring. Neutron irradiation tends to reduce survival by increasing early lysis. The " $\gamma$  reactivation" of neutron killed cells increases survival by reducing early lysis in both lines;  $\gamma$  exposure also tends to increase the number of abortive colonies (data not shown).

It must be emphasized that the trends noted here, although reproducible, occur at specific and critical dose levels. There are changes in the pattern of response; above 1-2 Gy  $\gamma$  rays produce early lysis as neutrons do beginning at the lowest dose (0.3 Gy). The observations noted here in general fit a pattern suggested by Calkins in 1967 [4] of induced repair where the character of response abruptly changes as the threshold of repair induction is crossed. To adequately understand radiation response, the thresholds for repair induction must be recognized along with the nature of the mechanisms of repair of DNA damage. Lethal but repairable damage can arise from radiation but also seems to develop in cell cultures in the natural course of subculturing of established lines, thus leading to the capacity of small (presumably repair inducing) doses of irradiation to improve the PE of irradiated cells over unirradiated cultures [3]. Radiation should be recognized as a complex and mixed agent, sometimes beneficial, in other circumstances very harmful. The patterns of abortive colony formation noted above are clearly different from our original expectations. A working hypothesis is proposed below which rationalizes many of the puzzling observations reported here.

Although a large and continual loss of reproductive cells is typical of tumors, cell cultures with a small growth fraction (low PE) are not widely used for radiobiological research. The disappearance of 50-80% of our cells from the growing population is too high and regular to believe that the missing cells arise from erratic random injuries particularly when it appears that many of the missing cells can be returned to the proliferating population by a treatment with low levels of ionizing radiation [3].

We postulate that low doses of  $\gamma$  radiation can return cells which would die and lyse (I 407) or fail to divide (Vero), into the viable population. This is attributed to some form of induced repair, and the induced repair is able to correct damage inflicted by neutrons thus leading to "reactivation" of neutron killed cells. The reactivated population arises from the least viable (lysing or non dividing cells) and not from the abortive colony formers. In fact in both cell lines the number of abortive colonies is increased not decreased by the gamma reactivation (induced repair). Since induced repair is a threshold phenomena, full comprehension and control of neutron therapy will require understanding of the nature and location of thresholds for inducing repair processes.

#### REFERENCES

- [1] J. Calkins, W. Harrison and M. Einspinner, "Reactivation of neutron killed mammalian cells by gamma irradiation: The observations, possible mechanism and implication, Strahlentherapie und Onkologie, Vol 166, pp 22-25, 1990.
- [2] M.M. Elkind, A. Han and K.W. Volz, "Radiation response of mammalian cells grown in culture. IV. Dose dependence of division delay and postirradiation growth of surviving and non-surviving Chinese hamster cells", J. of the National Cancer Institute, Vol 3, pp 705-721, April 1963.
- [3] J. Calkins, M. Einspinner, D. Blocher and W. Greer, "Response of two mammalian cell lines to low gamma ray doses", International Journal of Radiation Biology, Vol 56, pp 869-875, 1989.
- [4] J. Calkins, "An unusual form of response in X-irradiated protozoa and a hypothesis as to its origin", International Journal of Radiation Biology, Vol 12, pp 297-301, 1967.

**VARIATION OF RELATIVE BIOLOGICAL EFFECTIVENESS WITH DEPTH OF  
KFSH NEUTRON THERAPY BEAM CALCULATED FROM THE LET SPECTRUM**

By F. Mahyoub\*, M. Obeid\*\*, J. Calkins\*, A. Kadachi\*\*, and A. Waheed\*\*

\*Biomed. Physics Dept., King Faisal Specialist Hospital & Research Centre, POB 3354, Riyadh 11211; \*\*Electrical Engineering Dept., King Saud Univ., POB 800, Riyadh 11421, Saudi Arabia

**ABSTRACT**

The LET distribution of neutron therapy beam produced by KFSH cyclotron (Cs-30) was measured using a low-pressure tissue-equivalent (Rossi) proportional counter. The measurements were made in air and at various depths and lateral distances in a water phantom. Using published RBE-LET relationships for 3 levels of survival, predictions of the effective RBE variation of our beam with depth and near the beam edges were made. It was observed that the effective RBE at the 80% survival level was about 3.5, a value approximating the therapeutic value used and in good agreement with some biological measurements using this neutron source.

**INTRODUCTION**

Fast neutron radiotherapy became available at the King Faisal Specialist Hospital and Research Centre in 1984, a p,n. neutron facility, and was previously described by Barral et al.[1]. Fast neutron therapy has advantages over conventional photon or electron radiation in the treatment of certain types of tumors such as salivary gland tumors, prostate tumors, soft tissue sarcomas, and others [2]. Dosimetry for clinical neutron therapy requires the specification of absorbed dose and the Relative Biological Effectiveness (RBE) which is related to the radiation quality of the beam used. The absorbed dose alone is not sufficient for the description and understanding of radiation quality because it reflects the average energy deposited in tissue, whereas biological effectiveness is due to the spectrum of local energy deposition in small, sensitive sites such as a cell or its subcomponents. Energy deposition in such a small volume may show considerable statistical fluctuation, which must be accounted for by an as yet undefined theory relating radiation quality to biological action. Therefore, the spatial distributions of absorbed dose and of radiation quality with tissue depth and with lateral distance from the beam axis are relevant factors in fast neutron therapy.

The RBE of the beam just outside the edge of the field is a most important observation since field edges are often placed to protect critical organs and since the field edge is not perfectly sharp, there may be significant dosage 1-2 cm from the beam edge, and the RBE at the beam edge could, due to neutron scattering, be significantly higher than in the geometrical field. Also, a precise description of the spatial distribution of radiation quality (LET spectrum) is the first step which can then be combined with published data on RBE vs. LET to give an estimation of the spatial variation of RBE within the treatment volume, eventually leading to a proper biologically based theory of neutron therapy.

A tissue equivalent proportional counter was used to determine the LET distribution of collimated neutron therapy beam. The measurements were performed in air and in water phantom to determine microdosimetric spectra at different depths on the axis and near the neutron beam edges. RBE-LET relationships for 1%, 10% and 80% survival combined with the microdosimetric spectra were used to compute the spatial variation of effective RBE in the water phantom (and in air outside the phantom).

**EXPERIMENTAL METHODS**

The therapeutic neutron beam was produced by bombardment of a beryllium target with 26 MeV protons produced by the Cs-30 cyclotron of KFSH; a lithiated polyethylene filter 4 cm thick, was used which "hardened" the neutron beam to an average energy of 11 MeV. The water phantom (water in an open lucite cube) had dimensions of 40.0 cm x 40.0 cm with 20 cm deep water was placed at 120.0 cm distance from the target, roughly simulating a head & neck patient. The field size at the surface of the phantom was 10.0 cm x 10.0 cm. A spherical tissue equivalent proportional counter (Far-West Technology) with an inside diameter of 1.27 cm (0.5 in.) filled with a tissue equivalent gas-mixture of 28.8% CO<sub>2</sub>, 2.75% N<sub>2</sub> and 67.54% CH<sub>4</sub> at a pressure of 5.63 cm Hg was used to simulate a tissue sphere of a diameter of 1  $\mu$ m. [3].

The proportional counter was calibrated with an internal 244 Cm source, alpha energy 5.80 MeV, and average stopping power of 81.7 KeV  $\mu$ m<sup>-1</sup> in tissue [4]. The electronics of the measurement system was composed of several ORTEC modules, including a 126 Preamplifier, 472 spectroscopic amplifier, and 2048 channel MCA. The energy deposition spectra for each spatial position constituted four subspectra measured with different gains. Following the procedure described in ICRU Report No. 36 on Microdosimetry [5]. The gains were chosen so that any two neighboring spectra had sufficient overlapping region that they could be matched to give the spectrum over a wide range.

**Analytical Methods**

The analysis of data was done by a computer code called MICDOSE using similar algorithm as used by W.H. Grant et al.[6] and H. Heintz, et al.[7] in computer codes ANALET and EVENT, respectively. The main steps of this code are the calculation of even size distribution  $P(Y)$ , after joining at the different subspectra. The relative dose distribution  $D(Y)$  and the dose weighted distribution  $YD(Y)$  vs.  $Y$ , where  $Y$  is the lineal energy in KeV  $\mu$ m<sup>-1</sup> was derived from the  $P(Y)$  distribution and normalized to have integral dose equal to unity. The MICDOSE code also calculates the Relative Biological Effectiveness RBEs for each point by using the values of RBE extracted from the three survival curves (1, 10, 80%)[8] and the values of  $YD(Y)$  distribution.

**RESULTS**

The microdosimetric spectra of the neutron therapy beam were measured on the central axis at four depths: 0.5, 5, 10 and 15 cm in our water phantom. Also, the spectra were measured at four lateral distances: 5, 6, 7 and 9 cm for each depth. Similar measurements were done at one distance from the target in free air for the purpose of comparison.

Fig. 1 represents the variation of  $YD(Y)$  vs.  $Y$  along the beam axis for different depths in the water phantom. While there is a large reduction of intensity over this range, the changes in LET spectrum are quite small. A small decrease in  $YD(Y)$  with depth is observed in the high energy (~10 KeV/ $\mu$  proton region of the spectra, while the low energy proton (50 -100 KeV/ $\mu$ ) component falls more (i.e. the beam hardens with depth). Corresponding to the beam hardening, the a component (100 - 500 KeV/ $\mu$ ) also increases.

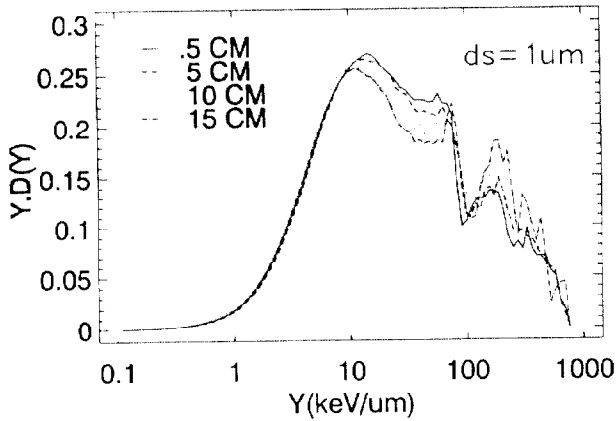


FIG. 1 MICRODOSIMETRIC SPECTRA MEASURED IN THE BEAM AXIS IN WATER PHANTOM FOR DIFFERENT DEPTHS

Fig. 2 represents YD(Y) vs. Y variation at the different distances off beam axis for .5 cm depth in the water phantom. In the beam, the same phenomena is observed as in Fig. 1, but outside the beam edges, the decreases in high energy proton region with depth becomes more important and YD (Y) near the proton edge increases significantly for all depths due to the relative importance of scattered neutrons which produce more high LET (low energy) recoil protons.

In the beam, the microdosimetric spectra for all depths have much the same features as at the 10 cm depth with only slight variations. However, a marked increase YD (Y) is observed outside of the beam near the proton edge (80 KeV/μ).

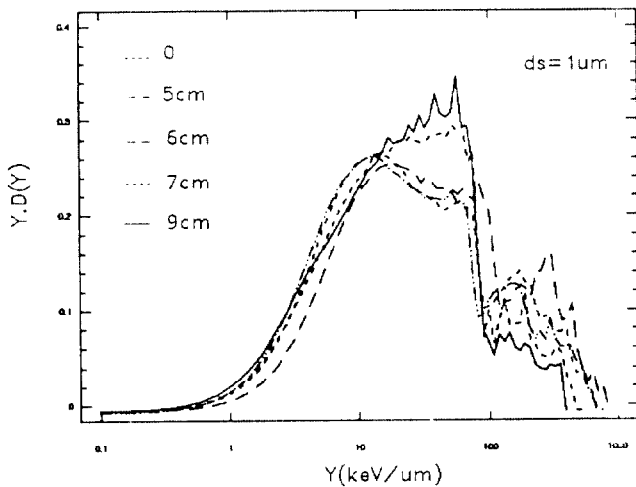


FIG. 2: MICRODOSIMETRIC SPECTRA AT 0.5 CM DEPTH IN WATER PHANTOM FOR DIFFERENT DISTANCES OFF BEAM AXIS

Fig. 3 represents a typical RBE x YD(Y) vs. Y on the beam axis at 0.5 cm depth in the water phantom for 1, 10 and 80% survival. Also, YD(Y) vs Y is included in the plots for comparison purposes.

Table 1 represents the values of  $Y_D$ , the mean lineal energy dose for all spectra at the different spatial position.

Table 2 represents the calculated values of the effective RBE for all microdosimetric spectra at the different spatial position at the 3 chosen survival levels.

Table 3 shows the dose rates at the points corresponding to the location of the YD(Y) values measured.

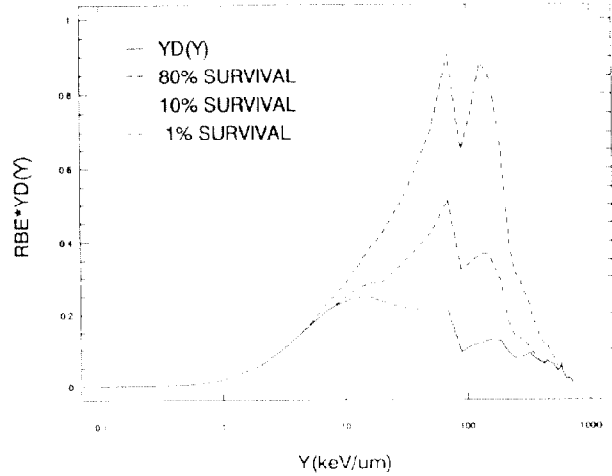


FIG 3 RBE\*YD(Y) VS Y IN THE BEAM AXIS AT .5CM DEPTH IN WATER PHANTOM

TABLE 1. VARIATION OF RELATIVE BIOLOGICAL EFFECTIVENESS FOR DIFFERENT SPATIAL POSITIONS (cm) IN WATER PHANTOM AND IN AIR.

LAT. DIST.	0.00	5.00	6.00	7.00	9.00	CELL SURVIVAL
DEPTH						
0.50	3.51	3.59	3.72	3.88	3.97	80%
	2.29	2.33	2.39	2.54	2.63	10%
	1.79	1.81	1.85	1.98	2.05	1%
5.00	3.59	3.58	3.75	3.96	4.07	80%
	2.33	2.31	2.43	2.56	2.66	10%
	1.82	1.87	1.88	1.98	2.07	1%
10.00	3.55	3.55	3.57	3.89	3.91	80%
	2.30	2.30	2.31	2.51	2.56	10%
	1.79	1.79	1.79	1.94	1.99	1%
15.00	3.55	3.56	3.70	4.03	4.09	80%
	2.29	2.31	2.39	2.59	2.65	10%
	1.77	1.80	1.85	1.99	2.04	1%
AIR	3.54	3.51	3.49	4.04	4.05	80%
	2.29	2.28	2.27	2.59	2.60	10%
	1.78	1.78	1.77	1.98	1.99	1%

TABLE 2. VARIATION OF DOSE MEAN LINEAL ENERGY YD [keV/um] FOR DIFFERENT SPATIAL POSITIONS (cm) IN WATER PHANTOM AND IN AIR.

LAT. DIST.	0.00	5.00	6.00	7.00	9.00
DEPTH					
0.50	65.10	68.30	65.90	51.30	44.20
5.00	67.70	73.00	61.10	51.30	47.10
10.00	68.70	70.60	69.30	55.30	48.90
15.00	75.30	68.00	65.60	53.40	47.70
AIR	68.60	64.80	71.70	58.60	57.90

Table 3. VARIATION OF DOSE RATE WITH POSITION

LATERAL DISTANCE (cm)	0	5	6	7	9
DEPTH (cm)					
.5	.3218	.2574	.0579	.0386	.0161
5	.252	.1967	.0882	.0459	.0252
10	.1727	.1485	.0984	.0484	.0259
15	.108	.0929	.0702	.0346	.0216



### DISCUSSION

The measurement we have made are in good accord with what might have been expected from neutron physics. Our beam is prefiltered by a 4 cm lithiated polyethylene filter, thus removing most of the low energy neutrons produced in the source. Our collimation system does not generate a large scattered neutron component. It is evident (Fig. 1) that there is some but minor beam hardening as the beam penetrates tissue. Our beam produces two high LET components which when folded with the corresponding RBE values are approximately equal (note the two equal peaks in figure 3 corresponding to LETs of ~80 and 150 KeV/ $\mu$ ). These two peaks arise from the low energy neutron produced recoil protons and the high energy neutron produced, n,  $\alpha$  reactions in C, N and O. Since the modifications of the fast energy neutrons as they penetrate tissue have opposite effects on the two components, the net result is that the RBE weighted effective beam remains almost constant with depth (Table 2). This situation would doubtless not apply to other fast neutron therapy facilities where the two high LET components might be quite different.

The principal concern which this study addresses is that the structures just outside the beam edge might receive an excessive dose through a combination of poor definition of the beam edge and a high RBE of radiation just outside the nominal beam because of a large low energy recoil proton component generated by neutrons scattered out of the beam. This research tend to dispel this concern. The RBE outside the geometrical beam rises modestly ( $\approx$  5-10%) because the scattered neutron component is largely compensated by the low level of the n,  $\alpha$  reaction outside the direct beam.

Our observations and approaches are clearly consistent with current reports regarding the clinical RBE of fast neutron beams[9]. We note that we obtain a value of  $\approx$ 3.5 for our RBE relative to Co  $\gamma$  rays (at 80% survival) and that the value of 3.5 is quite consistent with the RBE value we observed for transformation and killing of C3H-10T-1/2 cells (Calkins, et al. submitted) and for killing of two primate line cells[10]. The effective clinical RBE we use for our neutron therapy protocol is 3.58 again consistent with our calculated values. Nevertheless, we have no real basis to expect that the RBE for 80% survival would be the proper value to apply in clinical neutron therapy. The neutron tumor dose increments we apply (1.55 Gy) correspond to about 10% survival and at this survival level the RBE would be much less, only about 2.3. The implication of the observation of such a high RBE is that perhaps it is the cells and tissues that receive lower doses incidental to the tumor therapy that are the actual limiting factor in neutron therapy. The results of studies of both hamster and primate cells imply that, contrary to many previous studies, there is an induction of repair which transfers response from a sensitive type to a resistant type at a definite threshold. Within this assumption, it is possible to use a single RBE factor for all survival levels between about 100% to about 20%. The single RBE factor turns out to be 3.5 for our observations (Calkins et al. submitted).

### REFERENCES

- [1] R.C. Barral, K.A. Merendino, and N. Feteih, "A Medical Cyclotron and Program at the King Faisal Specialist Hospital and Research Centre", Riyadh, Saudi Arabia: in Proceedings of IEEE, Transactions on Nuclear Science, 1983, Vol. NS-30, No. 2, pp. 1777-1780.
- [2] M. Catterall, and D. Bewley, Fast Neutrons in the Treatment of Cancer, Academic Press, 1979.
- [3] H.G. Menzel, "Advances in Dosimetry for Fast Neutrons and Heavy Charged Particles for Therapy Applications", IAEA-AG-371/3 Vienna, 1984.
- [5] "Microdosimetry", ICRU Report 36, 1983.
- [6] W.H. Grant et al., "Automatic Analysis of Empirically Derived LET Spectra", Health Physics, Vol. 22, pp. 351-354, April 1972.
- [7] P.H. Heintz et al., "Neutron Energy Spectra and Dose-Distribution Spectra of Cyclotron-Produced Neutron Beams", Medical Physics, Vol. 4, No. 3, May/June 1977.
- [8] G.W. Barendsen, "Response of cultured cells, tumors, and normal tissues to radiations of different linear-energy transfer", Curr. Top. Radiat. Res. Q. 4, 293-355, 1968.
- [9] H.G. Menzel, P. Pihet and A. Wambersie, "Microdosimetric specification of radiation quality in neutron radiation therapy", Int. J. Radiat. Biol., Vol. 57, No. 4, pp. 865-883, 1990.
- [10] J. Calkins, M. Einspinner, D. Blocher and W. Greer, "Response of two mammalian cell lines to low gamma ray doses", International Journal of Radiat. Biol., Vol. 56, pp. 869-875, 1989.

## SPECIFICATION OF RADIATION QUALITY FOR HIGH-LET PARTICLE THERAPY: MICRODOSIMETRIC APPROACH

P. Pihet<sup>1</sup>, H.G. Menzel<sup>2</sup>, A. Wambersie<sup>3</sup>, R.E. Grillmaier<sup>1</sup>

1. Universität des Saarlandes, FR Biophysik und Physikalische Grundlagen der Medizin, Homburg (Saar), Fed. Rep. of Germany.

2. Commission of the European Communities, DGXII, B-1049-Brussels, Belgium

3. Université Catholique de Louvain, Cliniques Universitaires St-Luc, 1200-Brussels, Belgium.

**Introduction**

The application of fast neutrons in cancer radiation therapy is based on the expectation that there is a biological selectivity for some tumours with regard to high-LET radiation, i.e. it is hoped that the differential biological effectiveness for tumour control and normal tissue complications is higher than in conventional low-LET therapy with photons and electrons. It is common in radiation therapy, and in radiation biology, to qualify the different types of radiations simply as low or high-LET radiation. The related implication that there is a simple bi-modal description of effectiveness or radiation quality, however, does not correspond to reality. In fact, the charged particles released by the interactions of fast neutron with tissue nuclei have LET values ranging over more than four orders of magnitudes. Moreover, the actual dose distribution in LET depends critically on the neutron energy, as does the biological effectiveness expressed as RBE. It appears somewhat paradox that, in spite of being the basis of the underlying rationale, high-LET radiation quality has been treated in a very simplistic way in neutron therapy practice, for example by using a clinical RBE values as single dose scaling factors to relate conventional photon and neutron treatments.

The complexity of radiation quality specification in neutron therapy is due to the fact that the biological effectiveness is dependent on neutron energy and that there is an inherent variation of biological sensitivity of different types of tissue and endpoints.

The neutron beams used by various therapy centres are of widely differing energies and, corresponding by radiobiological experiments have revealed considerable differences in RBE between the various neutron beams [1][2][3]. Although these biological experiments provide the necessary primary information there is no generally accepted procedure to decide on a factor to be used to account for these differences. In addition, at some facilities RBE variations have been observed inside irradiated phantoms, in particular with increasing depth [4][5][6]. In spite of this evidence, there is no quantitative and widely accepted specification in radiation quality used in neutron therapy practice. The obvious discrepancy between the accuracy requirement for absorbed dose delivery of  $\pm 3.5\%$  (expressed as one relative standard deviation, [7]) and the lack of an adequate method for accounting for radiation quality differences and variations calls for an urgent practical solution of the problem [10][11][12].

**Criteria for radiation quality specification in neutron therapy**

The requirement of high accuracy in the delivery of absorbed dose to the target volume in radiation therapy is determined by the steepness of the dose-response curves for tumour control and normal tissue complications [8]. In photon and electron therapy, the accuracy requirements can be met by optimization of dosimetry, irradiation techniques and treatment procedures. In neutron and other high-LET therapy, the difference and variations in radiation quality should be specified with comparable accuracy.

For principal reasons a single parameter specification of radiation quality is preferable in clinical practice. At least, if the difference in biological effectiveness of neutrons and photons is considered, the applicability of a single conversion factor is, however, limited in view of the well known variations of RBE with

dose, dose per fraction, biological effect and type of tissue. However, if the biological effectiveness of different neutron therapy beams, i.e. neutrons within a limited energy range, are compared a single parameter characterization appears more promising and justified. Such a conversion factor has been given, the name clinical neutron intercomparison factor (CNIF) [9]. This factor is expected to be adequate for comparing the biological effectiveness between different neutron beams. The remaining problem was to establish a method to evaluate the factor with the required accuracy.

This paper is aimed at showing the considerable improvement achieved in specifying radiation quality for neutron therapy by using microdosimetric techniques and radiobiological experiments [11][12].

The microdosimetric approach is used to derive biological weighting factors for absorbed dose which fulfils the criterion of meeting the accuracy requirements for absorbed dose. This weighting factor is based on combined radiobiological and microdosimetric measurements and should be used in support of establishing CNIF values with increased reliability and will provide the possibility to take into account RBE variations of clinical relevance at a given facility. Another criterion to be met by any radiation quality specification for clinical applications is that it has to be valid for relevant biological endpoints, in particular, for late effects in normal tissue.

**Empirical biological weighting functions**

Results of microdosimetric measurements at neutron therapy facilities have been reported by many authors (for references see [10][11][12]). They have revealed that the measured spectra provide detailed information on the secondary radiation components and that they are very sensitive to variations of irradiation parameters such as primary neutron energy, field size, position in phantom and shielding. More recently, a systematic microdosimetric intercomparison of all European neutron therapy centres has been carried out under the auspices of the EORTC [12]. The biological intercomparisons of most of these beams were performed [3]. These correlated microdosimetric and radiobiological investigation was used to derive a biological weighting function  $r(y)$  in dependence of the microdosimetric quantity lineal energy,  $y$ . With the only assumption of the existence of a correlation between the RBE of a given neutron beam and the shape of the microdosimetric dose distribution, the function  $r(y)$  was obtained by a numerical optimization procedure, so that the integral R:

$$R = \int r(y) \cdot d(y) \cdot dy$$

reproduces the RBE ratios between any of the investigated beams and one neutron beam chosen as a reference. Such a procedure is well known in other applications and has been used to evaluate empirically biological weighting functions [13][14]. Assuming an initial guess function for  $r(y)$ , the parameters of the function  $r(y)$  are optimised by successive iterations in order to match the calculated parameter R and the experimental RBE ratio for each the investigated neutron beam. The biological results available and used in the analysis were growth inhibition in *Vicia faba* and early effects in mice. The resulting functions  $r(y)$  have shapes

similar to that of the well known RBE-LET relationships [ 10] [ 11] [ 12 ]. However, in detail, they depend on the biological system and the dose level. A comprehensive statistical analysis of the result showed that for the RBE values and microdosimetric data available, the overall uncertainty of R is less 3 % ( $\pm 1$  standard deviation within the neutron energy range relevant to therapy) [ 11] [ 12 ].

The empirical procedure proposed for the determination of the biological weighting function therefore meets the above given accuracy requirement and thus enables the determination of CNIF with sufficiently good accuracy. However, it has to be kept in mind, that the results obtained to date are restricted to the given biological endpoints, to the dose levels available for the analysis and to the neutron energy range of the therapy beams used. Combined microdosimetric and radiobiological experiments with endpoints and dose levels of clinical relevance are urgently required to reduce the restrictions of the applicability of the procedure.

#### Concluding remarks

The briefly described empirical procedure and the obtained results have shown that radiation quality specification for clinical purposes meeting the accuracy requirements is possible. In the future the evaluation of biological weighting functions has to be extended to other, clinically relevant endpoints. It is suggested that this microdosimetric approach is taken account of when new radiobiological experiments are being designed.

It should also be emphasized that the microdosimetric investigations of neutron therapy beams have achieved a number of improvements for the concept of therapy. First of all, the results document very clearly that the separation of photon and neutron dose components is only one, and a relatively small one at that, of the problems of radiation quality specification and that the offered microdosimetric alternative is much more comprehensive. The method has been shown to be able to account for small differences and variations of radiation quality for example with penetration in phantom. The achievable high accuracy for R, the microdosimetric parameter to estimate the biological effectiveness of a neutron beam with a given energy relative to that of a neutron reference beam, provides severe constraints for the experimental RBE values and thus contributes towards reducing the confidence limits.

The method must be recommended also to radiation therapy with other particles such as protons and, in particular, heavy ions. The experience gained with neutron therapy suggests strongly that the principle of combining dedicated radiobiological experiments with microdosimetric measurements is applied to heavy particle therapy from the beginning. There is, however, a need to modify suitably the experimental method with regard to complex size and possibly simulated diameter.

Finally, it should be mentioned that in radiation protection dosimetry, simple dedicated microdosimetric instruments have become available. It is possible to develop corresponding instrumentation for therapy applications in order to facilitate the still laborious microdosimetric method and make it accessible to routine use.

#### References

- Hall, E.J. and Kellerer, 1979, *Review of RBE data for cells in culture*. Proc. of Symp. — 3rd Meeting on Fundamental and practical aspects of the application of fast neutrons and other high LET particles in clinical radiotherapy. edited by G.W. Barendsen, J.J. Broerse and J.J. Breur, 171-174, .
- Zywietz, F., Menzel, H.G., Van Beuningen, D., and Schmidt R, 1982, *A biological and microdosimetric intercomparison of 14 MeV d-T neutrons and 6 MeV cyclotron neutrons*. Int. J. Radiat. Biol., **42**, 223-228 .
- Beauduin, M., Gueulette, J., de Coster, B.M., Gregoire, V., Octave-Prignot, M., Vynckier, S., Wambersie, A, 1989, *Radiobiological intercomparisons of fast neutron beams used in therapy*. Proc. of Symposium — EORTC-Heavy Particles Therapy Group Meeting, Munich, October 1987. *Strahlentherapie und Onkologie*, **165**, 263-267.
- Zeitz, , L., Canada, T.R., Djordjevic, B., Dymbort, G., Freeman, R., McDonald, J.C., O'Neil, J. and Laughlin, J.S. *A biological determination of the variation of fast neutrons field quality with depth, RBE and OER*. *Radiat. Res.*, **63**, 211-225 (1975)
- Gueulette, J., Breteau, N., Sabattier, R. and Wambersie, A., 1984, *RBE of p(34)+Be neutrons for early intestinal tolerance in mice. Radiobiological intercomparison between Orléans (p(34)+Be neutrons) and Louvain-la-Neuve (d(50)+Be neutrons)*. Proc. of Symp. — High LET particles in radiation therapy. Proc. EORTC Workshop. Orléans, May, 1983. J. Battermann, J.P. Le Bourgeois, A. Wambersie and N. Breteau, *Journal Européen de Radiothérapie*, **5**, 175-179 .
- Bewley, D.K., Cullen, B.M., Astor, M., Hall, E.J., Blake, S.W., Bonnett, D.E. and Zaider, M. *Changes in biological effectiveness of the neutron beam at Clatterbridge (62 MeV p on Be) measured with cells in vitro*. *Brit. J. of Radiobiology*, **62**, 344-347 (1989).
- Mijnheer, B.J., Batterman, J.J. and Wambersie A., 1987, *What degree of accuracy is required and can be achieved in photon and neutron therapy ?* *Radiotherapy and Oncology*, **8**, 237-252 (a).
- Wambersie, A. and Gueulette, J. ,1984, *Accuracy required in radiotherapy and in neutron therapy*. IAEA STI/PUB/643. Proc. of Symp.—Advances in Dosimetry for Neutrons and Heavy Charged Particles for Therapy Applications, Vienna 1982. IAEA Vienna. IAEA-AG-371/1, 11-26 .
- Wambersie A. and Battermann J.J. ,1985, *Practical problems related to RBE in neutrontherapy*. Proceedings of the 3rd Meeting on Progress in Radio-Oncology, Vienna, 1985.
- H.G. Menzel , P. Pihet and A. Wambersie *Microdosimetric specification of radiation quality in neutron radiation therapy*. *International Journal of Radiation Biology*, 1990, **57**, 865-883.
- Pihet, P., 1989, *Etude microdosimétrique de faisceaux de neutrons de haute énergie. Applications dosimétriques et radiobiologiques*, Thesis (Louvain-la-Neuve: Université Catholique de Louvain).
- Pihet, P., Menzel, H.G., Schmidt, R., Beauduin, M. and Wambersie, A.,1990. *Biological weighting function for RBE specification of neutron therapy beams. Intercomparison of 9 European Centres*. Proceedings of the 10th Symposium on Microdosimetry. Rome, Radiation Protection. Dosimetry, (in press).
- Varma, M.N. and Bond, V.P., 1982, *Empirical evaluation of cell critical volume dose vs. cell response function for pink mutations in Tradescantia*. Proceedings of the 8th Symposium on Neutron Microdosimetry, Jülich, September 1982. (Luxembourg: CEC, EUR 8395 EN, 439-450 .
- Zaider, M. and Brenner, D.J. ,1985, *On the microdosimetric definition of quality factors*. *Radiation Research*, **103**, 302-316 .

THE EFFECTS OF FRACTIONATED DOSES OF FAST NEUTRONS ( $42\text{MeV}_{d+\text{Be}}$ ) ON THE NORMAL TISSUE OF THE PIG

M.E.C. Robbins, D.W.H. Barnes, J.W. Hopewell and J.M. Sansom

CRC Normal Tissue Radiobiology Research Group,  
 Research Institute (Univ. of Oxford), Churchill Hospital, Oxford OX3 7LJ, and  
 MRC Radiobiology Unit, Chilton, Didcot OX11 0RD, UK.

The early and late effects of fractionated doses of fast neutrons ( $42\text{MeV}_{d+\text{Be}}$ ) were studied in the skin, lung, kidney and rectum of the pig. These results were compared with those for photon irradiation and RBE values calculated. The RBE for damage to dermal tissue, expressed as necrosis after 10-20 weeks, was greater than that for early moist desquamation, but only for total doses given as  $\sim 2\text{Gy}$ /fraction of X rays. For dermal and subcutaneous tissue atrophy, scored from 26-104 weeks, the variation in RBE values with X ray dose/fraction did not differ significantly with the observation period. These RBE values were similar to those for dermal necrosis, although values tended to decrease with increasing latency for doses of  $\sim 2\text{Gy}$ /fraction. Results for the lung showed no significant variation in RBE for early and late effects. In the rectum, however, a significant difference was noted, with RBE values of 2.0 and  $>3.0$  for acute and late effects, respectively, for photon doses of 5-8Gy/fraction. Very severe late effects were seen for doses that were initially well tolerated. For late radiation damage to the skin, lung and kidney, the RBE was  $\sim 3.0$  for X ray doses of  $\sim 2\text{Gy}$ /fraction.

Introduction

Fast neutrons were first used in radiotherapy in the United States nearly 50 years ago, but the late effects resulting from such treatments were so severe that the initial trial was curtailed [1]. With the realisation that the RBE increased with decreasing dose/fraction it appeared that the severe late normal tissue complications previously reported [1] could have been due to the use of too high a dose. The radiobiological findings and the favourable clinical results of Catterall et al. [2] resulted in a revived interest in the clinical use of fast neutrons. However, the increased risk of late normal tissue morbidity still appeared to be a major limitation in the use of fast neutrons [3-5]. This could reflect difficulties in obtaining an adequate dose-distribution with the first generation of neutron beams although it should be noted that late morbidity was still a problem with neutrons produced by higher energy cyclotrons [6].

This paper reviews the results of an extensive experimental study designed to determine the RBE for higher energy neutrons ( $42\text{MeV}_{d+\text{Be}}$ ) specifically for early and late effects on the normal tissues of the pig [7-9]. These studies were carried out using the Variable Energy Cyclotron (VEC) at the Atomic Energy Research Establishment (AERE) Harwell. This produced fast neutrons with an average energy of  $14\text{MeV}$ , similar to that of the new hospital based high energy cyclotron ( $62\text{MeV}_{p+\text{Be}}$ ) at the Clatterbridge Hospital, Merseyside, UK. Both early and late effects of fractionated doses of fast neutrons were studied in the skin, lung, kidney and rectum and compared with those after photon irradiation. RBE values were calculated. A large animal model allowed the irradiation of tissue volumes and hence dose distributions comparable with those found clinically.

Materials and Methods

Female pigs of the Large White strain were used. The animals were brought in to the animal house when 12-weeks-old (20-25kg) and allowed an acclimatization period of at least 2 weeks before any experimental procedures were undertaken. All procedures were carried out under anaesthesia using a 2% halothane, 70% oxygen and  $\sim 30\%$  nitrous oxide gas mixture.

Irradiations and the assessment of damage

[1] Skin: Prior to irradiation  $16\text{cm} \times 4\text{cm}$  fields were marked by tattooing with India ink on the left and right flank of each pig. For X irradiations (250kV X rays, HVL 1.4mm Cu; FSD 50cm; dose rate  $\sim 69\text{cGy}/\text{min}$ ) 2-4 fields on the left flank, separated by 4cm, were irradiated. Fields on the contralateral flank acted as controls; the exit doses ( $<8\%$ ) have not been shown to produce any late radiation-induced changes in the skin. For irradiations with fast neutrons only 2 fields were marked out on the left flank of each pig, separated from each other by 12cm. A single control site was marked in the centre of the right flank, positioned between the irradiated fields on the left flank. The exit dose was  $\sim 30\%$  of the applied dose after neutron irradiation. The characteristics of the neutron beam have been detailed previously [10]. Neutrons were produced by the bombardment of a 2mm thick, gold-backed, beryllium target with  $42\text{MeV}$  deuterons (SSD 150cm; dose rate  $\sim 54\text{cGy}/\text{min}$ ). Full skin build-up was provided by 10mm of tissue equivalent material, taped to the skin surface.

Irradiations with X rays were with either a single dose or fractionated doses given as 6 or 14F/18 days, and 6, 14 or 30F/39 days. Fast neutrons were also given as a single dose or as 6 or 12F/18 days, and 6, 12 or 30F/39 days.

Pigs were penned individually indoors and the skin sites scored weekly by at least 4 observers for 16-20 weeks after irradiation. Skin reactions were assessed in terms of the severity of erythema and presence or absence of moist desquamation or dermal necrosis [7]. Iso-effect doses for the early epithelial response and subsequent dermal reaction to each fractionation schedule were derived by establishing, at each dose level, the incidence of moist desquamation and dermal necrosis. Dose-effect curves were fitted by probit analysis and  $\text{ED}_{50}$  values ( $\pm\text{SE}$ ) calculated.

At regular intervals from 26 to 104 weeks after irradiation the degree of late radiation-induced damage to the cutaneous and subcutaneous tissue was assessed by comparing the lengths of the long axis of the irradiated skin fields with those of a comparable field on the opposite flank of the same pig. The ratio of the lengths of the irradiated/control sites represented the "relative field length". Measurements taken at 26-52 weeks and 65-104 weeks were converted into quantal data. At each dose level and for each

fractionation regime the proportion of skin fields showing a 'relative field length' of  $<0.9$ ,  $<0.875$ ,  $<0.85$  or  $<0.825$  was assessed. These data were used to calculate  $ED_{50}$  values ( $\pm SE$ ) for these 4 different levels of effect.

[11] Lung: Prior to irradiation the position of the fully ventilated basal lobe of the left lung was determined fluoroscopically and included in a 10cm x 20cm triangular shaped field tattooed on the overlying skin. This field was irradiated with either single or fractionated doses of X rays and fast neutrons. The irradiation schedules were the same as those outlined for the skin.

Lung function tests were performed prior to irradiation and at 13-week intervals for up to 104 weeks after irradiation. Each animal was tested twice on each occasion using a  $^{133}\text{Xe}$  washout technique [9]. Changes in the gas exchange capacity of the irradiated lung were compared with that of the contralateral unirradiated lung. The results from these lung function tests were converted into quantal data on the basis of the percentage of lung function tests showing a  $\geq 15\%$  impairment in function in the irradiated lung compared with the unirradiated lung in the same animal.  $ED_{50}$  values ( $\pm SE$ ) were determined for the early pneumonitic (13-26 weeks) and for the late fibrotic (39-104 weeks) phases of damage after irradiation.

[11] Kidney: Prior to irradiation the position of both kidneys was determined by intravenous pyelography and the right kidney included in an 8cm x 12cm field tattooed on the overlying skin. In each animal this field was irradiated with either X rays or fast neutrons. Doses were given as a single dose, as 6 and 12F/18 days, or 6, 12 or 30F/39 days for fast neutrons, and as a single dose, as 6 and 14F/18 days, or as 6, 12, 14 and 30F/39 days for X rays.

Before irradiation and at intervals of 4-104 weeks after irradiation renal function was assessed by renography [11]. This allowed the determination of a functional index (FI). The FI, expressed as a percentage, is defined as the ratio of the uptake function for  $^{133}\text{I}$ -hippuran of the irradiated kidney to that of the contralateral unirradiated kidney in the same animal. Irradiated kidneys for which the FI was  $\leq 30\%$  were defined as having no significant function. RBE values were calculated based on the maximum dose at which function was still observed, the minimum dose at which no function was observed, and an intermediate "iso-effect dose" between these two effect levels.

[iv] Rectum: A 10cm length of the rectum of the pig was irradiated with either single doses or fractionated doses involving one fraction/week i.e. 6F/5 weeks of fast neutrons or  $^{60}\text{Co}$   $\gamma$  rays. The latter schedule avoided severe acute damage, the weekly interfraction interval allowing regeneration of the mucosal epithelium. Acute damage was assessed by the reduction in crypt cellularity counted in histological sections from rectal biopsies taken serially from individual pigs 1-10 days after irradiation. Late damage was determined on the basis of severe morbidity.

### Results

[1] Skin: Following X irradiation a significant increase in the iso-effect dose for moist desquamation was seen when the fraction number increased from 5-14 given over 18 or 39 days ( $p < 0.0005$ ). The slight decrease in iso-effect for X ray doses given in 30F compared with 14F/39 days (Fig. 1) was not significant. No significant effect of fraction number was seen following neutron irradiation. However, a significant time factor was noted, the increase in irradiation time

from 18-39 days being associated with an  $\sim 20\%$  increment in total dose.

A log-log plot of the  $ED_{50}$  values for dermal necrosis versus fraction number is shown in Fig. 2. A good linear correlation was obtained between 1-30 fractions for X rays, and between 6-30 fractions for fast neutrons. Increasing the irradiation time had little effect; moreover, fractionation of the fast neutron dose has little effect on the  $ED_{50}$  values for doses given in  $\geq 6$  fractions. The variation in the RBE of fast neutrons, with respect to the X ray dose/fraction, is shown in Fig. 3. For moist desquamation, the RBE increased with decreasing dose/fraction down to  $\sim 5\text{Gy}/\text{fraction}$ ; with dose/fractions of  $\geq 5\text{Gy}$  the RBE showed no further change. This suggested an upper limit to the RBE for moist desquamation of  $\sim 2.75$ . In contrast, the RBE for later dermal necrosis appeared to increase linearly for dose/fractions down to  $\sim 2\text{Gy}$  X rays when the RBE was  $\sim 3$ .

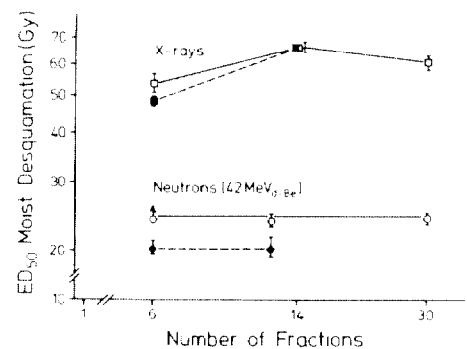


Fig. 1. Log-log plot of  $ED_{50}$  values ( $\pm SE$ ) for moist desquamation in pig skin against the number of fractions of X rays or fast neutrons ( $\bullet, \square$ ). Fractionated irradiation was given in 18 ( $\blacksquare, \bullet$ ) or 39 ( $\square, \circ$ ) days. (Redrawn from [7]).

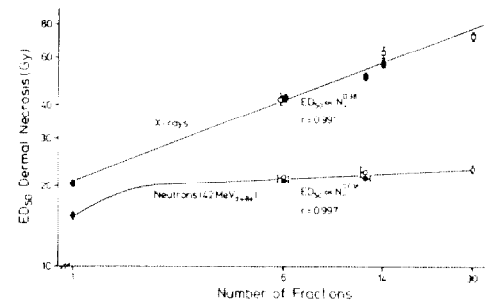


Fig. 2. Log-log plot of  $ED_{50}$  values ( $\pm SE$ ) for late dermal necrosis in pig skin against the number of fractions of X rays or fast neutrons. For key see Fig. 1. (Redrawn from [7]).

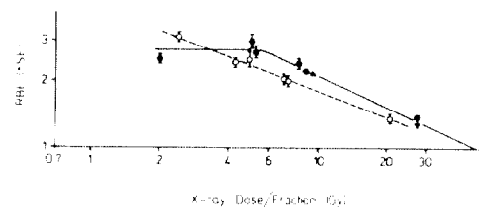


Fig. 3. Log-log plot of the RBE ( $\pm SE$ ) for early moist desquamation ( $\bullet$ ) and late dermal necrosis ( $\circ$ ) in pig skin as a function of X ray dose/fraction. (Redrawn from [7]).

A log-log plot of RBE against X ray dose/fraction for later cutaneous and subcutaneous skin damage is shown in Fig. 4. A good linear correlation was obtained for the time periods of 26-52 weeks and 65-104 weeks after irradiation when the data for 6F/39 days were excluded; the low RBE values for the latter reflected the higher than anticipated  $ED_{50}$  values for changes in "relative field length" following neutron irradiation. Fig. 4 also includes the plot for dermal necrosis, and indicates little variation in RBE with X ray dose/fraction over the observation period 10-104 weeks after irradiation. However, the RBE showed a tendency to decrease with increasing latency for X ray doses/fraction of  $\sim 2$ Gy.

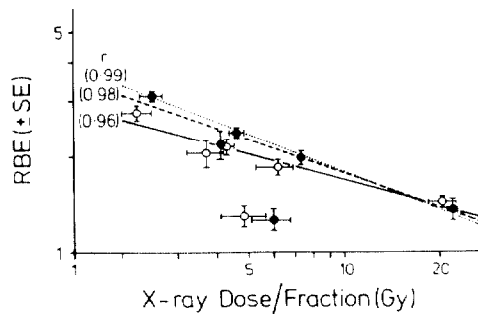


Fig. 4. Log-log plot showing the variation in RBE with X ray dose/fraction for changes in "relative field length" at 26-52 weeks (●); 65-104 weeks (○); and for dermal necrosis after 10-20 weeks (○). (Redrawn from [8]).

[i] Lung: There was no significant difference in the relationship between RBE and X ray dose/fraction for both early and late radiation damage to the lung (Fig. 5). The RBE for fast neutrons decreased with increasing fraction size. For the combined data the relationship was adequately described by a straight line with a slope of  $-0.52 \pm 0.1$ . For X ray doses/fraction of  $\sim 2$ Gy, the RBE, like that for late skin damage, was  $\sim 3.0$ .

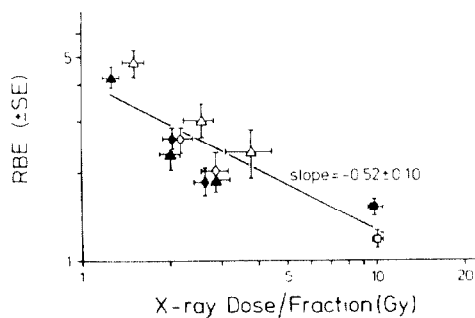


Fig. 5. Log-log plot of the RBE (±SE) against X ray dose/fraction for both early (13-26 weeks □, ○, △) and late effects (39-104 weeks ■, ◆, ▲) in pig lung. Fractionated irradiation was given in 18 (○, ◆) or 39 days (△, ▲). (Redrawn from [9]).

[ii] Kidney: There was no marked effect of fractionation or overall treatment time after fast neutron irradiation. The changes in RBE with X ray dose/fraction are shown in Fig. 6. Due to the low iso-effect dose for 12F of X rays given in 18 as compared with 39 days the RBE depended on the overall

irradiation time. The increase in RBE with decreasing dose/fraction was most marked for irradiations given in 39 days as compared with those given in 18 days; the slopes of the linear regression lines were  $-0.68 \pm 0.06$  and  $-0.25$ , respectively.

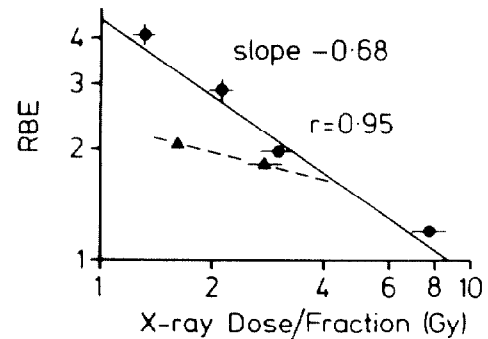


Fig. 6. Log-log plots of the RBE for renal damage against X ray dose/fraction. Fractionated irradiation was given in 18 (●) or 39 days (▲).

[iv] Rectum: A comparison of the dose-related reduction in the cellularity of the rectal mucosa between 1-10 days after irradiation with single doses of  $^{60}\text{Co}$  γ rays and fast neutrons suggested a RBE of  $\sim 2.0$  for photon doses of 5-10Gy. No late reactions were seen in the animals up to 104 weeks after irradiation. In marked contrast, severe late damage, consisting of severe rectal and pelvic oedema/fibrosis, was seen following fast neutron irradiation with 6 weekly fractions of 3 and 4Gy; acute rectal changes were minimal representing only a transient reduction in crypt length. Animals had to be killed between 60-184 days after irradiation due to severe morbidity. Irradiation with 6 fractions of 6 and 8Gy of  $^{60}\text{Co}$  γ rays produced only a slight narrowing of the rectal lumen after 39 weeks, and there were no deaths related to rectal complications. Based on these results a RBE of  $>3.0$  was estimated for late rectal damage.

#### Discussion and Conclusions

Studies in pig skin after irradiation with either X rays or fast neutrons have indicated a higher RBE for late dermal necrosis than for early epithelial damage, but only when total doses were given as  $\sim 2$ Gy/fraction X rays. This result helps to explain some of the disagreements that have been voiced on the basis of results from clinical trials with fast neutrons [12,13]. Duncan et al. [13] reported an increased incidence of late effects in skin and subcutaneous tissues for comparable tumour control in patients treated for squamous cell carcinoma. Photon doses of 55Gy were compared with 15.5Gy of fast neutrons, both given as 20 fractions/4 weeks i.e. a dose of 2.75Gy/fraction of photons. In contrast, treatment with 12 fractions/4 weeks with fast neutrons showed a close correlation between early and late effects on the skin and subcutaneous tissues [12]. A similar conclusion was reached based on the results of the present studies in pig skin when the two 12 fraction schedules were compared. Moreover, for 12 fractions/18 days there appeared to be significant sparing of late damage after fast neutron irradiation compared with that seen after X rays [7], suggesting that a few large dose fractions given in a short time period may be optimal for fast neutron therapy.

Assessments of dermal and subcutaneous damage at 26-104 weeks after irradiation produced similar RBE values to those for dermal necrosis after 10-20 weeks. However, the RBE values for fast neutrons did tend to

decrease slightly with increasing latency for X ray doses of ~2Gy/fraction.

For X ray doses given as ~2Gy/fraction the RBE for fast neutrons for dermal injury was ~3.0. With increasing fraction size the RBE values for the lung and kidney declined more than those for dermal and subcutaneous tissues. For doses given as ~5Gy/fraction X rays the RBE values for these 'late organ' responses were lower than that for acute epithelial damage (2.75) to pig skin, further supporting the use of a few fractions in a short overall treatment time for fast neutron therapy.

In the case of pelvic irradiation the RBE for late rectal injury was significantly greater than that for early damage i.e. >3.0 compared with 2.0 for doses of 6-8Gy/fraction X rays. Very severe late effects consisting of severe rectal and pelvic oedema with fibrosis were seen after neutron irradiation, despite these doses being well tolerated in the acute phase of injury. Clinical evidence for severe morbidity following pelvic irradiation has been reported previously [4,5] after irradiation with lower energy neutrons. Thus the previously reported morbidity of fast neutron therapy would appear to represent a true difference in biological effect and not simply an artifact due to poor dose distribution from lower energy neutrons [5]. The limited blood supply to the pelvis may result in the area being particularly prone to radiation-induced vascular damage with resultant ischaemia, loss of tissue and fibrosis [14]. An increased physical dose for neutrons to tissue with a high fat content may also play a role [15]. The precise mechanisms involved remain unclear, but in view of the current results and the earlier clinical findings the use of fast neutrons in the treatment of pelvic tumours should be attempted only with extreme caution.

#### References

- [1] R.S. Stone, Neutron therapy and specific ionization, *Am. J. Roentgen.*, 59, 771-785, 1948.
- [2] M. Catterall, I. Sutherland and D.K. Bewley, First results of a randomised clinical trial of fast neutrons compared with X or gamma rays in treatment of advanced tumours of the head and neck, *Br. Med. J.*, 2, 653-656, 1975.
- [3] R.D. Crnitz, F.W. Bradley, K.L. Mossman, F.M. Fender, M.C. Schnell and C.C. Rogers, Clinical observations of early and late normal tissue injury in patients receiving fast neutron irradiation, *Int. J. Radiat. Oncol. Biol. Phys.* 6, 273-279, 1980.
- [4] W. Duncan, J.R. Williams, G.R. Kerr, S.J. Arnott, P.M. Quilty, A. Roger, R.H. MacDougal and W.J.L. Jack, An analysis of the radiation related morbidity observed in randomized trial of neutron therapy for bladder cancer. *Int. J. Radiat. Oncol. Biol. Phys.*, 12, 2085-2092, 1986.
- [5] R.S. Pointon, G. Read and D. Greene, A randomized comparison of photons and 15MeV neutrons in the treatment of carcinoma of the bladder, *Br. J. Radiol.*, 58, 219-224, 1985.
- [6] L. Cohen, F.R. Hendrickson, J.A. Mansell, M. Awschalom, A. Hrejisa, R. Kaul and I. Rosenberg, Late reactions and complications in patients treated with high energy neutrons p(66MeV) and Be(49MeV), *Int. J. Radiat. Oncol. Biol. Phys.*, 7, 179-184, 1981.
- [7] J.W. Hopewell, D.W.H. Barnes, M.E.C. Robbins, J.M. Sansom, J.F. Knowles and G.J.M.J. van den Aardweg, The relative biological effectiveness of fractionated doses of fast neutrons ( $42\text{MeV}_{d+\text{Be}}$ ) for normal tissues in the pig. I. Effects on the epidermis and dermal vascular/connective tissue, *Br. J. Radiol.*, 61, 928-938, 1988.
- [8] J.W. Hopewell, D.W.H. Barnes, M.E.C. Robbins, M. Corp, J.M. Sansom, C.M.A. Young and G. Wiernik, The relative biological effectiveness of fractionated doses of fast neutrons ( $42\text{MeV}_{d+\text{Be}}$ ) for normal tissues in the pig II. Late effects on cutaneous and subcutaneous tissues. *Br. J. Radiol.* (in press) 1990.
- [9] M. Rezvani, D.W.H. Barnes, J.W. Hopewell, M.E.C. Robbins, J.M. Sansom, P.J.V. Adams and R. Hamlet, The relative biological effectiveness of fractionated doses of fast neutrons ( $42\text{MeV}_{d+\text{Be}}$ ) for normal tissues in the pig. III. Effects on lung function, *Br. J. Radiol.* (in press) 1990.
- [10] D.T. Goodhead, R.J. Berry, D.A. Bance, P. Gray and J.B.H. Stedeford, High energy fast neutrons from the Harwell variable energy cyclotron. I. Physical characteristics, *Am. J. Roentgen.*, 129, 709-716, 1977.
- [11] M.E.C. Robbins, M. Soper and Y. Gunn, Techniques for the quantitative measurement of individual kidney function in the pig, *Int. J. Appl. Radiat. Isot.* 35, 853-858, 1984.
- [12] M. Catterall, R.D. Errington and D.K. Bewley, A comparison of clinical and laboratory data on neutron therapy for locally advanced tumours, *Int. J. Radiat. Oncol. Biol. Phys.*, 13, 1783-1791, 1987.
- [13] W. Duncan, J.A. Orr, S.J. Arnott, W.J.L. Jack and G.R. Kerr, An evaluation of fast neutron irradiation in the treatment of squamous cell carcinoma in cervical lymph nodes, *Int. J. Radiat. Oncol. Biol. Phys.*, 13, 1793-1796, 1987.
- [14] T.F. Todd, Rectal ulceration following irradiation treatment of carcinoma of the cervix uteri, *Surg. Gynecol. & Obstet.*, 67, 617-631, 1938.
- [15] H.R. Withers, H.D. Thames and L.J. Peters, Biological bases for higher RBE values for late effects of neutron irradiation, *Int. J. Radiat. Oncol. Biol. Phys.* 8, 2071-2076, 1982.

## THE TENTH YEAR OF THE ORLEANS NEUTRON THERAPY FACILITY

Sabattier R.<sup>1</sup>, Goin G.<sup>2</sup>, Breteau N.<sup>1</sup>

1. Service de Radiothérapie, CHR, B.P. 6709, 45067 ORLEANS Cedex 2 (Fr)
2. CERJ-CNRS, 3A, rue de la Férollerie, 45071 ORLEANS Cedex 2 (Fr)

20 September 1990 will be the tenth birthday of the first neutron beam at the Orleans neutrontherapy facility.

20 January 1991 will be the tenth birthday of the first treatment.

Up to 1989, 1004 patients have been treated with fast neutrons according to three different protocols: mixed schedule, neutrons boost, neutrons only.

Distribution of patients is reported on table 1.

Tumour location	Number of patients
High grade astrocytomas	219
Uterine cervix	146
Bronchus carcinomas	116
Rectum	113
Head and Neck	137
Sarcomas	91
Prostate	48
Bladder	28
Others + metastasis	106
<b>Total</b>	<b>1004</b>

Table 1: Distribution of patients treated at the Orleans neutrontherapy facility from 1981 to 1989.

Pilot studies have been initiated and managed with parisian centers: neutrons boost for rectum carcinomas and for bronchus carcinomas, neutrons boost and concentrated irradiations for high grade astrocytomas.

For other tumor types or locations, protocols are derived from the current international practice (1).

Clinical results are in general good agreement with published data but the actual trend is to increase the proportion of neutron dose for mixed schedule and boost.

1990 is a tenth birthday for the technical staff of the neutron facility and this work shortly reports some technical data of clinical relevance.

From 1981 to 1989 treatment plannings became more and more sophisticated but basic data for dosimetry and radiobiology have not been modified.

Table 2 reports some physical and technical steps.

1980 :	- DOSIMETRY with ionization chambers according to ECNEU protocol.
	- RELATIVE BIOLOGICAL EFFICIENCY (2).
	- MICRODOSIMETRY.
1982 :	- IRREGULAR IRRADIATION FIELDS (3).
	- NEUTRON SPECTRUM with activation detectors (4).
1983 :	- SEMI-THICK BERYLLIUM TARGET : optimisation of the target/filter thicknesses (5).
	- INHOMOGENEITIES : depth dose distributions for lung inhomogeneities.
	- A150 CALORIMETER : direct calibration in the Orleans neutron beam of chambers in term of absorbed dose (6).
1985 :	- FLATTENING FILTERS, COMPENSATORS.
1986 :	- RADIOBIOLOGICAL INTERCOMPARISON (7).
	- EORTC MICRODOSIMETRIC INTERCOMPARISON (8).
1987 :	- RADIOPROTECTION with TE proportional counters (9).
1989 :	- New 3D TREATMENT PLANNING SYSTEM with CT scan data (Theratronics).

Table 2: Physical and technical steps at the Orleans Neutrontherapy Facility.

The optimum target and hydrogenous filter thicknesses for dose rate and depth dose were derived from the results in table 3.

$\Delta E$ (MeV)	FILTER THICKNESS (cm)	DOSE (%)	Dmax/2 (cm)
34	1	100	10.5
	4	73	11.0
	6	<u>60</u>	<u>11.3</u>
15.8	1	82	11.3
	4	<u>61</u>	<u>12.0</u>
	6	52	12.2
11.8	1	69	11.6
	4	53	12.2
	6	45	12.4
8.5	1	56	11.8
	4	43	12.3
	6	37	12.5

Table 3: p(34)+Be neutron beam : dose rate and penetration as a function of target thickness and beam filtration.

The underlined data are related to the original thick target and the semithick one now in use. Column :

- 1- Proton energy lost in the target.
- 2- Total hydrogenous filter thickness (10 mm perfluor for light simulation and additional polyethylene filter).
- 3- Relative dose at Dmax per unit proton charge, normalized for the thick target with the minimum filter thickness.
- 4- Depth of Dmax/2 for a 10cm x 10cm field and SSD 135 cm.

The main physical characteristics of the p(34)+Be(15.8) Orleans clinical neutron beam are listed in table 4 (10).

SSD	(cm)	169
Dose rate at Dmax	(cGy.min <sup>-1</sup> . $\mu$ A <sup>-1</sup> )	0.27
Depth of Dmax/2 in water	(cm)	12.8
Build-up: 0.9 Dmax	(cm)	0.2
Dmax	(cm)	0.7
$D_g / D_0 (n+g)$ :	(%)	5.2
- 2 cm		7.0
- 10 cm		
80%-20% penumbra width,	(cm)	1.9
-10 cm in water		

Table 4: Physical characteristics of a 10 cm x 10 cm reference field for the filtered neutron beam p(34)+Be(15.8)

As far as treatment planning is concerned, irregular fields are routinely planned since 1982 with no limitations for the field shapes up to 19cm x 19cm (3). Dose attenuation through the 20cm thick iron blocks is more than 97 % for a narrow beam.

Combinations of the different heavy collimator devices and basic filtrations routinely used do not significantly affect the beam quality. So conclusions were derived from the dosimetric data and the many microdosimetric spectra on axis and off axis for several configurations partly reported in (8).

Calculations of dose distributions are performed with a Theraplan-Theratronics computer.



When necessary, compensator filters are designed to optimise dose distribution: so filters are routinely used in the place of wedge and bolus since 1989.

Fields are daily confirmed with ordinary therapy verification films (10).

Radiation hazards around the collimators and the treatment-room were reported elsewhere (9-11): the low level of induced activity is mainly due to the medium neutron energy.

The cyclotron and the neutrontherapy facility have been running since 10 years without large technical breakdowns.

During the four last years only two treatment days were cancelled but without modification of the overall treatment time for any patient.

This aspect can be pointed out as conclusion from the running Orleans experience. Nevertheless, in this short special paper, it would be necessary to repeat that such special therapies should be considered by clinicians, physicists and technicians like classical therapies and conducted in the same way.

#### References :

1. N. Breteau, R. Sabbattier. Cahiers Cancer, Vol.2, 3, pp : 146-151, 1990.
2. J. Gueulette, N. Breteau, R. Sabbattier, A. Wambersie. J. Eur. Radiother., Vol.5, 3, pp : 176-179, 1984.
3. R. Sabbattier, N. Breteau. Proceeding of the fifth Symp. on Neutron Dosimetry. EUR. 9762 EN. Luxembourg CEC, pp : 1037-1046, 1985.
4. C. Clément. Note technique L.M.R.I. 84/133 MAI.
5. R. Sabbattier, G. Goin, L. Le Polotec, N. Breteau. Proceeding of tenth Int. Conf. on cyclotrons and their applications. IEEE 84 CH, 1996-3, pp : 483-485, 1984.
6. J. Caumes, A. Ostrowsky, K. Steinschaden, M. Mancaux, M. Cance, J.P. Simoen, R. Sabbattier, N. Breteau. Strahlenth. Onkol., 160, pp : 127-128, 1984.
7. B. Destembert, J. Gueulette, M. Leclerc, R. Sabbattier, N. Breteau. In SIN Jahresbericht, Swiss Institut for nuclear research. Med. Newsletter, 9, pp : 44-47, 1987.
8. P. Pihet. Thesis, Louvain-La-Neuve, 1989.
9. S. Vynckier, R. Sabbattier, A. Kunz, H.G. Menzel, A. Wambersie. Radiation Protection Dosimetry. Vol. 23, 1/4, pp : 269-272, 1988.
10. R. Sabbattier, B. Destembert, N. Breteau. Strahlenth. Onkol., Vol. 166, pp : 86-89, 1990.
11. R. Sabbattier, P. Pihet, J.C. Bajard, M. Noale, H.G. Menzel, N. Breteau. Radioprotection, Vol. 24, 2, pp :123-132, 1989.

THE ORLEANS EXPERIENCE IN TREATMENT OF SOFT TISSUE SARCOMAS WITH FAST NEUTRONS

N. Breteau, M. Demasure, B. Belgadi, B. Destembert, A. Favre.  
Centre Hospitalier Régional, Service de Radiothérapie, B.P. 6709, 45067 ORLEANS (Fr)

Since 1981, 63 patients with soft tissue sarcomas have been treated at the Orleans Neutrontherapy Facility. Results were evaluated in 1989.

23 Patients had to be excluded : 8 were lost of follow-up immediately after treatment and 15, referred for palliative treatment, received inadequate doses.

19 patients have been referred for neutrontherapy after a first series of X-Rays. 13 were treated using a photon-neutron mixed schedule regimen and 8 patients have been treated with neutrons.

The patient distribution according to histology is given on table 1.

Histology	Number
Fibrohistiocytosarcoma	10
Fibrosarcoma	6
Liposarcoma	5
Leiomyosarcoma	4
Synoviosarcoma	2
Rhabdomyosarcoma	2
Chordoma	5
Miscellaneous	6
<b>TOTAL</b>	<b>40</b>

Table 1 : Patient distribution according to histology.

Concerning the 40 evaluable patients, the sex ratio is balanced and the mid age is 47 years. The mid follow-up is 42 months (range from 12 to 94 months). 28 patients had trunk or abdominal locations (respectively 11 and 17), 11 had a limb tumor and one had a very advanced tumor of oral cavity. 11 patients had complete surgical resection, 12 had incomplete resection and 17 had inoperable tumors.

Immediate local control was observed in 32 patients. 8 relapsed from 10 to 22 months after treatment, 3 of them profited by surgical or brachytherapy salvage.

Table 2 gives the local control rate according to surgical procedure. Results for local control are summarized on Figure 1.

Local status	Persistent local control	Recurrence	Persistent disease
Surgical act			
Complete resection n = 11	9 (82 %)	2*	-
Incomplete resection n = 12	9 (75 %)	3**	-
Gross tumour or inoperable n = 17	6 (35 %)	3	8

\* 1 surgical salvage, 1 brachytherapy salvage  
\*\* 1 surgical salvage, 1 relapse out of field limits

Table 2 : Local control according to surgical procedure

At the time of evaluation, 22 patients were alive without evidence of disease with a mid follow-up of 30 months. 7 out of the 18 deceased patients were locally controlled.

As far as complications are concerned, side effects were not evaluable in 14 patients, 9 because of local control,

3 because of an additional treatment (2 surgery, 1 brachytherapy). For the last 2 patients, the only information was that they were locally free of disease.

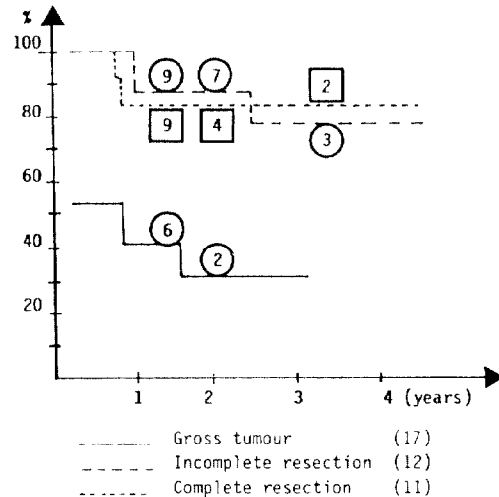


Figure 1 : Local control (Kaplan Meyer method)

After surgical act, 86 % of patient were alive with no evident disease.

When gross tumour was present, only 30 % of patients were alive and disease free. For the small number of analysed patients, there was no evidence of difference in local control according to the neutron dose proportion.

Institutions	Number of patients*	Local control (%)
Essen + Heidelberg 1983	60	31 (52 %)
Hammersmith, 1987	50	26 (52 %)
Hamburg, 1987	45	27 (60 %)
TAMVEC, 1980	29	18 (62 %)
Fermilaboratory, 1984	26	13 (50 %)
Seattle, 1986	21	15 (71 %)**
Louvain-La-Neuve, 1982	19	4 (21 %)
Orleans, 1990	17	6 (35 %)
Amsterdam, 1981	13	8 (61 %)
NIRS, 1979	12	7 (58 %)
Edinburg, 1986	12	5 (42 %)
MANTA, 1980	10	4 (40 %)
<b>Overall</b>	<b>314</b>	<b>164 (52 %)</b>

\* Patients treated de novo or for gross disease after surgery are included but not patients treated postoperatively for microscopic residual disease or for limited macroscopic residual disease.

\*\* Two-year actuarial data.

Modified from Wambersie (1990)

Table 3 : Review of the local control, rates for soft tissue sarcomas treated definitively with neutrontherapy.

For non operated patients, the local control rate as the results reported by Louvain-La-Neuve and Manta is generally worse than the other published results (table 3) (1). It must be partly explained by the high proportion of

very large tumours : 75 % of ours patients had tumour size larger than 10 cm (table 4).

Tumor size diameter	8 - 10 cm	11 - 28 cm
Local control	4 / 4	2 / 13

Table 4 : local control according to tumor size.

At the present time we intend to select patients with medium sized tumor for a whole treatment with neutrons only.

Reference :

1. Wambersie A., Fast neutron therapy at the end of 1988 - a survey of the clinical data. *Strahlenther. Onkol.*, 166, pp. 52-60 (Nr 1), 1990.

## NEUTRON THERAPY WITH $p(65) + \text{Be}$ NEUTRONS AT THE UCL CYCLOTRON OF LOUVAIN-LA-NEUVE

F. RICHARD, J. GUEULETTE, J. P. MEULDERS, P. PIHET, S. VYNCKIER and  
André WAMBERSIE

Université Catholique de Louvain, Unité de Radiothérapie, Neutron- et Curiothérapie,  
Cliniques Universitaires St-Luc, 1200-Brussels (Belgium)

### 1. Introduction

The neutron therapy programme at Louvain-la-Neuve is carried out with the cyclotron "CYCLONE" of the Université Catholique de Louvain designed for physics experiments (16). The cyclotron is located in the University Campus at the Physics Institute at 25km from the Cliniques Universitaires in Brussels.

The isochronous variable-energy cyclotron manufactured by CSF (France) accelerates different types of charged particles. Deuterons can be accelerated at energies ranging from 13 to 50 MeV and protons can be accelerated up to about 90 MeV. Beside medical applications, it is used for research in physics and chemistry as well for isotope production.

### 2. Description of the facility

The treatment room and related medical facilities are located one level below the main level of the cyclotron. This permits the use of a vertical therapeutic neutron beam by bending the deuteron or the proton beam.

Up to end of 1981, neutron beams used for therapeutic applications were produced by bombarding a 10mm thick Beryllium target with 50 MeV deuterons (16). This Beryllium target was mounted in a 7mm thick brass support, cooled with water. The maximum available deuteron energy at Cyclone (50 MeV) was selected. In a second stage, from 1982 up to now, neutron beams produced by bombarding a thicker (17mm) Beryllium target with 65 MeV protons were used (10). This change was made in order to improve the physical selectivity of the irradiation.

However to improve the  $p(65)+\text{Be}$  beam quality some modifications have been performed (9). Neutron spectra produced by protons on Beryllium differ in shape from those produced by deuterons, the former having 2 parts: a high energy extending almost to the energy of the incident protons and an intensive low energy component. A filtration with an homogeneous material such as polythene is then necessary to attenuate this low energy component.

The choice of the adequate filter, is always a compromise between an increase in depth dose and a reduction in the dose rate: at Louvain-la-Neuve, a 2cm thick polythene filter was selected.

Finally, in the prospect of initiating proton beam therapy (protons can be accelerated at CYCLONE up to about 90 MeV), the use of neutron beams produced by the same particles would be more practical if neutron therapy and proton therapy would be performed during the same session.

The collimation system consists of a fixed shielding and a series of interchangeable inserts (16). The shielding itself consists of a proximal part ("a precollimator") and a distal part in which the different inserts can be fitted and rotated along their vertical axis. The distal part is conical and consists of a steel mould filled with a mixture (50%) of epoxy and borax.

The precollimator, 50cm steel, which determines the largest available field (25cmx25cm) contains two independent transmission ionization chambers used as monitors and located about 25cm below the target.

The interchangeable inserts are cylindrical in shape; their height is 80cm and their external diameter 40cm. The proximal part (50cm) is a mixture of iron and epoxy and the distal part (30cm) is a mixture (50%) of borax and epoxy, which ensures an efficient definition of the beam. A set of 12 inserts is available with field sizes ranging from 6cmx8cm to 16cmx20cm (at a TSD of 157cm.). The field sizes can be modified -6% to +13% by varying the TSD from 147cm to 177cm. Due to their weight, positioning of the inserts requires an electro-hydraulic device.

### 3. Characteristics of the beams

The physical selectivity which can be reached with 50 MeV neutron beams is slightly better than that obtained, in usual conditions, with  $^{60}\text{Co}$  (10). For example, for a 10cmx10cm field at a TSD of 157cm, the 50% absorbed dose, on the axis, is obtained at 13.6cm in depth.

Irregular shaped fields are frequently used by inserting iron or better tungstene shielding blocks (12cm thick) (3) (4). These blocks are used to protect critical normal tissues. They are positioned on a perspex table just above the patient. The interposition of this perspex table (of 5mm thick required to support the heavy shielding blocks) destroys nearly completely the skin sparing.

This fact could be clearly noticed clinically (more heavy skin reactions), and was confirmed by measurements performed with a parallel plate ionization chamber..

For 50 MeV neutron beams skin sparing can be recovered completely (or even improved) by inserting 2mm lead beneath the perspex of the table; the surface dose then decreases down to 43%.

Improvement of skin sparing (surface dose: 41%) is observed by closing the collimator aperture with a 2 mm lead shield, which absorbs the charged particles produced inside the collimator.

#### 4. Activation problems:

Production of neutron beams from protons on Beryllium raises some activation problems (9). It has been observed that after several treatments with p(65)+Be neutrons, activation in the treatment room raised by a factor 2 if compared with activation levels after d(50)+Be treatments. In the beam axis, a significantly increase of activation irradiation was observed. Measurements indicated that this was mainly due to activation of the brass support of the Be target. A mechanical system, supporting two targets was then constructed in such a way that after each treatment, the irradiated target is automatically removed out of the beam line. A new target configuration was used since 1982.

A 17mm thick Beryllium target was used to raise the dose rate. Carbon was chosen as backing material to lower the gamma component and to reduce the low-energy component in the neutron spectra. The neutron beam was filtered with a hydrogenous material to further eliminate this low-energy component.

The 17mm Beryllium target together with the 10mm Be target are inserted in a movable brass support which allows the production of neutrons either by 65 MeV protons or by 50 MeV deuterons. The design of the new target assembly offers the possibility of transmitting the accelerated protons directly

#### 5 Radiobiology:

Different types of RBE determinations were performed: they were a part of the protherapeutic radiobiological program carried out at Louvain-La-Neuve.

The RBE varies, within large limits, as a function of the dose per fraction and the biological effect. For example, the RBE for the late tolerance of the central nervous system is particularly high. Relations between RBE and dose per fraction for early intestinal tolerance in mice were measured. Early intestinal tolerance was assessed from LD50 after selective abdominal irradiation. RBE increases with decreasing dose per fraction but reaches a plateau value of 2,6 when the gamma dose per fraction becomes smaller than about 3 Gy

Different RBE values were observed depending on biological system. For all the systems, RBE increases when decreasing dose.

The variation of neutron RBE as a function of energy was determined for different neutron beams.

An increasing RBE with decreasing neutron energy of the beam was observed.

#### 6. Clinical results

From the radiobiological data available, one could expect that hypoxic, slowly growing and well differentiated tumours would be a good indication for fast neutrontherapy.

It is now well recognized that the main indications for neutrontherapy are

- 1- Salivary gland tumours
- 2- Some head and neck tumours
- 3- Malignant melanomas
- 4- Soft tissue sarcomas
- 5- Prostatic adenocarcinomas

From March 1978 to December 1989, a total number of 1175 patients were treated at Louvain-La-Neuve (Table I)

##### A. Prostatic adenocarcinomas

From October 1979 to December 1988, 159 patients were treated for prostatic adenocarcinomas : 33 stage A, 12 stage B, 62 stage C and 32 stage D (8).

The present analysis, performed in March 1989, includes 62 patients with stage C, having a minimum follow-up of one year

In 34 patients, the tumour was present at the moment of neutrontherapy and in 28 patients, the treatment was started after TURP. The local control rate reaches 98% at one year, 95% at two years 82% at three years and 85% at 4 years.

The survival rate reaches 93% at one year, 82% at two years and 66,5 at three years and 57% at 4 years.

##### B. Soft tissue sarcomas:

Hundred evaluable patients with locally advanced soft tissue sarcomas were treated from March 1978 to March 1987 (6). They were analyzed in September 1987. The minimum follow-up was 6 months.

Excluding 22 intra-abdominal and 3 intrathoracic localizations, 75 patients are analyzed.

In a first group of 47 patients treated after radical surgery, a persistent local control was achieved in 91,5%.

In a second group of 28 patients with "gross" tumour present at the time of neutrontherapy, the local control was observed in only 15%. Survival rate is nearly independent on the presence or not of "gross" tumour at the time of neutron therapy (70% and 68% in the first and second group respectively).

Severe complications were observed in 12 cases (16%)

A correlation between complication rate and field size was observed. The large field sizes reflect generally the large initial tumour extent.

### 2 About the near future:

In October 1983, the therapeutic irradiations were stopped for 6 months in order to allow the construction of a second treatment room and the extension of the medical buildings. A new control desk has been developed including a dedicated HP86B computer. New monitoring systems have been developed and are now used for routine treatments.

The second treatment room is located at the same level and is adjacent to the first one. This room will be equipped with a horizontal beam and will be operational for 65 MeV neutrons in 1989.

Two 43° bending magnets bring the proton beam the main Cyclotron level down to the level of the treatment room.

Combination of a fixed vertical beam and of a fixed horizontal beam was preferred to an isocentric mounting. The vertical beam will be equipped with a variable multileaf collimator while the horizontal beam will be used with a set of interchangeable inserts.

The multileaf variable collimator designed by Dr. BRAHME is now under construction in our workshop in Louvain-La-Neuve. Of course, the length of the leaves had to be increased and adapted to the 65 MeV neutron beams.

Proton beam therapy is foreseen in the second irradiation room with the horizontal beam: 90 MeV protons are available. The Bragg Peak was measured at 6cm in depth in phantom. This proton beam appears to be suitable to treat choroidal melanomas, some cerebral lesions in children as well as some superficial tumours of the head and neck area.

### References

1. M. BEAUDUIN, J. GUEULETTE, J.P. MEULDERS, M. OCTAVE-PRIGNOT, B.M. DE COSTER and A.WAMBERSIE: Efficacité biologique relative (EBR) et effet oxygène (OER) des neutrons produits à partir de deutérons de 50 MeV et de protons de 34, 45, 65 et 75 MeV chez *Vicia Faba*. C.R. Soc. Biol., **178**, pp 219-223, 1984.
2. J. GUEULETTE, M. OCTAVE-PRIGNOT and A. WAMBERSIE: RBE of d(50)+Be neutrons, as a function of the dose per fraction, for early intestinal tolerance in mice. J. Eur. Radiother., **5**, n°3, pp 180-182, 1984.
3. F. RICHARD, J.P. MEULDERS, S. VYNCKIER, M. OCTAVE-PRIGNOT, A. POSSOZ and A.WAMBERSIE: Present status of the treatment planning for d(50)+Be Neutron Beams and mixed schedules at "cyclone". Supplement to strahlentherapie, **77**, pp 178-184, 1981 in G. Burger, A. Breit and J.J. Broerse (Ed) "Treatment planning for external beam therapy with neutrons" Urban and Schwarzenberg, Munchen-Wien, Baltimore, 1981.
4. F. RICHARD, S. VYNCKIER, S. MARQUEBROEUCQ, P. ROBERT, J.P. MEULDERS and A. WAMBERSIE: Recent development of the neutrontherapy facility at the Cyclotron "cyclone" in LLN. M.H. Schraube, G. Burger and J. Booz (Eds): fifth Symposium on neutron Dosimetry, Beam Dosimetry (vol 2), Munich- Neuherberg, 17-21 September 84. Commission of the European Communities, Eur 9762 en, Brussels Luxembourg, volume II, pp 1009-1017, 1985.
5. F. RICHARD, J. GUEULETTE, A. DUTREIX, J. VAN DAM and A. WAMBERSIE: RBE/Dose relationships for 650 MeV Helium ions, Californium-252 neutrons and fast neutrons obtained using 3 criteria in vegetal systems. Proceedings of third workshop on heavy charges particles in Biology and Medicine. GSI, Darmstadt, July 3-5, 1987.
6. F. RICHARD, L. RENARD and A. WAMBERSIE: Neutrontherapy of soft tissue sarcomas at the Louvain-la-Neuve Cyclotron-Interim results 1987. Workshop on Fast Neutron Radiotherapy, Neuherberg- Munich, October 16-17, 1987. (In Press)
7. F. RICHARD, L. RENARD, J. BONTE, J. VAN DAM and A. WAMBERSIE: Neutrontherapy of locally advanced uterine cervix carcinoma at Louvain-la-Neuve. Proceedings of the International workshop on Particle Therapy Meeting of the EORTC. Heavy Particle Therapy Group, Essen, October 28 and 29, 1988 (In Press).
8. F. RICHARD, N. BRETEAU, L. RENARD et A. WAMBERSIE: Current results of neutron therapy of locally advanced prostatic carcinomas (Stage C) at the UCL-Cliniques St Luc (Brussels). European Journal of Cancer and Clinical Oncology, vol 23, n°8, p1249, 1987.
9. S. VYNCKIER, P. PIHET, J.M. FLEMAL, J.P. MEULDERS and A. WAMBERSIE: Improvement of a p(65)+Be neutron beam for therapy at Cyclone, Louvain-La-Neuve. Phys. Med. Biol., vol 28, n°6, pp 685-691, 1983.
10. S. VYNCKIER, P. PIHET, M. OCTAVE-PRIGNOT, J.P. MEULDERS and A. WAMBERSIE: Comparison of neutron therapy beams produced by 50 MeV deuterons and 65 MeV protons on Beryllium. Acta Radiologica (Oncology Radiation therapy, Physics Biology), **21** Fasc 4 pp 281-287, 1982.
11. S. VYNCKIER, J.P. MEULDERS, P. ROBERT and A. WAMBERSIE: The protontherapy program at the cyclotron "cyclone" of Louvain-La-Neuve (first dosimetric result). J. Em. Radiother., **5**, pp 245-247, 1984.
12. S. VYNCKIER, F. RICHARD, J.P. MEULDERS and A. WAMBERSIE: Radiation protection at the neutron therapy facility in Louvain-La-Neuve. Proceedings of the EORTC Heavy Particle therapy Group, Clatterbridge May 1-3, 1986. The British Journal of Radiology, **60**, pp 310, 1987.
13. S. VYNCKIER, P. PIHET, J.P. MEULDERS, F. RICHARD and A. WAMBERSIE: Radiation protection at the Neutrontherapy facility at LLN. Annales de l'Association Belge de Radioprotection, vol 12, n°4, pp 303-313, 1987.
14. S. VYNCKIER, F. VANNEST, F. RICHARD, C. MICHEL, R. DEMEURE and A. WAMBERSIE: Quality control on patient positioning for neutron therapy using a PET- Scan proceedings of the international workshop on Particle therapy, Meeting of the EORTC. Heavy Particle therapy Group, Essen, October 28 and 29, pp 67, 1988.
15. A. WAMBERSIE: Radiobiological bases of fast neutrontherapy. Criteria for selecting the application modalities. J. Belge Radiol., **61**: pp 583-603, 1978.
16. A. WAMBERSIE, J.P. MEULDERS, F. RICHARD and M. OCTAVE-PRIGNOT: The fast neutron therapy at the Cyclotron "cyclone", Louvain-La-Neuve. J. Belge. Radiol., **61**, pp 571-582, 1978.

**PROSTATIC ADENOCARCINOMA (Stage A,B and C) TREATED BY  
NEUTRON THERAPY AT UCL LOUVAIN-LA-NEUVE**

F. RICHARD, L. RENARD AND A.WAMBERSIE

Université Catholique de Louvain, Unité de Radiothérapie, Neutron-et  
Curiothérapie, Cliniques Universitaires St-Luc,  
1200-Brussels (Belgium)

From March 1978 to December 1988, 1047 patients were treated at the UCL Cyclotron of Louvain-la-Neuve.

Due to the high energy neutrons available (d(50)+Be neutrons up to 1982 and later on p(65)+Be neutrons), a special effort has been made to treat deep seated tumours, mainly gynaecological tumours and prostatic adenocarcinomas (Table I) (1,2)

Among the 192 patients, with prostatic tumours, referred to neutrontherapy, 159 completed their treatment.

A combination of p (65)+Be neutrons and 18 MV X rays was used. The RTOG protocol designed for locally advanced tumours (C and D<sub>1</sub>) was followed but 3 neutron fractions and 2 photon fractions are given per week (2 Gy photon equivalent per session). (3)

A total dose of 50 Gy photon equivalent was delivered to a target volume encompassing the prostate and the pelvic nodes, with a boost of 16 Gy "photon equivalent" limited to the prostatic area.

A clinical RBE of 3 was chosen for d(50) + Be neutrons and 2.8 for p(65)+Be neutrons.

Sixty two patients were treated for stage C disease. Due to the excellent tumour response and tolerance observed for these locally extended tumours, some patients with more limited tumours were also referred to neutron therapy (33 stage A and 32 stage B patients). In addition, 32 stage D patients were treated.

Only the result obtained for the 62 patients with stage C disease are analyzed in the present paper. The tumour was present (biopsy only) in 34 cases and a trans-urethral resection of prostate (T.U.R.P) was performed in 28 cases.

The local recurrence rates and survivals are presented in table II (follow-up 1-5 years).

The clinically observed recurrences, as well as the positive biopsies in patients with no clinical evidence of local recurrence, are scored local failure.

At 2 years (n=39), 32 patients were alive and NED; 4 patients died with metastases but no local recurrence, 2 patients died with local recurrence and metastases and 1 patient died from intercurrent disease.

At 3 years (n=27), 15 patients were alive and NED. Three patients had a persisting positive biopsy but no clinical evolution. Six patients died with metastases but no local recurrence, 2 patients died with local recurrence and metastases and 1 patient died from intercurrent disease (Table III).

At 4 years (n=21), 9 patients were alive and NED; 1 patient was alive with a positive biopsy but no clinical evidence of evolution, 2 patients were alive with metastases but no local recurrence. Six patients died with metastases but no local recurrence, 2 patients died with local recurrence and metastases and 1 patient died from intercurrent disease.

Early and late tolerance was excellent and, in general, the patients could keep a normal social (and professional) life.

No severe complication was observed in the 62 patients treated for stage C. Only one severe complication (urethral structure and necrosis of the prostatic area) was observed in one patient, with stage A of prostatic adenocarcinoma treated with radiation after multiple TURP.

These data confirm the promising results of the pilot study by Franke (4,5) and the conclusions of the randomized trial initiated by the RTOG and reported by Russel (3).

**REFERENCES**

1. WAMBERSIE, A., MEULDERS, J.P., RICHARD, Fr. and OCTAVE-PRIGNOT, M.  
The fast neutrontherapy facility at the Cyclotron "Cyclone", Louvain-La-Neuve.  
*J. Belge Radiol. - Belgisch Tijdschr. Radiol.*, **61**, 571-582, 1978.
2. VYNCKIER, S., PIHET, P., FLEMAL, J.M., MEULDERS, J.P. and WAMBERSIE, A.  
Improvement of a p (65) + Be neutron beam for therapy at Cyclone, Louvain-La-Neuve.  
*Phys. Med. Biol.*, vol. 28 n° 6, pp. 685-691, 1983
3. RUSSELL, K.J., LARAMORE, G.E., KRALL, J.M., THORAMX, F.J., MAOR, M.H., HENDRICKSON, F.R., KRIEGER, J.N. and GRIFFIN, J.W.  
Eight years experience with neutron radiotherapy in the treatment of stages C and D prostate cancer: updated results of the RTOG 7704 randomized clinical trial. *Prostate* **11**: 183-193, 1987
4. FRANKE, H.D., LANGENDORFF, G. and HESS, A.  
Die strahlenbehandlung des prostata-carcinoms in stadium C mit schnellen neutronen, pp 175-185.  
*Verhandlungsbericht der Deutschen Gesellschaft für Urologie*, 32. Tagung 1980. Springer-Verlag, Berlin-Heidelberg-New-York, 1981
5. FRANKE, H.D.,  
Effect of fast neutrons on "radioresistant" undifferentiated prostatic cancer stage C/D1. Proceedings of the Annual Meeting of the EORTC Heavy Particle Therapy Group: Fast Neutron Radiotherapy, Klinik für Strahlentherapie und Radioonkologie, Westfälische Wilhelms  
Universität, Münster (Fed. Rep. of Germany), April 1990.

TABLE I

Total number of patients treated at the cyclotron "Cyclone" of Louvain-la-Neuve (March 1978 - December 1988)

Tumour type / site	YEAR										Total	
	1981	1982	1983	1984	1985	1986	1987	1988	1989	1990		
Soft tissues sarcomas	5	17	21	14	10	11	6	15	9	13	18	139
Osteosarcomas	2	7	4	7	4	2	-	-	8	3	8	45
Gynaecological tumours	6	42	35	32	29	20	17	26	30	40	45	330
Head and neck tumours	3	2	-	-	-	1	7	6	4	4	23	23
Bladder carcinomas	1	5	8	12	12	7	3	11	11	11	10	91
Bronchus carcinomas	-	9	24	13	9	4	6	16	5	8	2	96
Prostate carcinomas	-	4	12	12	10	11	19	20	15	29	52	192
Salivary gland tumours	-	2	2	3	2	-	-	-	3	3	3	18
Miscellaneous	-	0	12	3	13	6	1	17	23	10	20	113
Total	17	96	110	96	89	62	52	120	118	121	150	1047

\* Break of 3 months in 1983 and of 6 months in 1984 for enlargement of the facilities.

Table II

Follow up	1 year		2 years		3 years		4 years		5 years			
	Biop.	TURP	Biop.	TURP	Biop.	TURP	Biop.	TURP	Biop.	TURP		
alive	25/25	19/22	44/47	91%	17/19	15/20	32/39	82%	8/11	10/16	18/22	82%
dead	-	-	-	-	-	-	-	-	-	-	-	-
recurrent disease	0/25	1/22	1/47	2%	1/19	1/19	2/20	5%	1/11	1/15	2/26	7.50%
positive biopsy (cases clinically controlled)	-	-	-	-	-	-	-	-	+	+	+	+
Total	0/25	1/22	1/47	2%	1/19	1/19	2/20	5%	1/11	1/15	2/26	7.50%
Local recurrence	-	-	-	-	-	-	-	-	+	+	+	+
Biop.	-	-	-	-	3/11	2/15	5/26	19%	2/6	1/7	3/13	23%
TURP	-	-	-	-	2/15	2/15	5/26	19%	2/6	1/7	3/13	23%

Table III

LOCAL RECURRENCE AND SURVIVAL AT 3 YEARS

	Tumour present TURP		TOTAL
Alive NED	6	9	15
Alive REC-META+	-	-	-
Alive REC+META+	-	-	-
Alive REC+META-	2***	1***	3***
Dead REC-META+	2	4	6
Dead REC+META+	1	1	2
Dead REC-META-	-	1*	1*
TOTAL	11	15	27
TOTAL LOCAL REC.	3/11***	2/16***	5/27***(18%)
Alive	8/11	10/16*	18/27*(66,5%)
*** patients with positive biopsy. No clinical evidence of evolution.			
* 1 patient dead from intercurrent disease			



## RESULTS OF COMBINED PHOTON-NEUTRON-RADIOTHERAPY FOR SOFT TISSUE SARCOMAS

J. Romahn<sup>1</sup>, R. Engenhardt<sup>1</sup>, B. Kimmig<sup>1</sup>, K.H. Höver<sup>2</sup>, M. Wannemacher<sup>1</sup>

<sup>1</sup>Department of Clinical Radiology (Radiotherapy), University of Heidelberg

<sup>2</sup>German Cancer Research Center, Heidelberg

### Introduction

Soft tissue sarcomas are locally aggressive tumors, that are capable of invasive and destructive growth and distant metastases. Frequency and onset of metastases depends on histopathological classification and more at all on histopathological grading (1).

Soft tissue sarcomas are relatively rare tumors, compared with carcinomas and other neoplasms. They account for about 1% of all cancers, but for 2% of all cancer deaths (1). Sarcomas are more often found in elder people, but there do not exist a predominant age group.

Embryologically they are of mesodermal and neuroectodermal origin, and they can show the whole spectrum of differentiation. Furthermore different types of differentiation can be found in one tumor and so there are existing a large number of different pathological subgroups.

The classification system of the World Health Organization (WHO) is based on 16 different tumor categories, but in about 10-15% a classification is not possible, so that these tumors are classified as "uncertain histological type" (2).

Clinical experiences show that histopathological classification do not play the major role in estimating tumor malignancy. Malignancy is determined in a grading system by assessment of different histopathological features as: cellularity, pleomorphism, mitosis frequency, necrosis, infiltration and invasive tumorgrowth (2). This procedure is

relative subjective, but it is the best tool to estimate the tumor prognosis and it helps to find the best treatment for the individual patient.

Different grading systems are used, three level systems as well as four level systems (3,4). The lifetable results are not very different, but different grading systems make communication among oncologist difficult, because especially "Grade II sarcoma" does not always mean the same.

Because of the fact, that different types of malignancy can be found in one tumor, needle aspiration techniques have to fail in evaluation of malignancy. So incisional biopsy is the appropriate technique.

The major problem in treatment of soft tissue sarcoma is to gain local control to primary tumor. The treatment of choice is surgery. Surgical treatment differs from hospital to hospital, depending on the surgeons and their experience in treating soft tissue sarcomas. Recurrences are possible after each surgical treatment, but Enneking pointed out, that recurrence rate depends on the possibility to achieve radical resection margins (5).

In spite to that fact, in the last few years experienced surgeons prefer limb salvage methods. This is the reason why radiotherapy had become more frequent in that period.

### Material and Methodes

In our collective we found a spectrum of surgical interventions ranging from local incision to muscle compartment resection. Since 1986 we treated 45 patients with soft tissue sarcoma. Distribution of sex and average age do not differ from literatur. 35 patients had only locoregional tumors, the remaining 10 patients had both, local disease and distant metastases at the beginning of radiotherapy.

In spite of the importance of a correct histopathological grading 50% of our patients remained unclassified.

40 patients underwent prior surgery, most of the patients several times. Only 5 patients got primary radiotherapy, because of inoperable tumorsituation or patients constitution.

31 of these patients underwent radiotherapy according to our mixed beam schedule from 1/86 to 6/89. A photon or electron therapy of 40 Gy in conventional fractionation was followed by a neutron boost with a medium neutron dose of 8.3 Gy. Neutrons were delivered with the 14 MeV DT-generator at the German Cancer Research Center, three times per week with a single total dose of 1 Gy. So we delivered a photonäquivalent dose of up to 70 Gy.

### Results

It was obvious that the intervalls between the surgical interventions became shorter and shorter from recurrence to recurrence. That was the reason to compare the last recurrence free interval before irradiation to that after radiotherapy. Medium recurrence free interval after radiotherapy was 2.2 years. Before radiotherapy the medium recurrence free interval lasted only 1.6 years. So onset of recurrence after radiation seemed to be prolonged.

31 patients treated with the mixed beam schedule, and 24 of them are still alive. The results of our patient group is shown in table 1.

Local recurrence was seen more often in the M 1 group, may be due to a worse grade of malignancy in these tumors.

Medium survival is now 3.5 years with a median of 3.1 years. This means, that in our collective 50% now have a recurrence free survival of more than 3 years.

Tab. 1:

		M <sub>0</sub>	M <sub>1</sub>
Number of patients:	31	24	7
Survival	24	21	3
Death	7	3	4
Cause of death:			
Local recurrence	4	1	3
Metastases	3	2	1

### Conclusion

The evaluation from Cantin and Mc.Neer (6) demonstrates that more than 80% of all local recurrences occur during the first 3 years. Our patients now have a median follow up of more than 3 years. That means, we are allowed to hope, that only 2 or 3 patients will get further local recurrences. Longer follow up period will make sure, whether this estimation was true or not.

Surgery still is the first mainstay in any treatment approach to achieve local control of soft tissue sarcoma. But in all recurrent sarcoma as well as in all those patients without a complete (R0) resection (limb sparing, inoperable tumor situation) radiotherapy is necessary to reach the results of radical surgery.

We see an indication for radiation therapy with fast neutrons especially in all those patients with low grade sarcoma, because of the low proliferation rate of these tumors and the high LET effect of neutron beams.

**References**

1. Enzinger F.M., Weiss S.W.: Soft tissue tumors; The C.V. Mosby Company (1983) 1-18
2. Enzinger F.M., Lattes R., Tortonoi R.: Histological typing of soft tissue tumors. International Histological Classification of Tumors No.3 Geneva, World Health Organization, 1969
3. Markhede G., Angervall L., Steiner B.: A Multivariate Analysis of the Prognosis after Surgical Treatment of Malignant Soft Tissue Tumors. *Cancer* 49:1721, 1982
4. Myhre-Jensen O., Kaae S., Madsen E.H.: Histopathological Grading in Soft Tissue Tumors. Relation to Survival in 261 Surgically Treated Patients. *Acta Pathol Microbiol Immunol Scand* 91:145, 1983
5. Eneking W.F.: Musculoskeletal Tumor Surgery. Churchill Livingstone, New York 1983
6. Cantin J., Mc Neer G.P., Chu F.C. The Problem of Local Recurrence after treatment of Soft Tissue Sarcoma. *Ann Surg* 168:47-53, 1968

## REVIEW OF MEDICAL TREATMENT WITH HEAVY CHARGED PARTICLE BEAMS

Joseph R. Castro, M.D.

University of California Lawrence Berkeley Laboratory  
 Building 55, Mailstop 121  
 Berkeley, CA 94720 USA

Abstract

Particle beams including both neutrons and charged particles have been studied in a number of medical facilities in several countries during the past 2 decades. Only in recent years have beam delivery techniques, treatment planning and clinical utilization of these beams begun to be optimized. Neutrons do not have a dose localization advantage when compared to standard X-ray therapy, but do offer some high LET biological advantages for certain types. Charged particles have distinct dose distribution advantages leading to a higher ratio of dose in the tumor compared to adjacent normal structures. This improvement of the therapeutic ratio has led to higher local control rates and prolongation of survival for a number of tumors adjacent to critical structures such as the brain and spinal cord. Heavy charged particles offer additional biological advantages to their physical dose localization parameters. Promise of improved control of unresectable, slowly proliferating tumors such as those arising in bone, soft tissue, prostate and salivary gland has been seen in preliminary studies. Further research in optimization of therapy techniques with heavy charged particles is warranted to maximize the potential benefit of the use of heavy charged particles in medical therapy.

Introduction

With the advent of improved diagnostic techniques for tumor localization, including computerized tomography (CT), magnetic resonance imaging (MRI), and positron emission tomography (PET), and reliable linear accelerators for hospital use, local and regional control of unresectable neoplasms has steadily increased. However, even with modern megavoltage radiotherapy, and multimodality treatment, including irradiation, chemotherapy and surgery, some human tumors remain resistant to therapy. Often their treatment by standard radiation techniques would require unacceptably high doses to nearby normal structures with loss of structural integrity or function. Heavy charged particle radiotherapy is almost unique in value where unresectable tumors lie in or near critical structures and may be the only treatment which can be successfully accomplished with preservation of quality of life.

Using heavy ion beams, significant advantages accrue in safely delivering high doses of radiation to tumors adjacent to the eye, brain, cranial nerves, spinal cord, heart, esophagus, kidney, intestine, bladder, and other vital structures.

This ability to deliver a lethal tumor dose while maintaining the dose to nearby critical structures at safe levels is a hallmark of heavy charged particle treatment, which we have termed dose-localization therapy. When this treatment is done with protons or helium ions, the physical dose-localization advantage is paramount [3,4,6], with heavier ions such as carbon or neon, the biological advantages of high LET energy deposition are also present. Evidence has been gathered both from laboratory experiments and preliminary human trials that the high LET component of heavy ion treatment is effective in destroying some tumors which are radioresistant to standard low LET X-ray treatment

[2,5,10,11,16,18]. The rationale for the use of heavy charged particles in the treatment of human cancers is therefore based on:

1. The precise delivery of radiation dose to the tumor with a significantly lower dose to surrounding normal tissues.
2. The deposition of biologically more effective high LET radiation, affording a higher chance of tumor destruction.

Over the past several decades, research studies in the use of these heavy charged particles have been undertaken at the University of California Lawrence Berkeley Laboratory. In the early 1970s with the availability of the Bevatron for biology and medicine, a series of pretherapeutic studies were begun on the biophysical effects of heavy ion beams of interest in the treatment of human cancers [1,2,18,19]. The effects on cells, tissues and tumors relative to heavy ions were studied extensively in the laboratory as support for the human clinical research trial which began in 1975.

The goals of the clinical research trial are:

1. To develop the best methods for clinical use of heavy ions in the treatment of human cancers.
2. To demonstrate the clinical effectiveness of these beams for various human tumors.

About 1200 patients have been treated starting with helium ions in 1975 and progressing to heavier ions such as carbon, neon, silicon and argon. However, extensive availability of neon ions for Phase I-II studies did not occur until 1981 (Table 1).

Current prospective trials underway at LBL include:

1. Randomized Phase III trial of helium ions versus I125 plaque therapy for uveal melanoma.
2. Randomized Phase II dose searching study for head and neck chordoma/chondrosarcoma.
3. Randomized Phase III trial for carcinoma of the prostate (neon vs megavoltage X-ray).
4. Randomized Phase II trial of helium versus neon for sarcoma, base of skull tumors, unusual histology.
5. Randomized Phase II dose searching study for glioblastoma of the brain.

Helium Ions

The hallmark of dose localization therapy with protons and helium ions is the superb dose distribution available secondary to the physical parameters of these beams. A high level of control can be achieved for unresectable tumors in critical locations because the tumor dose can be increased by 20-40% over that

Table 1

Patients treated at LBL	
1975 - 1989	
Helium Only	616
Helium + Xray	157
Neon Only	88
Neon + Other	282
Other Heavy Ions	29
TOTALS	1172

possible with low LET Xray therapy.

Clinical trials with protons or helium ions have shown excellent tumor control results in a number of tumor sites [3,4,7,15,20] in the skull, orbit, nasopharynx, paranasal sinuses, and for soft tissue and bony tumors in other parts of the body. We have now treated about 40 patients with the helium ion beam for tumors of the paranasal sinuses and nasopharynx invading the base of skull, paraaortic lymphatic metastases, or unresectable soft tissue tumors in the retroperitoneum or pelvis. In these selected patients, long term local control rates of approximately 60% have been achieved.

We have also treated 123 patients with helium charged particle irradiation for chordoma, chondrosarcoma, or meningioma of the skull base or juxtaspinal area after partial surgical excision. Overall control of tumor in the irradiated volume was obtained in 78 of 123 patients (63%), with tumor control rates greater than 80% in patients with small tumors (less than 20 cc). The median followup in 86 living patients is 34 months and in all 123 patients is 31 months, range 4-153 months. Crude local control rates are highest in meningioma (84%) followed by chondrosarcoma (65%) and chordoma (60%). The actuarial survival calculated by the Kaplan-Meier method is 68% at 5 years and 50% at 9 years post treatment.

The results of treatment in 328 patients with localized melanoma arising in the choroid lining of the eye were also excellent [8,12,13,14]. A local tumor control rate of 97% with followup from 3 to 139 months (median: 48 months) was achieved. Nine of 328 patients with local failure of initial helium ion treatment received further treatment with enucleation (5 pts), reirradiation (3 pts) or laser therapy (1 pt). Tumor control was excellent at all studied dose levels of 5000-8000 centiGray equivalent.

Overall, 85% of patients have avoided the need for enucleation of their eyes and a significant number have kept useful vision. Of 291 patients who had pretreatment visual acuity of 20/400 or better, 145 (50%) retained useful post treatment vision of 20/400 or better (Table 2). The actuarial survival is 80% at 5 years, because about 20% of patients have developed distant metastases, a rate which is the same when using surgical removal of the eye as local treatment for the tumor in the eye. Risk factors for the development of metastatic disease outside the eye have been studied and we hope to develop adjuvant treatment for patients at high risk for metastases.

We are currently carrying out a randomized trial to better define the role of helium ions versus 125 Iodine plaque therapy in the treatment of melanoma of the eyes. One hundred sixty patients have been entered in this Phase III study which will help to define which lesions are best treated with charged particles and which might be well treated by plaque therapy. We also envision the future use of proton or helium beams to treat other tumors of the eyes such as retinoblastoma in infants in order to prevent the need for enucleation.

For more than 100 patients with esophageal, pancreatic, gastric and biliary tract tumors, helium ion therapy was well tolerated but produced only a modest improvement in local control and little impact on survival [9]; these results might be improved in the future with dynamic conformal charged particle therapy where higher tumor doses might be possible.

Limitations on beam availability at UCLBL have not permitted that all possible tumor sites for proton or helium ion therapy be tried as yet. Collaborative studies with the Massachusetts General Hospital-Harvard Cyclotron Department of Radiation Medicine, the Proton Treatment Facility at Loma Linda Medical School, the National Institute of Radiological Sciences of Japan, and the University of Heidelberg-GSI, Darmstadt, West Germany are planned or underway to increase the numbers of patients entered in clinical research trials [17].

#### Heavier Ions

For high LET ions such as carbon, neon or silicon, significant biologic potential is added to the physical dose attributes of charged particles. These ions are more effective in destroying hypoxic tumors and can overcome some of the normal repair mechanisms of radiation damage. With the use of their advantageous dose distributions, the major radiation damage is largely confined to the tumor volume rather than nearby normal tissues. Preliminary studies have been done with neon ions at LBL with promising results in several sites especially in tumors of bone and soft tissue with slow growth rates. Other potentially valuable ions such as carbon or silicon have been tested only sparingly because of limited beam availability. Although patient numbers are relatively small because of the need for proceeding slowly to assure patient safety, and the advanced nature of the neoplasms, we have accrued 239 patients in the preliminary neon ion research trial [10].

For locally advanced tumors of the salivary gland, prostate gland, bone and soft tissue, biliary tract, nasal cavity, nasopharynx and paranasal sinus, there are local control rates which range from 40-90% (Table 3). These tumors are often not completely resectable and tend to be resistant to standard radiotherapy, probably because of their ability to repair low LET radiation damage. We believe these results are promising in comparison to results with standard Xray therapy and are currently carrying out additional prospective trials to further define the role of high LET charged particle radiotherapy in the treatment of cancer.

Other advanced tumors such as those arising in the pancreas, stomach or esophagus did not fare so well although the results were at least equal to standard radiation modalities. This is felt to be due to the proximity of intestine which limited the dose, even using heavy ions, and the radioresistance of these tumors. It is planned to restudy these tumors in the future with the scanned beam delivery techniques and with radiosensitizing drugs to try to augment the

Table 2  
Results in Helium Ion Radiotherapy  
Lawrence Berkeley Laboratory  
1975 - 1988

Tumor Treated	Pts	Local Control	Median Followup
Chordoma Chondrosarcoma Meningioma	123	78/123 (63%)	31 mos (4-153 mos)
Other Tumors (Skull, sinuses, soft tissue)	38	25/38 (65%)	25 mos (2-133 mos)
Uveal Melanoma	328	319/328 (97%)	46 mos (3-146 mos)

effect of heavy ion irradiation on these tumors.

We also continue to search for reasons to explain why some tumors are susceptible to high LET charged particle therapy. We believe the ability to deliver higher local doses with charged particles is part of the explanation, but there are important biological reasons which require further elucidation. Since some tumors are resistant to standard radiotherapy, effective predictive assays are needed which would determine in advance if an individual's tumor was more susceptible to high LET charged particle radiotherapy than other modalities of treatment. Such techniques as pretherapy sampling of an individual tumor to determine its growth characteristics or radiation sensitivity would enable improved selection of patients for high LET therapy and could lead to treatment tailored to an individual patient.

Optimization of beam delivery and treatment techniques including three-dimensional dynamic conformal particle therapy will permit improved irradiation of irregular tumors. Such a scanning beam technique is now being developed at UCLBL and should lead to further advances in tumor control. Coupled with improved treatment delivery, improvements in therapy planning will include better techniques to localize the tumor, optimization of 3-dimensional radiation treatment planning, refining techniques for transfer of data from one imaging modality to another such as from MRI scans or PET scans, integration of PET scanning into radiation treatment planning and improved systems for monitoring patient positional stability during the treatment.

One of the unique attributes of heavy charged particles is the possibility to utilize a small beam of radioactive particles such as  $^{19}\text{Ne}$  to be injected into the tumor just prior to treatment. This radioactive beam emits positrons which can be measured outside the body by their X-ray emission. Thus the stopping area of the charged particles can be accurately imaged and matched to the previously determined tumor volume. This technique was developed at UCLBL and has been successfully demonstrated in both animal and human studies. It has great potential as a clinical tool to independently verify the accuracy of treatment planning and delivery.

It has been estimated that 5-10% of patients treated with curative radiotherapy could benefit from heavy charged particle treatment, either with light ions such as protons or helium ions or heavier ions such as carbon. With approximately 200,000 cancer patients treated definitively with radiotherapy per year in the United States, this suggests that as many

as 10,000 patients per year could benefit from charged particle therapy.

As a national need for 4-6 such centers might exist in the United States, we propose continuation of the heavy charged particle radiation oncology program in the form of a Biomedical Heavy Ion Center at LBL for continued studies in heavy ion medicine and biology. Using the existing space, shielding, and local injector, a strong-focused synchrotron could be realized for less than the cost of a proton center alone at a new off-site facility. This would provide both proton and heavy ion research capabilities with an in-place, experienced team of physicians, physicists, biologists, biophysicists, accelerator engineers, computer scientists and other personnel. Such a center would be hospital-optimized and benefit from the highly sophisticated medical resources in this area. In addition to medical studies, important biological and physical research could also be accomplished such as studies of effects of cosmic particles which would be encountered in manned space flights.

Similar proposed heavy ion facilities at NIRS, Japan, GSI-Heidelberg, Germany and/or EULIMA (European Community) would be vital for continued study of heavy ion medicine. A comprehensive program, benefiting from expertise in such fields as medicine, biology, biophysics, accelerator physics and engineering, radiation chemistry, genetics, computer science and biostatistics is needed. Only through multidisciplinary research can we determine the most effective use of heavy ions in medicine and biology.

#### Summary

1. Protons and helium ions are highly effective in irradiation of many locally advanced, unresectable tumors adjacent to critical structures.
2. High LET ions such as carbon or neon ions have important biological properties in addition to dose localization parameters which may make them more effective in treating some human tumors.
3. A new Biomedical Heavy Ion Center is proposed at UCLBL to continue the biophysical and clinical studies in heavy ion medicine.

Table 3

## Phase I-II Neon Ion Trial Results

Site	Neon	Results with Standard Therapy UCSF
Glioblastoma Brain	Med Survival-13.7 mos (n=13 pts)	Med Survival-9-12 mos
Nasopharynx, Paranasal Sinus	Loc Con-16/24 (67%) Med Follow=18 mos (4-85 mos)	Loc Con-21%
Salivary Gland	Loc Con-11/14 (79%) Med Follow=13 mos (5-91 mos)	Loc Con-28%
Prostate	Loc Con-12/13 (92%) Med Follow=28 mos (11-60 mos)	Loc Con-60%
Sarcoma	Loc Con-21/36 (58%) Med Follow=15 mos (3-76 mos)	Loc Con-28%
Pancreas, Stomach, Biliary Tract	Loc Con-10/78 (15%) Med Survival-8 mos	Loc Con-20%

Loc Con = Local control in irradiated area. Med Follow = Median followup from time of radiotherapy. Med Survival = Actuarial medial survival (Kaplan-Meier method).

AppendixDefinitions

**Heavy Ion** - Electrically charged nuclei of chemical elements. The term "Heavy" is somewhat arbitrary but it typically implies an ion heavier than protons or helium.

**LET** - Linear Energy Transfer refers to the rate at which energy is deposited as it passes through tissue. It does this by ionizing (stripping electrons from) the atoms that it encounters. LET depends on the type of radiation and its energy. In general, the more massive the particle and the greater its charge, the higher its LET. Xrays, protons and helium ions are characterized by low LET whereas carbon, neon and silicon ions are examples of high LET radiations.

**RBE** - Relative Biological Effectiveness is a term that compares the effects of different types of radiation, generally with the standar being Xrays. Radiations that have high LET also have high RBE for effects on human tissues or tumors.

**Heavy Charged Particles** - These particles are the electrically charged nuclei of chemical elements. They may range in mass from light elements like hydrogen (protons) or helium to nuclei many times heavier like carbon, neon, silicon or iron.

**Treatment Planning** - Process of using tumor imaging studies such as CT (computer tomographic scans) and a powerful computer to map out the radiation dose distribution in the body. Such plans are optimized to find the best way to irradiate a patient's tumor.

**MRI** - Magnetic Resonance Imaging scanning makes use of magnetic fields to image structures within the body.

**PET** - Positron Emission Tomography scanning images radiation produced by certain trace radiochemicals injected into the body and gives both an anatomical and

physiological picture of the imaged organs.

**Megavoltage Irradiation** - (Low LET) Irradiation produced generally by linear accelerators for hospital use in treating human tumors, in ranges from 4-20 MeV. These are usually Xrays but electron beam therapy in similar energy ranges may be employed for relatively superficial treatment.

References

1. E.A. Blakely, J.T. Lyman, G.T.Y. Chen, J.R. Castro, P.Y. Chang and L. Lommel, "Radiobiological Studies for Helium Ion Therapy of Uveal Melanoma," *Int. J. Rad. Onc. Biol. Phys.*, vol. 11, Supp. 1, p. 134, September 1985 (abstract).
2. E.A. Blakely, J.R. Castro, M.M. Austin-Seymour, G.T.Y. Chen, L. Lommel and M.J. Yezzi, "Clinical and Cellular Radiobiological Studies of Silicon Ion Beams," *Int. J. Rad. Onc. Biol. Phys.*, vol 10, Supp. 2, October 1984 (abstract).
3. A.M. Berson, J.R. Castro, P. Petti, T.L. Phillips, G.E. Gauger, P. Gutin, J.M. Collier, S.D. Henderson and K. Baken-Brown, "Charged Particle Irradiation of Chordoma and Chondrosarcoma of the Base of Skull and Cervical Spine: The Lawrence Berkeley Laboratory Experience," *Int. J. Rad. Onc. Biol. Phys.*, vol. 15, No. 3, pp. 559-565, September 1988.
4. J.R. Castro, J.M. Collier, P.L. Petti, V. Nowakowski, G.T.Y. Chen, J.T. Lyman, D.E. Linstadt, G. Gauger, P. Gutin, M. Decker, T.L. Phillips and K. Baken-Brown, "Charged Particle Radiotherapy for Lesions Encircling the Brain Stem or Spinal Cord," *Int. J. Rad. Onc. Biol. Phys.*, vol. 17, No. 3, pp. 477-484, September 1989.

5. J.R. Castro, G. Gademann, J.M. Collier, D. Linstadt, S. Pitluck, K. Woodruff, G. Gauger, P. Gutin, T.L. Phillips, W. Chu and S. Henderson, "Strahlentherapie Mit Schwere Teilchen Am Lawrence Berkeley Laboratory Der Universitat Von Kalifornien," Strahlentherapie Und Onkologie, vol. 163, No. 1, pp. 9-16, 1987.
6. J.R. Castro, G.T.Y. Chen and E.A. Blakely, "Current Considerations in Heavy Charged Particle Radiotherapy," Radiation Research, vol. 104, No. 2, pp. S263-S271, November 1985.
7. J.R. Castro and M.M. Reimers, "Charged Particle Radiotherapy of Selected Tumors in the Head and Neck," Int. J. Rad. Onc. Biol. Phys., vol. 14, No. 4, pp 711-720, April 1988.
8. M. Decker, J.R. Castro, D. Linstadt, P.L. Petti, J.M. Quivey and D. Char, "Ciliary Body Melanomas Treated with Helium Particle Radiation," presented at the 1989 annual meeting of the American Society for Therapeutic Radiology and Oncology in San Francisco, CA, October 1989. In press, Int. J. Rad. Onc. Bio. Phys.
9. D. Linstadt, J.M. Quivey, J.R. Castro, Y. Andejas, T.L. Phillips, J. Hannigan and M. Gribble, "Comparisons of Helium Ion Radiation Therapy and Split-Course Megavoltage Irradiation for Unresectable Adenocarcinoma of the Pancreas," Radiology, vol. 168, pp. 261-264, 1988.
10. D. Linstadt, J.R. Castro and T.L. Phillips, "Results of the Phase I-II Neon Trial at Lawrence Berkeley Laboratory, in press: Int. J. Rad. Onc. Bio. Phys.
11. D. Linstadt, E.A. Blakely, T.L. Phillips and J.R. Castro, "Radiosensitization Produced by Iododeoxyuridine with High Linear Energy Transfer Heavy Ion Beams," Int. J. Rad. Onc. Biol. Phys., vol. 15, No. 3, pp. 703-710, September 1988.
12. D. Linstadt, D. Char, J.R. Castro, T.L. Phillips, J.M. Quivey, M. Reimers, J. Hannigan and J.M. Collier, "Vision Following Helium Ion Radiotherapy of Uveal Melanoma: A Northern California Oncology Group Study," Int. J. Rad. Onc. Biol. Phys., vol. 15, pp. 347-352, August 1988.
13. D. Linstadt, J.R. Castro, M. Decker, J.M. Quivey, D. Char and T.L. Phillips, "Long Term Results of Helium Ion Radiotherapy for Uveal Melanoma," presented at the 1989 annual meeting of the American Society for Therapeutic Radiology and Oncology in San Francisco, CA, October 1989. In press, Int. J. Rad. Onc. Bio. Phys.
14. V. Nowakowski, G. Ivery, J.R. Castro, D. Char, D.E. Linstadt, D. Ahn, T.L. Phillips, J.M. Quivey, M. Decker, P.L. Petti and J.M. Collier, "Metastases in Uveal Melanoma Treated with Helium Ion Irradiation," in press: Radiology.
15. V. Nowakowski, J.R. Castro, P.L. Petti, J.M. Collier, I. Daftari, D. Linstadt and T.L. Phillips, "Charged Particle Radiotherapy of Paraspinal Tumors," presented at NCI Workshop on Effects of Superior Dose Distributor in Bethesda, MD, April 1989. Submitted: Int. J. Rad. Onc. Biol. Phys.
16. M. Reimers, J.R. Castro, D. Linstadt, J.M. Collier, S. Henderson, J. Hannigan and T.L. Phillips, "Heavy Charged Particle Radiotherapy of Bone and Soft Tissue Sarcoma: A Phase I-II Trial of the University of California Lawrence Berkeley Laboratory and the Northern California Oncology Group," Am. J. Clin. Oncol. (CCT), vol. 9, No. 6, pp. 488-493, December 1986.
17. H.J. Suit, T.G. Griffin, J.R. Castro and L.J. Verhey, "Particle Radiation Therapy Research Plan," in Radiation Oncology Research Directions 1987. Am. J. Clin. Oncol. (CCT), vol. 11, No. 3, pp. 330-341, June 1988.
18. C.A. Tobias, E.A. Blakely, E.L. Alpen, J.R. Castro, E.J. Ainsworth, S.B. Curtis, F.Q.H. Ngo, A. Rodriguez, R.J. Roots, T. Tenforde and T.C.H. Yang, "Molecular and Cellular Radiobiology of Heavy Ions," Int. J. Rad. Onc. Biol. Phys., vol. 8, pp. 2109-2120, December 1982.
19. C.A. Tobias, E.L. Alpen, E.A. Blakely, J.R. Castro, A. Chatterjee, G.T.Y. Chen, S.B. Curtis, J. Howard, J.T. Lyman and F.Q.H. Ngo, "Radiobiological Basis for Heavy Ion Therapy," M. Abe, K. Sakamoto and T.L. Phillips, eds. Treatment of Radioresistant Cancers. North Holland: Elsevier Biomedical Press, 1979, pp. 159-183.
20. S.R. Zink, J.T. Lyman, J.R. Castro, G.T.Y. Chen, J.M. Collier and W.M. Saunders, "Treatment Planning Study for Carcinoma of the Esophagus: Helium Ions Versus Photons," Int. J. Rad. Onc. Biol. Phys., vol. 14, No. 5, pp. 993-1000, May 1988.

Supported by USPHS NIH-NCI CA19138 and DOE Contract AC03-76SF00098.



# HEAVY-CHARGED-PARTICLE RADIOSURGERY FOR INTRACRANIAL VASCULAR DISORDERS

## CLINICAL RESULTS OF 350 PATIENTS

J. I. Fabrikant,\* R. P. Levy,\* G. K. Steinberg,+ G. D. Silverberg,+ K. A. Frankel,\* M. H. Phillips,\* J. T. Lyman\*

\*Donner Laboratory and Donner Pavilion, Lawrence Berkeley Laboratory, University of California, Berkeley, California 94720 and

+Division of Neurosurgery, Stanford University Medical Center, Stanford, California, 94305, USA

**Abstract:** Under multi-institutional approved protocols, we have treated over 375 patients with inoperable intracranial arteriovenous malformations with stereotactic charged-particle (helium ions) Bragg peak radiosurgery at Lawrence Berkeley Laboratory. We have had a long-term dose-searching clinical trial protocol in place with two university centers and have followed more than 230 patients for more than 2 y. Doses ranged initially from 45 to 35 GyE, and now doses of 25, 20, 15 and, under special circumstances, 10 GyE, depending on a number of factors, are being evaluated. This represents a relatively homogeneous dose distribution with the 90% isodose to the periphery of the lesion. For complete radiation-induced obliteration, there is a relationship of dose and volume primarily, and location secondarily. When the entire arterial phase of the AVM has been included in the radiosurgical field, the rates for complete obliteration 3 y post-treatment are: 90-95% for volumes  $\leq 4$  cm<sup>3</sup>, 90-95% for volumes  $> 4$  cm<sup>3</sup> and  $\leq 14$  cm<sup>3</sup>, 60-70% for volumes  $> 14$  cm<sup>3</sup>. The total obliteration rate for all volumes up to 60 cm<sup>3</sup> is approximately 80-85%. Results on relationships between dose, AVM obliteration, and complications are presented.

### Introduction

The potential for Bragg ionization peak irradiation with heavy-ion beams as a method for producing discrete focal and lamellar lesions in the brain is derived from two clinical observations: (a) heavy-ion radiosurgery avoids the morbidity and mortality associated with extensive neurosurgical procedures; and (b) alternative methods, such as cryosurgery, electrothermal surgery and X-rays, provide poor spatial definition and lack of reliability in confining the reaction of the brain to injury [1]. At Lawrence Berkeley Laboratory we have developed stereotactic heavy-charged-particle Bragg peak radiosurgery for treatment of surgically-inaccessible intracranial arteriovenous malformations [1,2,3]. Narrow beams of accelerated heavy-charged particles are directed stereotactically to defined intracranial targets. The precision of our treatment planning and beam delivery system assures improved dose localization and dose distribution of the Bragg ionization peak throughout the arteriovenous malformation, generally with little or no neurovascular or parenchymal injury to adjacent vital brain structures. We have thus far treated over 375 patients with intracranial arteriovenous malformations, 50 of whom are children 18 years or younger, initially at the 184-inch Synchrocyclotron and currently at the Bevatron. Based on evaluation using cerebral angiography, computerized tomography and magnetic resonance imaging, and position emission tomography and radioisotope scanning of selected patients, together with extensive clinical neurologic followup, it appears that stereotactic heavy-charged-particle Bragg peak radiosurgery obliterates high-flow intracranial arteriovenous malformations and protects against further intraparenchymal brain hemorrhage with reduced morbidity and no treatment-associated mortality. The current procedure still has two major disadvantages: the prolonged latent period and relatively low but finite incidence of neurologic sequelae. Considerable research is required before it can offer the possibility of complete recovery in all patients. At present we consider the procedure only for selected patients with intracranial arteriovenous malformations in whom the potential surgical risk is considered unacceptably high, and patient selection is constrained by specifically defined patient protocols.

### Method

The 165 MeV/amu helium-ion beam-line configuration for stereotactic cerebral irradiation with the Bragg ionization peak at the Lawrence Berkeley Laboratory Bevatron has been reliably tested [4]. In the standard configuration the helium-ion beam line has a range of about 15.0 cm to the Bragg peak, with very sharply delimited lateral and distal borders. This range is decreased to the desired value by the insertion of a computer-controlled water-column absorber in the beam path. For clinical applications the charged-particle beam can be shaped to conform to the configuration of the arteriovenous malformation and to any diameter from less than 6 mm to over 60 mm. Physical dose measurements indicate an unmodified Bragg peak-to-plateau ratio of about 5. The maximum dose in the Bragg peak within the brain is approximately three or more times greater than the plateau or entrance dose at the skin; there is virtually no exit dose. The beam is modulated to adapt to a variety of radiosurgical conditions; the modified Bragg ionization curve and its transverse profile for stereotactic radiosurgery of an intracranial arteriovenous malformation will vary depending on the depth and location of the lesion within the brain.

The 80% Bragg peak width along the unmodulated beam path is less than 3 mm, but can be spread out to any desired width to approximately 50 mm or more using specially-designed water-absorber modulation. The nuclear charge and mass of the helium ion are larger than those of the proton; therefore, the multiple scattering and the range straggling with the helium ion are less for the same range in tissues, resulting in a sharper beam for stereotactic radiosurgery [4]. The primary advantage of narrow beams of heavy-charged particles in radiosurgical treatment deep within the brain is the ability to confine the dose to a discrete volume of tissue. The improved physical dose distributions are made possible by the relatively small amount of multiple scattering and range straggling and by the rapid fall-off of dose with depth beyond the end of the Bragg peak. These same physical characteristics require a stringently accurate assessment of, and compensation for, inhomogeneities in the tissue in order to accomplish precision radiosurgery with focal charged-particle beams.

The aim of the radiosurgical procedure for treatment of arteriovenous malformations is to use a focal charged-particle beam to irradiate the main arterial feeders and abnormal shunting vessels of the malformation proper and to include, as completely as possible, the whole cluster of pathologic shunting vasculature within the radiation field [1,3]. The entire compartment of this vascular unit must be included in the target volume, and an optimal therapeutic situation is present when the entire arteriovenous malformation can be covered by a sufficient and uniform radiation dose. We now know that the biologic basis for this change involves deterministic radiation injury to the vascular endothelial cells and their supporting biochemical architecture, repair, intimal proliferation, media degeneration and thrombosis.

### Treatment Planning

Treatment planning for stereotactic heavy-charged-particle radiosurgery for intracranial vascular disorders integrates anatomic and physical information from the stereotactic cerebral angiogram, stereotactic CT scans, and magnetic resonance images for each individual patient using computerized treatment-planning calculations for isodose contour display [3,4]. The data are used for three-dimensional target contouring and conversion to relative stopping power values, for improved dose distribution and dose localization. Multiple-entry angles and beam ports are chosen and contoured apertures and compensators are fabricated to confine the high-dose Bragg ionization peak to the contoured target of the arteriovenous malformation while protecting adjacent critical structures in the brain. Head immobilization is achieved with the stereotactic thermoplastic mask fixed in the stereotactic frame which are integral components of the system's patient-positioning apparatus, the Irradiation Stereotactic Apparatus for Humans. The medical cave at the Bevatron and the stereotactic positioning system are designed so that the helium-ion beam path is coincident with the stereotactically-determined isocenter of the patient-positioning apparatus [1,2,3].

The dose to the central axis of the arteriovenous malformation, the aperture shape and size, tissue-equivalent compensators, the number of beam ports, the beam angles for delivery and the range and modulation of the Bragg peak all determine the isodose contour configurations. Currently, total doses up to 25 GyE, applying an RBE of 1.3 for the helium-ion spread Bragg peak, are delivered to treatment volumes ranging from 100 mm<sup>3</sup> to 70,000 mm<sup>3</sup>. In the initial stages of our dose-searching protocols, doses of 35 to 45 GyE were used. Since vascular obliteration occurred in the lower dose levels of each protocol group, we lowered the doses delivered incrementally. At present, we have found that the optimal dose inducing obliteration of the arteriovenous malformation with the smallest risk of neurologic sequelae depends on a number of factors and appears to lie in the range of 15 to 25 GyE using the helium-ion Bragg ionization peak [5,6]. Dose selection depends on size, shape and location of the arteriovenous malformation within the brain and a number of other factors including the volume of normal brain that must be traversed by the plateau portion of the charged-particle beam. The average treatment volume for most patients ranges from 1,500 mm<sup>3</sup> to 16,000 mm<sup>3</sup>. Most often treatment occurs through 3 to 5 entry portals, most frequently 4 noncoplanar beams, and is delivered daily in 1 or 2 days, depending on the treatment volume (e.g., in 1 day if the volume is 4,000 mm<sup>3</sup> or less) and the volume of normal brain tissue traversed by the beam. The dose to the critical normal brain structures adjacent to the arteriovenous malformation is considerably less than the dose to the target volume because fall-off to 10% of the central dose occurs within 4 to 6 mm, and is within 2 to 3 mm along the lateral margins of the beam.

Figs. 1 and 2 are examples of the isodose contours for stereotactic heavy-charged-particle Bragg-peak radiosurgery in patients with arteriovenous malformations of the brain, defined by the inner region of white dots. In Fig. 1 the arteriovenous malformation is in the brain stem and the helium ion beam was collimated by an 8 mm circular aperture; treatment was carried out using four coplanar ports in one day to a volume of 250 mm<sup>3</sup> within the brain stem to a dose of 45 GyE. In Fig. 2 the arteriovenous malformation is in the deep white matter, the cortex, and the central nuclei of the left cerebral hemisphere; seven noncoplanar ports were used and a dose of 25 GyE was delivered to a volume of 54,000 mm<sup>3</sup> in 2 days.

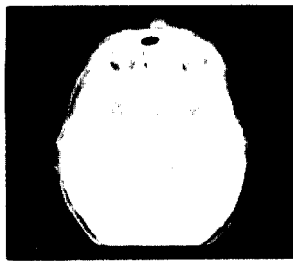


Fig. 1. Stereotactic helium-ion Bragg peak radiosurgery in a 38 year old patient with an arteriovenous malformation of the brain stem (defined by the inner ring of white dots). Isodose contours are shown superimposed on a central CT scan. The helium-ion beam was collimated by an 8 mm circular aperture. Treatment was performed using four coplanar ports in 1 day to a volume of 250 mm<sup>3</sup> within the brain stem; the dose was 45 GyE.

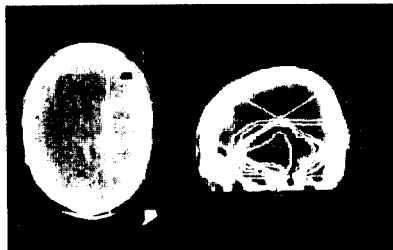


Fig. 2. Stereotactic helium-ion Bragg peak radiosurgery treatment plan for a large left temporal and deep central arteriovenous malformation in a 39 year old man. The helium-ion beam was collimated by 61 x 50 mm and 55 x 42 mm individually-shaped brass and cerrobend apertures; 25 GyE was delivered to the lesion (defined by the inner ring of white dots) using seven noncoplanar ports in 2 days to a volume of 54,000 mm<sup>3</sup>. The 90% contour borders precisely on the periphery of the lesion. There is a rapid dose fall-off to the 70% level, and the 10% isodose contour completely spares and protects the contralateral hemisphere.

Clinical Results

The clinical objectives of the radiosurgical procedure are to achieve changes in the intracerebral hemodynamic condition, resulting in (a) reduction or elimination of subarachnoid or intraparenchymal brain hemorrhages with their associated morbidity and mortality, (b) decrease in progressive or fixed neurologic deficits, (c) lower frequency of seizures, and (d) fewer subjective complaints, including frequency and intensity of headaches [1,6]. Nearly all patients have received clinical and neuroradiologic followup evaluations frequently since treatment; about two-thirds of the patients have had 60 months followup review, and extended review to 9 years has now been done on a regular basis where feasible. Preliminary observations in all patients, both adults and children, thus far treated indicate that the clinical objectives are being achieved in the majority of patients. The first 230 patients have been evaluated clinically to mid-1989; about 85-90% of the patients have excellent or good neurologic clinical grade, about 5% of the patients have poor neurologic clinical grade, and 5% had progression of disease and died, or died as a result of unrelated intercurrent illness.

In our Lawrence Berkeley Laboratory-Stanford University Medical Center patient series, we examined 101 consecutive patients to 72 months of follow-up. The Drake clinical grade at last followup is shown in Table 1 [6]. Seizures improved in 63% of patients, headaches in 68% and neurologic deficit in 27%. Progressive neurologic deficit stabilized in 55%. Outcome was excellent in 58% and good in 36% of patients [6].

Table 1  
Clinical Grade at Last Follow-up in 101 Patients

Presenting Clinical Grade	Excellent	Good	Poor	Dead
Excellent 68	53 (78%)	12 (18%)	2 (3%)	1 (17%)
Good 29	5 (17%)	21 (72%)	2 (7%)	1 (4%)
Poor 4		1 (25%)		3 (75%)
All Grades 101	58 (57%)	34 (34%)	4 (4%)	5 (5%)

Cerebral angiography illustrates changes in cerebral vessels at intervals following stereotactic radiosurgery. Hemodynamic changes are manifested by a decrease in blood flow through the pathologic cluster of vessels and a decrease in size of the feeding arteries, shunts and draining veins. Anatomic changes include progressive decrease in the size of the arteriovenous malformation until stabilization or total disappearance of the lesion occurs. The hemodynamic changes occur successively and are usually observed before the anatomic changes. Neuroradiologic followup to the end of 1989 indicate overall that for complete angiographic obliteration 3 years after treatment the obliteration rates are: 90-95% for volumes <4 cm<sup>3</sup>, 90-95% for volumes ≥4 cm<sup>3</sup> and ≤14cm<sup>3</sup>, and 60-70% for volumes >14 cm<sup>3</sup>; for all volumes up to 70 cm<sup>3</sup> it has been approximately 80-85% after 3 years [6,7]. Our Lawrence Berkeley Laboratory-Stanford University clinical series showed an overall complete malformation obliteration rate of 29% at 1 year, 70% at 2 years, and 92% at 3 years following helium-ion irradiation. (Table 2) [6]. The rate and extent of arteriovenous malformation obliteration appear to be threshold phenomena directly related to treatment volume and dose. Malformations smaller than 4 cm<sup>3</sup> (2 cm diameter) thrombosed more rapidly and more completely (94% complete obliteration at 2 years, 100% at 3 years) than larger lesions. Intermediate-sized malformations had an obliteration rate of 75% at 2 years and 95% at 3 years, while the larger lesions (>3.7 cm diameter) had an obliteration rate of 39% at 2 years and 70% at 3 years.

Table 2  
Stereotactic Radiosurgery Results at 3 Yr (230 Patients)

AVM Volume (cm <sup>3</sup> )	% of Patients	Obliteration Rate
≤4	49%	90-95%
>4 and ≤14	33%	90-95%
>14	18%	60-70%
All Volumes	100%	80-85%

Occlusion occurred most completely in the high-dose (30 to 45 GyE) group of patients. In our Lawrence Berkeley Laboratory-Stanford University series, this also occurred in the intermediate dose group; 24 to 28 GyE proved to be quite effective (Table 3). Following complete obliteration we have not seen subsequent angiographic reappearance of the malformation, even when prior embolization was performed.

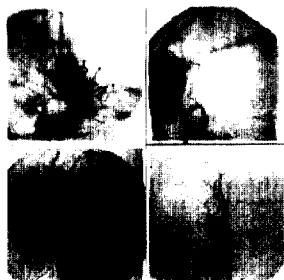
Table 3  
Complete AVM Obliteration vs. Treatment Dose

Dose (GyE)*	1 yr	2 yr	3 yr
11.5 - 20	4/18 (22%)	6/10 (60%)	6/6 (100%)
24 - 28	5/23 (22%)	17/23 (74%)	19/21 (90%)
30 - 45	9/16 (56%)*	16/18 (89%)**	18/19 (95%)

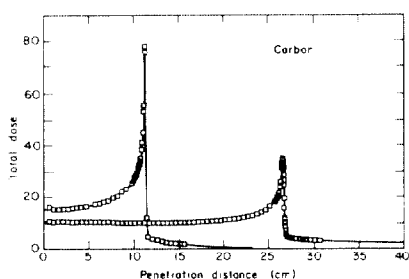
\* p = 0.057    \*\* p = 0.008    + RBE = 1.3

Fig. 3 illustrates the cerebral angiograms of a patient with recurrent seizures and progressive motor and sensory changes due to a steal phenomenon resulting from a deep right cerebral (frontal-temporal) arteriovenous malformation. Cerebral angiograms (upper) demonstrate the size, shape and location of the high-volume, high-flow malformation and the feeding vessels arising from branches of the middle cerebral artery. The anterior cerebral artery and its branches do not fill. Cerebral angiograms (lower) 1 year after stereotactic helium-ion Bragg peak radiosurgery (dose 35 GyE); demonstrate complete obliteration of the

arteriovenous malformation with redistribution of the normal cerebral blood flow. There is now filling of the anterior and posterior cerebral arteries and their branches and this is associated with a reversal of the steal syndrome.



**Fig. 3.** A 39 year-old woman with a right frontal-temporal arteriovenous malformation (volume 3,700 mm<sup>3</sup>). Upper: Cerebral angiograms show the size, shape and location of the malformations and its feeding vessels originating from the right middle cerebral artery and associated with a severe vascular steal phenomenon. Lower: Cerebral angiograms 1 year after helium-ion Bragg peak radiosurgery (dose 35 GyE) demonstrate complete obliteration of the malformation. The patient remains neurologically intact 7 years after treatment. There has been complete reversal of the vascular steal syndrome and return of normal regional cerebral flow patterns.



**Fig. 4.** Dose profiles for carbon-ion beams at the Bevatron suitable for radiosurgery of intracranial targets (range approximately 15.0 cm) and for radiotherapy of deep body targets (range approximately 25.0 cm). See text.

#### Complications

From the followup available we can conclude that by stereotactic heavy-charged-particle Bragg peak irradiation of the feeding arteries and shunts, total and irreversible angiographic obliteration of deep arteriovenous malformations is possible in a large number of patients, and protection against rehemorrhage with reduced morbidity and mortality occurs in over 80% of patients. The rate of moderate and serious complications combined is approximately 15-17%, but this is confined almost completely to the high-dose treatment group (30 to 45 GyE) in the initial stages of the dose-searching protocol. In the most recent analyses, no complications appear to occur at doses less than 20 GyE [6]. However, even at these rates, the cure rates are relatively high in this high-risk patient population, and the serious complications encountered may be considered acceptable in view of the potential for spontaneous intracranial bleeding and profound neurologic sequelae, morbidity and mortality, associated with the natural history of this disease in untreated patients [1,3,5,6,7].

#### Future Directions

Based on parameters derived from measured Bragg curves of protons (Harvard cyclotron), and helium, carbon and neon (Bevatron), for the particles and energies considered with increasing particle charge, the peak height reaches a maximum with carbon and then decreases, the Bragg peak width narrows, the distal fall-off gets steeper, and the exit dose increases (Table 4) [4,8]. The helium-ion beam is superior to a proton beam because of the higher peak-to-plateau ratio, more rapid dose fall-off and smaller beam deflection and suffers only in the modest exit dose. With the improved dose localization and dose distribution characteristics afforded by heavier-ion beams we will investigate the biologic and physical

characteristics and the relationships of helium and carbon-ion beams for stereotactic radiosurgery. Utilizing various ions, and total doses, we will define the optimal conditions and parameters for stereotactic heavy-ion Bragg peak radiosurgery for focal disorders in the brain, including intracranial arteriovenous malformations and tumors, while achieving improved protection of normal brain structures.

**Table 4**  
Heavy Charged Particle Beams for Stereotactic Radiosurgery

Characteristic	Protons	Helium	Carbon	Neon
Energy (MeV/u)	160	150	308	425
90% dose range (mm)	149.0	141.0	159.5	155.5
Peak-plateau ratio	3.6	5.1	5.15	4.6
80% peak width	6.0	2.7	1.5	1.2
Distal fall-off (%/mm)	20	43	60	75
Exit dose (%D <sub>max</sub> )	0	~ 18	~ 8	~ 11

At the Lawrence Berkeley Laboratory Bevatron accelerator high-energy particle beams of carbon and neon are available for biomedical research [4,8]. Of these beams, carbon has particularly good potential in stereotactic radiosurgery with the Bragg peak (Figure 4), and the physical characteristics of carbon beams lend themselves to 3-dimensional conformal treatment planning for radiosurgery. There are three general properties of this beam that are important: First, the carbon beam has less scattering and straggling than protons and helium ions by a factor of about 1.6 (helium) or 3.4 (protons) [6]. Consequently, the Bragg curves obtainable have greater peak-to-plateau ratios and can be aimed more accurately without affecting adjacent structures. Second, near the peak of the Bragg curve the dose of the carbon beam is much greater than at the plateau, perhaps by a factor of 5. Combined with an dose-equivalent of about 2.5 to 3 in the Bragg peak, the peak-to-plateau RBE ratio is significantly greater than comparable helium beams [4]. Therefore, if the peak is stopped in the target volume of the brain, relatively greater effects can be reached in the lesion with less dose; the adjacent critical structures of the brain will be better protected from radiation effects. Third, it is possible to localize the stopping points of the beam inside the head by the use of a radioactive carbon beam. This will make it feasible to stop the beam precisely at the appropriate depth within the brain [1].

It is our belief that heavy-ion beams, such as carbon, combined with beam raster scanning will allow improved dose distribution and dose delivery of localized irradiation in the central nervous system. It can be expected that many of the large intracranial arteriovenous malformations, small lesions, such as pituitary microadenomas, brain stem gliomas, isolated brain metastases and similar intracranial disorders can now be approached successfully. Furthermore, localization of very discrete focal lesions can be achieved in vital brain centers to treat certain diseases, such as Parkinson's disease, or for the control of pain and for such conditions as brain-stem cryptic arteriovenous malformations in children.

#### References

- [1] J.I. Fabrikant, J.T. Lyman and K.A. Frankel, *Radiat. Res.* 104 [Suppl] (1985) S-244.
- [2] J.T. Lyman, L. Kanstein, F. Yeater, J.I. Fabrikant and K.A. Frankel, *Med. Phys.* 13 (1986) 695.
- [3] J.I. Fabrikant, K.A. Frankel, M.H. Phillips and R.P. Levy, in *Cerebral Vascular Diseases of Childhood and Adolescence*, eds. M.S.B. Edwards and H.J. Hoffman (Williams and Wilkins, Baltimore, 1988) p. 389.
- [4] J.T. Lyman, M.H. Phillips, K.A. Frankel, J.I. Fabrikant, R.P. Levy, *International Workshop on Proton and Narrow-Photon Beam Therapy*, Oulu, Finland (1989) 43.
- [5] R.P. Levy, J.I. Fabrikant, K.A. Frankel, M.H. Phillips, J.T. Lyman, *Neurosurgery* 24 (1989) 841.
- [6] G.K. Steinberg, J.I. Fabrikant, M.P. Marks, R.P. Levy, K.A. Frankel, M.H. Phillips, L.M. Shuer, G.D. Silverberg, *NEJM* (1990) in press.
- [7] J.I. Fabrikant, M.H. Phillips, R.P. Levy, K.A. Frankel and J.T. Lyman, *EULIMA Workshop on the Potential Value of Light Ion Beam Therapy*, Nice, (France 1989) 233.
- [8] M.H. Phillips, K.A. Frankel, J.T. Lyman, J.I. Fabrikant, R.P. Levy, *Int. J. Radiat. Biol. Oncol. Phys.* 18 (1990) 211

## HEAVY-CHARGED-PARTICLE RADIOSURGERY OF THE PITUITARY GLAND: CLINICAL RESULTS OF 840 PATIENTS<sup>1</sup>

R. P. Levy, J. I. Fabrikant, K. A. Frankel, M. H. Phillips,  
J. T. Lyman, J. H. Lawrence, C. A. Tobias

Donner Pavilion and Donner Laboratory, Lawrence Berkeley Laboratory  
University of California at Berkeley, Berkeley, CA 94720 USA

**Abstract:** Charged-particle beams manifest advantageous properties for stereotactic radiosurgery of the brain. The beams have Bragg ionization peaks at depth in tissues, finite range and are readily collimated to any desired cross-sectional size and shape by metal apertures. Since 1954, 840 patients at Lawrence Berkeley Laboratory (LBL) have been treated with stereotactic charged-particle radiosurgery of the pituitary gland for various localized and systemic disorders. This report discusses the clinical and endocrinologic results in that patient series. The optimal choice of dose and fractionation schedules must be determined for the treatment of different intracranial disorders, in order to improve the cure rate and to minimize potential adverse sequelae.

### Introduction

Since 1954, nearly 6,000 neurosurgical patients world-wide have been treated with stereotactic charged-particle radiosurgery of the brain for various localized and systemic disorders [7]. Therapeutic efficacy has been clearly demonstrated for selected disorders, e.g., pituitary adenomas and intracranial arteriovenous malformations [6,7]. The first therapeutic clinical trial using accelerated heavy-charged particles in humans was performed by Lawrence, Tobias and their colleagues at Lawrence Berkeley Laboratory (LBL) for the treatment of endocrine and metabolic disorders of the pituitary gland, and as suppressive therapy for adenohypophyseal hormone-responsive carcinomas (e.g., breast and prostate cancer) and diabetic retinopathy [2,3,5]. Since then, stereotactically-directed focal charged-particle irradiation has been used at LBL to treat 840 patients to destroy tumor growth and/or suppress pituitary function; this includes patients with acromegaly, Cushing's disease, Nelson's syndrome, prolactin-secreting adenomas, chromophobe adenomas, metastatic breast carcinoma and diabetic retinopathy (Table 1) [7]. The initial 30 patients were treated with plateau proton beams. Subsequently, almost all of these patients were treated with plateau helium-ion irradiation, although selected patients with larger tumor volumes and more recent patients received Bragg peak helium-ion irradiation. In acromegaly, Cushing's disease, Nelson's syndrome and prolactin-secreting tumors, the therapeutic goal in the 443 patients treated has been to destroy or inhibit the growth of the pituitary tumor and control hormonal hypersecretion, while preserving a functional rim of tissue with normal hormone-secreting capacity, and minimizing neurologic injury [3,4]. An additional group of 34 patients was treated for nonsecreting chromophobe adenomas [3]. In the earlier years of the pituitary

irradiation program at LBL, many patients with various hormone-responsive disorders underwent stereotactic helium-ion irradiation, in order to effect hormonal suppression of the disease by induction of hypopituitarism [2]. This included 183 patients with metastatic breast carcinoma and 169 patients with diabetic retinopathy, as well as selected patients with prostatic carcinoma and other hormone-responsive malignancies [7].

### Methods

#### Physical Properties of Charged-Particle Beams

Beams of accelerated-charged particles have several physical properties that can be exploited to place a high dose of radiation preferentially within the boundaries of a deeply-located intracranial target volume [6,7]. These include: (1) a well-defined range that can be modulated so that the beam stops at the distal edge of the target, resulting in little or no exit dose beyond the Bragg ionization peak; (2) an initial plateau region of low dose as the beam penetrates through matter, followed by a region of high dose (the Bragg peak) at the end of the range of the beam and deep within the tissue, which can be adjusted to conform to the length of the target, so that the entrance dose can be kept to a minimum; and (3) very sharp lateral edges that can readily be made to conform to the projected cross-sectional contour of the target, so that little or no dose is absorbed by the adjacent normal tissues.

#### Radiosurgery

**Plateau Region:** When accelerated-charged-particle beams of sufficiently high energy, and hence greater depth of penetration, are available, radiosurgery can be performed with the plateau portions of the narrow beams, using several intersecting coplanar or noncoplanar arcs or multiple discrete stereotactically-directed intersecting beams. In this configuration, through-and-through irradiation techniques are employed, so that the plateau ionization regions pass through the entire brain [11]. The high-dose regions attained with the plateau irradiation technique are usually as sharply-delineated as those attained with the Bragg peak technique (see below); differences tend to be relatively minor for small target volumes (e.g., pituitary gland). With this technique, consideration of the tissue inhomogeneity normally encountered in the head is not important, but accurate stereotactic localization of the intracranial target volume and precise isocentric technique are essential. Stereotactic plateau-beam radiosurgery has been employed at LBL for irradiation of the pituitary gland since 1954 [7,11].

A beam delivery system was developed at the LBL 184-inch Synchrocyclotron using 230 MeV/amu helium ions in the plateau ionization region, which provided precise dose-localization and dose-distribution. Patient immobilization was accomplished by the integrated stereotactic mask and frame and an isocentric stereotactic apparatus (ISAH), and assured precision of dose-localization within 0.1 to 0.3 mm [9]; continuous and discontinuous rotation about the isocenter was achieved in two of three orthogonal planes. The optimal treatment procedure ensured that the optic chiasm, hypothalamus, and outer portions of the sphenoid sinus received less than 10% of the central-axis pituitary dose [11]. Until the introduction of high-resolution CT scanning and currently, MRI scanning, it was necessary to define the precise location of the pituitary gland, optic chiasm, nerves and tracts, and the adnexae of the cavernous and sphenoid sinuses with pneumoencephalography and polytomography.

Treatment was delivered in 6 to 8 fractions over 2 to 3 wk in the first few years of the program, and in 3 or 4 fractions over 5 d subsequently. The dose was necessarily high in order to overcome the radioresistance of the pituitary gland. However, the dose to adjacent cranial nerves and temporal lobes was considered to be a limiting factor rather than dose to the pituitary gland; the medial aspect of the temporal lobe received 36 Gy during longer courses of therapy,

Table 1  
CHARGED-PARTICLE RADIOSURGERY OF  
THE PITUITARY GLAND AT UCB-LBL [a]  
1954 to Present

Disorder	Patients Treated
Pituitary Tumors (total)	475
Acromegaly	318
Cushing's Disease	83
Nelson's Syndrome	17
Prolactin-secreting	23
Nonfunctioning Adenomas	34
Pituitary Suppression (total)	365
Diabetic Retinopathy	169
Breast Cancer	183
Prostate Cancer	3
Ophthalmopathy	3
Other	7
<b>Total</b>	<b>840</b>

[a] UCB-LBL: University of California at  
Berkeley - Lawrence Berkeley Laboratory

<sup>1</sup>This research was supported by the Office of Health and Environmental Research, U.S. Department of Energy Contract DE-AC03-76SF00098.

and 30 Gy to the same region during shorter courses of treatment. As the dose fell off rapidly from the central axis, the dose to the periphery of larger pituitary targets (e.g., acromegalic tumors) was considerably less than the peripheral dose to smaller targets (e.g., Cushing's disease).

**Bragg Peak:** Each charged-particle beam can be directed stereotactically to place individually-shaped three-dimensional high-dose regions precisely within the brain by adjusting the range, by spreading the Bragg peak, by introducing tissue-equivalent compensators, and by using an appropriately-shaped aperture [6,7]. Several entry angles and coplanar and/or noncoplanar beam ports are directed stereotactically so that the high-dose regions of the individual beams intersect within the target volume. This technique provides considerable flexibility of choice of beam direction for multiport stereotactic treatment planning for 3-dimensional conformal therapy, with a much lower dose to immediately-adjacent and intervening normal brain tissues, and complete protection of the largest proportion of the normal brain tissues. For helium, the relative biologic effectiveness (RBE) in the Bragg ionization peak is assumed to be approximately 1.3, based on *in vitro* and *in vivo* studies [1].

For Bragg peak pituitary irradiation, the beam delivery system described above has been modified using 165 MeV/amu helium-ion beams at the LBL Bevatron, by means of range adjustment, tissue compensation, and spreading of the Bragg peak. The tumor and its relationships to adjacent neural structures are defined on stereotactic MRI scans, and the radiosurgical target is delineated. The radiosurgical treatment plan is designed in order to place higher dose in the tumor mass lying within the sella and lower dose in any tumor mass extending into extrasellar tissues. A detailed description of treatment planning for pituitary radiosurgery using the Bragg peak of the helium-ion beam is the subject of a separate report in this symposium.

## Results

### Acromegaly

Stereotactic helium-ion beam irradiation has proven to be very effective as the treatment of acromegaly. Maximum dose to the pituitary tumor in 318 patients treated ranged from 30 to 50 Gy, most often delivered in 4 fractions over 5 d. Marked clinical and biochemical improvement was observed in most patients within the first year, even before a significant fall in serum growth hormone level was noted. A dramatic and sustained decrease in hormone secretion was observed in most patients; the mean growth hormone level decreased nearly 70% within 1 y, and continued to decrease thereafter (Figure 1). Normal levels were sustained during more than 10 y of follow-up. Comparable results were observed in 65 patients who were irradiated with helium ions because of residual or recurrent metabolic abnormalities persisting after surgical hypophysectomy. Most of the treatment failures after helium-ion irradiation apparently resulted from inaccurate assessment of extrasellar tumor extension [3,4,8].

### Cushing's Disease

Cushing's disease has been treated successfully by stereotactic helium-ion irradiation in 83 patients (aged 17-78 y) [3,4]. Mean basal cortisol levels and dexamethasone suppression testing returned to normal values within 1 y after treatment, and remained normal during more than 10 y of follow-up. Doses to the pituitary gland ranged from 30 to 150 Gy, most often delivered in 3 or 4 daily fractions. All 5 teenage patients were cured by doses of 60 to 120 Gy without inducing hypopituitarism or neurologic sequelae; however, 9 of 59 older patients subsequently underwent bilateral adrenalectomy or surgical hypophysectomy due to relapse or failure to respond to treatment. Of the 9 treatment failures, 7 occurred in the earlier group of 22 patients treated with 60 to 150 Gy in 6 alternate-day fractions; when the same doses were given in 3 or 4 daily fractions, 40 of 42 patients were successfully treated [8]. The marked improvement in response with reduced fractionation in this group of patients has helped provide the clinical rationale for single-fraction treatment with stereotactically-directed beams of heavy-charged particles.

### Nelson's Syndrome

Helium-ion beam treatment has been used in 17 patients with Nelson's syndrome. Treatment dose and fractionation were comparable to that in the Cushing's disease group, i.e., 50 to 150 Gy in 4 fractions. Six patients had had prior pituitary surgery, but had persistent tumor or elevated serum ACTH levels. All patients exhib-

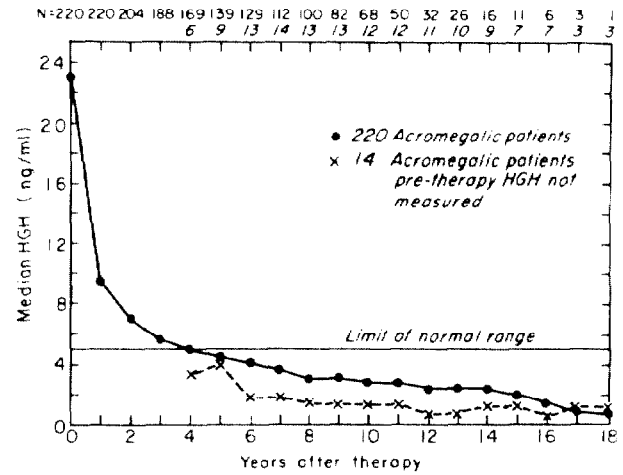


Figure 1. Changes in plasma human growth hormone (GHG) levels in 234 patients with acromegaly one or more years after stereotactic helium-ion (230 MeV/u) plateau radiosurgery at the University of California at Berkeley - Lawrence Berkeley Laboratory 184-inch Synchrocyclotron. At the top of the graph are the numbers of patients used to calculate the median plasma levels for each time interval following radiosurgery. Fourteen patients did not have pre-radiosurgery GHG measurements, but their GHG levels determined 4 to 18 years after radiosurgery are comparable with those of the other 220 patients. Excluded from this series were 63 patients who had undergone prior pituitary surgery and 5 patients whose pre-radiosurgery growth hormone levels were less than 5 ng/ml. The 20 patients in the series who subsequently underwent pituitary surgery or additional pituitary irradiation were included until the time of the second procedure. (From J. H. Lawrence, "Heavy particle irradiation of intracranial lesions," in R. H. Wilkins and S. S. Rengachary (eds): *Neurosurgery*. New York: McGraw-Hill, 1985, pp. 1113-1132.)

ited marked decrease in ACTH levels, but rarely to normal levels. However, all but one patient had radiologic evidence of local tumor control [3,4]. One patient who had presented with invasive tumor had progressive suprasellar extension following irradiation; this patient died postoperatively after transfrontal decompression.

### Prolactin-Secreting Tumors

In 23 patients with prolactin-secreting pituitary tumors, serum prolactin levels were successfully reduced in most patients following helium-ion irradiation. Of 20 patients followed 1 y after irradiation, 19 had a marked fall in prolactin level (12 to normal levels) [3,8]. Treatment dose and fractionation were comparable to that in the Cushing's disease and Nelson's syndrome groups, i.e., 50 to 150 Gy in 4 fractions. Helium-ion irradiation was the sole treatment in 17 patients; the remaining patients were irradiated after surgical hypophysectomy had failed to provide complete or permanent improvement.

### Complications of Pituitary-Tumor Radiosurgery

Variable degrees of hypopituitarism developed as sequelae of attempts at subtotal destruction of pituitary function in about a third of the patients, although endocrine deficiencies were rapidly corrected in most patients with appropriate hormonal replacement therapy. Diabetes insipidus has not been observed in any pituitary patients treated with helium-ion irradiation [8].

Complications in 318 acromegalic patients treated with helium-ion irradiation were relatively few and limited almost exclusively to those patients who had received prior photon treatment. Of 7 patients who had previously undergone unsuccessful photon irradiation, 3 patients subsequently developed focal and readily-controlled seizures due to limited temporal lobe necrosis; 3 patients developed mild or transient extraocular palsies; 2 patients had partial field deficits. Thereafter, previously irradiated patients were excluded from the protocol [10]. Temporal lobe injury, but no cranial nerve dysfunction, occurred in only 2 of 283 patients treated solely with plateau helium-ion irradiation; both were cases treated in the initial series, and who had received higher radiation doses than were used in later years [8].

Neurologic sequelae of stereotactic radiosurgical treatment have been infrequent in the Cushing's disease group of patients. One patient developed asymptomatic visual field deficits 18 mon after treatment. Two patients developed rapid progression of ACTH-secreting pituitary adenomas (i.e., Nelson's syndrome) following bilateral adrenalectomy that had been performed after helium irradiation failed to control the tumor growth adequately. Two patients developed transient partial third nerve palsies 6 to 7 y after helium-ion treatment [8].

#### Hormone-Dependent Metastatic Carcinoma

Between 1954-1972, stereotactically-directed proton (initial 26 patients) or helium-ion beams (157 cases) were used at LBL for pituitary ablation in 183 patients with metastatic breast carcinoma. Patients received 180 to 320 Gy stereotactic plateau helium-ion beam irradiation to the pituitary gland, in order to control the malignant spread of carcinoma by effecting hormonal suppression through induction of hypopituitarism [2]. Treatment resulted in a 95% decrease in pituitary cellularity with connective tissue replacement within a few months. At lower doses, the magnitude of cellular loss was dependent on the dose to the periphery of the gland [11]. Many patients experienced long-term remissions. Eight cases of focal radiation necrosis (including asymptomatic necrosis found at autopsy) limited to the adjacent portion of the temporal lobe occurred; all were from an earlier treatment group of patients entered in a dose-searching protocol who had received higher doses to suppress pituitary function as rapidly as possible [10]. Clinical manifestations of temporal lobe injury and transient 3rd, 4th, and 6th cranial nerve involvement occurred in only 4 of these patients.

#### Diabetic Retinopathy

Between 1958-1969, 169 patients with proliferative diabetic retinopathy received plateau helium-ion focal pituitary irradiation. This was done to follow the effects of pituitary ablation on diabetic retinopathy and to control the effects of insulin- and growth hormone-dependent retinal proliferative angiogenesis which could result in progressive blindness. The first 30 patients were treated with 160 to 320 Gy delivered over 11 days to effect total pituitary ablation; the subsequent 139 patients underwent subtotal pituitary ablation with 80 to 150 Gy delivered over 11 days. Most patients had a 15-50% decrease in insulin requirements; this result occurred sooner in patients receiving higher doses, but ultimately both patient groups had comparable insulin requirements. Fasting growth hormone levels and reserves were lowered within several months after irradiation. Moderate to good vision was preserved in at least one eye in 59 of 114 patients at 5 years after pituitary irradiation (J.H. Lawrence, unpublished). Of 169 patients treated, 69 patients (41%) ultimately required thyroid replacement and 46 patients (27%) required adrenal replacement. There were 4 deaths from complications of hypopituitarism. Focal temporal lobe injury was limited to an early group of patients that had received at least 230 Gy in order to effect rapid pituitary ablation in advanced disease; 4 patients in this high-dose group developed extraocular palsies. Neurologic injury was rare in those patients receiving doses less than 230 Gy (J.H. Lawrence, unpublished).

#### Pathologic Changes

Autopsies were performed on 15 patients who had been treated with plateau helium-ion irradiation of the pituitary [12]. Ten of these patients had been treated for progressive diabetic retinopathy with average doses of 116 Gy delivered in 6 fractions. All patients demonstrated progressive pituitary fibrosis. Five patients with eosinophilic adenomas received an average of 56 Gy in 6 fractions. These adenomas developed cystic cavitation, suggesting greater radiosensitivity of the tumor than the surrounding normal anterior pituitary gland, which in turn proved to be more radiosensitive than the posterior pituitary gland. However, no radiation changes were found in the surrounding brain or cranial nerves, demonstrating that the accelerated heavy-charged-particle plateau beams created a sharply delineated focal pituitary lesion without injury to the adjacent critical brain structures.

#### Discussion and Conclusions

Stereotactic heavy-charged-particle helium-ion radiosurgery of the pituitary gland has proven to be a highly effective method of treatment for a variety of endocrine and metabolic hormone-dependent conditions, alone or in combination with surgical hypophysectomy.

Since 1954, 840 patients have received stereotactically-directed focal plateau or Bragg peak helium-ion pituitary irradiation at LBL to suppress pituitary function and/or control tumor growth; this includes patients with acromegaly, Cushing's disease, Nelson's syndrome, prolactin-secreting adenomas, metastatic breast carcinoma and diabetic retinopathy. In the great majority of patients with pituitary tumors, this method has resulted in reliable control of neoplastic growth and suppression of hypersecretion, while generally preserving a rim of functional pituitary tissue. Variable degrees of hypopituitarism resulted in a number of cases, but such endocrine deficiencies and associated metabolic dysfunction were readily corrected with appropriate hormone supplemental therapy.

Clinical protocols for stereotactic helium-ion Bragg peak radiosurgery for pituitary microadenomas and recurrences following surgery are in progress at LBL, in order to make use of the uniquely advantageous dose-distribution and dose-localization properties inherent in the Bragg ionization peak. Improved anatomic resolution now possible with multiplanar MRI and CT scanning has made possible better localization of pituitary microadenomas and adjacent neural structures, and more accurate assessment of extrasellar tumor extension. These recent neuroradiologic advances should result in improved cure and control rates for pituitary tumors and related intracranial disorders, decreased treatment sequelae, and a decrease in the number of treatment failures previously found to have resulted from inaccurate assessment of tumor extension.

#### References

- [1] E. A. Blakely, F. Q. H. Ngo, S. B. Curtis, et al, "Heavy-ion radiobiology: cellular studies," in J. T. Lett (ed): *Advances in Radiation Biology*, New York: Academic Press, 1984, vol. 10, pp. 295-389.
- [2] J. H. Lawrence, "Proton irradiation of the pituitary," *Cancer*, vol. 10, pp. 795-798, 1957.
- [3] J. H. Lawrence, "Heavy particle irradiation of intracranial lesions," in R. H. Wilkens and S. S. Rengachary (eds): *Neurosurgery*, New York: McGraw-Hill, 1985, pp. 1113-1132.
- [4] J. H. Lawrence, J. A. Linfoot, "Treatment of acromegaly, Cushing disease and Nelson syndrome," *West J Med*, vol. 133, pp. 197-202, 1980.
- [5] J. H. Lawrence, C. A. Tobias, J. A. Linfoot, et al, "Heavy particles, the Bragg curve and suppression of pituitary function in diabetic retinopathy," *Diabetes*, vol. 12, pp. 490-501, 1963.
- [6] R. P. Levy, J. I. Fabrikant, K. A. Frankel, et al, "Stereotactic heavy-charged-particle Bragg peak radiosurgery for the treatment of intracranial arteriovenous malformations in childhood and adolescence," *Neurosurgery*, vol. 24, pp. 841-852, 1989.
- [7] R. P. Levy, J. I. Fabrikant, K. A. Frankel, et al, "Charged-particle radiosurgery of the brain," *Neurosurg Clin North America*, 1990 (in press).
- [8] J. A. Linfoot, "Heavy ion therapy: alpha particle therapy of pituitary tumors," in J. A. Linfoot (ed): *Recent Advances in the Diagnosis and Treatment of Pituitary Tumors*, New York: Raven Press, 1979, pp. 245-267.
- [9] J. T. Lyman, C. Y. Chong, "ISAH: A versatile treatment positioner for external radiation therapy," *Cancer*, vol. 34, pp. 12-16, 1974.
- [10] L. W. McDonald, J. H. Lawrence, J. L. Bern, et al, "Delayed radionecrosis of the central nervous system," in J. H. Lawrence (ed): *Semiannual Report. Biology and Medicine. Donner Laboratory and Donner Pavilion. Fall 1967*, UCRL Report No. 18066, Berkeley: Regents of the University of California, 1967, pp. 173-192.
- [11] C. A. Tobias, "Pituitary radiation: radiation physics and biology," in J. A. Linfoot (ed): *Recent Advances in the Diagnosis and Treatment of Pituitary Tumors*, New York: Raven Press, 1979, pp. 221-243.
- [12] K. H. Woodruff, J. T. Lyman, J. H. Lawrence, et al, "Delayed sequelae of pituitary irradiation," *Hum Pathol*, vol. 15, pp. 48-54, 1984.

## Detector Systems for Clinical Beam Delivery Systems

T. R. Renner, W. T. Chu, B. Ludewigt, K. Milne, M. Nyman, and R. Stradtner  
Lawrence Berkeley Laboratory, Berkeley, California  
and  
D. Senderowicz  
SynchroDesign Inc., Berkeley, California

### Abstract:

Detectors used in beam delivery systems for controlling and monitoring heavy charged-particle beams for clinical use have special requirements place on their response time, size, spatial resolution and reliability. A 30 cm by 30 cm transmission, ionization detector with 0.5 cm spatial resolution is now being developed for use with a raster scanning beam delivery system being built. The electronics for this system requires the development of a specially designed integrated circuit.

### Introduction

The treatment of humans with radiation requires real-time monitoring of the radiation. The accurate delivery of the prescribed dose is essential to affect the desired cure and to prevent the deleterious consequences of an overdose of radiation. The fact that humans are being exposed to the radiation and that the radiation has the potential to harm, as well as help, makes the design and construction of monitoring systems and detectors different from their traditional usage in physics. Dynamic beam delivery systems in particular require such active monitoring systems.<sup>1,2</sup>

Detector systems for radiotherapy and radiosurgery have three main functions: 1) the measurement of the dose being delivered to the patient in real time, so that the radiation can be terminated at the appropriate amount, 2) the measurement of the spatial distribution of the radiation delivered to insure the patient prescription is satisfied, and 3) the monitoring of the radiation delivery for the control of the radiation transport system. Monitoring the spatial distribution of dose is particularly important because the radiation must be modified as it comes from the source before being used clinically. The heavy charged-particle beams from the accelerator undergo range changes, spatial deflection, and nuclear interactions before reaching the patient. For beam transport purposes the monitoring must be independent of these modifications to facilitate beam line tuning and to minimize mistakes introduced from changes in the beamline setup.

### General Philosophy

Our experience with treatments at the Biomed facility at the Bevalac has lead us to several principals in the design and operating of detectors for clinical use. The first is that the detector system should be independent of the rest of the beam transport and beam delivery system. No *a priori* assumptions should be made as to what the other systems are doing. The detector system should work at all times with a response time sufficient to provide monitoring systems and human operators information on the radiation's status.

Second, the system must be reliable and safe. An acceptable fault rate can only be achieved by having redundant systems. Three independent systems for monitoring the dose and terminating the radiation are advisable; each system independently able to terminated the treatment. While this moderately increases the likelihood of a system not working properly and hence preventing a treatment, it is safer than a system with fewer monitors. If a system fails to work properly and the fault is not detected, there can be one of two consequences. The working systems will prevent an overdose or the broken system will terminated the treatment too soon. The latter can be corrected in subsequent treatments after the problem has been solved. Three systems makes assessing which system isn't working easier.

An additional method for assuring a systems reliability and safety is a method of checking the detectors without the use of radiation. The detector, its electronics, the dosimetry system and the entire treatment system can be tested with this simulation capability. The pre-treatment testing of new software and hardware saves time and effort in debugging and increases confidence in the treatment system's performance.

Third, the detector should detect a quantity directly proportional to the dose, the fundamental quantity of interest. The direct measurement of dose in the patient can not be easily done so that an indirect method must be used. To maintain a strict proportionality between the monitoring detector and the delivered dose, a fixed geometry relating the measured to the delivered dose is necessary. A calibration can then be made of detector response with dose delivered to a phantom setup identical to the actual treatment conditions. To achieve a proportionality close to unity, a simple relationship between the two is desired. Placing a detector as near the patient and as far downstream of beam modifying devices as possible helps insure that what is being measured is what the patient is receiving.

These considerations have lead us to the development of large-area, transmission ionization detectors that are segmented into many smaller, independent-areas. Dose distributions, distribution centroids and second moments can be measured in real time and displayed for the operator convenience or monitored via hardware and/or software. These detectors, used with known gases and known ionization volumes, can measure dose via the ionization produced by the radiation traversing the detector. This dose can be related to dose delivered to tissue via the relative stopping power ratio of tissue to gas. Since the monitor detectors can not be located in the tumor volume, as mentioned a further calibration is needed of the monitor detectors in terms of dose delivered to the tumor. A comparison between a calibrated reference detector, placed at the isocenter inside a phantom, and the monitor detector provides this conversion factor.



### Specifications

To specify the requirements of the dose measuring device, the range of dose to be measured must be known. For most clinical purposes this is between 1.0 milliGy and 10 Gy - a range of five orders of magnitude. A further complication is the time structure of the radiation. High dose rates produce high currents which must be integrable by the electronics. Currents lasting a few milliseconds as large as  $10 \mu\text{A}$  can be produced by the high frequency components in the time structure of the radiation extracted from the accelerator.

The minimum current produced in clinical systems is on the order of a few pA. Small volume detectors, short duration radiation pulses, or short integration times are sources of such currents. In these cases the signal to be measured must be distinguishable from noise in the system. For this reason charge integration is the preferred method because only low frequency noise is a significant noise source; otherwise, the noise signal is integrated out by the integrator. For systems currently used a noise level of a fraction of a pA are obtainable. This noise level presents no real problem during patient treatments where the typical currents are in the nanoampere to microampere range.

A further constraint on the design of detector systems are their size and spatial resolution. An area to be monitored as large as 30 cm by 30 cm is clinically useful with a spatial resolution on the order of a centimeter or less. Some applications such as measuring the penumbras of dose delivered near critical structures require a few millimeter resolution over 10 centimeter distances. This can be achieved with segmentation of the detector's collection foil. Large numbers of independent electronic channels are then required to maintain the independence of each element. Finally detector systems placed near the patient must be as unobtrusive as possible so that the valuable space near the patient is preserved for other beam-modifying devices.

The required response times of a detector system is dominated not by the detector response, but by the method of terminating the radiation. Response times less than a fraction of a second are necessary for passive scattering system to achieve the desired dose accuracy. With active beam-delivery systems millisecond response times are required for dose monitoring and termination in the case of a delivery-system failure. A failure in the beam extracting system of the accelerator that results in an instantaneous high beam current should be detected by other means than an ionization chamber which is susceptible to saturation. Secondary emission monitors are best suited for this purpose.

### Detector Choices

For ionization detectors the choice of gas is governed by the needed absolute accuracy of the system. The energy to make an ion pair,  $W$  value, are well known for only a few gases.<sup>3</sup> The density,  $W$  factor and relative stopping power of the gas in part determine the ionization produced by the beam of radiation.<sup>4</sup> The foil separation determines the radiation's pathlength thru the detector and hence the amount of charge produced. Nitrogen at atmospheric pressure and temperature is used because of its well known  $W$  value.<sup>5</sup>

The foil separation in all the detectors at the Bevalac have been standardized to 1 cm for ease of construction. Large area foils separated by 1 cm and placed at a relative high potential with respect to one another might be expected to bow from the mutual force between them. Calculations show that this force is negligible and, in practice, no bowing is observed. Since one of the foils is placed at a high voltage, careful electrical separation of it from nearby grounded structures is required. A gap of 0.3 cm between the high voltage foil and grounded surfaces is typically used in our chambers. A second detail of foil design is the extension of a grounded region around the active collection region. This grounded region insures a uniform electric field in the region where charge is being measured.<sup>6</sup> The produced ionization is not distorted by skewed electric field lines it follows migrating to the collection foil. A nominal extension of 2 cm is adequate for most foil geometries.

Since the chambers operate in a transmission mode, as little material in the beam path minimizes the detector's impact on the radiation. Kapton foils on the order of  $25 \mu\text{m}$  thick can be used to make a practical detector  $\sim 200 \mu\text{m}$  thick. Gold plating of the foils to a thickness of  $\sim 0.5 \text{ mg/cm}^2$  creates a conducting surface. With printed circuit board techniques a desired pattern can be etched for collecting the ionization charge. Several kinds of collection patterns have been made for different purposes. Figure 1 shows a detector used to measure onedimensional dose distributions with fine spatial resolution.

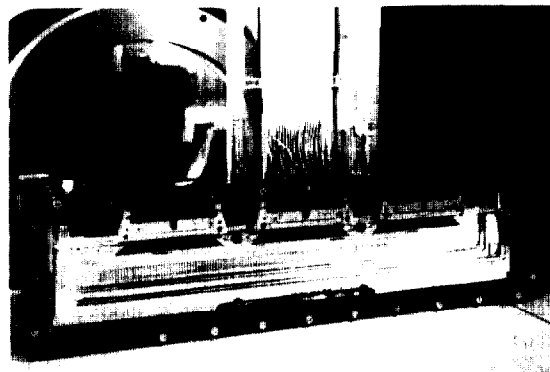


Figure 1 shows an ionization chamber that is segmented into 144 individual elements. Each element is 2 mm by 1 cm in area.

**Special Features** An important development in the construction of such multisegmented ionization chambers has been a method for extracting the signals from each element.<sup>7</sup> This has been done by moving the signal leads from the collection side of the foil to its backside. There are three advantages to doing this. 1) A great deal of area is gained to layout the signal leads. 2) Collection no longer occurs on the leads themselves since they are away from any electric field. 3) The entire collection area can be used for construction of well defined collection electrodes in symmetric patterns. By using printed-circuit board techniques the signals can also be easily connected to the electronics via edge connectors and cabling.



### Electronics

The most successful means of integrating the charge from an ionization collection element has been the recycling integrator or charge to pulse converter.<sup>8,9</sup> Their major advantages are their large dynamic range, exceptional linearity and excellent noise immunity. A simple integrator designed for use at the highest current levels suffers at low current levels; the small output signal is difficult to discriminate from noise and is difficult to digitize with sufficient resolution. A variable ranging system, another alternative, has two problems; the proper range must be selected before the measurement is made and the selection must be correct. Too coarse a resolution results in a dose measurement inaccuracy; too fine a resolution leads to saturation of the electronics and a wrong dose measurement.

Limitations: Recycling integrators also have limitations. The noise in the system determines the smallest charge measurable. Above some input current the recycling integrator will saturate. As saturation is approached a maximum output frequency is maintained and unaccounted charge is stored until the recycling integrator can catch up, with some penalty in linearity. At saturation the input will no longer appear as a virtual ground and the charge measured will be incorrect.

Bias: A small, fixed current input to each channel to offset unknown biases also checks that each channel is operating. A background subtraction eliminates any effect of this bias on the true charge measurement.

Integrated Circuit The largest obstacle to multiple channel systems is their cost. Toward the goal of reducing this cost, an integrated circuit is being developed with 16 channels per chip. The chip will have selectable charge quanta of 1, 10 and 100 pC per output pulse. The dynamic range will cover from 0.1 to  $10^7$  hertz. A 24 bit scaler and a preset scalar will be built into the integrated circuit along with a saturation detection circuit. A calibration bus will allow the individual calibration of each of the channels on a chip. A built in bias circuit will automatically adjust the input to maintain a fixed positive output to account for any unknown biases in the system.

### Conclusion

A 3600 element ionization chamber is being developed along with a special integrated circuit to measure in real-time the doses delivered with the raster scanning beam delivery system. This system will allow independent monitoring of the radiation during a patient treatment along with beam's characteristics. Measurement of two dimensional dose distributions will be possible with a clinically useful spatial resolution.

### References

1. W. T. Chu, T. R. Renner, and B. A. Ludewigt, "Dynamic Beam Delivery for Three-Dimensional Conformal Therapy," Proceedings of the EULIMA Workshop on the Potential Value of Light Ion Beam Therapy, eds. P. Chauvel and A. Wambersie, November 3-5, 1988, Nice, France, EUR 12165 EN, 295-328, (1989).

2. T. R. Renner, W. T. Chu, B. A. Ludewigt, J. Halliwell, M. A. Nyman, R. P. Singh, G. D. Stover, R. Stradtner, "Preliminary Results of a Raster Scanning Beam Delivery System," to be published in the Proceedings of the IEEE Particle Accelerator Conference, Chicago, April 1989.

3. "Average Energy Required to Produce an Ion Pair," ICRU Report 31, 1979, International Commission on Radiation Units and Measurements, Washington, D.C.

4. "Determination of absorbed dose in a patient irradiated by beams of x or gamma rays in radiotherapy procedures," ICRU Report 24 (1976), International Commission on Radiation Units and Measurements, Washington, D.C.

5. J. W. Boag, and T. Wilson, "The saturation curve at high radiation intensity," Brit. J. of Appl. Phys., 3, 222, (1952).

6. J. W. Boag, "Distortion of the electric field in an ionization chamber due to a difference in potential between guard ring and collector," Phys. Med. Biol. 9, 25-32, (1963).

7. Renner, T. R., W. T. Chu, B. A. Ludewigt, M. A. Nyman, R. Stradtner, "multisegmented ionization chamber dosimetry system for light ion beams," NIM A281 640-648, (1989).

8. E. Shapiro, "Linear seven-decade current/voltage-to-frequency converter," IEEE Trans. Nucl. Sci. NS-17, 335-344, (1970).

9. J. H. McQuaid, "Recycling integrator for measuring nanoampere currents," The Review of Scientific Instruments, 36, 599-600, (1965).

Work supported by US Dept. of Energy, Contract No. DE-AC03-76SF00098 and by National Cancer Institute under grant CA 30236.

## CHARGED PARTICLE SPOT SCANNING METHOD: EFFECTS OF MOTION ON DOSE HOMOGENEITY

Mark Phillips\*<sup>†</sup>, Eros Pedroni<sup>†</sup>, Reinhard Bacher<sup>†</sup>, Hans Blattmann<sup>†</sup>,  
Terence Bochringer<sup>†</sup>, Adolf Coray<sup>†</sup>, Stefan Scheib<sup>†</sup>

\* Research Medicine and Radiation Biology, Lawrence Berkeley Laboratory,  
1 Cyclotron Road, Berkeley, CA 94720, USA

† Division of Radiation Medicine, Paul Scherrer Institute  
CH-5232 Villigen-PSI, Switzerland

### Abstract

A spot scanning technique has been developed using a proton beam at the Paul Scherrer Institute (PSI) cyclotron. The depth-dose curves and lateral dose fall-off were measured and were used as input to a computer modelling program that calculates the dose distribution in a volume of water. Beam scanning parameters—speed and order of beam spot deposition—from the PSI method determined the position of the beamspot as a function of time. Respiration motion was modelled using a sinusoidal function. Beamspot size and position, number of fractions, order of scanning, respiration amplitude, respiration frequency, and direction of respiration were systematically varied. The dose homogeneity was determined by calculating the standard deviation (rms) of the resulting dose distribution and the maximum variation from the mean dose. The results of the calculations provide insight into the maximum tolerable patient motion, and are being used to improve the design of the entire beam delivery system.

### Introduction

Charged particles, such as protons and heavier ions, have better dose localization characteristics than photons. Past and current facilities have used charged particle beams that have been broadened by scattering to achieve uniform dose distribution across the beam profile and use collimators to restrict the beam to the target volume. Dose uniformity in the direction of beam propagation is achieved by “stacking” successive Bragg peaks of incrementally decreasing range. Recently, there has been much interest in the use of narrow beams of charged particles that are magnetically steered. Such scanning methods offer the ability to truly optimize the dose localization within the tumor volume, as well as offering a flexible and rapidly reprogrammed beam delivery system. Magnetic scanning can easily be implemented in the beam optics of an isocentric beam transport system, permitting the design of the gantry to be reduced to dimensions similar to those used in conventional therapy.

One of the major objections to using scanned beams has been the difficulty in achieving a uniform 3-dimensional dose. When broad, scattered fields are used, the dose at any point within the volume relative to some reference point is fixed. Variations in dose rate apply uniformly throughout the volume, and the incident beam has a well-defined profile. When using scanned beams, the dose at any point is independent of the dose at any other point. The first requirement, therefore, is a reliable and accurate dose monitoring and delivery system.

Scanning systems also must contend with the possibility that between the times of application of dose at two positions the tissue may move as a result of patient respiration or motion. This can result in two adjacent beams overlapping to produce a “hot” spot, or in two adjacent beams being widely separated so that there is a “cold” spot between them. This problem can be reduced by using large beams that have gradual dose fall-off, with the tradeoff being that the resolution of dose localization is reduced. Small, sharp beams can conform the dose precisely to the target volume, but are sensitive to patient motion. At PSI, we are seeking to find a suitable compromise between the two extremes that is clinically relevant and useful. Using experimentally measured beam profiles, we have performed computer simulations in order to assess the critical parameters and their effect on the dose homogeneity when respiratory motion is present.

### Methods and Materials

#### Beam Scanning

A detailed description of the PSI spot scanning method has been presented earlier in this conference [8]. A 600 MeV proton beam is degraded to 214 MeV and reanalyzed. A kicker magnet turns the beam “on” and “off” by steering it through a narrow aperture or into a beamstop. A sweeper magnet steers the beam in the X direction (along the body axis). The beam passes through two ionization chambers which monitor the total dose and the position, respectively. A range shifter consisting of 0.46 cm water-equivalent plastic sheets which can be inserted into the beam moves the Bragg peak in the Z direction. A patient transporter moves the patient to provide the third axis of spot positioning.

The dose is delivered in a series of discrete spots, each placed 0.5 cm apart. The spot is scanned sequentially first in the X direction. Then a range shifter plate is inserted and the spot is moved in the Z direction, and the X axis is scanned again. This continues until the plane is scanned. Then the patient transporter moves the patient up 0.5 cm and the next plane is scanned. This sequence is continued until the entire volume is scanned. One can also irradiate every second or third spot along one or more axes (definition of *rescanning multiplicity* along that axis) and then rescan the volume a number of times to fill in the missing spots in an attempt to randomize the tissue motion relative to the spot placement and achieve a more uniform dose distribution. To the extent that the width of the spot is larger than the effective step size between spots used with a particular multiplicity, the dose applied on a single

rescanning cycle should be quite homogeneous. In this limit, multiplicity rescanning and fractionation (complete rescanning) should have similar effects.

#### Computer Model

A representative dose volume of 1 liter ( $10 \times 10 \times 10$  cm) was used for calculations. In the absence of motion, beamspot separations of 0.5 cm (X), 0.5 cm (Y), and 0.46 cm (Z) were used. The points at which the dose was calculated were typically separated by 0.5 cm in all three directions. That this was a sufficiently fine spacing was checked by performing calculations with spacings down to 0.2 cm. The measured Bragg peak and the width of the Gaussian beam were stored in lookup tables and were used to determine the dose at surrounding dose grid points for each position of the beamspot.

Respiration was simulated using a sinusoidal function:  $A_r \sin(2\pi T/T_r + \phi)$ . The direction of motion,  $A_r$ , was either X, Y, or Z. The position of each beamspot was calculated by coordinating the respiratory motion with the time dependent position of the beamspot, as defined by the beamspot velocities ( $v_x = 500$  cm/sec,  $v_y = 25$  cm/sec, and  $v_z = 2$  cm/sec) plus the reaction time of the system for turning off the beam. Multiple fractions were simulated by repeating the calculations with a random initial phase. The phase was considered constant throughout a single fraction.

Analysis of the 3-dimensional dose distribution was performed either graphically or analytically. The RMS dose uniformity was defined as the standard deviation of the dose within a volume that excluded the dose fall-off at the borders of the scanned volume. The maximum deviation of the dose relative to the mean dose was also calculated.

#### Results and Discussion

The dose uniformity in the absence of motion is 1% due to the small ripple resulting from the narrowness of the Bragg peak in the Z direction. Perpendicular to the beam propagation direction, the dose is very uniform. At a depth of 23.7 cm, the lateral dose fall-off is 1.48 cm from 90% to 10%. At the end of the range of 28.7 cm, the dose fall-off in the distal direction is 0.67 cm from 90% to 10%.

Motion due to respiration introduces a number of variables that can affect dose homogeneity: (a) respiration amplitude,  $A_r$ , (b) respiration period,  $T_r$ , (c) respiration axis,  $A_r$ , (d) number of fractions, F, and (e) multiplicity, M. The effects of these are complicated by the interaction between the time-dependent deposition of dose at each spot and the motion of the irradiated volume. Such an interaction was manifested in the pronounced variation in the RMS dose homogeneity from calculation to calculation when the motion was along the slowest axis (Y) of beam scanning. The variability was significantly less when the motion was in the Z direction, and was negligible when along the X (fastest) axis.

The motion of an organ due to respiration strongly depends on the location of the organ and the forcefulness of the respiration and can range from 0 to 5 or 6 cm. Traditionally, consideration of the blurring effects on the edges of the dose distribution because of respiration has been included in the marking of a margin about the tumor when defining the tumor volume. Ohara and colleagues [7] quote a value of 2 cm when the tumor

is close to the diaphragm. It seems reasonable to limit the spot scanning technique to those cases where the size of the beam spot is not smaller than the motion of the target volume.

The possibility of synchronizing the radiation with respiration was explored by Ohara for photons and was found to confer a marked benefit. The same idea can be applied to the spot scanning technique, and its implementation would be very simple since the irradiation control system is already part of the technique. We have not included synchronization in our simulation since we are exploring the worst possible cases.

The dose uniformity was the worst for motion along the Y axis, since the beam scanning velocity in this direction was comparable to the respiration velocity. Scanning along X proceeds virtually instantaneously with respect to respiration motion and was the least sensitive to respiration. Scanning in Z is intermediate in speed and effect with regards to respiration. Fig. 1 illustrates the effect on the RMS dose homogeneity as a function of  $A_r$  for motion along the X, Y, and Z axes.

To assess the effect of the size of the beam, the Gaussian width was doubled with respect to the values plotted in Fig. 1. The lateral dose fall-off from 90% to 10% increased to 3.2 cm. In the absence of motion, dose uniformity was approximately equal to that with the narrower beam. For  $F = 1$ ,  $M = 1.1, 1$ ,  $T_r = 5$  sec, and  $A_r = Y$ , the dose uniformity was 3% for  $A_r = 1$  cm, and 4% for  $A_r = 2$  cm.

Fractionation had a considerable effect on the dose uniformity in all cases, as shown in Fig. 2. The standard deviation of the dose decreased approximately proportional to the square root of the number of fractions, as did the maximum deviation from the mean dose. Regardless of the direction of the motion, the RMS dose uniformity was less than 4% for 15 or more fractions. Increasing the multiplicity also lowered the standard deviation and maximum deviation of the dose, although not as much as the fractionation did. This may be caused by the fact that fractionation is a statistical averaging of the motion about every beamspot, whereas the rescanning with increasing multiplicity does so only to the extent that the dose from a beamspot overlaps the location of adjacent beamspots.

The interaction between respiration period and the multiplicity was difficult to predict. In general, no appreciable effect on the dose uniformity was seen when the respiration period was varied between 1 and 10 sec (60 to 6 breaths/min). Increasing the multiplicity had the general effect of improving the dose uniformity.

Kanai and colleagues [3,4] also demonstrated a scanning system with protons that achieved very good dose uniformity. They used a collimator to produce a beam that was square in cross-section with very sharp edges. References [3] and [4] do not deal with motion of the patient, but given the sharp beamspot they used, their system would most probably be very sensitive to patient motion. Levin and colleagues [5] calculated that a proton scanning system would not be practical because of the extreme sensitivity of the dose uniformity to patient motion or beamspot misplacement. However, their calculations utilized beamspots with very sharp dose fall-off at the edges.

These results, when added to those presented in this paper, demonstrate the importance of (a) the dose fall-off at the edges of the beam and (b) the importance of statistically averaging spatial fluctuations in the dose. Very sharp beams provide good conformation at the edges of the target volume but can-

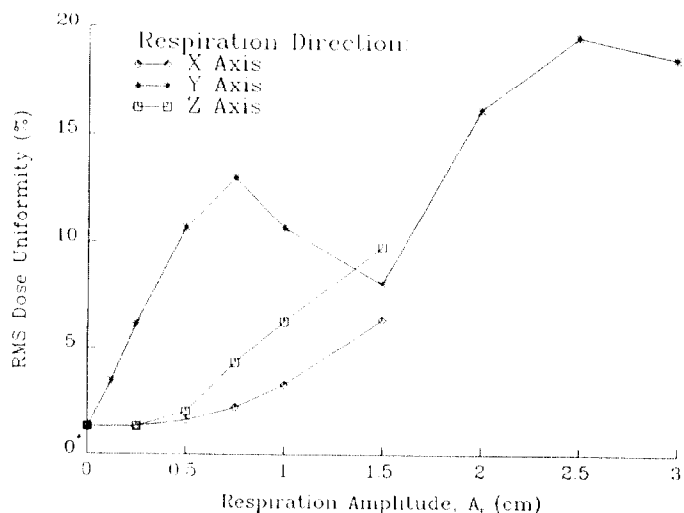


Figure 1: RMS dose homogeneity ( $100 \times$  standard deviation / mean dose) as a function of respiration amplitude,  $A_r$ , for motion along the X, Y, and Z axes. It would not be practical to use spot scanning with the given beam size when respiration motion was greater than approximately 1 cm.

not tolerate much motion. Broader, Gaussian, beams are much more robust but sacrifice the sharpness at the tumor borders. The addition of a small multileaf collimator (covering the swept beam) and the use of ridge filters could cure this problem without giving up the main advantages of the spot scan method, i.e. complete automation on a compact gantry system. The dose uniformity is significantly enhanced, as expected, by rescanning the volume many times. In addition, it appears that the direction of respiration motion and the direction of the slowest direction of spot scanning is an important factor in reducing dose inhomogeneity. Dose homogeneity, however, is not the only factor to be considered. Respiration synchronization is the only method that results in improvement at the edge of the field as well.

The results of our calculations need to be interpreted in light of current practice and theory regarding the required uniformity of dose in radiotherapy. Recent articles have addressed the issue of precision and accuracy in radiotherapy [1,6]. These articles, and the ICRU Report 24, recommend an accuracy of approximately 5%. It is also stated [6] that in practice the dose uncertainty is approximately 4% with photons and 6-8% with neutrons at a specified point, and that the uncertainty at other points within the target volume will be higher. The early results of our experimental work and computer simulations provide confidence that such standards can be met using the spot scanning method. They are also providing an important input into the design process so that decisions as to the use of collimators, respiration synchronization, and other components can be made that will result in a clinically useful system.

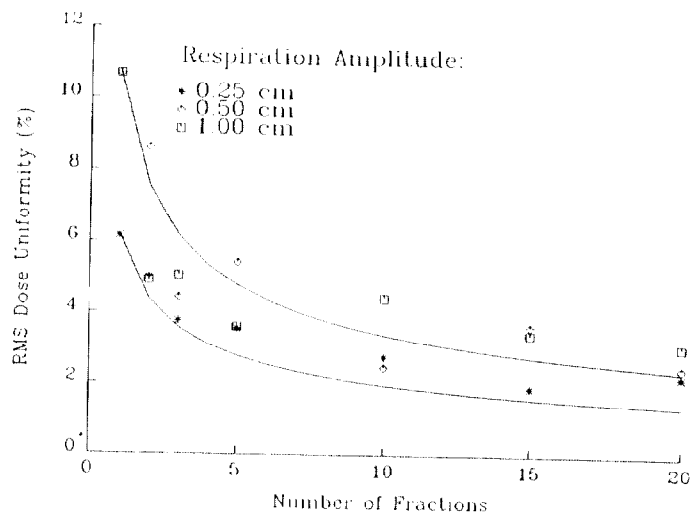


Figure 2: RMS dose uniformity plotted as a function of number of fractions for three different values of respiration amplitude,  $A_r$ . The solid lines are plots of the dose uniformity at  $F=1$  divided by the square root of the number of fractions.

## References

- [1] A L Boyer, T Schultheiss. Effects of dosimetric and clinical uncertainty on complication-free local tumor control. *Radiotherapy and Oncology*, 11: 65-71 (1988).
- [2] ICRU Report 24. Determination of absorbed dose in a patient irradiated by beams of X- or gamma-rays in radiotherapy procedures. International Commission on Radiation Units and Measurements, Woodmont Avenue 7910, Washington, DC 20014, USA, 1976.
- [3] T Kanai, K Kawachi, Y Kumamoto, H Ogawa, T Yamada, H Matsuzawa, T Inada. Spot scanning system for proton radiotherapy. *Medical Physics*, 7: 365-369 (1980).
- [4] T Kanai, K Kawachi, H Matsuzawa, T Inada. Three-dimensional beam scanning for proton therapy. *Nuclear Instruments and Methods*, 214: 491-496 (1983).
- [5] C V Levin, R Gonin, S Wynchank. Computed limitations of spot scanning for therapeutic proton beams. *Int J Biomed Comput*, 23: 33-41 (1988).
- [6] B J Mijnheer, J J Battermann, A Wambersie. What degree of accuracy is required and can be achieved in photon and neutron therapy? *Radiotherapy and Oncology*, 8: 237-252 (1987).
- [7] K Ohara, T Okumura, M Akisada, T Inada, T Mori, H Yokota, M J B Calaguas. Irradiation synchronized with respiration gate. *Int J Radiation Oncology Biol Phys*, 17: 853-857 (1989).
- [8] E Pedroni, R Bacher, H Blattmann, T Boehringer, A Coray, E Egger, M Phillips, S Scheib. Cancer therapy with 200 MeV protons at PSI. Development of a fast beam scanning method and future plans for a hospital based facility. European Particle Accelerator Conference, Nice, France, June, 1990.

## EULIMA BEAM DELIVERY

F.J.M. Farley and C. Carli  
 Eulima Feasibility Study Group  
 Laboratoire du Cyclotron, Centre Antoine Lacassagne  
 227 Avenue de la Lanterne, 06200 Nice, France

## Abstract

The stopping light ion beam must be scanned through the tumour in three dimensions, laterally and in range. Range changing with a fixed energy cyclotron implies a degrader. The optimum beam condition at the degrader is calculated, and it is shown that the increase in phase space by multiple scattering is acceptable. Range straggling and projectible fragmentation are also tolerable.

In contrast to conventional radiotherapy (x-rays, cobalt) the light ion beam from EULIMA and similar machines can be exactly localized, laterally to  $\pm 1.5$  mm, and in range to 5 mm. This allows the tumour to be treated precisely by scanning in three dimensions over a designated volume of arbitrary shape. The beam delivery system must accomplish this reliably and safely at reasonable cost.

- This requires lateral (x-y) deflection by a fast magnet
- Variable range
- Variable exposure time to achieve a uniform biologically effective dose, see Fig 1.
- Position sensitive monitors
- Rapid switch off in case of malfunction

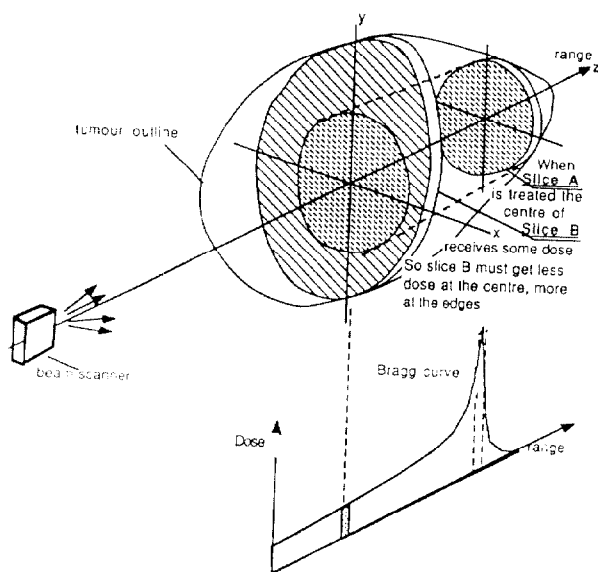


Fig. 1 3 D Conformal Therapy

Fig 1 shows a typical treatment plan. By adjusting the range, the Bragg curve is placed successively at various depths. Each depth slice is scanned in the x-y plane over the tumour cross-section at that depth; Note that when distal slice A is treated, the centre of central slice B will receive some dose. This must be compensated when slice B is treated, by giving more dose at the edges than at the centre. Therefore in general each slice requires a carefully computed non-uniform dose.

In any scanning system tissue movement is a problem. An unfortunate correlation between movement and scanning period could cause part of the system to be overdosed while other parts receive nothing. Internal organs move cyclically in synchronisation with breathing and heart beat. Synchronizing the beam with respiration is one possibility [1], and the pulse could also be included, implying an accelerator with plenty of intensity to spare and good on/off control. The alternative is to repeat the scan many times and hope that unforeseen correlations will cancel out. Hope is a virtue, but we prefer not to depend

upon it when lives are at stake.

## Lateral scanning

The scanning across the x-y plane may be either continuous (called "raster scan") or intermittent (called "pixel scan").

## Pixel scan

The target plane is treated at a triangular mesh of points, Fig 2, with spacing  $p$ , and a Gaussian beam spot of standard deviation  $\sigma$ .

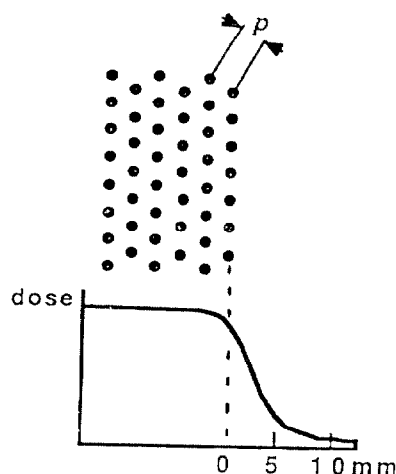


Fig. 2 Pixel Scanning

If  $\sigma \geq 0.5 p$  the dose is uniform to 1.2%. The edge definition depends on  $\sigma$  and is shown in Fig 2 for  $\sigma = 2.5$  mm,  $p = 5$  mm. This is good enough to delineate a cross-section of arbitrary shape by choosing which pixels to treat. The procedure would be as follows: beam off - move spot to pixel - beam on until desired dose is reached - repeat for next pixel.

We see the following advantages for the pixel scan

- flexible shape in each plane
- each pixel is dosed separately giving flexible dose distribution
- no collimators
- no beam when spot is moving
- no error from magnet rise time or transient oscillations
- no error from beam intensity fluctuations
- conceptually simple computer control
- good security

An essential technical prerequisite is a means of switching the beam on and off. With a cyclotron this can be done at low energy in the injection line, because the particles only spend  $60 \mu\text{s}$  inside the machine and the beam loading is negligible. However with a synchrotron using resonant ejection to get a long burst it takes several milliseconds to cut the beam; therefore a fast beam switch needs to be included in the transport system, and this is expensive.

The time available per pixel is determined by the desired maximum treatment time (5 mn), the number of pixels ( $10^4$  for a one litre tumour), and the number of times one scans the tumour in each session (say 10). This gives 3 ms per pixel, to include spot settling time, on/off switching and treatment.

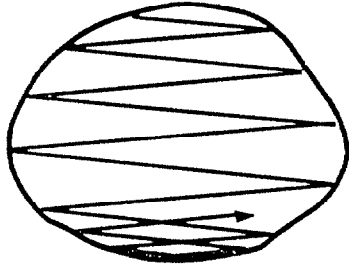


Fig. 3 Raster Scanning

Raster scanning

With equally spaced parallel lines, spacing  $p$ , a Gaussian spot of standard deviation  $\sigma$  gives a dose uniform to 2.83 % if  $\sigma \geq 0.5 p$ . In principle a cross-section of any shape can be delineated (Fig 3), but it requires the horizontal turning points to be correlated with vertical position and there will be some overdose at the turning points where the spot velocity is less. In general the intensity can be modulated by varying the spot velocity. Note that at Berkeley the raster scan gives a rectangular field and collimators are used to define the exact tumour shape, so the turning points are screened.

The main advantage of the raster scan is that no on/off switch is needed in the beam. It requires :

- a steady beam
- precise control of scan velocity
- fast magnet response with no undesirable transients

Disadvantages are :

- probable overdose at turning points or collimator needed
- rapid beam fluctuations cannot be compensated
- faster magnet response will be needed and this means more power.

Scanning in range

Typically the depth required in tissue is 5 cm (min) to 20 cm (max). (Shallower tumours could be treated by low energy proton machines). The corresponding particle energies for carbon are 140-340, and for oxygen 170-420 MeV/nucleon. With a synchrotron there is no problem in varying the extraction energy. A cyclotron however has a fixed extraction energy, so it will be necessary to reduce the energy by passing the beam through a slab of matter (called the degrader) of variable thickness. However the degrader has several undesirable effects which must be analysed :

- a) increase of the beam phase space by multiple scattering
- b) increase of the momentum spread by energy straggling
- c) fragmentation of the incoming particle, giving lighter ions of roughly the same velocity with a longer range in the patient.

Multiple scattering

At any point along the beam axis we assume that in the horizontal phase space defined by

$$\mathbf{X} = \begin{pmatrix} x \\ \theta \end{pmatrix}$$

the distribution of particles is Gaussian, with the one standard deviation contour defined by the ellipse

$$\bar{\mathbf{X}} \sigma^{-1} \mathbf{X} = 1 \tag{1}$$

The symmetric matrix

$$\sigma = \begin{pmatrix} \sigma_{11} & \sigma_{12} \\ \sigma_{12} & \sigma_{22} \end{pmatrix} \tag{2}$$

Then specifies the beam shape and area, and is transformed according to

$$\sigma' = \mathbf{R} \sigma \bar{\mathbf{R}} \tag{3}$$

where  $\mathbf{R}$  is the usual transport matrix (3). The overall variance of the distribution in the  $\theta$ -direction is  $V_\theta = \sigma_{22}$ .

We consider how the matrix  $\sigma$  is changed by a degrader of finite thickness  $t$ , adding the effects of multiple scattering in each larger  $dt$  to the effect to the drift distance  $dt$ . For drift alone

$$\mathbf{R} = \begin{pmatrix} 1 & dt \\ 0 & 1 \end{pmatrix}$$

so applying (3)

$$d\sigma/dt = \begin{pmatrix} 2\sigma_{12} & \sigma_{22} \\ \sigma_{22} & 0 \end{pmatrix} \tag{4}$$

For scattering alone

$$d\sigma_{22}/dt = d\theta_{rm}^2 = \mathbf{K}(t) \tag{5}$$

with  $\mathbf{K}(t) = 200 Z^2/A^2 p^2 \beta^2 X_0$  for a projectile of charge  $Z$ , mass  $A$  velocity  $\beta c$ , and momentum  $p$  in MeV/c, in a degrader of radiation length  $X_0$ .  $\mathbf{K}$  varies with  $t$  because  $p$  and  $\beta$  are changing. Adding (4) and (5) gives the total change in  $\sigma$ ,

$$d\sigma/dt = \begin{pmatrix} 2\sigma_{12} & \sigma_{22} \\ \sigma_{22} & \mathbf{K} \end{pmatrix} \tag{7}$$

For a degrader of total thickness  $t$ , (7) can be integrated term by term to give at the output

$$\sigma_{out} = \sigma_{do} + \sigma_s \tag{8}$$

where  $\sigma_{do}$  is the matrix expected at the end of the degrader due to the drift distance only and the effect of the scattering is entirely included in

$$\sigma_s = \begin{pmatrix} C & B \\ B & A \end{pmatrix} \tag{9}$$

with

$$A(t) = \int_0^t \mathbf{K} dt, \quad B = \int_0^t A dt, \quad \text{and} \quad C = 2 \int_0^t B dt \tag{10}$$

Note that  $\sigma_s$  is independent of the phase space of the incoming beam, and depends only on the properties of the degrader, plus the beam momentum. In general the beam emittance, that is the area of the ellipse in phase space is

$$\pi \epsilon = \pi \sqrt{\det(\sigma)}$$

The emittance is not changed by drift distance only so the input beam emittance is given by

$$\epsilon_{in}^2 = \det(\sigma_{in})$$

In (8) we now vary the components of  $\sigma_{do}$  keeping the emittance fixed, to find the condition for minimum emittance  $\epsilon_{out}$  at the output with scattering included. One finds for the optimum beam,

$$\sigma_{do} = (\epsilon_{in}/\epsilon_s) \sigma_s \tag{11}$$

where

$$\epsilon_s^2 = AC - B^2 \tag{12}$$

That is the components of the unscattered beam must be proportional to the components of  $\sigma_s$ , with magnitudes adjusted to give the correct determinant. Substituting in (8), one finds in this case, for the output emittance including scattering

$$\epsilon_{out} = \epsilon_{in} + \epsilon_s \tag{13}$$

In summary, if the shape of the input beam is optimized the increase in emittance due to the degrader is  $\epsilon_s$ ; this is only a function of the degrader characteristics and adds linearly to the input emittance.

The integrals in equation (10) have been evaluated for various materials, slowing down a beam from 20 cm range in water to 5 cm range. The results are given in Table 1 for beams of fully stripped carbon.

Table I  
 Degradar parameters for C<sup>12</sup> beam slowing down from 20 cm range-in-  
 tissue to 5 cm

Material	$\rho$	X <sub>0</sub> cm	thickness cm	$\epsilon_s$ mm.mrad
Li	0.53	155	34.5	6.25
H <sub>2</sub> O	1.00	36.1	15.0	5.10
Be	1.85	35.3	10.0	2.23
B <sub>4</sub> C	2.52	20.7	7.1	2.06
graphite	2.26	18.8	7.5	2.42
Cu	8.96	14	2.5	3.55

The density of the degrader is significant, as well as the thickness in radiation lengths, and for this reason boron carbide turns out to be the best material. (Diamond would be even better, but is not available in the required thickness). The output emittance of 2.06 mm.mrad (one standard deviation) for B<sub>4</sub>C is encouraging. However the one standard deviation ellipses, in horizontal and vertical planes together, only contain 16 % of the particles. To pass 40% of the particles we must double the emittance in both planes to 4 mm.mrad, which is comparable to synchrotron output beams with no degrader. As the cyclotron has plenty of intensity to spare we can sacrifice the rest of the beam and still have more particles.

One concludes that multiple scattering in the degrader is not an impediment for a light ion cyclotron.

Energy straggling

For a thin layer with a projectile of charge Z, velocity  $\beta c$ , in a target of charge Z<sub>T</sub>, the variance V in energy increases as

$$dV/dt = 4\pi n e^4 Z^2 Z_T (1 - \beta^2/2)/(1 - \beta^2) \quad (14)$$

where n is the number of target atoms per cm<sup>3</sup>. Projecting to the end of the degrader and integrating, the final variance is

$$V = \int_{E_{in}}^E \left\{ \frac{dE}{dX}(E_{in}) \right\}^2 \frac{dV}{dt} dt \quad (15)$$

Degrading a carbon ion beam from 20 cm range in water to 5 cm range gives  $dp/p = 0.5\%$ . If non-dispersive bends are used this should not be a problem for the beam optics.

Fragmentation

It is intended to place the degrader close to the cyclotron, so that fragments with the wrong magnetic rigidity will be lost in the bending magnets. As fragments in general have the same velocity as the incoming projectile, only those with the same Z/A as the projectile need be considered. Light fragments of the same Z/A have much smaller dE/dx and longer range. Therefore only the fragments produced in the final layers of the degrader will have the same rigidity as the main beam.

Partial cross-sections for carbon and oxygen beams of 2.1 GeV/n in a beryllium target for deuteron production are 32<sup>9</sup> and 417 nb respectively ; for helium production 383 and 501 nb. At 100 Mev/n the cross-sections will be smaller. Other fragments are much less probable. For oxygen penetrating 10 cm of beryllium one finds that d<sup>2</sup> + He<sup>4</sup> together are 10 % of the beam ; but allowing for the different dE/dx we expect only about 1% of the beam to have the correct rigidity.

Therefore fragmentation does not seem to be a serious problem provided that a momentum selection is made after the degrader.

Beam layout

A preliminary drawing of the EULIMA beam delivery system is given in Fig 4. Initially there will be one vertical and one horizontal beam, both with scanners. Further beams can be added as indicated.

References

- [1] K. Ohara, T. Okumura, M. Akisada, T. Inada, T. Mori, H. Yokota and M. Calaguas, *Int. J. Oncology Biol. Phys.* 1989, 17, 853
- [2] T. R. Renner, W. Chu, B. Ludewigt, J. Halliwell, M. Nyman, R. P. Singh, G. D. Stover and R. Stradtner, "Preliminary results of a raster scanning beam delivery system" Particle Accelerator Conference, Chicago 1989
- [3] K.L. Brown, D.C. Carey, C. Iselin and F. Rothacker, 1980, CERN Yellow report 80-04
- [4] N. Bohr, *K. Dan Vidensk Selsk. Mat. Fys. Medd.* 1948, , 18  
 K.H. Schmidt, E. Hanelt, H. Geissel, G. Münzenberg and J.P. Dufour, *Nuch. Instr and Meth.* 1987, A260, 287
- [5] D.L. Olsen, B.L. Berman, D.E. Greiner, H.H. Huckman, P.J. Lindström and H.J. Crawford, *Phys. Rev. C*, 1983, 28, 1602

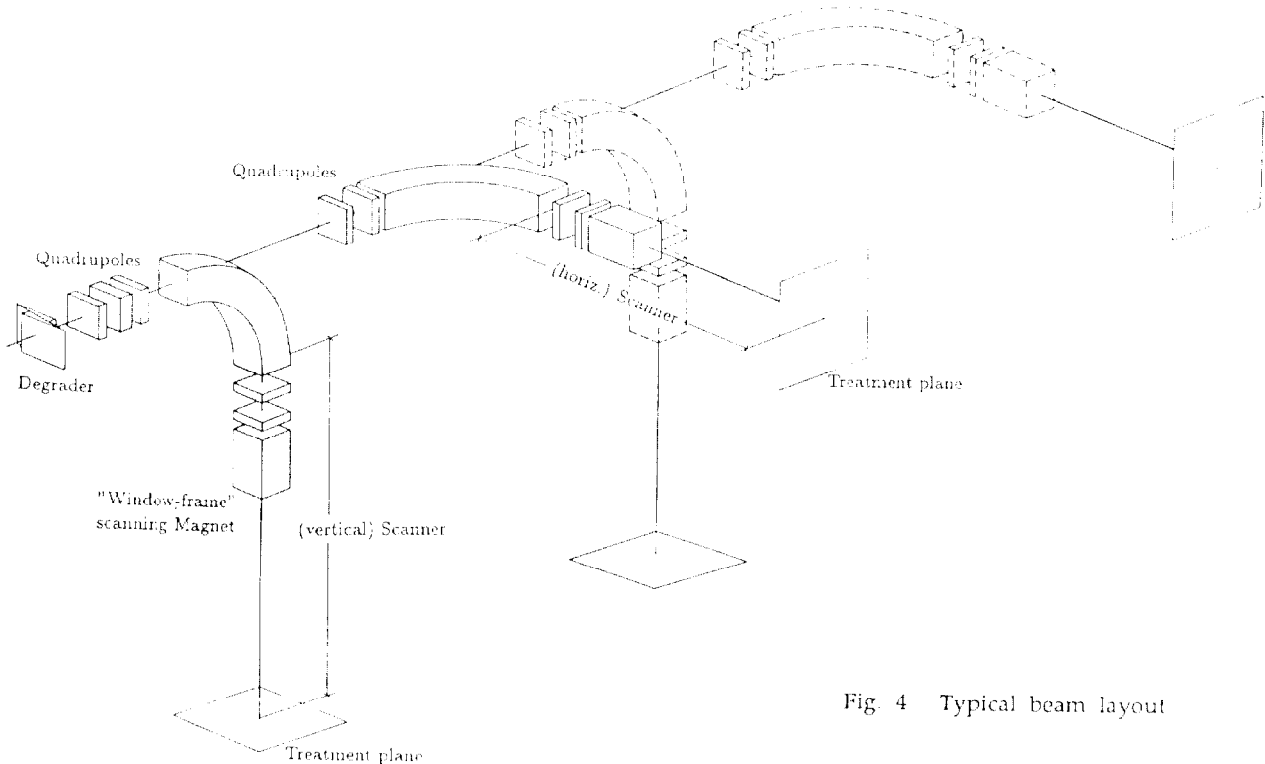


Fig. 4 Typical beam layout

APPROACH TO BORON NEUTRON CAPTURE THERAPY IN EUROPE:  
GOALS OF A EUROPEAN COLLABORATION ON  
BORON NEUTRON CAPTURE THERAPY

Detlef Gabel  
Department of Chemistry  
University of Bremen  
Box 330 440  
D-2800 Bremen 33

**Abstract:** A European Collaboration on Boron Neutron Capture Therapy has been founded in 1989. This Collaboration wants to create all necessary conditions to establish neutron capture therapy as a clinical therapy in Europe. For this, two main goals are being pursued:

1. To initiate, at the High Flux Reactor in Petten (The Netherlands) clinical trials of glioma and melanoma
2. To create conditions that other tumors can be treated at this and at other sites.

In this paper, the approach towards clinical trials of gliomas with boron neutron capture therapy is detailed. The necessary development of an epithermal neutron beam, and the necessary healthy tissue tolerance studies are discussed in view of the particularities of the radiobiology of boron neutron capture therapy.

#### Introduction to Boron Neutron Capture Therapy

Boron neutron capture therapy (BNCT) is based on the high cross section of the boron-10 nuclide for thermal neutrons. Upon capture, the boron nucleus disintegrates into highly energetic alpha- and lithium-7 particles. One event liberates enough energy to, in principle, kill a cell. The nuclides that are present in the body (hydrogen, nitrogen, carbon, oxygen) possess such low cross sections for thermal neutrons that already modest amounts of boron (in the order of several tens of microgram boron per gram tissue) suffice to deliver a substantially increased dose to that tissue.

BNCT was tried clinically in the United States in the late 1950's and early 1960's. These trials resulted in a failure, and were consequently abandoned. In Japan, clinical trials for glioma (Hatanaka, since 1968) [1] and melanoma (Mishima, since 1987) [2] are being pursued. World-wide, a greatly increased interest in BNCT can be observed. This interest is based on the fact that we now know which factors led to the failure of BNCT in the past. Problems were encountered with the poor penetration of the thermal neutron beam into tissue, a poor differential between tumorous and healthy tissue of the boron compounds used, and an excessive radiation dose especially to the skin.

Better boronated tumor seekers are now available. More is known about the radiation biology of the dose components that are encountered in BNCT. Finally, epithermal neutron beams are accessible that permit to treat tumors at depth.

For the above-mentioned Goal 2, namely the treatment of tumors other than gliomas and melanomas, it will be necessary to develop new and improved tumor seekers. This requires advances in boron chemistry, and an intense collaboration of boron chemists with, e.g., biochemists and biologists. The development of other neutron sources, also part of Goal 2, aims at existing research reactors and their conversion or modification to extract sufficiently intense epithermal neutron beams. Of great potential usefulness are accelerator-based neutron beams. The physical and technical feasibility is presently under experimental evaluation.

Here, emphasis will be placed on the approach to Goal 1. It is the aim of the European Collaboration to initiate clinical trials of glioma by the end of 1991.

#### Epithermal Neutron Beams for BNCT

As mentioned above, a thermal neutron beam was used in the past, and is being used currently, for BNCT. Thermal neutrons (i.e. neutrons having a kinetic energy corresponding to room temperature, around 0.025 eV) are capable of being captured immediately by all elements in the body, and therefore have only a limited depth to which they can penetrate before reacting. Epithermal neutrons, i.e. neutrons in the energy range of 1 eV to 10 keV, cannot as such be captured efficiently by the atoms of the body. They will, however, lose energy through collisions, and thus will eventually reduce their energy to thermal values. In biological material, the maximum thermal neutron flux occurs at around 2 cm depth, with many neutrons penetrating much further.

Beams of epithermal neutrons can be produced by filtration from fission spectrum neutrons obtained from a reactor, or spallation neutrons obtained from an accelerator. These beams, because of incomplete filtration, will contain a number of fast neutrons (i.e. neutrons with energies far above 10 keV), and gamma photons emerging from the reactor and produced in filter and structural materials.

#### Determination of the Biological Effects of Neutron Beams

In order for such beams to be useful, their biological effect on the tissue present in the beam must be known. The biological effect of the beam will determine which dose can be administered to the target volume (containing the tumor and healthy tissue) without inducing unacceptably high damage. This must be known before clinical trials can be embarked upon.

Two different approaches to this (and any similar) problem can be envisaged. One approach would be to arrive at the exact conditions of the clinical trial from known basic facts (the deductive approach). The alternative approach would be empirical (the inductive approach).

In principle, it would be of great reassurance if treatment of BNCT could rely on deduction from known principles. It would then be necessary to identify and quantify the different components to the biologically effective dose in the target, to quantify the biological response to these different dose components, and to tailor, with these data, the incident beam such that the tumor receives a maximum dose, while healthy tissue is not inflicted an unpermissibly high dose.

As will be detailed below, this approach is presently not feasible in BNCT, and perhaps might never be possible.

In BNCT, there are a variety of dose components that contribute to the total dose. For an epithermal neutron beam, which would allow to treat tumors at depth and thus overcome some of the problems encountered in the initial clinical trials, these dose components come from the incident beam (mainly fast neutrons and gamma photons), and from neutron capture reactions of the thermal neutrons generated with hydrogen (giving rise to a 2.2 MeV gamma photon) and nitrogen (generating a carbon-14 ion and a proton of an energy of 0.56 MeV available for ionization).

In addition to the doses associated with the epithermal beam impinging on the target, there is a dose component generated by the  $^{10}\text{B}(n,\alpha)^7\text{Li}$  capture reaction wherever boron is present in the irradiation volume.



Depth-dose profiles for the different dose components will have shapes like those shown in Fig. 1 for the epithermal neutron beam of the Medical Research Reactor of the Brookhaven National Laboratory [3].

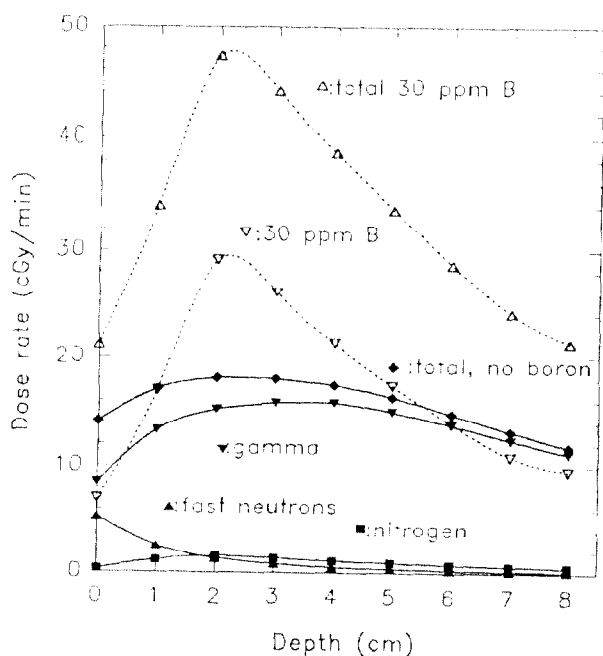


Fig. 1. Depth-dose profiles in a cylindrical phantom of the epithermal beam of the Brookhaven Medical Research Reactor. (Data adapted from [3])

The necessary information about these different dose components would have to come from adequate physical dosimetry of the different beam components in the different volume elements in the target. In conventional radiotherapy, a sum of all dose components, multiplied when indicated with their appropriate RBE values, would give a good estimate of the actual expected dose in each of the volume elements of the target.

There are considerable problems to estimate the biologically effective dose associated with the boron capture reaction. These problems cannot be solved easily, and might perhaps elude estimation altogether. This arises from the fact that the alpha and the lithium particles generated in the boron capture event have, in biological tissue, ranges that are commensurate with the dimensions of a cell. Thus, the energy deposited in the nucleus of a cell will depend considerably on the location of the boron capture event in relation to the cell nucleus [4]. (The energy deposited in the nuclei of single cells has been termed "hit size" by Bond [5], in order to differentiate it from dose, which is an average quantity. Subsequently, "hit size" will be used to indicate the energy deposited in a cell nucleus.) Calculations by Gabel for typical cells [4] have indicated that the hit sizes from this reaction might vary by almost a factor of 10, depending on whether the same amount of boron is distributed uniformly throughout the tissue or whether present only on the surface of the cells. (The latter case might arise when antibodies are used to carry boron.) Furthermore, because of the energy and the high LET values of the two particles, Poisson statistics will result in a large variation of hit sizes. Analysis of cell biological experiments [4], taking into account the statistical variations of hit sizes, infers the existence of a Hit Size Effectiveness Function [5]. This implies that not every cell whose nucleus receives a hit size from the  $^{10}\text{B}(n,\alpha)^7\text{Li}$  reaction, will die as a consequence. The probability of reproductive death will increase with increasing hit size.

For these reasons, the concepts of "dose" and "RBE" can be misleading in BNCT.

As a consequence, only an empirical, i.e. inductive, approach towards BNCT can be followed in a given therapy situation with a given compound. This will be reflected in treatment planning.

#### Treatment Planning in BNCT

In conventional radiotherapy, considerable effort is devoted to maximize the dose to the tumor and at the same time spare healthy tissue. This is achieved by tailoring the beam shape for each of several irradiation ports.

In BNCT, the approach must be different. This is due to the fact that the incident beam is not as such of therapeutic efficacy. Upon collision with a sufficient number of atoms, the epithermal neutrons have reduced their energy such as to be captured by boron (and hydrogen and nitrogen). During the process, the initial direction of the neutrons will gradually be lost, and consequently the edges of the beam will become diffuse in comparison with conventional therapy beams. A broad range of penetration depths will exist for these neutrons (in marked contrast to the Bragg peak observed for accelerated heavy particles). Therefore, not only will the beam be diffuse laterally, but also vary considerably in its dose to tissue along the beam axis. The hydrogen capture reaction gives rise to long-reaching gamma photons, which in the absence of boron are responsible for the major fraction of the dose deposited in tissue, and will add to the broadening of the beam.

In BNCT, the hit size to a tumor cell is due mostly to the hit size from boron, and thus cannot be influenced by the shape and properties of the external beam. Treatment planning is indeed achieved by the choice of compound. Therefore, the properties of the beam are of greatly reduced importance, as far as its lateral and depth profiles are concerned. This is illustrated in Fig. 2. In conventional radiotherapy, the hit size to one cell is very close, if not identical, to the hit size to its immediate neighbors. In BNCT, each cell will receive a hit size which is due to a very great extent only to the amount of boron this very cell has accumulated.

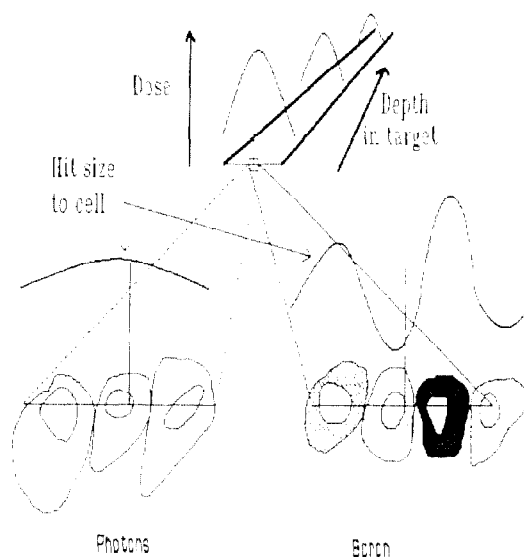


Fig. 2. Schematic presentation of hit sizes to cells in a target from photons, compared to hit sizes from the  $^{10}\text{B}(n,\alpha)^7\text{Li}$  reaction. The target will attenuate the beam and, in the case of a neutron beam, broaden it. In the case of photons, hit sizes to adjacent cells will be similar, if not identical. Hit sizes to cells in BNCT will be dependent mostly on the boron accumulation in each of the cells, and will therefore vary greatly between one cell and its immediate neighbors.

In healthy tissue, one will have to expect that boron will be present in different cells in different amounts. The determina-

tion of boron concentrations averaged over as little as several cells, not to mention weighable amounts of tissue, will not allow to draw conclusions for the hit size to each of the cells present. In order for this to be predicted, the distribution of boron in each of these cells and their immediate neighbors needs to be known. There are presently no techniques to measure this. In the tissues of an individual patient, this distribution will remain unknown even if such techniques were available.

#### The Safety of BNCT Treatment

In order to initiate clinical trials with BNCT, as with any other new therapy modality, it must be made plausible that the treatment does not carry an undue risk to the patient; indeed, it must be made sure, in the case of BNCT and in conjunction with its earlier failure, that the risk to the patient is minimal. To ensure safety is of primary concern for the initial treatment planning; efficacy of treatment is consequently not as important in the first steps. Therefore, the effect of the therapy on healthy tissue must be estimated. A thorough study of the tolerance to the therapy of healthy tissue exposed to the beam must thus be conducted.

Healthy tissue tolerance will be studied in dogs. The dogs will be given  $\text{Na}_2\text{B}_{12}\text{H}_{11}\text{SH}$  (BSH) in different amounts, and they will then be exposed to different neutron levels. BSH is used by Hatanaka [1] for treating gliomas, and will be used in the initial study in Europe. From the initial studies on healthy tissue tolerance in dogs carried out in the United States, as well as from the dose-depth profiles of such beams in phantoms, the likely tissue at risk is not the skin, but tissue at a few centimeters depth (i.e. brain tissue) (see also Fig. 1). White matter necrosis would occur with such treatment, and this will take several months to develop. (In previous experience of the late 50's and early 60's, skin was the most radiosensitive organ. This was due to both the high boron concentration in the skin and the simultaneous use of a thermal neutron beam. With beams of moderate mean energy, and using the presently available boron compounds, skin is no longer the dose limiting healthy tissue.)

From a knowledge of the dose components at different depths, operational factors can be derived when this study includes different levels of boron concentration and neutron exposure. These factors then allow the necessary exposure planning.

Due to the importance of localization of boron, the maximally tolerated dose will be compound dependent. Thus, studies with one compound (e.g. BSH) will not yield much information for the treatment using a different boron compound (e.g. p-dihydroxyboryl phenylalanine). Equally, studies for one target organ (e.g. brain tissue) cannot, even for the same compound, be transferred easily to other treatment areas.

In order to transfer results from this animal study to patients, the pharmacokinetics of the boron compound needs to be known in both. The European Collaboration therefore has placed great emphasis on a thorough pharmacokinetic study of BSH in brain tumor patients.

#### Requirements on the Epithermal Neutron Beam

The quality of the incident neutron beam is, of course, of great importance for the success of the treatment. As detailed above, there are not only epithermal neutrons present in the beam, but also unwanted components. These include fast neutrons and gamma photons. The number of fast neutrons relative to those of epithermal neutrons, expressed as the mean energy of the beam, should be as low as possible. This can be achieved by filtering away neutrons of unwanted energy by means of suitable filter materials. Filter materials of potential use are: aluminum, sulfur, deuterium, oxygen, titanium. There is a price to be paid for heavy filtration, in terms of loss of intensity of the beam.

Gamma photons have to be absorbed by the use of appropriate shielding material. Shielding materials include bismuth

and argon (liquid).

Extensive calculations of these different filter and shielding materials have been carried out for the High Flux Reactor (HFR) in Petten (The Netherlands). The first goal was to explore which range of mean energies, beam intensities, and gamma contaminations can be achieved. With these data at hand, and based on the projected healthy tissue tolerance, beam design goals were defined. These are:

Neutron fluence	$\geq 10^9 \text{ n cm}^{-2} \text{ s}^{-1}$
Mean neutron energy	$\leq 8.1 \text{ keV}$
Incident gamma dose	$\leq 0.5 \text{ Gy} / 3 \cdot 10^{12} \text{ n cm}^{-2}$

The neutron fluence of this beam would be enough to deliver a therapeutic dose, in a single session, in a period of around one hour. Most probably, a fractionated treatment will be aimed for. This is based on the general practice and experience in conventional radiotherapy, the unavoidable and considerable gamma component to the total dose, and the limit to which radiation can be delivered to the skull without inducing unwanted side effects.

A beam with the above characteristics will be achieved by combinations of aluminum, sulfur, titanium, cadmium, and liquid argon as filter materials. All other materials were found to be less useful for the beam construction.

The filter will be installed in the HB11 beam hole of the HFR, during the summer break of 1990.

#### The Next Steps

Following the installation of the beam, its physical parameters will be carefully measured and compared with the calculated values. Extensive dosimetry in phantoms will be carried out and complemented by cell survival assays. Thereafter, the above-mentioned study of healthy tissue tolerance will begin. It is anticipated that clinical trials can start towards the end of 1991.

#### Acknowledgments

I am greatly indebted to all members of the European Collaboration for their great enthusiasm for and cooperation in this project. I am grateful to R.G. Fairchild and M.L. Griebenow for communicating essential information prior to publication, and for stimulating discussions. The work of the European Collaboration is supported, on a supra-national level, by the Commission of the European Communities, which is gratefully acknowledged.

#### References

- [1] H. Hatanaka, Boron-Neutron Capture Therapy for Tumors. Niigata, Nishimura, 1986.
- [2] Y. Mishima, C. Honda, M. Ichihashi, H. Obara, J. Hiratsuka, H. Fukuda, H. Karashima, T. Kobayashi, K. Kanda and K. Yoshino, "Treatment of malignant melanoma by single thermal neutron capture therapy with melanoma-seeking  $^{10}\text{B}$ -compound", Lancet, Vol. II, pp. 388-389, 1989.
- [3] R.G. Fairchild, J. Kalef-Ezra, S.K. Saraf, S. Fiarman, E. Ramsay, L. Wielopolski, B. Laster and F. Wheeler, "Installation and testing of an optimized epithermal neutron beam at the Brookhaven Medical Research Reactor (BMRR), in Proceedings of the Workshop on Neutron Beam Design, Development and Performance for Neutron Capture Therapy, Plenum Press, New York, in press, 1990.
- [4] D. Gabel, S. Foster and R.G. Fairchild, "The Monte-Carlo Simulation of the Biological Effect of the  $^{10}\text{B}(n,\alpha)^7\text{Li}$  Reaction in Cells and Tissue and Its Implication for Boron Neutron Capture Therapy", Radiat. Res. Vol. 111, pp. 14-25, 1987.
- [5] V.P. Bond, M. Varma, C.A. Sondhaus and L.E. Feinendegen, "An alternative to absorbed dose, quality, and RBE at low exposures", Radiat. Res. Vol. 104, pp. S52-S57, 1985.

## PROGRAMME FOR ACCELERATOR-BASED NEUTRON CAPTURE THERAPY

A. Andersson<sup>5</sup>, J.-O. Burgman<sup>5</sup>, J. Capala<sup>5</sup>, J. Carlsson<sup>5</sup>, H. Condé<sup>3,5</sup>,  
 J. Crawford<sup>9</sup>, S. Graffman<sup>8</sup>, E. Grusell<sup>5</sup>, A. Holmberg<sup>5</sup>, E. Johansson<sup>5</sup>,  
 O. Jonsson<sup>5</sup>, B.S. Larsson<sup>6</sup>, B. Larsson<sup>5</sup>, P. Lindström<sup>1,5</sup>, B. Norling<sup>5</sup>,  
 L. Pellettieri<sup>2</sup>, O. Pettersson<sup>5</sup>, J. Pontén<sup>4</sup>, M. Pråhl<sup>5</sup>, A. Roberto<sup>6</sup>,  
 K. Russel<sup>5</sup>, H. Reist<sup>9</sup>, T. Rönnqvist<sup>3,5</sup>, L. Salford<sup>7</sup>, S. Sjöberg<sup>1</sup>,  
 B. Stenerlöv<sup>5</sup>, P. Strömberg<sup>5</sup>, and B. Westermark<sup>4</sup>

Departments of chemistry<sup>1</sup>, neurosurgery<sup>2</sup>, neutron research<sup>3</sup>, pathology<sup>4</sup>,  
 radiation sciences<sup>5</sup>, and toxicology<sup>6</sup>, Uppsala university, Uppsala, Sweden;  
 Departments of neurosurgery<sup>7</sup> and oncology<sup>8</sup>, University of Lund, Lund, Sweden;  
 and the Paul Scherrer Institut<sup>9</sup>, CH-5232 Villigen, Switzerland

Boron neutron capture therapy (BNCT), with slow neutrons, is based on the large cross-section of the stable boron isotope,  $^{10}\text{B}$ , for thermal neutron capture. Upon capturing a neutron, the  $^{10}\text{B}$  nucleus is transformed to a highly excited  $^{11}\text{B}$  compound nucleus that promptly disintegrates into two antiparallel, highly energetic and cell-killing fragments, one  $^4\text{He}^{+2}$  and one  $^7\text{Li}^{+3}$  ion, with ranges of 9 and 5 micrometers respectively. By more or less selective accumulation of  $^{10}\text{B}$  in suitable chemical form, to levels of 10 mg/kg or more, in or in close contact with the target cells, the probability of target cell sterilization is significantly increased, after therapeutic slow-neutron irradiation.

BNCT was originally conceived in 1936<sup>1</sup>. Partly for lack of basic knowledge, partly for technical reasons, it took half a century to introduce the idea clinically and get it accepted on the basis of favourable treatment results<sup>2</sup>. BNCT is at present used in Japan, in cases of malignant brain tumours and skin melanoma, using thermal neutrons from fission reactors. Also in preparation are reactor-based facilities for intermediate energy neutrons ("keV neutrons") that would permit more efficient irradiation of deep-lying targets, without the concern for damage to the skin and other intervening tissues<sup>3</sup>. The appropriate energy range is around 10 keV, in single or opposing field BNCT. When the aim is multidirectional irradiation, as in our programme, somewhat higher energies, say 10 - 100 keV could be used, without undue risk of damage caused by recoiling nuclei. A rotating source would also permit some tailoring of the neutron capture probability distributions within the brain or the body. Taken together with the difficulties connected with the safety of nuclear reactors in hospital environments - be it a real problem or not - the desired ver-

satility in configurating the keV neutron fields in BNCT calls for studies of the usefulness of accelerator-produced neutrons for multidirectional intermediate energy neutron irradiation. Thus the production of keV neutrons by spallation reactions induced by accelerated protons in heavy element targets has been studied as part of a Swedish-Swiss collaboration<sup>4</sup>. The aim is the design of a keV neutron source that could be rotated relative to the patient. Indirectly, the successful operation of such a device could be a step towards the introduction of hospital-based BNCT.

#### A spallation neutron source for BNCT

Various target-moderator combinations have been tried using 72 MeV protons from the Philips Injector Cyclotron I at the Paul Scherrer Institut (PSI). The experimental neutron spectra thus found have been compared to and supplemented by theoretical calculations<sup>5</sup>. A proposal for a prototype facility for accelerator-based BNCT with the high-current PSI Injector Cyclotron II is now in preparation<sup>6</sup>. In this proposal the concept of a rotating proton beam hitting a ring-shaped spallation target in the depth of a moderator structure is introduced. In this paper, this idea is referred to, and the biological and clinical implications discussed. The related programme of chemical and biological research is also briefly reviewed. Here we limit ourselves to problems concerned with treatment of cerebral disorders, but the new concepts and findings may help to pave the way for the use of BNCT in cases of infiltrating neoplasms, including pathological vessels, and regional metastatic disease in the abdomen or in extremities. Whether accelerator-based BNCT would be eventually useful against systemic disease, by whole-body keV neutron irradiation, is still hard to say.

When medium-energy protons are stopped in a heavy metal target, such as tungsten, the evaporation neutron spectrum shows a peak energy of less than 2 MeV. By proper choice of moderator material and configuration, it is possible to reduce the energy of the bulk of these neutrons to the energy interval suitable for BNCT with keV neutrons. The 72 MeV proton beams available at the injector cyclotrons are well suited for the design study, and for the eventual biological and clinical tests with the planned prototype neutron source for BNCT. This was demonstrated in the first experiments with low-current proton beams from the Philips Injector Cyclotron I that included measurements of moderated spallation neutron spectra by time-of-flight techniques, and the mapping of neutron capture probability distributions in a perspex phantom<sup>7</sup>. Results of these experiments and Monte Carlo calculations show good agreement. The work shows that thermal neutron fluences suitable for BNCT in the depth of the brain could be produced by keV neutron fields emanating from a tungsten target bombarded with less than 0.2 mA beams of 72 MeV protons.

Special attention has to be paid to the cooling and maintenance of the spallation target, where many kilowatts of heat will be produced. In one possible solution (Fig. 1), the horizontal proton beam scans continuously over a ring-shaped spallation target, 50 cm in diameter, which is buried in a semi-spherical Fe + D<sub>2</sub>O moderator. This configuration permits the neutrons to reach the patient's head from many directions, so as to reduce the keV neutron flux in the skin and skull.

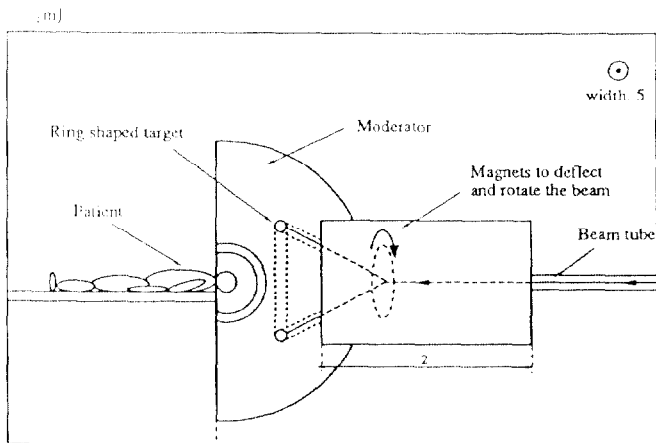


Fig. 1. Layout of a possible design of a spallation source for keV neutron therapy in cases of intracerebral disease. The 72 MeV proton beam enters from the right. Moderator: 1.05 m Fe + 8 cm Pb + 20 cm D<sub>2</sub>O.

With the target-moderator geometry shown in Fig. 1, the boron neutron capture dose has a maximum at a depth of 2 cm in the phantom. The depth-dose then decreases linearly (Fig. 2). At 10 cm depth, the neutron capture dose is still 40% of the peak dose. The situation is comparable or better than the very best neutron capture distributions that can be expected at nuclear fission reactors, particularly since the dose is nearly constant in any chosen plane perpendicular to the beam axis (Fig.3). The associated dose of fast neutrons and gamma rays is comparatively low.

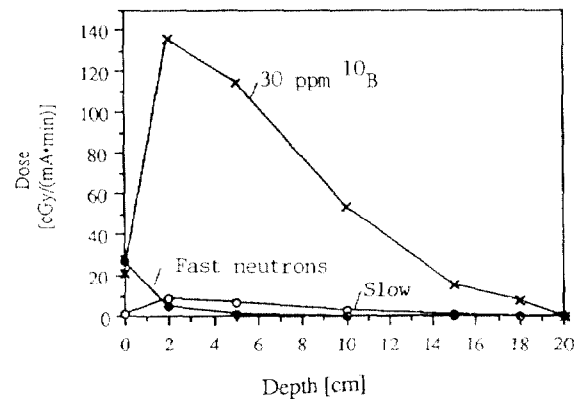


Fig. 2. Absorbed neutron doses on the axis of symmetry. Gamma dose levels are indicated in Fig. 3.

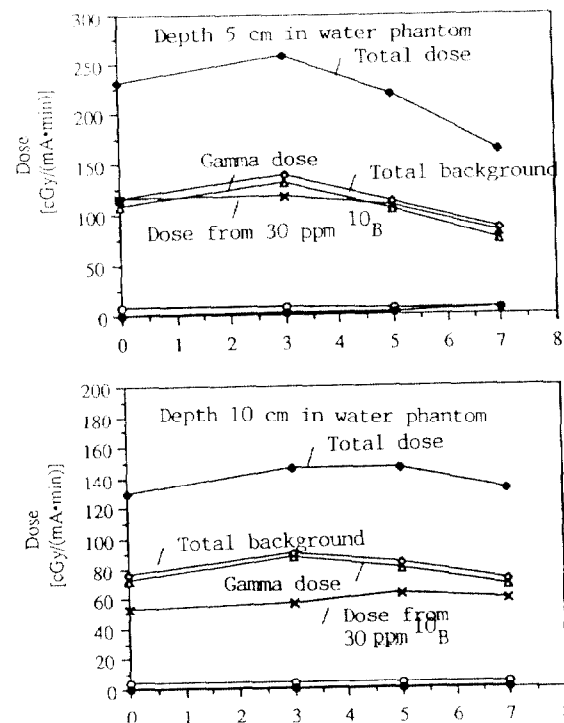


Fig. 3. Total dose and dose fractions in planes perpendicular to the axis of symmetry. Upper curves at 5 cm depth, lower curves at 10 cm depth.

Clinical aims of BNCT with keV neutrons and related  
chemical and biological studies

This programme is closely connected with the European Collaboration on BNCT<sup>3</sup>. The primary goal is a useful BNCT for advanced malignant brain tumours and for inoperable vascular malformations, as a supplement to existing methods of surgery, stereotaxic radiosurgery, and radiotherapy. A basic philosophy is to consider BNCT as an adjuvant therapy, in the context of precise external photon or charged particle therapy. By such a combination of modalities it should be possible to further optimize radiotherapy for maximum benefit of the patient. The bulk of a primary tumour, or the nidus of an arterio-venous malformation, where the density of target cells is high could then be treated with a relatively high dose, while peripheral or scattered target cells in surrounding tissues could be more selectively attacked by the highly cell-killing fragments of disintegrating boron nuclei.

To meet the clinical expectations, the aim of our chemical and biological research is to develop and test a variety of principles that would be useful for directing  $^{10}\text{B}$  to tumour cells, or to the endothelium of pathological vessels. In a number of basic scientific projects, we therefore address problems of boron compound synthesis and cytoaffinity, boron pharmacokinetics in animal models and human subjects, as well as the radiobiology of neutron capture reactions in tumour cells, tumour models, and healthy tissues. A main theme is the design of boron-loaded biomolecules with specificity for the target cells. The epidermal growth factor, EGF, conjugated with boron-loaded dextrane is the latest and most promising example<sup>7</sup>. EGF-dextrane conjugates are being tested with favourable results, in experiments on cultured human glioma cells and in tumours transplanted into immunodeficient mice or rats.

Awaiting the availability of heavily boron-loaded, cell-seeking biomolecules, such as EGF or suitable antibody fragments, the radiobiological study is based on low-molecular weight boron compounds with affinity for melanin<sup>8</sup>. In this way  $^{10}\text{B}$  could be accumulated in melanotic melanoma cells that are useful in model experiments, in vitro as well as in vivo. The effects of neutron capture on endothelial cells are similarly studied by use of boronated dextrane, at relatively high concentration, in the medium of cell cultures or in the blood of experimental animals<sup>9</sup>.

References

1. G. L. Locher, Biological effects and therapeutic possibilities of neutrons. *Am. J. Roentgenol. and Radium Ther.*, 36 (1936) 1.
2. H. Hatanaka, S. Kamano, K. Amano, S. Hojo, K. Kano, S. Egawa, and H. Yasukochi, Clinical experience of boron-neutron capture therapy for gliomas - a comparison with conventional chemo-immuno-radiotherapy. In: H. Hatanaka (Ed.), "Boron Neutron Capture Therapy for Tumors, Nishimura Co. Ltd, Niigata, Japan, 1986, pp. 349-378.
3. D. Gabel, Approach to neutron capture therapy in Europe: goals of a European Collaboration on boron neutron capture therapy. In these proceedings.
4. H. Condé, E. Grusell, B. Larsson, E. Ramström, T. Rönqvist, O. Sornsuntisook, S. Villa, J. Crawford, H. Reist, B. Dahl, N. G. Sjöstrand, and G. Russel, Status report on the development of a spallation source for neutron capture therapy. In: R. G. Fairchild et al. (Eds.), "Clinical Aspects on Neutron Capture Therapy", Plenum Publ. Corp., New York 1989, pp. 319-323.
5. P. Strömberg, Pers. comm. 1990.
6. J. F. Crawford, H. Condé, K. Elmgren, E. Grusell, B. Larsson, B. Nilsson, H. Reist, T. Rönqvist, G. Russel, and O. Pettersson, Neutron beams for capture therapy produced by 72 MeV protons, To be presented at the 4th Int. Conf. on Neutron Capture Therapy, Sydney, Australia, December 1990.
7. S. Sjöberg, G. Bergson, G. Adolf, P. Lindström, J. Carlsson, B. Larsson, A. Andersson, C. Jacek, A. Holmberg, B. Westermark, and J. Pontén, Synthesis of low-molecular weight boron compounds and their conjugation to EGF-dextrane and other tumour-seeking substances. Internal report, March 1990. (The project spokesperson is Dr Stefan Sjöberg, Department of chemistry, Uppsala university, Box 531, S-751 21 Uppsala, Sweden)
8. B. S. Larsson, B. Larsson, and A. Roberto, Boron neutron capture therapy for malignant melanoma: An experimental approach, *Pigment Cell Research* 2 (1989) 356.
9. B. Larsson, J. Carlsson, H. Börner, J. Forsberg, A. Fourcy, and M. Thellier, Biological studies with cold neutrons. An experimental approach to the LET problem in radiotherapy. In: "Progress in Radio-Oncology II, K. H. Kärcher et al. (Eds.), Raven Press, New York 1982, pp. 151-157.

Acknowledgements

The experimental work has been financially supported by the Swedish Cancer Society, the Swedish Medical Research Council, The Swedish Natural Science Research Council, and the Swedish Board of Technical Development.

## A NEUTRONIC STUDY OF AN ACCELERATOR NEUTRON IRRADIATION FACILITY (ANIF) FOR BORON NEUTRON CAPTURE THERAPY (BNCT)

T.X. Bruce Qu, Thomas E. Blue, Reinhard A. Gahbauer, James Blue  
The Ohio State University, Nuclear Engineering Program, Dept of Mechanical Engineering  
206 West 18th Avenue, Columbus, Ohio 43210-1107

### ABSTRACT

The major components of an Accelerator Neutron Irradiation Facility (ANIF), for Boron Neutron Capture Therapy (BNCT), are a radio-frequency quadrupole (RFQ) proton accelerator, a  ${}^7\text{Li}$  target, and a moderator assembly. Neutrons generated by bombarding the  ${}^7\text{Li}$  target with 2.5 MeV protons are too energetic to be used for BNCT, and are moderated as they traverse the moderator assembly to the patient. The design of the moderator assembly for an Accelerator Epithermal Neutron Irradiation Facility (AENIF) is described and compared with the design of the moderator assembly for an Accelerator Thermal Neutron Irradiation Facility (ATNIF). From the performance evaluation of the two designs we conclude that, with different moderator assemblies, a 30 mA 2.5 MeV RFQ proton accelerator can be used to treat both superficial and deep lesions from melanomas and gliomas.

### I. INTRODUCTION

Boron Neutron Capture Therapy (BNCT) is an experimental technique for the treatment of highly malignant tumors that are resistant to other treatment modalities. It is based upon the  ${}^{10}\text{B}(n,\alpha){}^7\text{Li}$  reaction. In BNCT,  ${}^{10}\text{B}$  containing compounds are administered to the patient. These delivery agents carry boron to the tumor, where it attaches to or is incorporated within the tumor cells. Then the tumor site is irradiated with thermal neutrons. The thermal neutron are absorbed by the  ${}^{10}\text{B}$ , producing short range high LET  ${}^4\text{He}$  and  ${}^7\text{Li}$  nuclei, which selectively destroy malignant cells that contain a sufficient amount of  ${}^{10}\text{B}$ .

Prerequisites for successful BNCT are boron containing compounds with good tumor specificity and a suitable source of thermal neutrons; that is, a source which can provide a large flux of thermal neutrons at the tumor site, and a small dose equivalent to the surrounding normal tissue. At the First and Second International Conferences on BNCT, an Accelerator Neutron Irradiation Facility (ANIF) for BNCT was proposed [1]. The major components of an ANIF are a radio-frequency quadrupole (RFQ) proton accelerator, a  ${}^7\text{Li}$  target, and a moderator assembly. Neutrons generated by bombarding the  ${}^7\text{Li}$  target with 2.5 MeV protons are too energetic to be used for BNCT, and are moderated as they traverse the moderator assembly to the patient. The design of the moderator assembly for an Accelerator Epithermal Neutron Irradiation Facility (AENIF) for the treatment of gliomas is described and compared with the design for an Accelerator Thermal Neutron Irradiation Facility (ATNIF) for the treatment of superficial melanomas. The performance of the AENIF

and the ATNIF is evaluated, and the neutron fields produced by the AENIF and the ATNIF are compared with reactor epithermal and thermal fields for BNCT.

### II. BACKGROUND

#### II.1 Glioblastoma and Melanoma

Boron Neutron Capture Therapy is presently being considered as a means for treating two types of tumors: glioblastoma multiforme and malignant melanoma. For glioblastoma multiforme, which occurs within the brain, the source neutrons should have energies in the range of 1 eV to 1 keV, in order to penetrate to the tumor in large numbers, without depositing too much energy at the skin's surface. The characteristics of the neutron sources for the treatment of melanomas may be very different from that of glioblastoma multiforme. For treatment of melanomas that spread superficially at the skin level, the thermal neutron flux should be as large as possible, and the contamination of the thermal neutron field by fast and epithermal neutrons should be as small as possible.

#### II.2 Neutronic Properties for the Moderator Assemblies

In order to treat glioblastoma and melanoma, two different moderator assemblies are required.

For the AENIF moderator assembly, the neutronic properties which a good moderator material should possess are (1) large  $\Sigma_s$ , the neutron scattering cross section; (2) moderate  $\xi$ , the average increase in the lethargy of a neutron per collision; and (3) small  $\Sigma_a(n,\gamma)$ , the neutron cross section for radiative capture. For the AENIF, a good reflector material should have large  $\Sigma_s$ , small  $\xi$ , and small  $\Sigma_a(n,\gamma)$ .

The neutronic properties of a good moderator material for the ATNIF moderator assembly are similar to those of a good moderator material for the AENIF, except that  $\xi$  should be as large as possible. Also, the neutronic properties of a good reflector material for the ATNIF are similar to those of a good reflector material for the AENIF, except that  $\xi$  may be large (although it need not necessarily be so).

### III. MODERATOR ASSEMBLY DESIGN

#### III.1 Figures of Merit for AENIF and ATNIF Moderator Assemblies

To assess the design of the AENIF moderator assembly, a figure of merit (FOM) is the epithermal neutron flux ( $\Phi_e$ ) at the irradiation point in air. A second FOM is the neutron kerma to epithermal and fast neutron fluence ratio, or average kerma factor, for a differential volume of tissue, at the irradiation point in air. To assess the design

of the ATNIF moderator assembly, a FOM is the thermal neutron flux ( $\Phi_t$ ) at the irradiation point in air. A second FOM is the Ratio of the Thermal neutron fluence to the epithermal neutron and Fast neutron fluence, RTF, at the irradiation point in air.

### III.2 Calculation Methods

The coupled neutron and gamma-ray transport calculations for the AENIF and ATNIF moderator assemblies and phantoms were performed using the three-dimensional multigroup Monte Carlo code MORSE-CG [5]. The multigroup cross sections used in the calculations came from BUGLE-80, a coupled, 47-neutron, 20-gamma-ray,  $P_3$ , cross-section library [3]. The kerma was assumed to equal the absorbed dose for both the neutron and gamma-ray dose for all points within the phantom. The kerma factors used for dose calculations also came from BUGLE-80. These kerma factors were derived for each of the 47 neutron and 20 gamma-ray groups by collapsing the 171-neutron, 36-gamma-ray MACKLIB-IV kerma factor library [4]. The neutron kerma factors were calculated for tissue, and for tissue with a  $^{10}\text{B}$  concentration of  $3 \mu\text{g}$  of  $^{10}\text{B}$  per gram of tissue, which is the  $^{10}\text{B}$  concentration of melanomas [5]. The tissue composition was assumed to be  $(\text{C}_5\text{H}_{40}\text{O}_{18}\text{N})_n$ .

There are five important components of the absorbed dose in BNCT: the absorbed dose due to  $^{10}\text{B}(n,\alpha)^7\text{Li}$  reactions, three components of the absorbed dose due to neutrons interacting with the elements in tissue, and the absorbed dose due to gamma rays which accompany the neutron beam as it enter the patient. The three components of the absorbed dose, due to neutrons interacting with the elements in tissue, are due to  $^1\text{H}(n,n')^1\text{H}$ ,  $^{14}\text{N}(n,p)^{14}\text{C}$ , and  $^1\text{H}(n,\gamma)^2\text{H}$  reactions. Our AENIF and ATNIF moderator assembly performance evaluation is based upon calculations of the dose equivalent in representative phantoms. Following Fairchild [6], in calculating the dose equivalent from the absorbed dose, we have assumed an RBE of 1.0 for the absorbed dose due to gamma rays, which accompany the neutron beam or which result from  $^1\text{H}(n,\gamma)^2\text{H}$  reactions (this sum is hereafter called the gamma ray absorbed dose); an RBE of 2.0 for the absorbed dose due to protons, which result from  $^1\text{H}(n,n')^1\text{H}$  or  $^{14}\text{N}(n,p)^{14}\text{C}$  reactions (this sum is hereafter called the neutron absorbed dose); and an RBE of 2.5 for the absorbed dose due to  $^{10}\text{B}(n,\alpha)$  reactions (hereafter called the boron absorbed dose).

## IV. RESULTS AND PERFORMANCE EVALUATION

### IV.1 AENIF

#### IV.1.1 FOMs

The optimization of the design FOMs for the AENIF resulted in the moderator assembly that is shown in Fig. 1. It consists of a cylinder of  $\text{BeO}$ , which is 25 cm in diameter and 22.5 cm in height, surrounded by a 30 cm thick alumina reflector. Also,  $0.01 \text{ g/cm}^2$  of  $^6\text{LiF}$  is placed at the moderator assembly exit window to reduce thermal neutron contamination at the irradiation point.

The moderator assembly yields at the irradiation point in air an epithermal neutron flux of  $3.1 \times 10^7 \text{ n/cm}^2\cdot\text{sec}$  per mA of proton

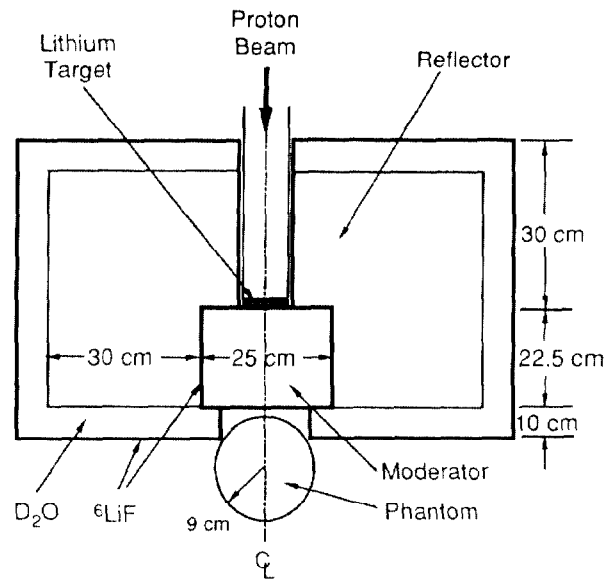


Figure 1. The configuration of the moderator assembly for AENIF. (side view)

current, with a neutron kerma to epithermal and fast neutron fluence ratio of  $4.9 \times 10^{-11} \text{ cGy}\cdot\text{cm}^2/\text{n}$ , which is equal to the kerma factor of a 5 keV neutron. The neutron spectra for the AENIF neutron field and the Brookhaven National Laboratory Medical Research Reactor (BMRR) BNCT beam are plotted in Fig. 2. As one can see, the neutron flux in the epithermal region (i.e. from 1 eV to 1 keV) is comparable for the AENIF operating at 30 mA and for the BMRR operating at 1 MW. For neutron energies greater than 20 keV but less than 300 keV, the neutron flux is relatively larger for the AENIF than for the BMRR. However, for neutron energies greater than 300 keV, the neutron flux for the BMRR decreases slowly, while the

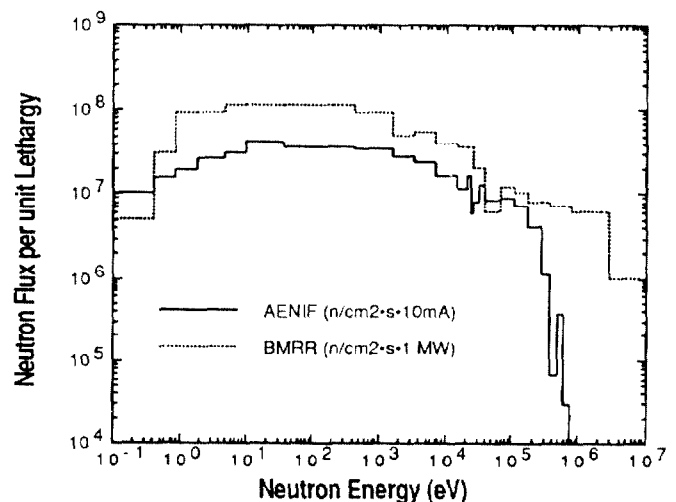


Figure 2. The neutron flux spectra for the AENIF and BMRR

neutron flux for the AENIF decreases precipitously, because the  ${}^7\text{Li}(p,n){}^7\text{Be}$  reaction does not produce neutrons with energies greater than 800 keV for a proton kinetic energy of 2.5 MeV. Despite the differences in the spectra above 20 keV, the average kerma factors for a differential volume of tissue irradiated in the two fields are nearly equal.

#### IV.1.2 Performance Evaluation

With the AENIF moderator assembly shown in Fig. 1, the maximum absorbed dose (MAD) rate to both normal tissue and tumor, in a 9 cm radius spherical head phantom, occurs at a depth of 3.5 cm. At this depth, the MAD rate is  $2.0 \times 10^{-4}$  Gy/s per mA of proton current for a  ${}^{10}\text{B}$  concentration of 10  $\mu\text{g/g}$  tissue and is  $3.4 \times 10^{-4}$  Gy/s per mA of proton current for a  ${}^{10}\text{B}$  concentration of 30  $\mu\text{g/g}$  tumor. Therefore, for a single session irradiation of 20 Gy to the tumor, the treatment time is about 33 min for a 30 mA beam [7].

### IV.2. ATNIF

#### IV.2.1 FOMs

The optimization of the design FOMs for the ATNIF, resulted in a moderator assembly consisting of a cylinder made of  $\text{D}_2\text{O}$ , which is 25 cm in diameter and 50 cm in height, surrounded by a 40 cm thick graphite reflector. The thermal neutron flux  $\Phi_t$  at the irradiation point in air is  $4.9 \times 10^7$  neutrons/ ( $\text{cm}^2 \cdot \text{sec} \cdot \text{mA}$ ) and the RTF is 32.

#### IV.2.2 Performance Evaluation

With a 20 cm x 40 cm x 80 cm rectangular parallelepiped phantom placed with its short axis along the moderator assembly centerline, 5 cm from the surface of the moderator, the thermal neutron flux at the center of the phantom surface is  $(2.5 \pm 0.2) \times 10^8$  neutrons/ ( $\text{cm}^2 \cdot \text{sec} \cdot \text{mA}$ ). The absorbed dose rates to tissue at the phantom surface with a  ${}^{10}\text{B}$  concentration of zero are  $(0.47 \pm 0.03)$  cGy/(min·mA) for neutrons and  $(2.0 \pm 0.4)$  cGy/(min·mA) for gamma-rays. The boron absorbed dose rate to tumor at the phantom surface is  $(3.2 \pm 0.2)$  cGy/(min·mA) for a tumor  ${}^{10}\text{B}$  concentration of 24  $\mu\text{g}$   ${}^{10}\text{B}$  per gram of tumor, which is the  ${}^{10}\text{B}$  concentration which has been reported for human melanomas which have been treated with BNCT [5]. The corresponding total (i.e. neutron plus gamma plus boron) dose equivalent rate to the tumor is 10.1 cSv/(min·mA). At this dose equivalent rate, the time which it takes to deliver 40 Sv to the tumor (the dose equivalent recommended to cure melanoma [5]) is 13.2 minutes for a 30 mA proton beam. For a tumor dose of 40 Sv, the corresponding total dose equivalent to normal tissue with a  ${}^{10}\text{B}$  concentration of 3  $\mu\text{g}$   ${}^{10}\text{B}$  per gram of tissue is 15 Sv. This is less than the 18 Sv normal tissue tolerance dose equivalent recommended in Ref. 3; and indicates the adequacy of our ATNIF thermal neutron field for the treatment of melanoma.

### V. CONCLUSION

We conclude that from a neutronic standpoint, a 30 mA 2.5 MeV proton accelerator can be used to treat both superficial and deep lesions from melanomas and gliomas. Different moderator assemblies are necessary for the optimal treatment of these tumor types. We have presented in this paper the two extremes; a

moderator assembly for superficial tumors and our previously designed moderator assembly for deep tumors.

### ACKNOWLEDGMENT

This work was supported in part by the National Cancer Institute under Grant 1 RO1 CA 47298-01 and by the U.S. Department of Energy under contract DE-AC02-76CH00016.

### REFERENCES

1. J.W. Blue, W.K. Roberts, T.E. Blue, R.A. Gahbauer, and J.S. Vincent, "A Study of Low Energy Proton Accelerators for Neutron Capture Therapy," in Proceedings of the Second International Symposium on Neutron Capture Therapy, edited by H. Hatanaka (Nishimura Co., Ltd. 1985), p. 147.
2. M.B. Emmett, "The MORSE Monte Carlo Radiation Transport Code System," ORNL-4972, Oak Ridge National Laboratory (Feb. 1975).
3. R. Roussin, "BUGLE-80, Coupled 47-Neutron, 20-Gamma Ray Group, P<sub>3</sub>, Cross Section Library for LWR Shielding Calculation Calculations," DLC-75, Radiation Shielding Information Center, Oak Ridge National Laboratory (1980).
4. Y. Gohar and M. A. Abdou, "MACKLIB, A Library of Nuclear Response Functions Generated with the MACK-IV Computer Program from ENDF/B-IV," DLC-60, Radiation Shielding Information Center, Oak Ridge National Laboratory (1978).
5. Y. Mishima et al., "First Human Clinical Trial of Melanoma Neutron Capture, Diagnosis and Therapy," *Strahlenther. Onkol.* 165 (1989), 251-254 (Nr. 2/3)
6. R.G. Fairchild, V.P. Bond, "Current Status of  ${}^{10}\text{B}$ -Neutron Capture Therapy: Enhancement of Tumor Dose via Beam Filtration and Dose Rate, and the Effects of These Parameters on Minimum Boron Content: A Theoretical Evaluation", *Int. J. Radiation Oncology Biol. Phys.*, Vol. 11, Num 4, April 1985, pp.832-840
7. C.K. Wang, T. E. Blue, and R. A. Gahbauer, "A Neutronic Study of an Accelerator-Based Neutron Irradiation Facility for Boron Neutron Capture Therapy," Nucl. Tech. 84, 93 (1989).



## STATUS REPORT ON THE INSTALLATION OF PROTON AND NEUTRON THERAPY IN CENTRE ANTOINE-LACASSAGNE.

P. Chauvel, P. Mandrillon, N. Brassart, J. Tuyn\*, J. Hérault,  
A. Courdi, J.L. Lagrange, M. Héry, F. Demard.

Centre Antoine-Lacassagne, Cyclotron Biomédical, 227 avenue de la Lanterne, 06200 - Nice - France

\*CERN, TIS Division, 1211 Geneva 23 - Switzerland

Abstract: In January 1987, the Centre Antoine-Lacassagne (CAL) was authorized to install the Medicyc cyclotron (65 MeV protons) for proton therapy and neutron therapy.

Construction of the final building to house the cyclotron and the radiotherapy, radiobiology and maintenance services began in January 1988 and has been completed in July 1989, allowing the reinstallation of the cyclotron, construction of beamlines and installation of treatment rooms.

### Characteristics of the Medicyc cyclotron

Medicyc is a fixed-frequency isochronous cyclotron designed by P. Mandrillon and built under his control for the Centre Antoine-Lacassagne to accelerate protons to an energy of 65 MeV. Close collaboration with CERN, CNRS and IN2P3, allowed the project to concretize. Presently, the characteristics of the magnet are as follows: length: 4m, height: 2.3m, width: 1.7m, weight: 140 tons, 4 spiraled sectors, 9 trim coils.

### Axial injection and central region:

Medicyc is a medical machine and this influenced initial design and further modifications as important as the decision to switch from positive to negative charged ions (H<sup>-</sup>) acceleration, in order to increase ion source duration of life and simplify extraction of proton beam. Consequently ion source was substituted, axial injection and central region redesigned, RF system and extraction modified.

H<sup>-</sup> ions are produced in a multicusp source supplied by Ion Beam Application (IBA, Louvain-la-Neuve). The source is mounted on a platform at 33 kV vertically above the axial injection line. A pseudo cylindrical inflector deflects the beam in median plane. The central region has been designed to accept a  $h=1$  for protons and  $h=2$  acceleration mode for deuterons and other fully stripped light ions. The new geometry operates at 24.8 MHz. Central magnetic field is around 1.7 Tesla.

### RF system

The RF system consists of two opposed dees with a 75 deg. aperture, now operating at 24.8 MHz after an

enlargement of the cone of the dee. The peak voltage is 50 kV. Each dee is independently excited by its own amplifier which is in turn driven by a master oscillator. The dees resonate as  $\lambda/4$  lines.

### Poles sectors and trim coils:

The azimuthally varying magnetic field is obtained in Medicyc by means of four pairs of spiraled sectors with hill and valley gaps of 130 and 280 mm, an average spiral of 60 deg./m. In order for a 24.8 MHz operation to be optimized, several sector modifications were necessary, notably in the extraction region.

For achieving isochronous magnetic field shape and better beam control, a total of nine trim coils are mounted on the surface of the sectors. Recent magnetic field measurements have shown that a satisfactory degree of field isochronization can be achieved with this trim coil arrangement. The final energy of 64.5 MeV will be reached at the extraction radius of 68.8 cm.

### Beam extraction and transport:

Initially designed and tested resonant extracting system was substituted by stripping extraction consisting of a 100  $\mu\text{g}/\text{cm}^2$  carbon foil mounted on a movable support. Following the stripper, the positive proton beam is transported 35 m down the beamline to the two treatment rooms equipped for neutron and proton therapy. The transport consists of a quadrupole pair at the cyclotron exit and a FODO channel consisting of two identical bending magnets and three equally spaced quadrupoles, which has unit magnification. This arrangement is followed, for the neutron therapy beamline, by a quadrupole pair and a vertical bending magnet directing the beam to the vertical neutron collimator. In order to reduce the cost of the focusing elements, the design seeks to achieve a small beam diameter throughout the transport system. The calculated beam size is within 2.4 cm, both horizontally and vertically. The bending magnets and the quadrupoles have been constructed by Bruker and Sigmaphi.

### Shieldings:

Shieldings necessary around the cyclotron, beam lines and treatment rooms were determined using the

formulas proposed by Braid, Tesch and Stevenson (IAEA Report, 1986), taking into account the radioprotection recommendations. As construction materials, barium concrete, concrete and earth were used. The choice between those materials is a result of a compromise between price and available space for a given mass surface density. Shieldings are in general equivalent to 2,40m concrete. The access to treatment rooms is through labyrinths avoiding the use of large heavy doors, costly and psychologically intolerable for patients.

The proton treatment room is located in front of beamlines deviation area and over the labyrinth of access to the neutron treatment room. Barium concrete was used to build the walls of proton room perpendicularly to the proton beamline, in order to increase the length of this room. The access labyrinth runs around two sides of the treatment room.

Covering of the deviation area, protontherapy room and partly cyclotron vault is made of movable concrete blocks, in order to facilitate further evolutions of the installation and allowing the access of the overhead travelling crane for heavy maintenance of the cyclotron.

#### Treatment rooms:

The beam leading to the proton treatment room is left to spread freely from the last dipole magnet and is collimated to 35mm before entering the treatment area. This diameter is the maximum width of the eye tumor. Only the central part of the beam is selected so as to obtain a flat dose profile. For an initial beam intensity of 120nA, only 9nA are transmitted, corresponding to a rate of 50pA/cm<sup>2</sup>.

Once inside the treatment area, the proton beam continues to travel in air before being modulated by a rotating plexiglass wheel with variable thickness angular sectors. The diameter of the beam is kept at 35mm by Al collimators mounted on the optical bench. At the end of the bench, it is finally collimated to the treated tumor shape. These arrangements follow closely those of Clatterbridge. The protontherapy chair has been built in the workshops of the Medical Research Council in Clatterbridge and set-up in May 90. Optical bench elements are now under construction.

The neutrontherapy room is located under the deflection area. Neutrons are produced in a Beryllium target which is retractable at the end of each treatment, avoiding unnecessary irradiation of the staff. The intensity of proton beam on target is around 15μA. The emerging neutron beam is defined to obtain fields varying from 5x5 to 25x25cm at 160cm from the target by using two collimators, the first one made of iron with a fixed aperture, while the second is a continuously adjustable

multileaf collimator of the Scanditronix design, modified for 65MeV p/Be neutrons and constructed by the "Cyclotron Research Center" in Louvain-la-Neuve and set up in Nice during April and May 90. This multileaf collimator consists in 44 independent steel leaves placed in two groups of 22 parallel and opposed leaves. Each leaf can reach and pass over the beam axis to obtain complex field shapes avoiding interposition of heavy metallic shielding blocks in the beam. The Oldelft treatment table equipped with a wooden couch has also been set up.

The choice of a vertical beam for neutrontherapy has been imposed by economical considerations and does not exclude a future isocentric gantry.

General design of the building took into account all these considerations together with medical ones.

#### General organization of the buildings:

The buildings are in two parts, one housing the cyclotron related facilities and one housing, for one third, technical workshops and offices, and for two thirds, medical and radiobiological facilities.

The technical building has been made with a metallic frame supporting on its whole length the overhead travelling crane. Under that structure are built the cyclotron vault, beamlines gallery and treatment rooms. Beside the cyclotron are located the mechanical workshop, electric power supply and cooling systems. The treatment rooms are between two areas devoted to future developments. The need for an underground level below the cyclotron and the possibility of superimposing the two treatment rooms induced us to design the building on two levels, with a basket supporting the beamlines at the upper level. In order to preserve all the future evolutions, the developmental areas have been left without intermediate floor.

The second building is also on two levels: patients will enter the facility at the upper level, where take place the protontherapy waiting room, laboratories devoted to radiobiology and, for the technical team, design office. The lower level receives electronics workshops and technical offices, and for the medical part, the neutrontherapy waiting room, radiotherapy and medical physics facilities. One fourth of the total surface of this building is devoted to further developments. This building has also been designed to be easily surmounted by three additional levels.

Lastly a third building could be added in the rear of the first one. It has been started by the installation of the command and controls room, placed at half-height of the technical building, behind and above the mechanical workshops. Further developments are also possible in this room, only one half of the surface being occupied by the

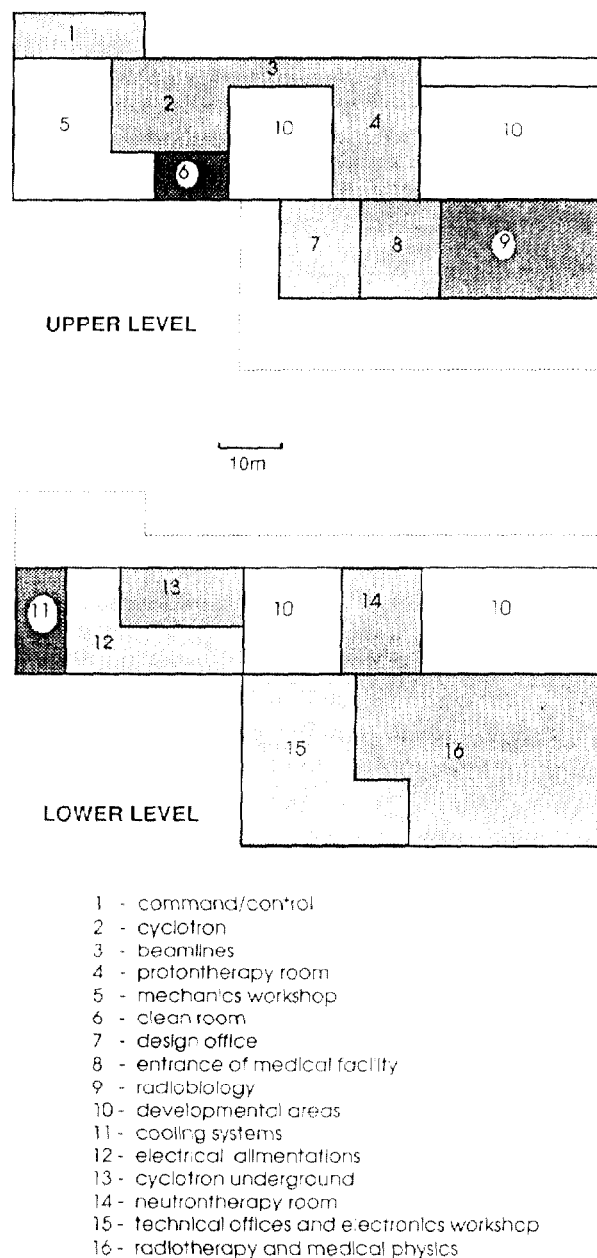
command and controls systems of Medicyc.

#### Medical programme:

Protontherapy will be the first application to start, firstly for ocular melanoma treatment, with the same protocols used in Boston, Villigen and Clatterbridge. Furtherly, we plan to use protons in the treatment of some relatively superficial head and neck tumours. The first treatments are planned in the very beginning of 1991.

Neutrontherapy would start a few months later. Main tumours concerned are: salivary gland and facial sinuses adenocarcinomas, bulky head and neck tumours and/or nodes, advanced prostatic carcinomas, soft tissue and bone sarcomas, cutaneous melanomas, rectal adenocarcinomas. The depth dose profile given by a  $p(65)+Be$  neutron beam authorizes the treatment of deep seated tumours, while avoiding side effects occurring in healthy tissues with low or medium energy neutrons; 50% of the entrance dose is given at a 16cm depth, compared to 10cm for cobalt and 6cm for 200kV. This depth dose profile looks like a 8MV photon beam from a modern LINAC. The facility in Nice will be the third in Europe (after Louvain-la-Neuve and Clatterbridge) to enter into the high energy neutron group ( $>60MeV$ ) encompassing, out of Europe, three machines: one in Fermilab(USA), one in NAC(South-Africa) and one in South-Corea. The interest for high energy neutrons has been clearly demonstrated by the RTOG(Radiation Therapy Oncology Group): there is a strong relation between low energy neutron and high complication rate. Increasing energy decreases complications and allows to treat deep seated tumours for which good results of neutrons are annihilated, due to high rates of severe problems occurring in healthy tissues.

But a lot of progresses remain achievable in the field of neutrontherapy and the absolute necessity of radiobiological research appears at evidence. This is the reason why the facility contains a large laboratory mainly devoted to radiobiology and cellular kinetics. Major progresses in neutrontherapy are to be expected of a better patients selection based not only on some radiosensitivity assays, but also on a better individual knowledge of cell kinetics parameters for both healthy and tumoural tissues. The laboratory will open during the second part of 1990. Main goals of our team for the near future are to set up short life isotope production and PET camera facility, in order to develop immunolabelling techniques, both for diagnosis and treatment. Furtherly, we plan to develop protontherapy at higher energy.



#### **CENTRE ANTOINE-LACASSAGNE BIOMEDICAL CYCLOTRON**

A COOPERATIVE GROUP AND COMMUNICATION NETWORK  
FOR PROTON AND NEUTRON THERAPY IN SOUTH EAST OF FRANCE:  
the S.E.R.A.G.(South-East Radiotherapy Group).

Chauvel P.<sup>1</sup>, M.D., Achard J.L.<sup>2</sup>, M.D., Bard J.J.<sup>2</sup>, Ph.D., Bolla M.<sup>3</sup>, M.D., Brassart N.<sup>1</sup>, Ph.D.,  
Carrie C.<sup>4</sup>, M.D., Chassard J.L.<sup>4</sup>, M.D., Clément R.<sup>7</sup>, M.D., Costa A.<sup>1</sup>, Ph.D., Coste G.<sup>6</sup>, Ph.D.,  
Courdi A.<sup>1</sup>, M.D., Delard R.<sup>8</sup>, Ph.D., Dionet C.<sup>2</sup>, M.D., Dubois J.B.<sup>8</sup>, M.D., Dussere A.<sup>3</sup>, Ph.D.,  
Garcia R.<sup>8</sup>, Ph.D., Gary-Bobo J.<sup>8</sup>, M.D., Gely S.<sup>8</sup>, M.D., Gérard J.P.<sup>5</sup>, M.D., Ginestet C.<sup>4</sup>, Ph.D.,  
Guillet J.P.<sup>6</sup>, Ph.D., Hay-Meng H.<sup>8</sup>, M.D., Hérault J.<sup>1</sup>, Ph.D., Héry M.<sup>1</sup>, M.D., Juin P.<sup>7</sup>, M.D.,  
Kerr-Picard C.<sup>8</sup>, M.D., Lagrange J.L.<sup>1</sup>, M.D., Marcié S.<sup>1</sup>, Ph.D., Mère P.<sup>9</sup>, M.D., Ollier P.<sup>10</sup>, M.D.,  
Pignon T.<sup>7</sup>, M.D., Porcheron D.<sup>7</sup>, Ph.D., Pourquier H.<sup>8</sup>, M.D., Puel G.<sup>9</sup>, Ph.D.,  
Reme-Saumon M.<sup>8</sup>, M.D., Resbeut M.<sup>6</sup>, M.D., Romestaing P.<sup>5</sup>, Rozan R.<sup>2</sup>, M.D., Schmitt T.<sup>9</sup>, M.D.,  
Sentenac I.<sup>5</sup>, Ph.D., Verrelle P.<sup>2</sup>, M.D., Veyssière J.<sup>7</sup>, Ph.D., Vrousos C.<sup>3</sup>, M.D., Waultier S.<sup>7</sup>, Ph.D.

<sup>1</sup>Centre Antoine Lacassagne - Cyclotron Biomedical, 227 avenue de la Lanterne 06200 Nice-France.

<sup>2</sup>Centre Jean-Perrin, 63011 Clermont-Ferrand <sup>3</sup>Hôpital de la Tronche, 38043 Grenoble

<sup>4</sup>Centre Léon-Bérard, 69373 Lyon <sup>5</sup>Centre Hospitalier Lyon-Sud, 69310 Pierre-Bénite

<sup>6</sup>Institut Paoli-Calmettes, 13273 Marseille <sup>7</sup>Hôpital de la Timone, 13385 Marseille

<sup>8</sup>Centre Paul-Lamarque, 34094 Montpellier <sup>9</sup>Hôpital Bellevue, 42100 Saint-Etienne

<sup>10</sup>"AcroSoft" 06560 Sophia-Antipolis

**Abstract:** Eight major radiotherapy departments participating in Public Health Service in South-East of France already joined the Centre Antoine-Lacassagne to prepare the exploitation of the Medicyc cyclotron for proton and neutron therapy. The solutions retained to facilitate a convivial working are presented. Due to the distances between participating sites, a communication network is included in these solutions.

### Introduction

The total cost of a facility comparable to the Medicyc cyclotron, buildings and related installations partly explains why there are so few installations of this kind, i.e. dedicated to cancer treatment, around the world. On the other hand, relatively small numbers of patients eligible for low energy proton therapy or for neutron therapy confirm the multiregional vocation of these installations, if one thinks relevant to treat more than a hundred patients per annum. On behalf of this assertion, a cooperative group has been set-up around the Centre Antoine-Lacassagne (CAL). In order to ensure the good efficiency of the group, a communication network is under elaboration.

### Composition and goals of the group

Eight major radiotherapy departments in South-East of France have already joined the group. They belong either to the French Comprehensive Cancer Centers (CCC) organization or University Hospitals (UH): CCC and UH in Marseilles (Institut Paoli-Calmettes and Hopital de la Timone), CCC in Montpellier (Centre Paul-Lamarque), UH in Grenoble (Hôpital de la Tronche), UH in Saint-Etienne (Hôpital Bellevue), CCC in Clermont-Ferrand (Centre Jean Perrin), CCC and UH in Lyons (Centre Léon Bérard and Hôpital Jules Courmont) accepted to closely collaborate with the Centre Antoine-Lacassagne in Nice. Due to this will, a large potential number of patients in South of France could benefit of proton and neutron therapy. This cooperative group remains widely open and hopes to enlarge the collaboration to other teams in and out of France, for example, in Italy and Spain, in order to propose to South European patients the possibility of heavy particle treatments and to South European physicians, physicists and radiobiologists to participate in research programmes in the field.

In order to work at its best and to ensure a

sufficient recruitment of patients, physicians, physicists and biologists have been invited to participate in the practical organization of the facility. The cooperative group is in charge of developing protocol for multicenter clinical trial and defining the logistics for patient recruitment. The group plans to function in a very convivial way, radiation oncologists coming in Nice to set up the treatment of their own patients and watch over its tolerance, while physicists will work in common on dosimetrics measurements, and participate together with other groups to intercomparisons and quality control campaigns. Direct collaboration of physicians coming in Nice to treat their own patients seems to be a good mean to ensure both a real interest of physicians in the practical organization and technical details of treatments, and keeping a close relation between physician and patient. This last point seems to be relevant and is in favour of a better psychological tolerance to treatment, avoiding to the patient the disastrous sensation to be a "stranger lost faraway from home". Furthermore, this collaboration ensures a large physicians and physicists upgrading in heavy particles therapy and could rise up interest in these techniques. This general point is very important for further developments in radiation oncology using heavy charged particles and/or high Linear Energy Transfer (LET) particles.

In its present composition, the cooperative group represents almost 10 000 new cancers irradiated per annum and covers 5 regions : Auvergne, Corse, Languedoc-Roussillon, Provence-Alpes-Côte d'Azur, Rhône-Alpes. This represents one fourth of the french population, and constitutes a sort of recruitment warrant.

Taking into account the distances between all institutions participating in the group, the set-up of a communication network and electronic mail became soon a necessity. This would allow a large exchange of information and a remote management for medical files, irradiation techniques, dosimetrics data, image transmission and data base.

#### Communication network:

##### Common medical files

based on the CAL computer systems, medical files will be created documented and exploited through a connected microcomputer from one or another

collaborating center. This allows an automatic procedure of file maintenance during the follow-up and facilitates statistical exploitation of multicentric clinical trials. Data concerning each patient will be directly entered into the computer at each step of the treatment and of the follow-up. This avoids a fastidious work to fill in a lot of sheets and afterwards transfer these data into the computer, repeating each time a lot of redundant data. Furthermore, this organisation facilitates the remote management of trials by each responsible from his own office. Beside the constitution of medical files, must be elaborated iconographical files allowing to keep in, after digitalization, the main informations from CT Scan and/or MRI, endoscopic views, whenever possible, pictures of skin status before and after treatment. Documents will be recorded either in each center before treatment and during follow-up or in CAL before and during treatment, and stored in the computer constituting a videodata base.

#### Irradiation techniques and dosimetrics data.

As for medical data a file will store the main parameters of irradiation techniques, treatment plans, simulation radiogramms and portal films. This technical file will be accessible for consultation and verification of treatments parameters by each member of the group from his own institution, through the same microcomputer, on a special screen.

#### Remote video consultation:

If, for one reason or another, a physician from a corresponding center could not come in Nice to set up the treatment of his patients we plan to have the possibility of a videophonic communication during which the essential close connection between physician and patients could be maintained.

- Furtherly, we plan to set up a bibliographic data base.

#### Technical solutions:

Present evolution of telecommunications in France, with both Minitel and Numeris (Large Scale Integration Services) gives us the possibility to set up such a communication network. The Teletel 2 system, on which is based the Minitel, allows us the possibility of a distant consultation of the data base at a low transmission rate, for a low cost. For applica-

tions implying a high transmission rate because of files size (such as digital images) the Numeris network will be used.

During the procedures of files updating or statistical exploitation, the whole data base will be loaded, via Numeris, on the exploitation site, in order to keep the connexion duration as low as possible. Inversely, ordinary consultation of a file is realized through Teletel network.

Such a hybrid architecture keeps the running costs very cheap, around 1500 FF per month, for an investment of 10 000 FF including the computer, connexion cards and comescope for image digitalization.

This communication network is developed for the Centre Antoine Lacassagne, by Acrosoft company in Sophia Antipolis and could further be connected to digital international networks.

### Conclusions

A cooperative group of radiation oncology departments representing 10 000 new cancers irradiated per annum has been set-up around the CAL facility to prepare the treatment protocols and logistics for patient recruitment both for proton and neutrontherapy. The structure remains open and new members, in and out of France are expected to join soon. In order to reinforce the convivial organization of the group and facilitate the circulation, updating and exploitation of medical and technical data related to treatments, a communication network is under elaboration.

## RECENT DEVELOPMENTS OF A HIGH-ENERGY PROTHONTHERAPY PROJECT IN ORSAY (France)

J.C. Rosenwald\*, J.L. Habrand\*\*, A. Bridier\*\*, D. Pontvert\*, P. Schlienger\*,  
M. Louis\*\*\*, J. Rouesse\*\*\*\*, A. Laugier\*\*\*\*\*, J.P. Camilleri\*

\* Institut Curie, Paris

\*\* Institut Gustave Roussy, Villejuif

\*\*\* CPO-Synchrocyclotron, Boite Postale n°1, F-91406 Orsay Cedex

\*\*\*\* Centre René Huguenin, St-Cloud

\*\*\*\*\* Assistance Publique, Hôpitaux de Paris

It has been decided some years ago that the Orsay Synchrocyclotron, located about 20 km from Paris and originally designed for physics research would be shut down at the end of 1989.

Since many years, the possibility of using this machine for medical application had been considered, the 200 MeV proton energy and the relatively high current output making it suitable for treatment of deep seated tumors. Although built in 1958, the machine was very well maintained, substantially upgraded in 1977, leading to a break down time less than 5 % in the last period.

It was therefore a unique opportunity to keep this machine running and convert it into a protontherapy facility.

### Feasibility study

A feasibility study was conducted from November 1987 to November 1988 in order to investigate the beam characteristics and decide if they were suitable for proton treatment. For this investigation, priority was given to proton beams in the range of 70 MeV since the higher demand was for eye tumors treatment, as practiced in a number of other places and for which such an energy is required.

A graphite block 12.8 cm thick was therefore introduced in the beam line, for energy degradation. It was found that it was necessary to place it upstream, before the beam deviation (*fig.1*), in order to avoid significant contamination from secondary particles.

The measured depth dose curve is presented on *fig.2*. The position of the Bragg peak is 4.5 cm in water, corresponding to an energy of 73 MeV consistent with the expected degradation, and the dose at peak is 4.5 times higher than at surface.

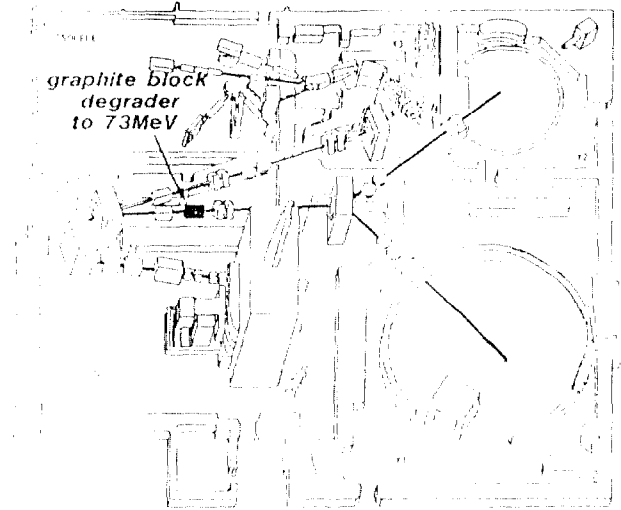


**Fig. 1**

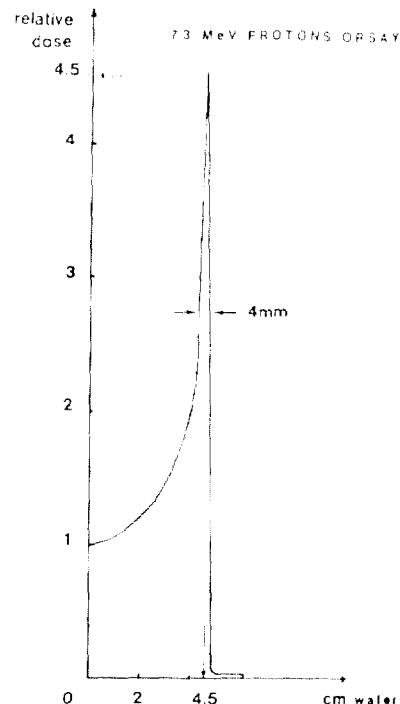


**Fig. 2**

A simplified range modulator was constructed (fig.3) consisting of a 4 steps perspex filter rotating in the beam, each step being weighted so that the Bragg peak addition for all steps results in average in a flat dose distribution over a 2 cm thickness. The obtained depth dose curve is shown on fig.4. The dose in the flattened part is now only 1.8 times higher than the surface dose.

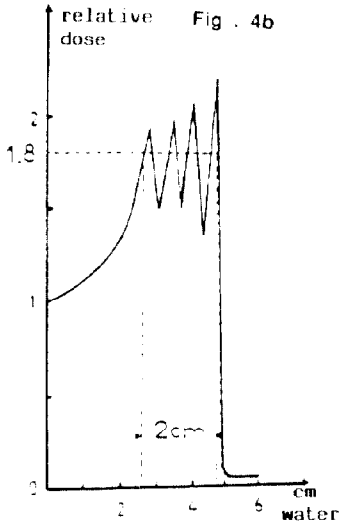


Fig.3

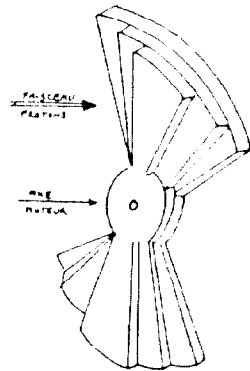


Fig.4

Some experiments have also been performed at 200 MeV, without any range shifter. The obtained depth dose curve is shown on fig.6. The position of the Bragg Peak is 25.7 cm in water and the dose at the peak is 4.3 times higher than at the surface. Such a depth can be considered as appropriate to treat practically all tumors, wherever they are located.

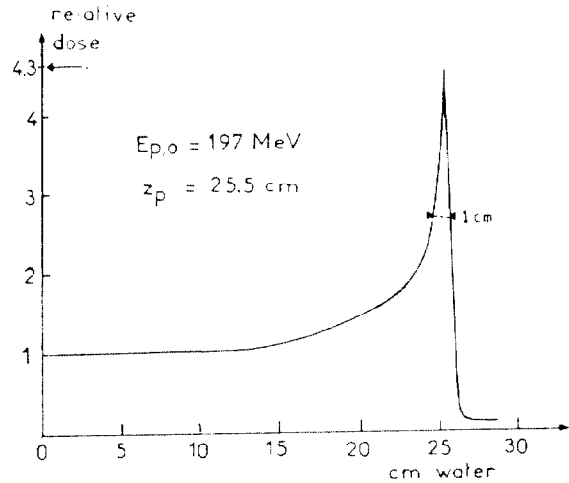


Fig.6

The dose distribution in planes perpendicular to the beam axis has also been investigated and by using appropriate scatterers and collimators, it was easy to obtain very flat dose profiles over a diameter of about 3 cm with a sharp fall off at the beam edge (fig.5).

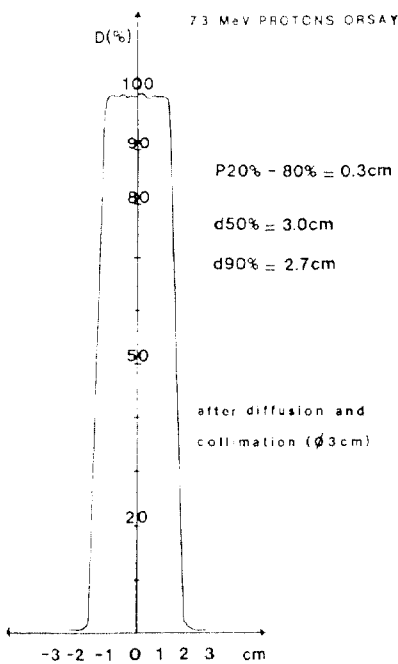


Fig.5

The beam stability and the available dose rate were also found perfectly suitable for protontherapy.

**Creation of the CPO  
(Centre de Protontherapie d'Orsay)**

After difficult negotiations with the French authorities, the decision to keep the machine in operation for protontherapy has finally been taken in December 1989 :

A new organism is founded jointly by the major hospitals of the Paris area involved in cancer treatment, namely Institut Curie, Institut Gustave Roussy, Centre René Huguenin and Assistance Publique-Hôpitaux de Paris. This organism, named CPO (Center for Protontherapy in Orsay) will own the Synchrocyclotron given by the CNRS and will have the responsibility of operating and maintaining the machine, as well as undertaking treatments. It will consist of about 20 persons, half being in charge of the machine (8 were already affected to the Synchrocyclotron) and half for medical application, whether hired by CPO or detached from participating hospitals.



### Project planning

It is planned to treat about 270 patients/year : 150 patients for ocular tumors, 20 patients for radiosurgery of brain arteriovenous malformations and 100 patients for other deep seated tumors.

The required modifications of the building and of the machine have started.

The eye treatments are expected to start in the first room at beginning of 1991. In the same room, it should be possible to treat brain lesions in summer 1991.

Another room for large field treatments will be equipped during year 1991 and should open for treatments at beginning of 1992.

A general assessment of the project by the health authorities will take place at the end of 1993.

If the project evolution is judged satisfactory, it is likely that it will continue and expand after 1993 with additional possibilities such as adjunction of imaging equipment and of a third room for radiobiological and physics experiments.

## Installation of a hospital-based protontherapy center in the province of Antwerp, Belgium

Prof. Dr. P. Scalliet, AZ Middelheim, Department of Radiotherapy, Lindendreef 1, B 2020 Antwerp.

### 1. Introduction

This report deals with the potential benefit and the overall costs of the implantation of a high energy accelerator of particles for medical use in the Province of Antwerp. We based our arguments on similar projects in the USA and in Europe, as far as beam production and the medical applications of proton beams are concerned.

Radiotherapy constitutes, together with surgery, one of the most efficient modalities of cancer treatment. The recent successes of chemotherapy remain, up to now, limited to infrequent forms of cancer (hematological cancers, germ cell tumors...), and it is likely that, unless dramatic and unexpected progress is made in cancer prevention or curing, radiotherapy will remain a treatment modality of choice in the foreseeable future. Any kind of further development of this technique is thus desirable.

If investments are to be planned in oncology, they can be affected either to basic biological research (immunotherapy, biological response modifiers...), whose potential benefit, although probable, is difficult to predict, or to the development of existing modalities of treatment, yet still susceptible of technical improvements, and whose benefit is reasonably foreseeable. The present project belongs to this second category.

### 2. Relevance of high energy protons

Among the different types of radiation, high energy proton beams offer the best achievable ballistic characteristics. Ballistic characteristics must be understood as the physical selectivity with which a proton beam drops its energy in a given volume, while considerably limiting the amount of energy (i.e. the dose) dissipated outside this volume. Indeed, the energy lost by a positive ion is inversely proportional to its kinetic energy, and as this kinetic energy is progressively dissipated as particles plunge into the medium (i.e. as the particles slow down in the depth), the amount of energy deposited *increases* with the depth. Hence, the dose delivered to the surface is comparatively much smaller than the one given in the depth, with a surface/depth ratio comprised between 1:4 and 1:5.

This distribution of the dose is exactly the reverse of what is observed with classical X-rays, where the dose decreases with depth. In summary, the advantage of proton beams owes to the combination of 2 characteristics: (1) the progressive increase in dose with the depth, followed by a sharp fall-off due to the sudden stop of the protons, and (2) the extremely sharp penumbra at the borders of the beam.

To the extent that normal tissue tolerance represents the actual limiting factor of radiotherapy, all technical improvement increasing the dose delivered to the tumor compared to the dose to the normal surrounding tissues is of potential benefit (selective ballistic). The relative radioreistance of some tumors may then to some extent be bypassed, since it is possible to increase the tumor dose without damaging the neighbouring healthy tissues. In fact, proton beams offer two main lines of progress: either decreasing the normal tissue dose for radiosensitive tumors (f.i. irradiation of a Hodgkin disease with a quasi null dose to the spinal cord), or increasing the tumor dose without exceeding the tolerance level of normal tissues (brain, lungs, pelvis...). Proton beams are thus particularly well adapted to the treatment of tumors lying close to critical structures. Essential progresses have been made along this line in the treatment of eye tumors and of tumors of the base of the skull (f.i. chordoma), with spectacular clinical results (7500 patients treated worldwide, of which more than 4000 were treated in Boston). It is also a particular attractive technique for the local treatment of pediatric tumors.

The shape of the proton depth-dose curve is thus very characteristic, with a peak at the end of the particle path where the dose is concentrated (the Bragg peak). However, the peak is far too narrow to be really useful for therapeutic applications (excepted perhaps for extremely small volumes), and different methods are used to spread it over a desirable depth depending on the clinical situation (either by varying the incident beam energy, or by the interposition of appropriated filters).

The choice of the energy depends on the tumor site to be treated. For small superficial volumes, like hypophyse or eye tumors, brain arteriovenous shunts, some pediatric tumors, a proton beam in the energy range of 90-100 MeV is sufficient (Bragg peak at 6-7 cm). These indications are however infrequent, and account for a proportion of tumors insufficient by itself to justify the investment in a new protontherapy machine in Belgium, since such a center is

almost operational in Louvain-la-Neuve (in close coordination with the neutrontherapy program). The creation of a Flemish center seems therefore of little interest. Indeed, competition in the treatment of small superficial tumors would result in an unoptimal recruitment, detrimental to the quality of treatment, to the scientific aspects of the program and, last but not least, to the patients.

On the contrary, the treatment of thoracic or abdominal deep seated tumors forms a much broader recruitment basis, as well as a research field of great interest. It requires the production of 200-250 MeV protons, whose Bragg peak is situated at 27-30 cm in depth. Such a depth is sufficient to face almost all the clinical situations, even in obese patients.

### 3. Choice of a heavy particle accelerator

The choice of a particle accelerator depends on the forecasted applications.

	<i>Beam Energy</i>	<i>Beam Intensity</i>
Radioactive isotope production	30 MeV	500 $\mu$ A
Fast neutron beams	55-60 MeV	10-20 $\mu$ A
Proton beams	200-250 MeV	1-2 nA

These different applications are hardly compatible in a single particle accelerator, to the extent that they require the construction of a variable energy machine of high cost and complex technology. Running costs are therefore comparatively high, which decreases the rentability expected from a partial commercial use. Moreover, organisational aspects inherent to a mixed use of a multipurpose installation are inordinately complex (the smallest breakdown stops the running application and delays the whole following program). Last but not least, it should be realized that a lot of interest in the project would be lost if the activities of a single facility were to be shared between different users, each being limited in his development by a short access to the beam. Most of the teams which attempted to develop such a program decided, after the feasibility study of a multipurpose cyclotron, upon a single application unit, as well for financial as for technical reasons.

A parallel can be made with the situation in computer technology. While the dogma has long been to centralize the different applications in a large sized computer, equipped with numerous working posts, the present trend is to connect smaller independent units into a network, allowing exchange of informations and programs without impairing the independence of each individual computer. A breakdown in one of the units does not stop the operations or access to the network, while any kind of defect in a centralized system irremediably blocks the totality of the applications.

Reasoning along this line, IBA preferred the concept of a simple isochronous cyclotron devoted to a single purpose, much easier to design and to operate (it is highly automatized), and therefore far less expensive in investments as well as in running costs.

#### 3.1 Radioactive isotopes production

A broad range of gamma radioactive isotopes can be manufactured from a beam of reduced energy but of high intensity (30 MeV - 500  $\mu$ A). A unit fitted with these characteristics offers a production capacity exceeding largely the needs of Belgium; one to 2 facilities would be sufficient to meet the need of larger countries, like France or Germany. As to the north american continent, about 15 units are in activity, with the possibility of increasing the production with university cyclotrons, in case of temporary excess in demand.

Installing a complete production unit, including the cyclotron, the beam transport system and the chemistry laboratories, would cost approximately 150 to 200 millions BF (the cyclotron alone costs 120 millions). If such a unit were to be installed in the Province of Antwerp, a good commercial network with the neighbouring countries would be mandatory, in order to ensure its financial rentability. As short-lived radioactive isotopes can be shipped by plane, any distance between the production and the place of delivery does not constitute an obstacle to this kind of development. As a matter of fact, the English Amersham company markets its products all around Europe.

#### 3.2 Neutron beams

The production of high energy neutron beams is still compatible with the manufacture of radioactive isotopes, provided some technical modifications of the original plans. The medical interest in fast neutrons lies in their increased

biological effectiveness, as has been experimentally largely demonstrated. With respect to cancer cell killing, they are 2 to 3 times more efficient than high energy X-rays. Sadly enough, their effectiveness is equivalently higher in damaging normal tissues, which makes their practical use rather delicate.

Seventeen neutron facilities are operational in the world (Belgium, Germany, England, France, Soviet Union, Poland, United States, Japan), but of quite disparate characteristics, which was, indeed, responsible for an evident lack of collaborative work between European institutions (difficult exchange of informations). As a consequence, and despite the efforts of each of the research team, the potential of neutron therapy remains a subject of debate. Unfortunately, this debate evolved recently into a passionate more than a scientific dispute (cf. the situation in England), which has somewhat clouded the real question of the value of neutron therapy. It is good to remind that the RTOG published, a few years ago, an interesting series of prostatic tumors treated either with photons or with mixed neutron/photon beams (this study was randomized). A definite advantage was demonstrated for the latter, with respect to 5 year survival. Other studies, however, failed to demonstrate an advantage (some of them even a disadvantage) in using fast neutrons, mainly in advanced head and neck localisations. Nevertheless, it should be realized that most of the trials were conducted with poorly performing neutron installations (similar to old 200 kV X-ray units). The last word is thus still to be said.

In conclusion, the development of a research project in neutron therapy seems risky in the present context. Moreover, the Louvain-la-Neuve facilities have a considerable advance in this field (more than 12 years experience), and, here again, any competition would be unlogical and detrimental to the community (including the patients).

### 3.3 Proton beams

The production of proton beams needs a machine with specific characteristics (very high energy, very low beam intensity), hardly compatible with other applications (radioactive isotope production). Until now, the majority of the operational proton centers (Boston, Uppsala, Villingen, Louvain-la-Neuve...) benefited from existing installations previously developed for nuclear physics research. This research turning toward much higher energies (cf. the CERN in Geneva or the Superconducting Super Collider SSC in USA), the destiny of these "old" plants was to be either destroyed, or converted for medical applications, when a motivated and dynamic radiotherapy staff was present in the vicinity. For these medical teams, the problem of investments was solved, since a high energy machine was already available (cf. the project in Orsay, France).

The development of new proton therapy facilities, within medical centers which had no existing cyclotron at their disposal, came up against obvious financial problems. The recent project in Loma Linda (USA) supplied a particularly dissuasive budget example, as his overall cost amounts to about 45 millions \$ (indeed, this was the forecasted cost, but it seems that the real price of the center will be even higher).

Three different technical solutions are conceivable for proton beam production.

1. The first type, of advanced technology, makes use of superconducting materials. Its advantages are not envisaged here. The major drawback, for an unbroken medical use, is the time necessary for the cyclotron to reach its working (extremely low) temperature, i.e. about 2 weeks. Any kind of breakdown which needs an intervention on the cyclotron means that the machine has to be stopped, warmed up until the repair can be carried out, and then cooled down back at its working temperature. The interruption lasts thus at least 3 to 4 weeks, which is hardly compatible with medical (as well as commercial) applications.

2. A second type is the synchrotron, a technology which was developed in the fifties for research in the nuclear physics, and reaching energies in the range of GeV. Its advantage over a classic isochronous cyclotron is its lightness (40-60 tons vs. 600 tons for a cyclotron in the past), and it remains a possible choice to the extent that the characteristics of a modern unit are compatible with a continuous medical use. An other theoretical advantage is that the proton beam can be extracted at a desired energy, allowing for the treatment of bulky volumes without the need for energy degrading filters. However, a major disadvantage of a synchrotron is its technical complexity, which implies higher investments and running costs (cf. Loma Linda). The beam output is also lower, implying longer irradiation sessions per patient, and thus less treatments per day, as compared to a classic isochronous cyclotron. This last problem seems however to be solvable in large installations, although still not solved today.

3. Logically, the choice must be turned to an isochronous cyclotron, of simple technical design, of comparatively low cost, and of lightened structure (120 tons) as compared to what has been done in the past. Its running output in proton therapy is also far below its maximal capacity, compared to a synchrotron which must run at its maximal power to supply for a sufficient beam output. This means that the decrease in output, due to the beam divergence induced by the interposition of energy degrading filters (see further), can be compensated by an

adaptation of the beam intensity, which helps to keep the time of a treatment session within normal limits (1 minute, or so).

The new IBA project supports the concept of a hospital-based isochronous cyclotron dedicated to a single application: the production of 230 MeV protons (Bragg peak at 30 cm depth). It makes use of a simple but modern technology, with an interesting predicted reliability and an overall cost of about 10 millions \$ (400-500 millions BF). The need for maintenance staff is reduced by a highly automatized design, decreasing the running costs accordingly. See the IBA report for more details.

## 4. Size of a proton therapy center

In principle, a single particle accelerator can supply several treatment rooms with an irradiation beam, provided several beam transport systems have been installed. In the initial IBA project, the cyclotron supplied 4 rooms with fixed beams (2 verticals, 2 horizontals).

### 4.1 Why four beams?

We have seen that the main advantage of protons beams is to deliver a high dose in depth while sparing the surface of an irradiated medium. However, apart for the smallest target volumes, the Bragg peak is too narrow for a direct clinical use and it is necessary to spread it over a realistic depth (i.e. 5 cm), depending on the tumoral size. This can be done by the interposition of filters of appropriate thickness, degrading the beam energy at a value corresponding to the desired Bragg peak depth. Unfortunately, the use of such filters increases the surface dose, which dissipates the surface-sparing effect of protons. As the surface is less protected, one may resort to multiple coaxial beams, convergent to the target volume. This technique, already in use since decades in classical X-ray therapy, imposes the design of an isocentric mounting, essential for the accuracy of the irradiation. The solution is to use a 270 or 360° rotating gantry, allowing for a convergent irradiation of the patient with multiple beam incidences. While this solution has proven to be technically feasible for the usual radiotherapy units (modern linear accelerators), it represents a technically complex and expensive problem for proton therapy (expensive is, of course, a question of proportion, since the gantry amounts certainly for at least 50 % of the price of a linear accelerator). For instance, the isocentric arms of Loma Linda (USA) costed as much as the particle accelerator itself. Therefore, IBA initially projected 4 fixed beams, the patient being moved from a room to another for its successive irradiations, depending on the number and incidences of the beams determined by the treatment schedule.

It is however easy to picture the extremely strict organisation imposed by such a solution. In order to reduce the loss of time, inherent to the passage of patients from one to another treatment room, it would be essential to develop a particularly strict time schedule. Moreover, any latency longer than, say, 15 minutes or more, between two successive fields in the same patient, could be biologically detrimental (in fast repairing tumors). And last but not least, fixed beams cannot offer the certitude of a rigorous treatment geometry, as compared to an isocentric mounting. This last solution seems thus warranted, exactly as it is the case in X-ray therapy (nobody treats deep seated tumors with fixed X-ray beams anymore).

Following contacts with Dr. Sc. A. Brahme (head of the department of medical physics, Radiumhemmet, Stockholm), it appeared that Uppsala University developed the concept of a reliable isocentric system for proton therapy, at a much lower cost than in Loma Linda. After some exchanges between the technical staff of IBA and Dr Sc A. Brahme, the company modified (and improved) the project, by replacing the four fixed beams by two isocentric gantry in two independant treatment rooms.

### 4.2 Number of treatment rooms

When a single cyclotron feeds a number of treatment rooms, it is necessary to successively commute the beam from one room to another, in function of the local need. If the beam is not immediately available, one waits (indeed, the patient waits) until it becomes free for irradiation. The probability that the patient moves increasing with time, while he is expected to stay absolutely motionless, the hazard of irradiation error increases in proportion. It is thus not only unrealistic but also potentially hazardous to provide a large number of rooms with a beam from a single unit. Moreover, the need for a stringent working time schedule increasing with the number of rooms, it is likely that the productivity of each room will be inversely proportionnal to this number, let alone the general discomfort for the patients and the staff (some patients move slower than others, suffer...).

Following some discussions with the company and with Prof. A. Wambersie, and on the basis of the experience of other centers, it seems that two treatment rooms for one particle accelerator represent an optimum (it remains possible to increase this number later on). It is estimated that in routine use about 400 patients can be treated yearly in each room. This means 800 patients per year for the center (in routine operations), which seems to be a reasonable recruitment basis for the Province of Antwerp.

### 4.3 Staff

The technical staff should include a civil ingeneer and 2 to 3 electronicians (A2), which would be sufficient for the routine maintenance of the cyclotron.

Three technicians per room must be sufficient (corresponding to the belgian norms for a linear accelerator), each taking on its own task: display of the irradiation parameters on the instrument panel, manipulation of the isocentric gantry and set up of the patient in the laser marks. A total of six full time technicians is thus necessary (nurses A1 in Belgium).

The physics staff must certainly be meaty, at least during the development phase (4 physicist), while 2 to 3 could be sufficient in the routine phase. The duration of the development period is however difficult to define, and may last several years.

One medical doctor for 200-250 new patients/year is the belgian norm (the desired norm, since most of our large centers do not meet this criteria). Four full staff members should therefore be foreseen, with a complement in residents at various stages of their training (exchange with other proton centers would certainly be of great interest).

Finally, the administrative management will require a few secretaries, this post being pooled in the financial analysis with the general administrative costs.

## 5. Financial analysis

The following analysis is, at this stage, purely indicative of the different orders of magnitude of the overall costs of the project.

### investments

proton center installation 400-500 millions BF

### annual running costs

#### Personnel

1 civil ingeneer and 3 electronicians A2	3.8
4 physicist	5.6
6 nurses A1 (technicians)	6.6
4 physicians	10

#### Cyclotron

electricity consumption	1.6
administration and disposables	7.5
maintenance	15

**total 46.5**

The electricity consumption is based on 180 kW, 8 hours a day, 5 days a week and 50 weeks a year. The post "administration and disposables" includes the administrative costs, the nursing disposable materials, the cleaning of the building... Maintenance means the yearly revision and the maintenance contract with the company.

If we leave the paying off of the investment out, the annual running cost is thus 46.3 millions BF. This amount must be divided by the number of patients to obtain the mean cost per treatment, that is to say 46.3/800 patients = 58.000 BF per treatment. The paying off of the investment, without interests, would cost 55-60.000 BF per patient. The total cost per treatment is thus about 120.000 BF per treatment.

This sum is to be compared with what has been recently calculated for a conventional radiotherapy department, treating 1000 new patients a year with two linacs (and all facilities). Taking the running costs as well as the paying off of the investments into account, the price of a treatment with X-rays is about 106.000 BF. This is much higher than the 55.000 BF that the belgian social insurances refund for a treatment with high energy X-rays (minimum 20 sessions) with blocks, wedges, a simulation and a computer dosimetry. A rapid solution to the structural deficit of radiotherapy in Belgium, through reevaluation of the intervention of the social insurances (which is forecasted in the coming months), would make the construction of a protontherapy center a financially possible project.

## 6. Research project

The presently available clinical experience is based on 8000 patients, of whom 60 % were treated in Boston, Harvard Cyclotron Laboratory (HCL), since 1961 (in close collaboration with the Massachusset General Hospital). Most of the indications were eye melanoma and some central nervous system tumors, considered as indications of choice for protontherapy. Only a few other localisations were treated, due to the very small number of operational centers. Outstanding results have been published.

As mentioned before, the Antwerp medical project will focus on deep seated tumors only, very briefly summarized here.

1. adult tumors : gynecological, urological and abdominal locally advanced tumors, lung tumors (limited stages)...

2. pediatric tumors : central nervous system (craniopharyngiomas, medulloblastomas, gliomas...) and thoraco-abdominal tumors in boost technique of residual localisations (neuroblastomas, rhabdomyosarcomas, Wilm's tumors, Ewing tumors...).

3. salvage therapy in recurrent tumors (f.i. rectal cancer).

4. replacement of some indications of brachytherapy ?

Along with the medical project, technical research programs will be developed :

1. cyclotron, beam transport system, isocentric gantry...

2. tridimensional targeting: tumor localisation, definition of target volumes, absorbed dose distribution...

3. on-line control of irradiation : PET scan, detection of patient movements and beam correction...

## 7. Situation of radiotherapy in the Province of Antwerp

The Province of Antwerp homes a population of 1.6 millions inhabitants, with Antwerp city as administrative center. Antwerp is the second belgian city in size (0.5 million inhabitants), after Brussel (1 million inhabitants), and almost the second european see harbour with respect to economic activities.

Six radiotherapy centers cover the province: AZ Middelheim (1 cobalt, 1 linac), St Vincentius (1 cobalt, 1 linac), St Augustinus (1 cobalt, 1 linac), Euwfeestkliniek (1 cobalt) in Antwerp city, St Elisabeth in Turnhout (1 cobalt) and St Norbertus in Duffel (1 cobalt, 1 linac). Table 1 summarizes this situation, in comparison with Brussel city and with Belgium.

	cobalt	linacs	population (millions)	unit/million cobalt	unit/million linac
Belgium	40	20	9.5	4.2	2.1
Brussel	10	8	1	10	8
Antwerp	6	3	1.6	3.75	1.8

It is clear from this table, that, both for cobalt units and for linacs, the Province of Antwerp is slightly underequipped as compared to the national average. With respect to Brussel, we must admit that the comparison is probably less relevant since Brussel benefits from one of the highest concentration of radiotherapy units in Europ, some of them being obviously not optimally utilized. Nevertheless, Antwerp would reach the average national value with two additional treatment units.

On the other hand, Belgium is in the leader group for cobalt units (on average old or very old units which need urgent replacement), but in the lower range for linacs, as compared to other european countries (f.i. The Netherlands, Germany or the scandinavian countries). Thus, we need more linacs, and we need also to replace some of our old cobalts, better by small linacs, which is the recognized international trend.

## 8. Conclusions

The investment in a protontherapy center seems to be medically highly justified, yet it implies the input of considerable financial efforts, whose rentability is not ascertained in the present context (due to low repayments from the health authorities). Nevertheless, protontherapy leading undoubtedly to better curative results, one may consider that, on a macroeconomic level, the restitution of a larger proportion of cured cancer patients to the active life represents a major economic profit. It is good to remind that the NCI has stopped paying (as a reasearch grant) for proton treatments at Boston HCL cyclotron, stating that, on the basis of the outstanding clinical results, the treatment expenses had to be supported by the social insurances, and no more by scientific research funds.

It is otherwise interesting to compare these costs to those of classical radiotherapy. It has been estimated that a new center, equipped with 2 linacs, a simulator and a computer planning system would cost approximately 180 millions BF (150 millions equipments and 30 millions for the building), i.e. 2/5 of the overall cost of a protontherapy center. Given the limited number of radiotherapy units in the Province of Antwerp, it is anyway necessary to forecast some development in this sector (see above). Investments in high energy linear accelerators could then be partly replaced by the installation of a proton accelerator, by using part of the development budgets allocated to cancer treatment.

## PRELIMINARY DESIGN OF A REDUCED COST PROTON THERAPY FACILITY USING A COMPACT, HIGH FIELD ISOCHRONOUS CYCLOTRON.

Y. Jongen\*, A. Laisné<sup>†</sup>, G. Lannoye<sup>°</sup>

\* Ion Beam Applications s.a;  
Chemin du Cyclotron, 2  
B - 1348 Louvain-la-Neuve  
(Belgium)

<sup>†</sup> Institut de Physique Nucléaire  
Orsay BP 1  
F - 91406 Orsay  
(France)

<sup>°</sup> Centre de Recherches du Cyclotron,  
Chemin du Cyclotron, 2  
B - 1348 Louvain-la-Neuve  
(Belgium)

### ABSTRACT

It is generally agreed that, among the different kinds of radiations usable for radio-therapy, high energy proton beams exhibit the best ballistic specificity. However, the development of proton therapy has been hindered by the size, cost and complexity of high energy accelerators. We have therefore tried to design not only an accelerator, but a complete proton therapy facility where the size, the investment, the complexity and the cost of operation would be minimized.

For a clinical therapy unit, reliability is of paramount importance, and we believe that the simplicity and sturdiness of the design is the key to reliability. This is why we selected a non-superconducting isochronous cyclotron as accelerator. The magnet is a high field (3.09 Tesla peak field, 2.165 Tesla average field at extraction) deep valley design, using 190 kW in conventional coils. The complete cyclotron is split in two parts at the median plane. The upper half can be quickly raised by one meter, using hydraulic jacks, allowing an unrestricted access to all cyclotron elements. This design feature, combined with a rapid pump downtime (30 min.) should contribute to maintain downtime of the accelerator to very low values.

The cyclotron would then feed two or three isocentric gantries. IBA has developed a new concept leading to isocentric gantries of reduced size and cost [1]. This new gantry design allows to reach infinite "source to patient distance" with a gantry not exceeding 2.5 m total maximum radius.

The dose delivery system has been reviewed to optimize dose accuracy, uniformity and speed of delivery. In the axial motion, the magnetic sweep is controlled by a dose integrator, guaranteeing an uniform dose irrespectively of minor intensity fluctuations.

### 1. Basic specifications for a proton therapy cyclotron

#### 1.1. Energy

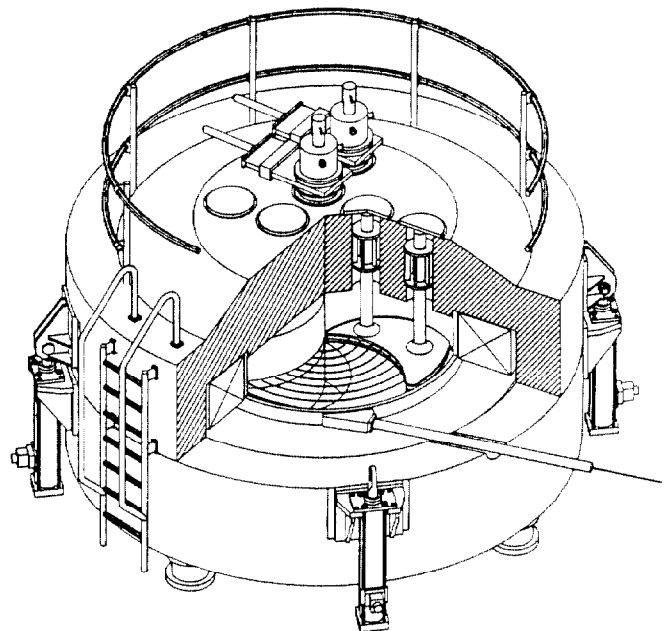
The energy required for a proton therapy cyclotron is entirely defined by the energy-range relation in tissues (quite equivalent to the range in water). The range at 175 MeV is approximately 20 cm, at 200 MeV, 27 cm and at 250 MeV the range is 37 cm. If passive beam flattening filters are used, some extra range must be provided to allow for the energy losses in the filters. However, in this case we intend to use beam scanning and such filters are not needed. Therefore, we feel that a maximum energy of 230 MeV, yielding a range of 32 cm is sufficient.

### 1.2. Intensities

Intensities needed for a proton therapy facility have been discussed by Goitein [2] [3]. To deliver the doses needed in one fraction (from 14 Gy for Choroidal Melanomas to 1.8 Gy for Pelvic tumors or Hodgkin's Disease) in one minute or less, using a scanned beam technique, an effective dose rate of  $5 \cdot 10^{12}$  protons/min or 13.5 nA is needed.

Allowing for losses in the beam delivery system (energy selection) the extracted beam intensity should exceed 30 nA, with the internal beam intensity being around 50 nA.

Delivering this kind of intensity with an isochronous cyclotron is, of course a trivial problem: isochronous cyclotrons can very easily achieve extracted beam intensities of tons of microamperes i.e. thousand time more than needed. The fact that we operate the accelerator so much below his maximum capacities is a key factor in achieving a very high level of reliability. This is in contradiction with synchrotrons working with low energy injectors where space charge limits are quite close for the highest intensities needed for radiotherapy.



### 1.3. Variable versus fixed energy

To locate the Bragg peak at the required depth within the tumor, it is necessary to vary the energy of the incident beam accordingly. This energy variation needs to be very fast, because the Bragg peak is so narrow that the irradiation of one field requires several successive passes with progressively decreasing energies.

In order to optimize the simplicity and reliability of the system, we have selected the solution of a very simple accelerator working continuously at the maximum energy, i.e. 230 MeV. Between the accelerator and the isocentric gantry, the energy is degraded to the value corresponding to the deepest range for the patient being currently irradiated. This first and largest energy reduction is done in such a way as to reduce the beam degradation caused by the scattering and straggling of the beam.

The modulation of the range is controlled by a second cylindrical rotating absorber located at the exit of the isocentric gantry.

## 2. The "CYCLONE 230"

The CYCLONE 230 cyclotron proposed by IBA is an isochronous, high field, non-superconducting cyclotron able to accelerate protons to 230 MeV.

### 2.1. The magnet system

The basic question in designing the magnet for a 230 MeV isochronous cyclotron is whether to use superconducting coils or not. In both solutions the field levels are rather similar: 3.09 Tesla on the hills, 0.985 Tesla in valleys, 2.165 Tesla average field at extraction radius, 1.74 Tesla average field at the center. Such field levels are mostly dictated by the requirement of obtaining adequate vertical focusing without having to use excessive spiraling of the sectors. The dimensions of both designs are therefore rather similar.

The advantages of a superconducting system are the reduction (possibly the suppression) of the iron for the return magnetic flux, a reduction of the electrical power required by the cyclotron in operation and, possibly, a reduction in the total investment costs.

On the disadvantage side of a superconducting system is the mechanical complexity of a split-coil cryostat, with very large forces involved, the potential problems associated with the liquid helium supply (from an attached helium liquefier or from batch transfers) and the very long thermal time constants of such a system: for a large mass, highly thermally insulated cryostat, warm-up or cool-down times are in excess of one week, yielding excessive down-time for a medical device, in case of problem.

The initial choice of the author is, therefore, to go for a classical, non superconducting design. Using the deep-valleys concept pioneered by IBA for non superconducting cyclotrons with the CYCLONE 30 series, it is possible to design a high field, non superconducting magnet for a 230 MeV cyclotron using no more than 185 kW of electrical power. The magnet section is illustrated in fig. 1, and the main parameters of the magnet are described in table 1. A number of steps have been taken to minimize the size and power consumption of the magnet, without compromising the optical qualities of the internal beam. The magnet gap in the hill regions decreases with radius, from 9.6 cm at the center to 0.5 cm at extraction, following an elliptical law [4]. The very small magnet gap at extraction is designed to provide a very sharp radial field fall-off, in order to simplify the beam extraction. For the same reason, the shape of the outer edge of the hills is patterned according to the shape of the orbit close to extraction and is not a circumference centered on the center of the machine like in other cyclotrons.

Another new technical feature of the CYCLONE 230 is that the azimuthal shape of the hills is not rectangular, like in other cyclotrons, but trapezoidal. The wider base of the hills reduces the magnetic saturation. This, in turn, results in an improved flutter and in a decreased power in the magnet coils.

To reduce also the main-coils power, the gap in the valleys was reduced to 60 cm. This value was found to be a reasonable compromise between the reduction of coil power and a convenient dimensioning of the R.F. system in the valley.

Using those values, we found that a good vertical focusing of the beam could be found with a 60° spiral angle of the sectors at extraction.

To facilitate maintenance, the cyclotron is split in two halves at the median plane. Using hydraulic jacks the upper half can be quickly (15') raised by one meter, so as to give an unrestricted access to the cyclotron median plane. Using this construction the cyclotron can be opened for maintenance or repair, closed, pumped down and restarted for operation in less than two hours. This is quite different from current superconducting cyclotron designs where an operation requiring access to the median plane implies a major dismantling and a loss of beam time for several days.

### Magnet system

number of sectors	4	
sector angle at the center	36°	
sector angle at extraction	53°	
hill field	3.09	T
valley field	0.985	T
average field at extraction	2.165	T
average field at center	1.739	T
magnetic induction	5.248 · 10 <sup>5</sup>	A.t
apparent current density in coils	153	A/cm <sup>2</sup>
actual current density in coils	214	A/cm <sup>2</sup>
power per coil	92	kW
weight of one coil	13.3	tons
weight of the iron	165	tons
Spiral angle	at the center	0°
	at extraction radius	60°

Table 1

### 2.2. The R.F. acceleration system

In a previous paper [5], we had proposed a "cyclotron without dees", i.e. a R.F. system where a pair of opposite hills would play the role of R.F. resonating structure. However, such a structure would lead to a sub-optimum design for the magnet and was, therefore, not selected in the present design.

Instead, we present a more classical R.F. system in which two dees are located in two opposite valleys. Those dees resonate on the fourth harmonic of the ions orbital frequency, i.e. 25.527 MHz × 4 = 102.11 MHz. This frequency falls in the F.M. broadcasting frequency range. It is therefore possible to find inexpensive standard broadcasting transmitters meeting the requirements of the system.

In the present design, each dee is supported by four vertical pillars, located symmetrically above and below the median plane. This design optimizes the simplicity, the mechanical stability of the dees and the cooling. In addition, a careful optimization of the diameter and length of each pair of opposed pillars allows to shape the amplitude of dee voltage versus radius.

### R.F. system

harmonic mode	H = 2	
dee voltage	100	kV
frequency	102.11	MHz
resonating system	2 dees in opposite valleys	
length of resonator	60	cm
capacitive loading estimated (each resonator)	58	pf
total RF power estimated for 100 kV	65	kW

Table 2

### 2.3. Vacuum system

Due to the moderate vacuum requirements of a positive ion cyclotron, a quite classical vacuum system can be used. In this case, we plan to reach the operational pressure of  $5 \cdot 10^{-6}$  mbar by a combination of 4 x 2000 l/sec oil-diffusion pumps located below the cyclotron and 4 x 3000 l/sec valved cryopumps located above the cyclotron. Due to the large pumping speed installed, in regard of the volume to be evacuated and of the surfaces to be outgassed, it is expected that an operational vacuum of less than  $10^{-5}$  mbar can be achieved less than 30 minutes after pump-down if the cyclotron has been vented to dry nitrogen.

### 2.4. Injection

The protons will be produced at the center of the cyclotron by a hot filament P.I.G. source introduced axially, through an air-lock. The life time of an ion source filament is expected to be in excess of one month, considering the very small arc currents required. Beam pulsing for the voxel scanning will be obtained by pulsing the arc voltage. Experiments have shown that rise and fall times of 15  $\mu$ sec or less could be achieved by this method.

### 2.5. Extraction

High efficiency extraction of high energy protons of an isochronous cyclotron is well known, but still quite difficult problem. However, in this case, three considerations allow significant simplification of the extraction system :

- the gap of the hills is decreased to 5 mm at extraction, allowing to reach a very steep magnetic field fall-off for the extracted beam
- as the extracted current is low (30 nA), a moderate extraction efficiency can be tolerated without causing an excessive machine activation
- unlike some physics experiments, proton therapy does not require the ultimate in beam emittance or energy resolution.

However, unlike cyclotron for physics, it is very necessary to obtain an extraction tuning that would be very uncritical and highly reproducible from day to day.

It is therefore the opinion of the authors that high extraction efficiency methods that are based on a high turn separation and on a very critical turn positioning in respect to the extraction devices should not be used in this case.

On the opposite, we plan to allow the acceleration of a rather large radial emittance and of a wide phase angle. The beam can then be considered as radially continuous at extraction, without any turn structure apparent anymore.

The extraction system based on such a beam structure has obviously a lower efficiency but this lower efficiency is obtained by very uncritical tunings.

The extraction system considered would use a septum magnet, followed by passive gradient correctors.

### 2.6. Control

The proposed cyclotron is a very simple, stable, uncritical and continuous device. The level of control required to achieve unattended operation of the cyclotron is therefore minimal, and the cyclotron should be considered as a mere accessory of the beam delivery system.

For the cyclotron control we plan to use a high level PLC based control system, basically similar to the system used in the lower energy CYCLONE 30 series. The human interface is made through graphical displays on a color screen, a keyboard and two virtual knobs (optical encoders) that can be allocated by software to any variable cyclotron parameter. The normal cyclotron operation is foreseen to be unattended, the cyclotron control being normally relayed to the beam delivery control desk.

### 3. Isocentric gantry

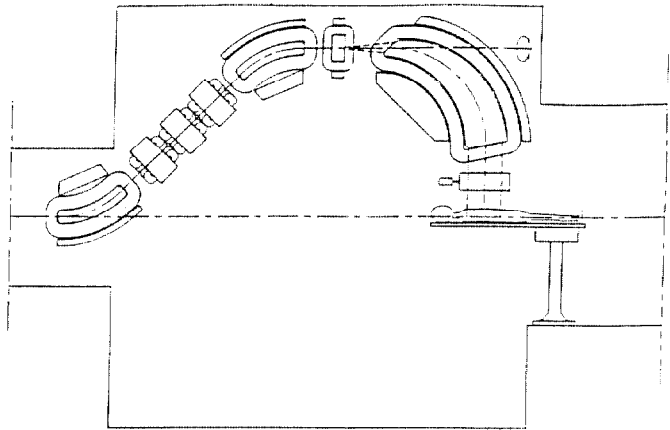
As a part of this proton therapy facility design, IBA has developed the concept of a more compact and simple isocentric gantry. This gantry is more fully described in another paper [1]. To cover the irradiation field, the beam is scanned in three dimensions. Range scanning is achieved by a cylindrically shaped, rapidly rotating absorber. The beam pulses are accurately synchronized to the absorber position so as to deliver beam only in the specific range.

Axial scanning is achieved by a sweep magnet located upstream of the final  $90^\circ$  magnet. Thanks to the optical features of the system, the beam reaching the patient is swept parallelly with a maximum amplitude of 40 cm. The effective source to isocenter distance is therefore infinite. The axial scanning speed is controlled by a dose integrator allowing an automatic correction of small beam intensity variations.

The transverse beam scanning is obtained by a slow rotation of the final  $90^\circ$  magnet around the axis of the incoming beam. By combining this motion with a slight gantry motion, a parallel beam translation, or even an arc therapy is also possible, reducing the skin radiation dose.

A conceptual mechanical structure has been designed. The reduced diameter of this gantry (5 meter, 16.4 feet) allows its installation in the therapy room of much more reasonable size.

Further calculation and engineering studies will be needed to confirm that the proposed structure is able to meet safely all design specifications.



### 4. Acknowledgements

Proton therapy is today a small and close knit community. Every progress is therefore more or less an achievement of the whole community and not of some groups or individuals. As newcomers in this community we would like to thank specially Michael Goitein, Monroe Rabin, Bernard Gottschalk and Ken Gall at MGH, Anders Brahme at the Karolinska, Eros Petroni and Hans Blattmann at P.S.I. and Pierre Scaillet at Middelheim, Antwerpen. It was through the informations they supplied to us and through the educating and simulating discussions we had together that we could improve and refine the design of this proton therapy facility.

### 5. References

- [1] A new concept of isocentric gantry for IBA's cyclotron based proton therapy facility. Y. Jongen, proceedings of the Loma Linda workshop - May 90.
- [2] "Clinical specification for a charged particle medical facility" Michael Goitein, proceeding of the Workshop on Accelerators for Charged-Particle Beam Therapy - Jan 25th, 1985- pp 41-65.
- [3] "Proton Beam Intensity" Michael Goitein -1/21/86-revised 3/19/86 -Report of the facilities working group -september 87 - 3 pages.(Facility general)
- [4] "IPN-ORSAY Project - First Machine Design Studies" - A. Laisné, 9th Conference on Cyclotrons and their Applications - Caen (Sept. 81) - 203.
- [5] "Preliminary Design of a Cyclotron-Based-Proton-Therapy Facility" - Y. Jongen, private communication.

# CANCER THERAPY WITH 200 MEV PROTONS AT PSI. DEVELOPMENT OF A FAST BEAM SCANNING METHOD AND FUTURE PLANS FOR A HOSPITAL BASED FACILITY.

Eros Pedroni<sup>†</sup>, Reinhard Bacher<sup>†</sup>, Hans Blattmann<sup>†</sup>, Terence Boehringer<sup>†</sup>, Adolf Coray<sup>†</sup>, Mark Phillips<sup>\*†</sup>, Stefan Scheib<sup>†</sup>

<sup>†</sup> Division of Radiation Medicine, Paul Scherrer Institute  
CH-5232 Villigen-PSI, Switzerland

<sup>\*</sup> Research Medicine and Radiation Biology, Lawrence Berkeley Laboratory,  
1 Cyclotron Road, Berkeley, CA 94720, USA

## Abstract

A new project for the treatment of deep seated cancers using proton beams has been started at PSI. The results of the first tests of the development of a fast beam scanning application technique (magnetic deflection of the focussed proton beam) performed in 1989 at PSI are summarized in this paper. The plans for the future construction of a beam line dedicated to proton therapy together with the new design of a very compact gantry are presented in the second part of the report. A very brief discussion on ideas and problems about a future hospital based facility for Switzerland terminates the presentation.

## 1. Introduction

The physical properties of proton beams are expected to bring significant improvements in cancer therapy by their large potential of improving dose localisation [1,2,3].

At PSI experience with cancer therapy with charged particles beams spans many years. Since 1981, 482 patients have been treated with negative pions using a dynamic scanning method developed for a 60 converging pion beams geometry (Piotron) [4].

Since 1985, 840 patients have received radiation treatment for uveal melanoma cancer (OPTIS project) using a 70 MeV proton beam at PSI [5].

The third new project of the medical division of PSI, namely charged particle therapy for deep seated tumors using protons of 200-250 MeV, is now underway [6,7,8].

Protons with variable energy and intensity suitable for proton treatment were available for test experiments starting from July 1989 at PSI. The beam is obtained by degrading the protons from 590 MeV (proton current of about  $20\mu A$ ) down to energies near 200 MeV (proton current of about  $1nA$ ). The beam is reanalysed in momentum and phase space in the second part of the beam line after the degrader. The present setup is provisional and is not adequate for the treatment of patients. The beam has been used in 1989 for the development of a new method of application of radiation, a **fast scanning of the focussed proton beam** inside the patient. Technical specifications and first results obtained with our apparatus are presented in section 2 of this report. Since the results were encouraging, the design of a new beam line dedicated to proton therapy has been proposed at PSI, accompanied by the design of a very compact isocentric gantry (with dimensions similar to those used for conventional treatments). These topics are briefly discussed in section 3. The final goal of the project is, however, to contribute to the realisation of a hospital-based proton facility, adapted to the needs of a small country like Switzerland.

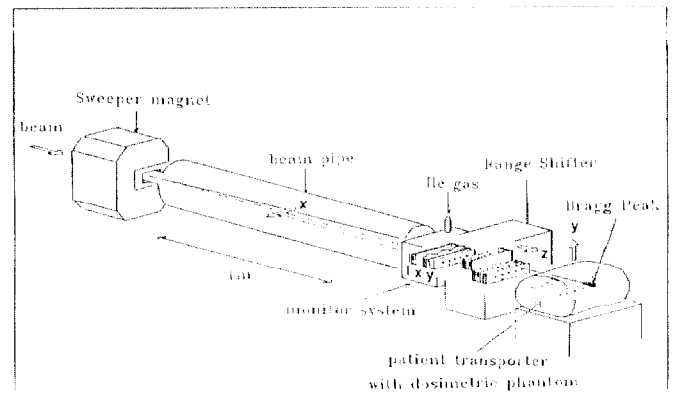


Figure 1: Layout of the experimental setup for the tests of the spot scan method.

## 2. Development of the spot scanning technique

The new dynamic treatment developed at PSI is based on the superposition of discrete dose spot applications. The dose at each single spot is well localised in space (in the lateral direction by maintaining the beam focus and in depth by the presence of the Bragg peak characteristic of all charged particle beams). The dose at a given position is applied by switching on the beam, measuring the quantity of applied radiation while the dose is being accumulated and by switching off the beam when the desired dose value for the spot has been reached. The focussed proton beam is then moved to the next spot position and the cycle is repeated. The full scan is performed under computer control by scanning the beam in three dimensions inside the patient's specific target volume, defined by the therapist using modern diagnostics like CT and MRI.

The basic apparatus is shown in Fig.1. The switching on and off of the beam is performed by a *fast kicker magnet*. The measurement of the dose delivery is performed with a *dose monitor system*. The motion, which is most often executed (in our case the horizontal) is performed by the magnetic deflection of the beam with a *sweeper magnet*. The depth of the beam in the patient is controlled by a *range shifter* system. The motion which is least frequently used is the vertical one and is performed by moving the phantom with a *patient transporter* system.

The advantages of the spot scanning method compared to the conventional method with passive scatterers in the beam is summarised in the following paragraph.



The dose can be exactly tailored in three dimensions according to the anatomical extent of the tumor (**three dimensional dose conformation**). The dose distribution may be shaped, if desired, according to a non-homogeneous dose prescription. The treatment is fully automated, multiple field irradiations are therefore performed more efficiently. Individual hardware like collimators, compensators, range shifter wheels, etc. can be avoided for routine treatments (but can be included as an option for special indications). A very small compact gantry can be designed for the spot scanning technique. The "discretisation" of the spot applications makes the method insensitive to beam instabilities. The electronics performing the dynamic treatment and the devices necessary to guarantee the safety of the treatment are simpler to realize for the discrete than for a continuous scan method.

The discrete spot scan technique easily permits the synchronisation of the treatment with the phase of breathing of the patient. The problem of organ movements during treatment and related dose errors, are discussed in a separate report [9].

#### Specifications for the dynamic scanning.

The spot size at the Bragg peak has dimensions of about 0.5 to 1.5 cm FWHM in the three directions, depending on the energy of the beam. We assume that scanning with the beam should be performed on a grid with a mesh size of typically 5 mm. Assuming a treatment volume of 1 liter and an irradiation time of about 2 minutes we calculate a total of about 10000 spots and a mean irradiation time of 12 ms per spot. If we want to control the dose at each spot individually at the 1% level we need to be able to switch off the beam with a reaction time of 120  $\mu$ s. The apparatus depicted in Fig.1 has been designed to satisfy these general specification goals.

The components in Fig.1 have been constructed and tested in the NA1 beam line during the beam period of 1989.

#### Fast kicker magnet.

Function: On-Off switching of the beam. The kicker magnet is a laminated C-shaped magnet with an effective field length of 23 cm and a magnetic field of 0.5 kGauss. The power supply allows the switching of the current in the magnet from 0 to 50 Amperes in 100  $\mu$ s with a rather high repetition rate (spot times as short as a few ms). The kicker magnet has been installed about 2.5 meters upstream of the last bending magnet of the beam line. A copper collimator with a horizontal slit of 4 mm width has been placed inside the gap of this bending magnet. The beam optics of the beam have been chosen with a sharp vertical focus at this collimator location. When the kicker is powered, the beam is deflected in the vertical direction by about 1.2 cm and is then completely stopped in the copper plate of the collimator. We measured the reaction time for the switching off of the beam by recording the rate in a small scintillation counter during the beam-on time and immediately after. The reaction time has been measured to be 50  $\mu$ s.

#### Integral dose monitor.

The monitoring of the dose is done with plane parallel ionisation chambers (gap 1 cm) covering the full beam (thin aluminized mylar windows mounted on rigid modular frames). The chamber modules are placed in a box filled with helium gas (at about 1 atmosphere) and are operated with 1 kV voltage, to guarantee a fast collection of the charges (ions and electrons) produced by the radiation in the gas. With 1 kV the overall reaction time of the full dose delivery system (fast kicker magnet controlled by the ionisation monitor) has been measured in the beam to be 135  $\mu$ s.

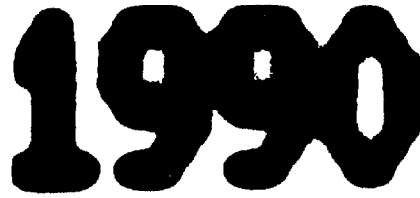


Figure 2: X ray film irradiated with the 200 MeV proton beam using the spot scanning method.

#### Position-sensitive monitor system.

The most frequent motion of the beam is performed by the sweeper magnet (see below). In order to check (on line) the proper functioning of the sweeper system the position of the deflected beam is measured immediately in front of the patient for each spot deposition during treatment. A position-sensitive helium monitor chamber has been built and placed in the same helium box as the integral monitor. The high voltage plane of this chamber is tilted with respect to the two parallel ground planes collecting the ionisation charges. By taking the ratio  $I_1/(I_1+I_2)$  of the charges collected on both sides of the tilted foil it is possible to measure the centroid of the beam. In the case of the x motion, the tilted foil has been shaped like a zigzag profile. Reproducibility measurements of the charge ratio recorded for time intervals as short as 5 ms were performed showing a position resolution better than 0.5 mm.

#### Range shifter.

The range shifter system consists of a stack of 40 polyethylene plates, each 4.5mm thick and with a size 2.5 cm x 20 cm in the direction perpendicular to the beam covering the entire region of the swept beam. The plates can be moved individually into the beam by pneumatic valves (but can be removed only collectively with the full stack). The time delay needed to bring one plate in the beam has been measured by an optical system to be less than 30 ms. The time for removing the full stack is longer (around 100 ms).

#### Sweeper magnet.

The magnet for sweeping the beam is of the same design as the fast kicker, but with a different power supply. The beam can be swept over a region of  $\pm 10$ cm in the patient at a distance of 2.5 m from the magnet by changing the magnet current over  $\pm 400$ Amp. The sweeping speed has been measured to be faster than 1cm/ms.

#### Simulation of dynamic treatments.

With the full apparatus as described above we performed first tests for the spot scanning method.

Fig.2 shows the capability of the spot scanning method to shape the dose according to very irregular target volumes. The X-ray film has been irradiated with the proton beam at 15 cm depth in the water phantom. The hardware used for the test for dynamic treatment with protons has been found to be within the original specifications. Although the treatment planning system for irregular volumes and with inhomogeneities has yet to be developed, the technical feasibility of the spot scanning technique has been demonstrated in practice.

### 3. Proposition for a dedicated proton facility at PSI

The next step of the project is the realisation of a new beam line with a dedicated area for the treatment of patients with a horizontal beam. At a later stage a compact gantry will be installed in the treatment area. The optics of the beam line have been designed in such a way to have a complete rotational symmetry of the beam (symmetric phase space and complete achromaticity) at the coupling point to the gantry.

A compact gantry with a diameter of only 3 to 4 m can be realised for the spot scanning method. The diameter is reduced considerably compared to other proposals by placing the sweeper magnet before bending the beam toward the patient (see Fig.3). The patient transporter system will be mounted directly on the gantry eccentrically with respect to the gantry axis. This reduces further the radius of the gantry system and acts as a counterweight for the magnets on the gantry. The rotation of the gantry must be accompanied by a counterrotation of the patient transporter system, maintaining the position of the patient horizontal at any angle of incidence of the beam.

The sweeping of the beam is performed only in the dispersion plane. This allows the gap of the magnets to be kept as small as possible. The arrangement of the scanning devices on the gantry is essentially the same as in Fig 1. The implementation of the sweeping in the beam optics of the gantry allows the design of the 90 degree magnet to be done in such a way as to displace the swept beam parallel to its direction (infinite source-to-skin distance). All three axes of scanning are in this way completely cartesian. This helps to make the treatment planning easier and reduces the skin dose.

The spot scanning method allows the addition of dose fields shaped like wedges into a single large homogeneous field. In this way it is possible to irradiate treatment volumes larger than allowed by the maximum range of scanning. This should permit us to keep the width of the pole tips of the 90 degree magnet rather small.

#### 4. Future plans for a hospital-based proton therapy facility

Any type of accelerator (synchrotron, synchrocyclotron, sector cyclotron) can in principle be utilized for proton therapy. The relative merits of any of these solutions are quite difficult to judge at present. From the point of view of reliability and simplicity of operation a sector cyclotron should be a very attractive solution. This machine should not present any problem with respect to beam intensity, which other solutions could possibly have. The cyclotron has the best possible time structure of the beam suitable for the realisation of a beam scanning technique with three dimensional conformation. With a sector cyclotron (or synchrocyclotron) the switching on and off of the beam can be done directly at the ion source (elimination of the fast kicker magnet). This possibility is also very attractive from the point of view of patient safety during treatment. The major drawback of these accelerator types is the fixed beam energy. Propositions for constructing cyclotrons or synchrocyclotrons with 2 or more fixed energies have been formulated recently [10,11].

The possibility to vary the energy (even on a pulse by pulse base) is probably the strongest argument in favor of the Fermilab compact synchrotron [12] for the Loma Linda proton facility, which will become operational this year and will be the first hospital-based proton facility in the world.

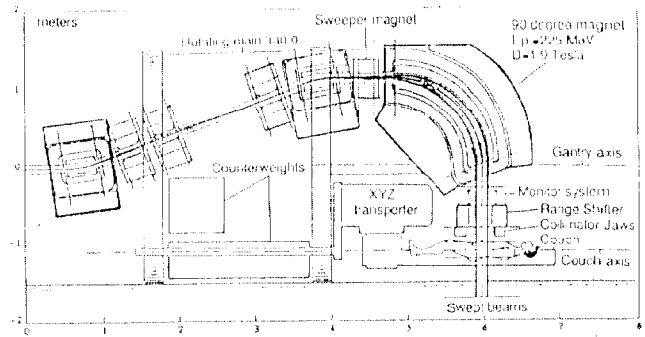


Figure 3: Schematic representation of the 360° compact gantry design for PSI.

One of the most important issues to be investigated with the new proposed beam line at PSI will be the importance in the practice of daily treatments of being free to choose the energy of the proton beam. This experience will be a major guideline for deciding on the accelerator type toward the realisation of the first hospital based facility for Switzerland.

This project is supported by a grant from the Swiss National Science Foundation (NFP18, 4018-25687).

## References

- [1] J.E.Munzenrider et al, *Strahlentherapie* 161(1985)756.
- [2] S.Graffmann et al, *Strahlentherapie* 161(1985)764
- [3] J.M.Slater et al. *Int. J. Rad. Oncol. Biol. Phys.*, Vol 14(1988)761.
- [4] C.F.v.Essen et al. *Int. J. Rad. Oncol. Biol. Phys.*, Vol 11(1985)217.
- [5] R.Greiner et al, *Muench. med. Wschr.* 131(1989)652.
- [6] Proton therapy project at PSI. Status report Nr 1 (June 1989). Dept. of Rad. Medicine, PSI.
- [7] Proceedings of the International Heavy Particle Therapy Workshop, PSI, Sept.15 to 20,1989.
- [8] H.Blattmann et al, *Strahlenther. Onkol.*, 166(1990),45.
- [9] M.Phillips et al, Dose Homogeneity ..., this conference.
- [10] H.G.Blosser, East Lansing, Michigan State University, USA, private communication.
- [11] Y.Jongen, PTCOG XII, Workshop on proton gantries ..., Loma Linda, Ca, USA, May 1990.
- [12] F.T.Cole et al. *Proc. of IEEE Particle Accelerator Conference*, 1987, pp. 1985.

## THE ACCTEK PROTON MEDICAL ACCELERATOR AND BEAM DELIVERY SYSTEM FOR CANCER THERAPY AND RADIOGRAPHY \*

Ronald L. Martin

ACCTEK Associates, 901 S. Kensington, LaGrange, IL 60525 USA

### Abstract

ACCTEK has developed prototype magnets and vacuum chambers for its concept of the proton medical accelerator under grants from the U.S. National Cancer Institute. The synchrotron would accelerate  $H^+$  ions to 250 MeV and utilize charge exchange extraction. Under development also is a beam delivery system consisting of a raster scanning magnet system and a rotating  $90^\circ$  bending magnet system. Conceptual ideas and progress on these systems are discussed. Also discussed are the feasibility of proton radiography and computed tomography with accelerators designed for proton therapy.

### 1. Introduction

ACCTEK Associates has been awarded grants from the United States National Cancer Institute for research and development on its concepts of a proton medical accelerator and a proton beam delivery system for radiation treatment of cancer. These are under the Small Business Innovative Research program applicable to all large U.S. Agencies with the purpose of commercializing technology developed with Federal funds.

The conceptual design of the Proton Medical Accelerator has been reported previously [1]. Briefly it would be a synchrotron to accelerate  $H^+$  ions to 250 MeV in a ring of small straight magnets of relatively small aperture, and utilize charge exchange extraction in a thin foil at any desired energy. To accommodate  $H^+$  ions without substantial losses due to magnetic stripping and neutralization by the residual gas the accelerator would operate with a peak field of 5.6 kG and a vacuum of  $10^{-10}$  Torr. The ring diameter would thus be relatively large, 13.7 m, and the ultra high vacuum would be achieved by nonevaporable Zr/Al getter strips, in an extruded aluminum vacuum chamber. Feedback from extracted beam current monitors to two fast orbit bumping magnets, would be utilized to control the extracted beam current. The nominal repetition rate would be 1 Hz, with 0.3 sec rise and fall time of the field and 0.4 sec at constant field to accommodate extraction for 0.3 sec. At this rate the average beam current would be 3nA. The magnets are designed for two times this rate of rise, 2 Hz with a 0.2 sec flat top or 3.3 Hz without flat top, with corresponding increase in the average current.

The SBIR grant on the Proton Medical Accelerator was completed in November 1989. Twelve small prototype magnets of accelerator quality were constructed at Argonne National Laboratory under a Work-For-Others contract. These are shown in Figure 1 in various stages of completion. They are arranged in an arc that is equal to the design value for the medical accelerator. Aluminum extrusion vacuum chambers were also produced and bent to the proper radius of curvature without serious distortion of water holes for baking and cooling nor distortion of the structure for mounting the getter strips

\* Work supported by Grant Nos. R44 CA41218 and R44 CA43407 from the National Cancer Institute

on the inside radius. This was an important issue not at all certain in the initial design.

The low field and use of many small straight magnets for the ring has led to some interesting alternatives because of the ease of increasing the field and redesigning the lattice layout. Many of these have been discussed previously [2] and are not repeated here.



Fig. 1. Prototype magnets for  $H^+$  accelerator, arranged on an arc of a circle of 13.7 m diameter.

### 2. Raster Scanning System

Under the current grant from the National Cancer Institute ACCTEK is developing a raster scanning system for 250 MeV proton beam delivery. This consists of a fast horizontal scanning magnet operating at 660 Hz followed by a slow vertical scanning magnet at 3 Hz as shown in Figure 2. The field scanned, with a lever arm of 3 m from the center of the vertical magnet, is 25 cm horizontally and 35 cm vertically. The arrangement is similar to one being developed at Lawrence Berkeley Laboratory [3] for raster scanning of heavy ions, although the ACCTEK system scans at a much faster rate. The rate is determined by the desire to complete a single scan of the entire area in 0.17 sec to accommodate 2 Hz operation of the accelerator.

The proposed scanning method is to scan a fixed field on each pulse and modulate the dose by controlling the extracted beam current. At a given depth the beam would be turned "on" when the leading edge of the sweeping beam intersected the desired contour of 100% dose at that depth and "off" when the trailing edge intersected the opposite boundary of that contour. The term "off" might mean reduction to a low value, say 5%, in order that the time of arrival of the beam at the end of the sweep can be detected by scintillators. The latter is but one link of a multielement safety system that is being

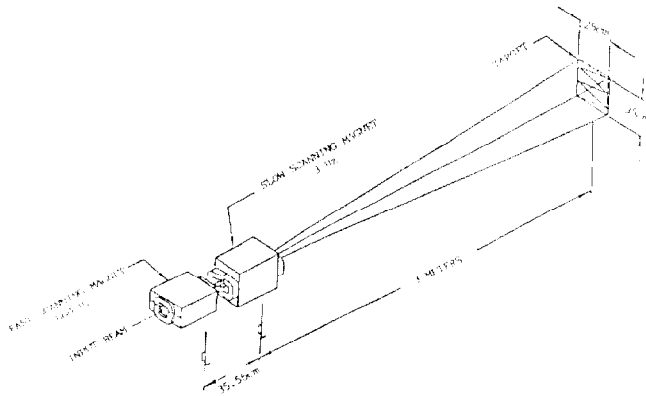


Fig. 2. Raster Scanning System

studied but will not be described. The transition from full dose to a low level is then about one beam diameter beyond the specified contour, with corrections for multiple coulomb scattering.

The scanning magnets being constructed are made of grain-oriented steel and are tape wound on a mandrel. The core is then cut, pole faces machined, and C cores assembled into H type magnets. The fast scanning magnet is made of 4 mil Selectron tape and the magnet steel is 8 3/4" wide, 4" high and 8" long. The gap is 1 3/4" x 0.787" high. The vertical scanning magnet is made of 12-mil Selectron tape and the magnet is 10" wide, 8 1/4" high, and 7 3/4" long. The gap is 3 1/4" wide by 2 1/32" high.

The proposed ability to control the extracted beam current with some precision has greatly simplified the design (and reduced the cost) of the power supply for the horizontal scanning magnet. Rather than producing a linear ramp, requiring a power supply with 200 kVA ratings and switching problems at zero current, it appears that a simpler resonant circuit will be adequate. The horizontal sweep speed will then vary with time so that the beam current will have to have a sinusoidal variation in order that the radiation dose remain uniform with time. This can be accomplished by inserting an ac wave in the feedback loop to the magnets that control the circulating beam position at the stripping foil in the accelerator.

The power supply for the vertical scanning magnet does not present a difficult problem because the power requirement is much lower at the slower sweep rate, and a jitter in zero crossing of the current is not nearly as critical. For this supply a linear ramp would be adequate. It is also possible to reduce the deviation from a straight line of the horizontal sweep by an order of magnitude (to 35 $\mu$  for a 1.5 mm vertical travel during one horizontal sweep) by the introduction of a small second harmonic current of the proper phase and amplitude into the vertical scan magnet supply.

The design of these power supplies is not yet complete but it is planned to test these ideas with a low energy beam.

### 3. Rotating Beam Delivery System

Also being developed as part of the SBIR grant is a low cost alternative to the 360° vertical gantry. It is proposed that a vertically downward directed beam, able to be rotated through an angle up to 60°, along with horizontal beams in the same and other treatment rooms, could serve most of the functions of the gantry and at much

lower cost. Capital and operating cost are seen as critical issues in the widespread development and utilization of proton therapy.

A schematic of the layout of such a system is shown in Figure 3. A 90° bending magnet system is capable of rotation about the incident beam axis to direct the beam vertically downward to a treatment room below beam level or to either of two horizontal beam treatment rooms at the beam level. A counterweight extends above the axis of rotation to balance the system.

It is believed, although a detailed study has not been carried out, that the shielding of each of the rooms is adequate that they could be utilized independently so that setup of a patient in one room could be performed while treatment was carried out in another. Such a flexibility of multiple treatment rooms is important for the economic feasibility of the proton treatment facility whereas the gantry system services only one treatment room per gantry. With the magnets in the 90° bending system turned off the beam emerging through the center of rotation could be transported downstream to be utilized in other treatment areas, possibly in a duplication of the layout shown.

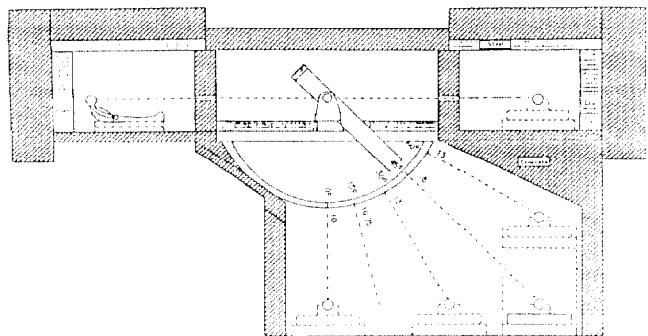


Fig. 3. 90° Rotating Magnet System for Beam Delivery to Three Treatment Rooms

Not shown, but important to the efficient utilization of this layout is a horizontal beam into the vertical treatment room at the patient level. In what might become the most widely used mode, treatment in this room could be carried out in 3 fields, two horizontal beams 180° apart (obtained by 180° rotation of the patient in the horizontal plane) and one vertical beam.

In the vertical treatment room variation in the incident angle through 0-45° requires patient motion in the horizontal plane. It is proposed to accomplish this by having the patient cart mounted on rails (lowest support), able to be rotated 360° (next support level), and finally laterally along the patient axis (upper support level). If treatment at 45-60° from the vertical is desired it might be accomplished by utilizing a vertical elevator as shown in order not to further extend the lever arm for treatment. It is believed that this patient motion can be accomplished with the speed and precision

with which a vertical gantry can be positioned and that multiple field treatment will be sufficient to reduce the dose to healthy tissue so that the missing flexibility (compared to a gantry) of treatment from below is not a serious drawback.

The raster scanning system described above, and diagnostics not described, would be carried on the rotating system and thus serve all three treatment rooms. It is designed for the minimum distance, 3 m, so that the longer distance, 5.5 m at 45°, can easily be handled. This variation of lever arm with angle does not present a problem to the raster scanning system, which will be under computer control.

A prototype of this rotating support system is under construction and its angular reproducibility will be demonstrated. Six small straight bending magnets of a type similar to those designed for the accelerator will be mounted on the support to provide 90° of bending, along with one quadrupole and the scanning magnet system described above. The total magnet weight is about two tons so that the total system with counterweight is just over four tons. It is anticipated that it can be rotated 90° in one minute.

#### 4. Proton Radiography

The application of protons to medical radiography was pioneered by A. Koehler and V.W. Steward at Harvard [4]. The initial work was extended at Argonne National Laboratory[5], at Los Alamos National Laboratory[6], and with alpha particles and heavier ions at Lawrence Berkeley National Laboratory[7]. The results clearly demonstrated the superiority of density resolution in soft human tissue of ion beams over x-rays at equivalent deposited radiation dose. This application of protons has not been pursued vigorously, however, because suitable proton beams did not exist to make this a practical technique. With the development of dedicated proton machines for cancer therapy, and especially of fast raster scanning beams, the advantages need to be reexamined.

While 300 MeV protons would be desirable for this application, the therapy beam of 250 MeV, with a range in soft tissue of about 38 cm water equivalent, is adequate for complete penetration of the head and most sections of average size humans. The low intensities required for a projection radiograph, a few times  $10^8$  protons, is sufficiently low that high quality proton beams can be produced at most machines by collimation. The capability for proton radiography can therefore be usefully developed at any dedicated therapy facility. Perhaps the most serious limitation of proton radiography is the loss of spatial resolution due to multiple coulomb scattering. The problem is minimized on the average, however, by knowledge of the transverse position of the entrance beam rather than that of the position at exit because of the cumulative buildup of angular divergence and beam size as the protons penetrate deeper into tissue.

Projection radiographs with protons in situ just prior to therapy could prove to be useful. It would directly check the patient alignment, and the calibration and operational status of the accelerator, transport, scanning system, and monitors. It could detect quantitatively any changes from previous treatment fractions, and any temporary problems that would affect the precision of dose delivery.

The potential for proton CT scanning also seems clear with raster scanning of a high quality proton beam. With a scanned beam size of  $1 \times 2 \text{ mm}^2$  and 360 line scans at 1° increments good computed cross sections should be obtained with  $10^3$  protons/ $2\text{mm}^2$ . The estimated dose for this procedure, provided scanning planes were no closer than 5 mm apart, is about 0.5 rem, comparable to or lower than that for an x-ray CT exposure. For upright patients, particularly applicable to images of the head, the time for a proton CT is only limited by the rate of rotation of the patient. A rotation period of 10 or 20 seconds seems reasonable. For reclining patients, of course, a gantry would be required for proton CT.

Not only is it anticipated that the proton CT scan will give more precise density data than x-ray scans, but it measures proton stopping power directly. The potential exists therefore of improving treatment planning by eliminating the use of CT conversion numbers with their uncertainty because of x-ray beam hardening.

Finally the use of proton CT as a stand alone technique independent of therapy seems sure to find wide application once the capability exists.

#### Acknowledgement

The author wishes to acknowledge the assistance on various phases of the work described here of: K. Thompson and R. Wehrle, Argonne National Laboratory, W. Praeg, ANL, retired, R. Swannstrom and A. Hassan, ACCTEK, and S. Kramer, Brookhaven National Laboratory.

#### References

- [1] R.L. Martin, "A Proton Accelerator for Medical Applications," *Nuc. Inst. Methods in Physics Res.* B24/25, 1987, pp. 1097.
- [2] R.L. Martin, "Modular Design of H<sup>+</sup> synchrotrons for Radiation Therapy," *Nuc. Inst. Methods in Physics Res.* B40/41, 1989, pp. 1331-1334.
- [3] J.E. Milburn, et.al., "Raster Scanning Magnets for Relativistic Heavy Ions," *IEEE Trans. on Nuc. Sci.*, N, 1987, pp. 2000-2002.
- [4] A.M. Koehler, "Proton Radiography", *Science*, Vol. 160, pp. 303, 1968; V.W. Steward and A.M. Koehler, "Proton Beam Radiography in Tumor Detection," *Science*, Vol. 179, 1973, pp. 913.
- [5] D.R. Moffett, et.al., "Initial Test of a Proton Radiographic System," *IEEE Trans. Nuc. Sci.*, NS-22, 1975, pp. 1749.
- [6] K.M. Hanson, et.al., "The Application of Protons to Computed Tomography", *IEEE Trans. Nuc. Sci.*, NS-25, 1978, pp. 657. *ibid*, NS-26, 1979, pp. 1635.
- [7] K.M. Crowe, et.al., "Axial Scanning with 900 MeV Alpha Particles," *IEEE Trans. Nuc. Sci.*, NS-22, 1975, pp. 1752; E.V. Benton, et.al., "Radiography with Heavy Particles," preprint, LBL-2887, Univ. California, 1975.

## FIRST BEAM IN A NEW COMPACT INTENSE 30 MeV H<sup>-</sup> CYCLOTRON FOR ISOTOPE PRODUCTION

B.F. Milton, G. Dutto, R. Helmer, R. Keitel, W.J. Kleeven, P. Lanz, R.L. Poirier, K. Reiniger, T. Ries, P.W. Schmor, H.R. Schneider, A. Sliwinski\*, J. Sura†, W. Uzat‡, and J. Yandon  
*TRIUMF, 4004 Wesbrook Mall, Vancouver, B.C., Canada V6T 2A9*  
 R. Dawson, M. Denhel, K.L. Erdman, W. Gyles, J. Sample, Q. Walker, and R. Watt  
*Ebco Industries Ltd., 7851 Alderbridge Way, Richmond, B.C., Canada V6X 2A4*

### Abstract

A new high intensity, 30 MeV H<sup>-</sup> cyclotron has been constructed for radioisotope production. It is a four-sector radial ridge design with two 45° dees in opposite valleys. An external multi-cusp dc source developed at TRIUMF generates the H<sup>-</sup> beam for injection into the cyclotron. Beam extraction is by stripping to H<sup>+</sup> in thin graphite foils. Two multiple foil stripper mechanisms produce two simultaneous external beams, of intensities up to 200 μA. Adjustment of the extraction foil position permits extracted beam energy variation from 15 MeV to 30 MeV. Results of magnet field mapping, vacuum, high power rf and beam tests will be described. A 30 MeV beam of intensity in excess of 250 μA has already been extracted along one beam line. On opposite beam lines two beams, one of 140 μA the other of 164 μA, for a total in excess of 300 μA, were simultaneously produced.

### 1. Introduction

The 30 MeV cyclotron (TR30) which is being built for isotope production by Ebco Industries Ltd. with the technical and design assistance of TRIUMF achieved first beam on May 9, 1990, within 17 months of project startup date. The basic specifications for the cyclotron [1-3] call for two external beams of current up to 200 μA and energy variable between 15 MeV and 30 MeV, with a total maximum beam intensity of at least 350 μA. More than 300 μA have already been extracted to date.

Figure 1 shows the cyclotron as it was undergoing commissioning tests recently. Design features are more readily apparent in the schematic view given in Fig. 2. The cyclotron is a four-sector compact design with radial ridge hills. The magnet is approximately square in shape, 2.3 m flat to flat, 1.26 m high



Fig. 1. The 30 MeV high intensity compact cyclotron.

\*on leave from SINS Swierk, Poland

†on leave from University of Warsaw, Poland

‡on leave from University of Manitoba

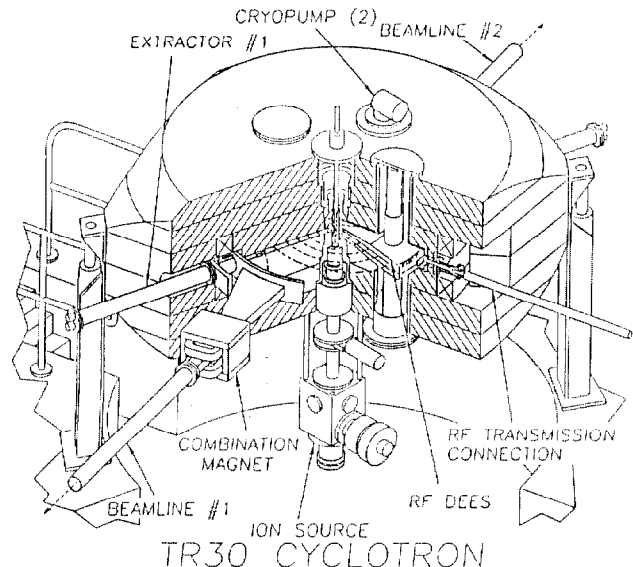


Fig. 2. Schematic view of the cyclotron.

and weighs approximately 46 tonnes. It is split at the midplane, so that four hydraulic jacks located at the corners of the yoke can elevate the upper part approximately one metre to allow access to the cyclotron interior. Two coils 37500 A-turn each mounted on the upper and lower poles provide the magnet excitation. Because of the fixed field operation, all magnetic field corrections were made by shimming during field mapping. No trim coils are needed.

Head room requirements in the cyclotron vault are minimized by installing the external H<sup>-</sup> ion source and injection line below the cyclotron. This arrangement has the additional practical advantage of avoiding the possibility of material flaking off the ion source filaments and falling onto any of the high voltage electrodes of the source or inflector. It does, however, require that the cyclotron be mounted over a 1.4 m deep pit.

The H<sup>-</sup> beam is injected vertically upward along the magnetic axis toward the centre where an electrostatic spiral inflector bends it into the median plane. Two 45° dees located in opposite valleys then provide acceleration at four gap crossings per orbit. The design voltage for the dees is 50 kV, and the operating frequency is 73 MHz, the fourth harmonic of the orbit frequency. The dees operate in phase.

Four large holes through the yoke in the dee valleys accommodate the coaxial stubs required to resonate the dees at the operating frequency. For magnetic symmetry there are four identical holes in the unoccupied valleys. Two of these are used as vacuum pump ports in which two 20 cm diameter cryopumps are installed.

Beam extraction is by stripping to H<sup>+</sup> in thin graphite foils. Two independent external beams are formed with two extraction probes travelling in opposite hill gaps.

The basic cyclotron parameters are given in Table I.

Table I. Principal cyclotron parameters.

Magnet	
Average field	1.2 T
Hill field	1.90 T
Valley field	0.55 T
Hill gap	4 cm
Valley gap	18 cm
Pole radius	76 cm
Number of sectors	4
Ampere-turns	$7.5 \times 10^4$
RF	
Frequency	73 MHz
Dee voltage	50 kV
Harmonic	4
Vacuum	
Pressure	$6 \times 10^{-7}$ Torr
Pumping	4000 $\ell/s$ ( $\text{H}_2\text{O}$ ), 1500 $\ell/s$ (air)
Ion source	
Type	$\text{H}^-$ cusp
Output current	7 mA
Emittance (normalized)	$0.34\pi$ mm-mrad
Bias voltage	25 kV

In order to test, at an early stage, the design of critical centre region components, a full scale model of the TR30 centre region was also built. A stable beam intensity of  $650 \mu\text{A}$  was measured at the fifth turn (1 MeV). This work is described in another paper presented at this conference [4].

## 2. Magnet

Initial magnet design calculations were done with the two-dimensional magnet code POISSON and were subsequently refined using the three-dimensional code TOSCA. To avoid the  $\nu_r = 2\nu_z$  resonance, the top surface of the hills were sculpted to reduce the flutter slightly and the hill width adjusted to achieve isochronism. The calculations achieved a field that was isochronous to better than 50 G at all points. A template was then prepared according to the calculated hill profile and used to machine the surface of the hills.

The magnet, first energized on August 4, 1989, achieved full field without difficulty. A shuttle coil field mapping system [5], borrowed from Texas A&M University and modified to suit the magnet, was used for the field mapping. Initial data indicated that the magnetic field was within 200 G of isochronism at the worst point, and within 50 G over most of the magnet. In fact the largest discrepancy was at the centre of the machine where four mounting holes, for central region components, had been drilled in the pole tip surfaces. This was rapidly corrected by raising the centre plug pole tips by 1 mm. The field was then within 50 G everywhere. Shimming was accomplished by varying the thickness of plates attached to the hill edges. Initially many small plates screwed onto a larger base plate were used. Once a reasonably isochronous field was achieved, this shape was used to cut a single plate for each hill edge. This procedure turned out to be extremely predictable and reliable. After shimming the magnetic field was isochronous to within  $\pm 5^\circ$  of rf phase. Reproducibility of the average field was better than 2 G after opening and closing the magnet. The tune diagram, calculated from the measured field data shows that the  $\nu_r = 2\nu_z$  resonance has actually been avoided. Small imperfection harmonics, generated by small rf liner attachment holes drilled in the pole faces, were overcome by using composite studs in the holes. Custom made studs were designed so that the part of the

stud below the hill face was steel and the part above was made of stainless steel. This reduced the first and second harmonic amplitudes to below 4 G everywhere.

## 3. RF System

The rf power is delivered to the dees through a motor tunable capacitor coupled to the  $50 \Omega$  transmission line that passes through a port in the vacuum tank wall. A tuning capacitor, located at the back of the dees and having actuators that pass through ports in the vacuum tank wall, provide a tuning range of 200 kHz for dee voltage balancing and resonance control. For ease of maintenance the entire rf amplifier system, which will consist of two combined 25 kW FM transmitters modified for operation at 73 MHz, is located outside the cyclotron vault.

Figure 3 shows the two dees being installed in the magnet. All copper surfaces of the dees, resonator stubs, and valley liners are water cooled to assure stable rf operation. Cooling water lines enter from the lower resonator so magnet opening is possible without disturbing the cooling circuits. The measured Q of the dee-resonator system is 5200, and the rf power necessary to establish the specified 50 kV dee voltage is 19 kW.

## 4. Ion Source and Injection Line

A compact version of the TRIUMF dc volume  $\text{H}^-$  multicusp ion source [6] has been tested. To reduce arc power the extraction electrode aperture was enlarged to 11 mm diameter. The normalized emittance of an extracted 7 mA  $\text{H}^-$  beam, measured at the 90% contour, 2 m downstream from the source was found to be  $0.34\pi$  mm-mrad. Arc power in this case was  $\approx 3.7$  kW and the  $\text{H}_2$  flow was 10 std cc/min. The current is observed to be stable to  $\pm 2\%$  over periods of 6 h.

A 1.3 m long injection line transports the beam from the source to the inflector. Beam line optics along this line, consisting of a solenoid and a quadrupole doublet, have been optimized together with the inflector to match the beam to the cyclotron [7]. Because of the intense bright beam available from the source no bunching is required.

## 5. Extraction and Diagnostic Probes

The simplicity of extraction is of course the main attraction of  $\text{H}^-$  cyclotrons. It is achieved by passing the  $\text{H}^-$  beam



Fig. 3. View of the dees in opposite magnet valleys.

through an appropriately positioned thin graphite foil (approximately  $200 \mu\text{g}/\text{cm}^2$ ) to strip off the electrons. The resulting  $\text{H}^+$  beam then deflects into the exit port. For an extraction foil locus that is very nearly linear and located in a hill gap, the  $\text{H}^+$  trajectories for the 15 MeV to 30 MeV beams exit the cyclotron through a valley, far from the defocusing effects of the hill fringe fields, and come to a common crossover point at the combination magnet location outside the magnet yoke.

Two diametrically opposite extraction probes, each carrying a five foil carousel of graphite foils, pass through 15 cm diameter holes in the magnet yoke and vacuum tank port, into the respective hill gaps. The probes are remotely adjustable in radial and transverse direction for energy variation and steering into the extraction beamline.

For magnetic symmetry there are two additional 15 cm holes opposite the two other hills. One of these is used to accommodate a water cooled radial diagnostic probe. As an injection diagnostic a pop-up probe to intercept the fifth turn is installed in a valley.

## 6. Control System

The control system, which is totally automatic and computer controlled, is based on an Allen Bradley PLC for monitoring and controlling individual power supplies and switches. These are connected by means of a proprietary communications network to two 20386 PCs with a 60 megabyte hard disc and running at a clock speed of 25 MHz.

Operator interaction is achieved by using a modular software program called Control View supplied by the same company. It controls all screen (mouse) and keyboard input/output and manages the multitasking operating system. It also maintains a current value database and is capable of interacting with up to 10,000 I/O points in the system.

Two 14 in. high-resolution color monitors are used to display a series of graphic screens on which the operating values of all of the power supplies, the states of switches and valves, and the readings of all relevant water flows, vacuum pressures, and temperatures in the system can be viewed.

Separate crates containing PLCs are used for the safety systems, target monitoring, and ion source control units. The latter, which is at a potential of 25 kV with respect to ground, is accessed through a fibre optical cable serial data link. The control program includes an RS 232 driver system and is thus capable of communicating with serial devices.

The system is easy to program and operate, and it is not difficult to write macro routines to simplify control and tuning procedures. As well as the built-in application packages other application routines have been written using the C-toolkit provided with the software. Microsoft C can also be used to create routines that will run in the multitasking environment.

## 7. Commissioning

Commissioning of the TR30 cyclotron has proceeded rapidly as components have been completed. The vacuum system has achieved a base pressure of  $8 \times 10^{-8}$  Torr and typical operating pressure with beam is  $6 \times 10^{-7}$  Torr. Initial tests began with beam blockers at 1 MeV. Quite quickly an injection line tune was demonstrated that gave  $200 \mu\text{A}$  at 1 MeV. The measured transmission efficiency from the ion source up to 1 MeV is 8% for a dee voltage of 49 kV and increases to 12% for a dee voltage of 51 kV. The beam blockers were then removed and

$1 \mu\text{A}$  of beam was accelerated to full radius. Checks performed with a radial probe showed that there was better than 95% transmission between 1 MeV and 32 MeV.

Following these tests we installed the two stripping foil mechanisms. By performing shadow measurements with the two strippers and the diagnostic probe, we verified that the beam was centered to within 4 mm. This also verifies that the maximum energy is greater than 30 MeV. As soon as a target became available we began extracting 30 MeV and in a matter of hours we had beam current in excess of  $100 \mu\text{A}$  on the target. On June 6 a 30 MeV beam of intensity in excess of  $250 \mu\text{A}$  was extracted from the machine (with  $230 \mu\text{A}$  reaching the production target system), a major milestone in a tight 18 months design and construction schedule. On June 7 two beams of  $164 \mu\text{A}$  and  $140 \mu\text{A}$  were simultaneously extracted on opposite beam lines, with a total beam intensity in excess of  $300 \mu\text{A}$  being accelerated. For these tests only one of the two transmitters was used, powered to 28 kW. The losses in the cyclotron were very low and small losses in the beam line were mainly at the protection slits which had been deliberately set to form a tight restriction for setup purposes. The commissioning team was pleased to find that most settings lie very near the calculated values. The rf system, the vacuum system, the extraction stripper and the control system have behaved extremely well so far. Overall component stability is very good.

Future commissioning work will aim at reliable high intensity operation with minimal operator intervention and extraction at several combinations of energies. It is expected that Nordion International who contracted the cyclotron and its building as a turn-key facility to Ebco, will be able to start isotope production on or before August 1, as originally planned.

## Acknowledgement

This isotope production cyclotron is the first cyclotron produced by Ebco and is an important example of technology transfer for TRIUMF. TRIUMF and Ebco would like to thank all those who have contributed to this 18 month endeavour with ideas, suggestions, hard work or support. A particular thanks goes to those colleagues from the international community who have given useful advice during design and construction.

## References

- [1] H.R. Schneider et. al., "A Compact  $\text{H}^-$  Cyclotron For Isotope Production", Proc. I<sup>st</sup> European Particle Accelerator Conference, Rome, 1988, p. 1502.
- [2] R. Baartman et. al., "A 30 MeV  $\text{H}^-$  Cyclotron for Isotope Production", Proc. of the IEEE Particle Accelerator Conference, Chicago, 1989, p. 1623.
- [3] B.F. Milton et. al., "A 30 MeV  $\text{H}^-$  Cyclotron for Isotope Production", to be published in the proceedings of the 12th Int. Conf. on Cyclotrons and their Applications, Berlin, 1989.
- [4] W. Kleeven et. al., "Status and Results from the TR30 Cyclotron Centre Region Model", these proceedings.
- [5] L.H. Harwood et. al., "Characteristics and Performance of the System Developed for Magnetic Mapping of the NSCL Superconducting K800 Cyclotron Magnet", IEEE Trans. on Nucl. Sci. NS-32, 3734 (1985).
- [6] K. Jayamanna et. al., "A Compact  $\text{H}^-/\text{D}^-$  Ion Source", these proceedings.
- [7] R.J. Balden et. al., "Aspects of Phase Space Dynamics in Spiral Inflectors", to be published in the proceedings of the 12th Int. Conf. on Cyclotrons and their Applications, Berlin, 1989.



APPLYING CHARGED PARTICLE PHYSICS TECHNOLOGY  
FOR CANCER CONTROL AT

LOMA LINDA UNIVERSITY MEDICAL CENTER, USA

James M. Slater, M.D., F.A.C.R.  
Chairman, Department of Radiation Sciences  
Loma Linda University Medical Center  
Loma Linda, California, USA

Abstract

The world's smallest proton synchrotron soon will begin to be used for patient treatments at Loma Linda University Medical Center in the United States, as part of an effort to apply and exploit high-energy physics technology for cancer control. Proton therapy has superior characteristics to accomplish this end, notably a dose distribution that facilitates the delivery of effective doses while sparing adjacent tissue. The characteristics are exploited in a synchrotron, designed and built in a cooperative effort among university, government and industry investigators, for treating patients. The characteristics and implications of this development are discussed.

Introduction

The precision of proton therapy underlies its clinical application. Exploiting that precision to its fullest, underlies the effort to apply high-energy physics technology for controlling cancer at Loma Linda University Medical Center. The classic intent of radiation oncology is to treat only diseased tissue, sparing normal tissue in the process. In practice, this ideal is often compromised so that all areas of risk may be encompassed. Normal tissue tolerances in those areas determine the dose that can be given; often, one insufficient to control a malignant tumor.

Because photons and electrons lose most of their energy near the point of entry, it often is difficult to concentrate a cancerocidal dose deep in the body. Photons and electrons also cause much secondary lateral scatter; surrounding normal tissues receive part of the dose, resulting in side effects. Attempting to circumvent these problems, radiation oncologists often irradiate the tumor through several portals with overlapping beams, building up the target volume dose and minimizing the dose to normal tissues. Using such strategies with protons, one can deliver higher doses of ionizing radiation with even greater precision.

The Clinical Problem

According to current information from the American Cancer Society,<sup>1</sup> more than one million Americans will develop some form of non-skin cancer in 1990. About three of every ten Americans will develop some form of cancer at some time in her or his life, and cancer affects three of every four families in some way. Among Americans receiving treatment for cancer localized to an anatomic region and theoretically amenable to control by locoregional therapies, disease, failure to control the local process occurs in 225,000 cases every year.<sup>2</sup> In addition, morbidity from disease and treatment causes unacceptable suffering in uncounted numbers of people. Such data give impetus to the search for more effective locoregional treatments.

History of Proton Therapy

The first proposal for the medical use of protons occurred in 1946,<sup>3</sup> when Robert Wilson published his landmark paper. Because protons deposit almost all their energy at any desired depth in the body, Wilson believed that patient trials should be undertaken on the accelerators then being built for high-energy physics research.

In the mid-1950's, proton beams were first employed on humans; 26 patients received pituitary irradiation for advanced breast cancer.<sup>4,5</sup> The second application of a physics research accelerator for proton therapy occurred in Sweden in 1957; by 1968, 69 patients had been treated.<sup>6,7</sup> Physicians working with Harvard Cyclotron Laboratory began employing a 160 million electron volt (MeV) proton beam for therapy in the early 1960's; pituitary adenomas were among the first tumors treated.<sup>8,9</sup> Large field radiation therapy began at Harvard in 1974, as the applications of the superior physical dose distribution of the proton beam to a range of tumors became apparent.<sup>10-12</sup> Proton beam therapy began in the Soviet Union in the mid-1960's;<sup>13</sup> the Japanese experience began in 1979, at Chiba; another facility opened at Tsukuba a few years later.<sup>14</sup> At the Paul Scherrer Institute in Villigen, Switzerland, proton beam therapy commenced in 1985.<sup>15</sup>

Interest in proton therapy grew rapidly as results were reported from early investigations. As a means of consolidating this interest and directing it to optimize the clinical potential of the modality, the Proton Therapy Cooperative Group (PTCOG) was formed in 1985. This group meets semi-annually to report to its international membership on the state of the science; works to design therapy facilities for institutions around the world; and drafts protocols for analyzing proton treatment in a scientific, cooperative manner. Through its newsletter, PTCOG tabulates the progress of proton and other charged particle therapies in institutions employing physics research accelerators for medical purposes. Currently, over 8,000 patients have been treated with protons in these and other institutions around the world.<sup>16</sup>

A Superior Beam for Clinical Radiation Therapy

Like conventional external beam irradiation, proton radiation therapy is directed to a tumor or other disease process, causing changes which kill irradiated cells or render them unable to function. In terms of their relative biologic effect (RBE), protons are similar to photons (the RBE of protons is generally accepted as being approximately 1.1, compared to cobalt).

A proton beam has almost no secondary lateral scatter and deposits most of its energy at the Bragg peak; little energy is deposited along the path until the peak is reached, and virtually no energy is deposited distal to it. By spreading out the Bragg peak through energy variation or other measures, the radiation oncologist can encompass the target volume.

Such precision means the radiation oncologist can increase the dose to the tumor while reducing the dose to surrounding normal tissues, allowing for higher tumor-destroying doses and a greater chance for locoregional disease control without stopping treatment because of side effects.

#### Demonstrated Effectiveness of Proton Therapy

Results from difficult-to-treat tumors show the benefits of the modality. Some ophthalmologists treat ocular melanoma, for example, by enucleation. Where protons or helium ions have been used, however, the cure rate is more than 95%, and most patients retain useful vision in treated eyes.<sup>17,18</sup> Pituitary tumors show similar results and, like small tumors of the eye, can be treated in one to three days on an outpatient basis.<sup>19</sup> Because of their proximity to the brain stem, tumors of the base of the skull are difficult to control. In contrast to conventional irradiation's control rates of 35% or less, proton and helium ion therapy have yielded control rates of approximately 85%, and patients can pursue daily activities after being treated.<sup>20</sup> Proton therapy has also been employed in non-cancerous processes, such as arteriovenous malformations of the brain.<sup>21</sup>

The precision of proton therapy has long been known, but applications have been limited because physics research accelerators were not designed for treating patients, and because many tumors could not be localized with the necessary precision. Since the mid-1970's, however, CT, MRI, SPECT, PET, ultrasound, improved conventional imaging modalities and improved means of contrast enhancement, have all increased the precision with which disease extent is defined. These improvements, combined with better understanding of the radiobiological effect of conventional and heavy charged particle irradiations, justify the expense and effort required to build a proton accelerator and facility designed for patient treatments.

#### Designing a Proton Accelerator for Medical Use

The Loma Linda accelerator is the smallest synchrotron in the world. It was designed from the start to be a patient-treatment machine, and reflects the input of physicians, physicists and engineers from around the world, via the efforts of PTCOG, which drafted its specifications, Fermi National Accelerator Laboratory, which designed and built it, and Science Applications International Corporation, which assisted in the design and installation at Loma Linda, and will market future, similar accelerators.

The requirements for a medical accelerator differ from a high-energy physics research accelerator. For example, the ability to vary the energy is critical, in order to encompass the varying anatomical configurations of tumors. A medical machine also must be simple to operate and easy to maintain, in contrast to one employed in a high-energy physics laboratory. Some of the characteristics of the Loma Linda synchrotron are indicated in Table 1.

Table 1  
LLUMC Accelerator; Goals of Design

Energy	70-250 MeV
Beam spill time	0.05-9.9 sec
Cycle time	2 sec.
Beam intensity	1 E 11 protons/pulse
Ion source	Duo-plasmatron 100 mA max. current 70 mA operational 30 kV
Linear accelerator	RFQ 2 MeV 20 microsec. pulse 20 mA output current
Synchrotron	Zero gradient Betatron tunes: @ extraction .5/1.36 @ flattop .6/1.30 Harmonic: 1 Single turn injection 20.05 meter circumf. Inject above transition Cycle time: 2,4,8 sec. Aperture: 5 x 10 cm. Extraction: 0.4-10 sec.

#### Expected Applications

Computer simulations show the benefits that can be expected when the modality is employed. In locally advanced cancer of the uterine cervix, for example, control is difficult to achieve with conventional irradiation because the needed large fields and high doses result in unacceptable doses to nearby vital structures. Proton beams will enable delivery of even higher doses, while still avoiding the nearby structures. The ability to spare the opposite parotid gland and mandible, while delivering high doses to tumors of the tonsillar region, suggests a role for proton therapy in such malignancies staged T2 or higher. In a series of carefully planned protocols, the patients who can benefit from proton therapy will be identified. As suggested in Table 2, it is expected that such studies will reveal several groups of patients who will benefit.

Table 2  
Anatomic Sites of Potential Application

CNS	Glioma; meningioma; cervical chordoma and chondrosarcoma; pituitary adenoma; acoustic neuroma; craniopharyngioma
H & N	Oropharynx; nasopharynx; larynx; hypopharynx
Thorax	Esophagus; lung
Abdomen	Pancreas; retroperitoneal soft tissue sarcoma; para-aortic nodes
Pelvis	Bladder; uterine cervix; prostate; unresectable or recurrent colo-rectal or endometrial carcinoma
Pediatric	Optic & brain glioma; pineal malignancies; Hodgkin's disease; retinoblastoma; medulloblastoma; rhabdomyosarcoma; neuroblastoma
Other	Hodgkin's, non-Hodgkin's lymphoma; soft tissue sarcoma; arteriovenous malformations

#### Initial Endeavors

Opening in 1990, the Loma Linda proton therapy facility is eventually expected to serve between 1000 and 2000 patients annually. The first patients will be treated with the stationary beam this autumn, with one of the gantries commencing operation the following

winter. Patients with eye and head & neck tumors will be treated first, with the stationary beam. Patients with tumors in other anatomic sites will be treated with the movable beam. One of the three gantries will be commissioned in winter, 1991, for this task. Experience with that gantry will be utilized for modifying the other two, if needed.

The Loma Linda facility will be a worldwide resource for research and learning about proton beam therapy. Researchers will investigate topics such as: dose escalation and time de-escalation protocols; radiobiologic effects of particle therapy; the physics and engineering of proton accelerators; simulated effects of outer-space radiation; and combined treatment modalities. A charged-particle database is being developed to assist in these efforts, and satellite and microwave communications systems will enable physicians to send patient images to LLUMC for therapy planning. Data generated by these studies will be made available to the general medical community, and will help physicians and patients determine whether proton therapy might be advantageous for them.

#### REFERENCES

- American Cancer Society, Facts & Figures, 1990.
- DeVita VT: "Principles of Chemotherapy." (In) VT DeVita, S Hellman, SA Rosenberg (eds), Cancer: Principles & Practice of Oncology (3rd ed). Philadelphia: Lippincott, 1989, pp. 276-300.
- Wilson RR: Radiological use of fast protons. *Radiology* 1946; 47:487-491.
- Tobias CA, Roberts JE, Lawrence, JH, Low-Beer BVA, Anger HG, Born JL, McCombs R, Huggins C: Irradiation hypophysectomy and related studies using 340 MeV protons and 190 MeV deuterons. *Peaceful uses of atomic energy* 1956; 10:95-96.
- Tobias CA, Lawrence, JH, Lyman J, Born JL, Gottschalk A, Linfoot J, McDonald J: Progress report on pituitary irradiation. In Haley TJ, Snider RS (eds): Response of the Nervous system to Ionizing Irradiation. New York, Little, Brown & Co., 1964; pp. 19-35.
- Larsson B, Leksell L, Rexed B: The use of high energy protons for cerebral surgery in man. *Acta Chir Scand* 1963; 125:1-7.
- Larsson B, Liden K, Sarby B: Irradiation of small structures through the intact skull. *Acta Radiol Ther Phys Biol* 1974; 13:512-534.
- Kjellberg RN, Shintani A, Frantz AG, Kliman B: Proton-beam therapy in acromegaly. *New Eng J Med* 1968; 309:689-695.
- Kliman B, Kjellberg RN, Swisher B, Butler W: Proton beam therapy of acromegaly: a 20-year experience. *Prog Endocr Res Ther* 1984; 1:191-211.
- Suit HD, Goitein M, Tepper J, Koehler AM, Schmidt RA, Schneider R: Exploratory study of proton radiation therapy using large field techniques and fractionated dose schedules. *Cancer* 1975; 35:1646-1657.
- Suit HD, Goitein M, Munzenrider JE, Verhey L, Gragoudas E, Koehler AM, Urano M, Shipley WU, Linggood RM, Friedberg C, Wagner M: Clinical experience with proton beam radiation therapy. *J Canad Assoc Radiol* 1980; 31:35-39.
- Suit HD, Goitein M, Munzenrider J, Verhey L, Davis KR, Koehler AM, Linggood RM, Ojemann RG: Definitive radiation therapy for chordoma and chondrosarcoma of base of skull and cervical spine. *J Neurosurg* 1982; 56:377-385.
- Ambrosimov NK, Vorobev AA, Zherbin EA, Konnov BA: Proton therapy at the cyclotron at Gatchina, USSR. *Proc Acad Sci USSR* 1985; 5:84-91.
- Tsunemoto H, Morita S, Ishikawa T, Furukawa S, Kawachi K, Kanai T, Ohara H, Kitagawa T, Inada T: Proton therapy in Japan. *Radiat Res* 1985; 8(Suppl):S235-S243.
- Blattman H (ed): Proton therapy of choroidal melanomas (OPTIS). *Swiss Institute for Nuclear Research Medical Newsletter* 1986; 8:32.
- Proton Therapy Co-operative Group (PTCOG): World-wide charged particle patient totals. *Particles* (PTCOG newsletter) June, 1989; #4:6.
- Gragoudas ES, Seddon J, Goitein M, Verhey L, Munzenrider J, Urie M, Suit HD, Elitzer P, Koehler AM: Current results of proton beam irradiation of uveal melanomas. *Ophthalmol* 1985; 92:294-291.
- Saunders WM, Char DH, Quivey JM, Castro JR, Chen GTY, Collier JM, Cartigny A, Blakely EA, Lyman JT, Zink SR, Tobias CA: Precision, high dose radiotherapy: helium ion treatment of uveal melanoma. *Int J Radiat Oncol Biol Phys* 1985; 11:227-233.
- Minakova EI, Kirpatovskaia LE, Liass FM, Snigireva RIA, Krymskil VA: Proton therapy of pituitary adenomas. *Med Radiol (Mosk)* 1983; 28:7-14.
- Saunders WM, Chen GTY, Austin-Seymour M, Castro JR, Collier M, Gauger G, Gutin P, Phillips TL, Pitluck S, Walton RE, Zink, SR: Precision, high dose radiotherapy: II. Helium ion treatment of tumors adjacent to critical central nervous system structures. *Int J Radiat Oncol Biol Phys* 1985; 11:1339-1347.
- Stein BM, Mohr JP: Proton therapy for arteriovenous malformations of the brain. *New Eng J Med* 1984; 310:656-657.

HIMAC PROJECT AT NIRS-JAPAN

Y. Hirao, H. Ogawa, S. Yamada, Y. Sato, T. Yamada, K. Sato, A. Itano, M. Kanazawa, K. Noda, K. Kawachi, M. Endo, T. Kanai, T. Kohno, M. Sudou, S. Minohara, A. Kitagawa, F. Soga\*, S. Watanabe\*, E. Takada\*\*, K. Endo\*\*\*, M. Kumada\*\*\*, and T. Matsumoto\*\*\*\*  
 National Institute of Radiological Sciences  
 4-9-1, Anagawa, Chiba-shi, 260, Japan

A heavy ion synchrotron complex for medical use is being constructed at Chiba, Japan. General feature and present status of this project are described.

Introduction

An original idea of the HIMAC (Heavy Ion Medical Accelerator in Chiba) Project was proposed at the High LET Radiotherapy Division in the US-Japan Cooperative Cancer Research Program in 1979 at Kyoto, Japan. In 1983, the Japanese government decided to promote the 10 year strategy for cancer initiative. The HIMAC Project has also been proceeding along it, towards the end of the program. It was approved in 1987 and is expected to complete and to start the first clinical trial in 1993.

The superiority of heavy ion therapy has been demonstrated through radiological experiments and clinical trials at Lawrence Berkeley Laboratory so far. Based on their results of heavy ion therapy and of neutron and proton therapies at NIRS, the HIMAC project has been proposed in years.

In the proposed facility, the maximum output energy should be 800MeV/u for silicon ions in order to realize a residual range of 30cm in human body. Such a high energy beam is also effective to produce radioactive beam of high quality for diagnosis and/or treatment. The area of beam irradiation must be enlarged to cover homogeneously whole area to be treated. The maximum diameter of the irradiation field is chosen at 22cm. Beam intensity should be sufficient to give a dose of 5Gy into the irradiation field within an allowed time duration of several to a few tens of seconds. For therapeutic purpose, vertical beam is indispensable requirement. The main parameters of the accelerator complex are listed in Table 1.

Table 1  
 HIMAC parameters

Ion source	Type	PIG & ECR from <sup>4</sup> He to <sup>48</sup> Ar q/A
Injector	Frequency Repetition rate Duty factor Acceptance	100 MHz 3 Hz Max. 0.3% Max. 0.6 π mm·mrad (normalized)
RFQ linac	Input/Output energy Vane length Cavity diameter Surface field Peak rf power	8 / 800 keV/u 7.3 m 0.6 m 205 kV/cm (1.8 Kilpatrick) 260 kW (70% Q)
Alvarez linac	Input/Output energy Total length Cavity diameter Average field Shunt impedance Surface field Peak rf power Focusing sequence	0.8 / 6.0 MeV/u 24 m (3 rf cavities) 2.20/2.18/2.16 m 1.8/2.2/2.2 MV/m 34 - 47 MΩ/m (effective) 150 kV/cm (1.3 Kilpatrick) 770/820/760 kW FODO (6.8 kC/cm Max.)
Synchrotron (for one ring)	Output energy Average diameter Focusing sequence Betatron tunes (H/V) No. of dipole magnet Dipole field No. of Q magnets Quadrupole field Long straight sect. Repetition rate Rise/flat-top time	100 - 800 MeV/u (q/A = 1/2) 41 m (12 cells, 6 s-periods) FODO 3.75 / 3.25 12 (3.4 m each) 0.11 (Min.) / 1.5 (Max.) T 24 (0.4 m each) 0.51 (Min.) / 7.6 (Max.) T/m 12 (5.0 m each) 1/2 Hz 0.7 / 0.5 s
Acceleration system	No. of cavities Frequency range Acceleration voltage RF power input	1 (one more is foreseen) 1.0 - 7.9 MHz (harmonic 4) 11 kV peak at 1 MHz 30 kW peak at 6 MHz
Vacuum system	Material of chamber Baking temperature Average pressure Pumps	SUS-316 L (0.3 mm thick) 200 °C 1 × 10 <sup>-9</sup> torr Sputter ion pumps Ti getter pumps Turbo molecular pumps
Extraction system	Type Length of spill	Fast & slow (1/3 resonance) up to 400 ns (slow)

Ion Source

Two types of ion sources are prepared for the injector system: a PIG and an ECR sources. The PIG source is used mainly for lighter ions, whereas the ECR source is expected to improve heavier ion capabilities of HIMAC. The ion source system is to cover at least from He to Ar. The injection energy to the linac is 8keV/u, and is realized by putting the sources on the high voltage platforms of maximum 60kV.

The PIG source is of a hot cathode type. The pulse operation of the system is expected to be effective for increasing both intensity and lifetime. The preliminary results show that the extracted beam intensities exceed the required values except for Si.

The plasma chamber of the ECR source is fed with a microwave source of 10GHz, 2.5kW. Two solenoids with return yokes generate axial magnetic field, whereas radial sextupole field is produced with NdFe permanent magnet installed outside the vacuum chamber.

Injector Linac

The injector system is composed of an RFQ and an Alvarez linacs, as shown in Fig.1. The output energies of the linacs are 0.8 and 6MeV/u, respectively. The injector is designed to accelerate heavy ions with a charge to mass ratio of higher than 1/7. The maximum repetition rate and duty factor are 3Hz and 0.3%, respectively.

The structure of the RFQ linac is of four vane type with single loop rf coupler. The total length of the vanes and the cavity diameter are about 7 and 0.6m, respectively. The entire cavity including the vanes themselves is divided into four sections. The peak rf power of ~300 kW, 100MHz is fed to the cavity through the single loop coupler. The maximum surface field on the vane top is ~200kV/cm (1.8 Kilpatrick).

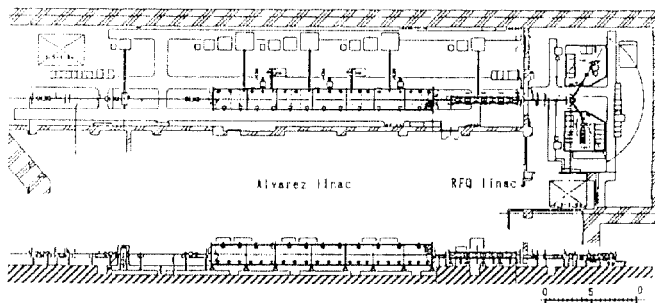


Fig.1. Layout of injector linac system including ion sources.

The operation frequency of the Alvarez linac is 100MHz as same as of the RFQ linac. A pulsed quadrupole magnet is equipped in every second drift tube, and a FODO type focusing sequence of quadrupole lenses is adopted. A transverse acceptance is 2.8π mm·mrad (normalized) with the highest field gradient of 6kG/cm and large enough to accept the output beam of 0.8π mm·mrad (normalized) from the RFQ. The peak rf power is estimated to be about 3.0MW in total. A diameter and a length of the linac cavity are about 2 and 24m, respectively. The cavity is separated into three sections and

Guest scientists: \* from INS, Univ. Tokyo, \*\* Fac. Sci. Univ. Tokyo, \*\*\* KEK, \*\*\*\* Dokkyou Univ. Med. School

rf power of about 1MW is fed to each of them through a loop coupler. The average axial fields of the sections are 1.8, 2.2 and 2.2MV/m, respectively. Following the Alvarez linacs, an equipment of charge exchange with a  $100\mu\text{g}/\text{cm}^2$  thick carbon foil is installed. Manufacturing of all parts of the injector system including the ion sources is proceeding as in the Fig.2, which shows the third section of the Alvarez.

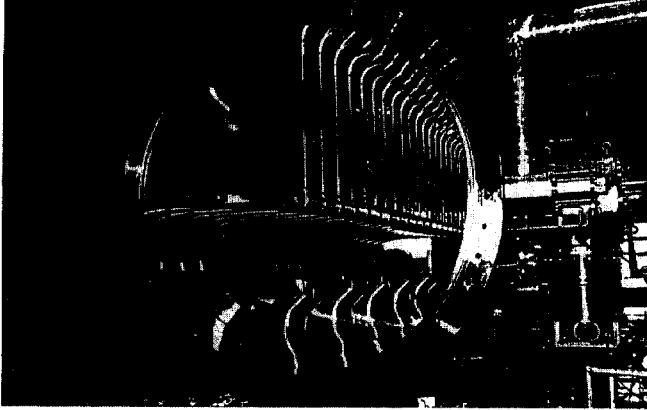


Fig.2. Inside view of the third section of Alvarez linac, seen from low-energy side.

### Synchrotron

The synchrotron consists of two rings, which are installed in the upper and lower floors and are operated independently of each other except the alternate injection and excitation. The output energy of each ring must be variable in a wide range from 100 to 800MeV/u. The two ring structure of the synchrotron is expected to make the operation mode much more flexible. The synchrotron can provide horizontal and vertical beams simultaneously at different energies for the two beam treatment or for two different treatments. In the future extension, two stage acceleration of the heavier ions will be possible. It will be also feasible that one of the rings is used as a storage ring, aiming at the treatment and diagnosis with radioactive beams and/or a single shot beam.

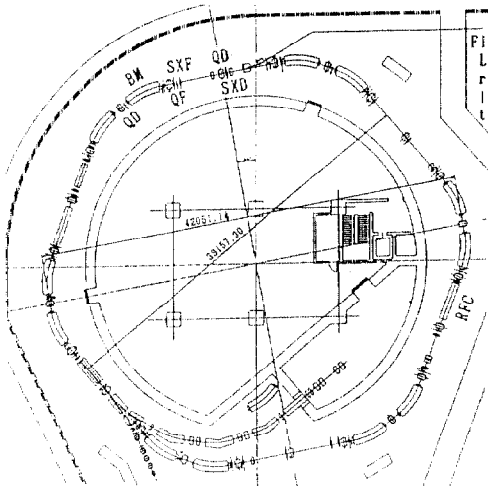


Fig.3. Layout of the upper ring of synchrotron, lower one is almost the same.

The layout of the upper ring is shown in Fig.3. The rings are of a separated function type with a standard FODO focusing sequence. An average diameter of the rings is about 41m. The maximum magnetic rigidity is 9.75Tm. The bending magnets are of sector type and have the maximum field of 1.5T. The quadrupole magnets have the maximum field gradient of 7.4T/m. The closed orbit distortion and the chromaticity are dynamically corrected with a set of steering magnets and with a set of

sextupole magnets, respectively. A multiturn beam injection scheme is adopted to increase the beam current by ten times. The horizontal and vertical acceptances of the rings are  $30\pi$  and  $3\pi$  mm·mrad in normalized values, respectively.

Two kinds of extraction modes, fast and slow extraction, are prepared for the upper ring, while only slow one for the lower ring. The extraction septum magnets for both modes are installed in the same long straight section in the upper ring. The slowly extracted beam is directed to the outside of the rings, whereas the pulsed beam is extracted to the inside. The slow extraction scheme uses a third order resonance. Beam spill time is to be longer than 400ms at 600MeV/u.

For each of two rings, a current source for the bending magnets of the maximum current of 2100A is composed of four sets of high power thyristor rectifier blocks working in 24 phases followed by a filter circuit. Two 24-phase thyristor current sources of the maximum current of 1600A are prepared for focusing and defocusing quadrupole magnets. The reactive power is dynamically compensated by 12-pulse thyristor controlled reactor (TCR) equipped parallel with a set of capacitors. These sources and TCR are controlled digitally by a computer. A feed-forward loop by the use of the computer will realize precise tracking of the current pattern. The repetition rate of pulse operation of them is varied in a range of 0.3-1.5Hz depending on extraction energies of the two rings. In a proposed current waveform, at 0.5Hz, a rising time and flat top time are 0.7 and 0.5s, respectively. The maximum value of the time derivative of the bending field is about 2T/s.

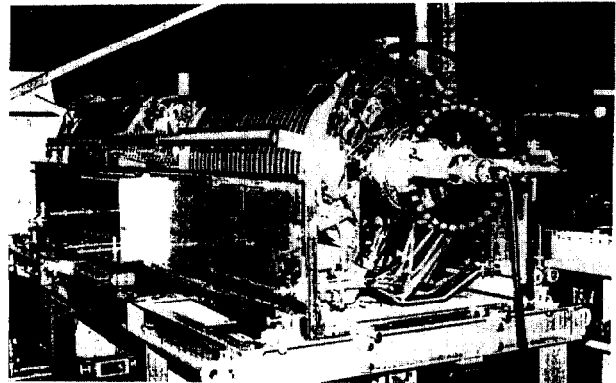


Fig.4. Rf acceleration cavity with a pair of  $\lambda/4$  resonators. Upper and side covers are removed.

The rf acceleration system has to have a wide frequency range from 1.0 to 7.8MHz, where a harmonic number of 4 is chosen. The cavity, installed in each ring, consists of a pair of ferrite loaded  $\lambda/4$  resonators as shown in Fig.4 and generates an acceleration voltage of 11kV. The cavity is powered by a single tetrode of the final rf power amplifier.

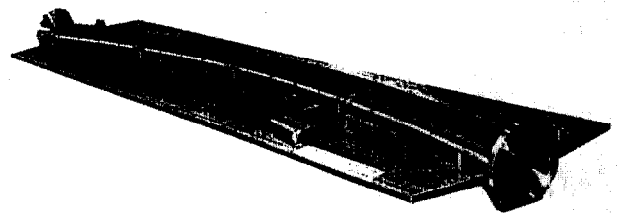


Fig.5. One section of vacuum chamber installed inside the bending magnets, made of 0.3mm thick SUS-316L reinforced by ribs.

The maximum rf output power is 30kW. The system is operated with feed-back loops in order to lock the rf frequency in the circulating beam bunches and to position the beam correctly, respectively.

An average vacuum pressure of an order of  $10^{-9}$  Torr is necessary to accelerate fully stripped ions with a negligible amount of beam loss. A combination of sputter ion pumps, titanium getter pumps and turbo-molecular pumps is chosen to realize such a pressure. All the vacuum chambers of the rings are bakable up to  $200^{\circ}\text{C}$ . The chambers installed inside the bending magnets are made of SUS-316L of 0.3mm thick reinforced by ribs to suppress the unwanted effects of eddy current due to varying magnetic field, as shown in Fig.5.

#### Beam Delivery System

The total layout of the beam delivery system is shown in Fig.6. The system consists of the vertical beam line which guides the beams up to  $600\text{MeV/u}$  from the upper synchrotron ring and the horizontal beam line which guides the beams up to  $800\text{MeV/u}$  from the lower one. A junction beam line is prepared to guide the horizontal beams into the vertical beam line. Two vertical treatment courses one of which reaches to the same isocenter of one of the horizontal one and biological irradiation course are prepared in the vertical beam line. The horizontal beam line has two horizontal treatment courses and two experimental rooms, one for physics and general, and another for secondary beam experiments. To get an efficient usage of treatment courses, it is necessary to switch beams rapidly from one course to the other within 5 minutes, keeping the reproducibility of the beam position within  $\pm 2.5\text{mm}$  at the isocenter.

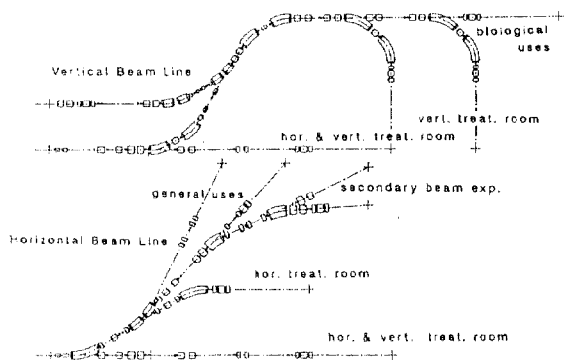


Fig.6. Total layout of horizontal and vertical beam delivery system.

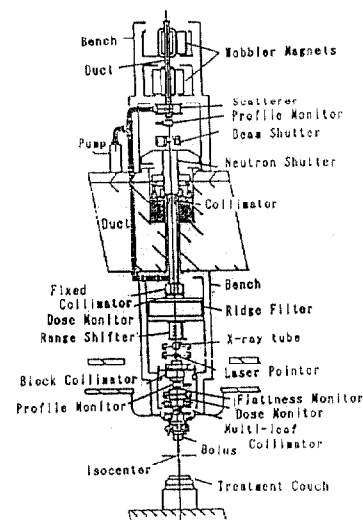
Concerning the secondary beam courses for the development of diagnostic and therapeutic applications of radioactive beams, the momentum spread of ions is expected to be  $\pm 0.2\%$  with analyzing magnets and a wedge degrader. The vertical beam line is also usable for the therapeutic applications of radioactive beams. The produced radioactive beams are transported to a vertical treatment course, and the precise stopping point of the beams in a patient's body is measured, and then, the treatment is carried out by stable ion beams having the same range as the radioactive beams.

#### Treatment devices

The medical requirement on the beam has a considerably unique feature, such as a broad and uniform beam, and specially modulated range distribution. To meet the required specifications, each treatment course comprises a scatterer, a pair of scanning magnets, a range shifter, a ridge filter, a multileaf collimator and several beam monitoring devices, as shown in Fig.7.

In case of heavy ion treatment, it is very important to set up a patient with regard to the delivered beam center and beam shape. The patient positioning system consists of a laser pointer, a digital X-ray TV, an X-ray CT, a treatment couch, a compensator holder and

Fig.7. Typical set of treatment devices, in the vertical beam course.



patient immobilization aids. The treatment couch is automatically controlled by the patient positioning computer linked to image verification devices.

The treatment planning is supported by a computer which has a compatible software with the patient's position image data. The main activity of the treatment planning system is the simulation of iso-effect dose distribution for heavy ion treatment, which takes into account inhomogeneous electron density and biological response factors in the body.

These treatment facilities are necessary to meet the specification of three dimensionally conformed (3D) irradiation, in order to prove that heavy ion therapy could be markedly better than the best use of other radiation therapies.

#### Building

The height of the building of HIMAC facility reaches to about 30m because of the necessity of vertical beam. Considering such a height and radiation shielding, more than half of the building is constructed under the ground level.

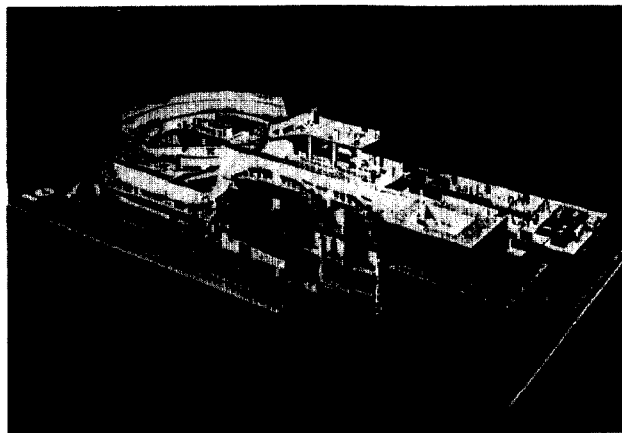


Fig.8. 1/100 scaled model of the total facility.

#### Acknowledgment

The authors have cooperated with many accelerator staffs of various laboratories as well as of NIRS, and also of industrial companies. The authors would express sincere thanks to the physicists, engineers and radiotherapists of domestic and foreign laboratories, especially of LBL, GSI and LNS, for their very helpful suggestions and valuable informations.

## PROGRESS OF THE FEASIBILITY STUDIES OF THE EUROPEAN LIGHT ION MEDICAL ACCELERATOR

P. Mandrillon, C. Carli, G. Cesari, F. Farley, N. Fietier, R. Ostojic, C. Roher  
EULIMA Feasibility Study Group, PS Division, CERN  
1211 Geneve 23, Switzerland

R. Dubois, P. Lefevre,  
CERN, 1211 Geneve 23, Switzerland

**Abstract:** A status report on the feasibility studies for the EULIMA medical accelerator project is given. Recent advances in the assessment of the various basic accelerator types for the facility are presented in terms of their advantages for heavy ion beam acceleration. Details of the technical studies of various critical subsystems for the superconducting separated sector cyclotron concept are also presented.

### Introduction

The main objectives of the European Light Ion Medical Accelerator (EULIMA) have been defined recently in terms of biomedical and technical issues in a series of expert meetings [1]. In order to take advantage of the biological and ballistic properties of high energy light ion beams for radiotherapy, the European Commission is in favour of implantation in Europe of a prototype accelerator, EULIMA, for carbon, oxygen and neon beams of energy up to 400 MeV/nucleon. The facility is expected to treat 1000 patients per year with beams that are to be delivered both horizontally and vertically. The beam intensity should be compatible with a three dimensional scanning beam delivery system. A supplementary radiation area should be available for research and development of new treatment methods, including diagnostics and treatment with radioactive beams of positron emitters such as  $^{10}\text{C}$ ,  $^{11}\text{C}$ ,  $^{15}\text{O}$  and  $^{19}\text{Ne}$ . The accelerator should be cost-effective, of compact size and highly reliable, as its pilot role should enable an assessment of the clinical value of the light-ion therapy and the need for similar installations elsewhere.

The feasibility study of the facility is being carried out by the EULIMA feasibility study group hosted by CERN. The study has concentrated on several important issues concerning the basic conceptual design of the accelerator and its specific facilities. A detailed analysis of the beam delivery system, including a design of the beam energy degrader (with implications on accelerator operation) has been done, and is reported elsewhere at this Conference [2]. Following the initial concept of a superconducting separated sector cyclotron as the accelerator for EULIMA, several issues pertaining to the RF design have been clarified [3].

In this report, we present the advances of the conceptual studies of the accelerator system, and discuss several features of the separated sector and box-type superconducting cyclotrons and of a conventional synchrotron, as the basic accelerator options. Several technical details of the separated sector superconducting cyclotron mechanical design and extraction system are also reported.

### Accelerator Conceptual Studies

#### Superconducting Cyclotrons

Previously, we have reported the basic features of the EULIMA accelerator based on the separated sector superconducting cyclotron [4]. The basic approach was that a machine with a bending constant of about 2000 MeV, needed to obtain the required 400-450 MeV/n  $^{12}\text{C}^{6+}$  or  $^{16}\text{O}^{8+}$  beam, could be built on the basis of a four-fold symmetric magnet excited by a single cylindrical superconducting coil, contributing as much as 50% of the necessary average magnetic field of about 3 T. This approach implies certain simplicity of the mechanical design, since the machine is of the open type, freely accessible in the valleys, and with a single cryostat. The beam is injected axially from an ECR ion source and accelerated in two RF cavities located in the valleys. The layout of the machine is shown in Fig. 1 and its operating parameters are summarized in Table 1 (SSC1).

As an alternative to the basic separated sector design aiming at the extracted beam energy of 430 MeV/n, a scaled down version, with the final energy of 340 MeV/n was also considered. Since the range of light ions scales as  $z^2/A$ , this design has the carbon beam in mind as the workhorse of the therapy programme as opposed to the oxygen beam in the basic design. The resulting design, with the basic parameters given also in Table 1 (SSC2), has hence been termed "carbon" machine, and obviously has smaller overall dimensions.

Further development of these solutions was primarily concentrated on the analysis of single particle dynamics in a highly spiraled magnetic field generated by the sectors, and in particular on the influence of magnet tolerances on the working diagram of the machine. Details of these studies are presented in ref [5]. Here, we note that the sector entrance angle and angular width as function of radius were precisely determined, as well as the dimensions of the main superconducting coil. The conductor cross-section was chosen, and the principles of the cryostat design laid out. The concept of trimming coils winding on the sector surface was considered, and their operation as harmonic coils conceived. As a consequence, the configuration of the extraction system could be studied and the mechanical properties of the structure analyzed. The results of these studies are presented below.

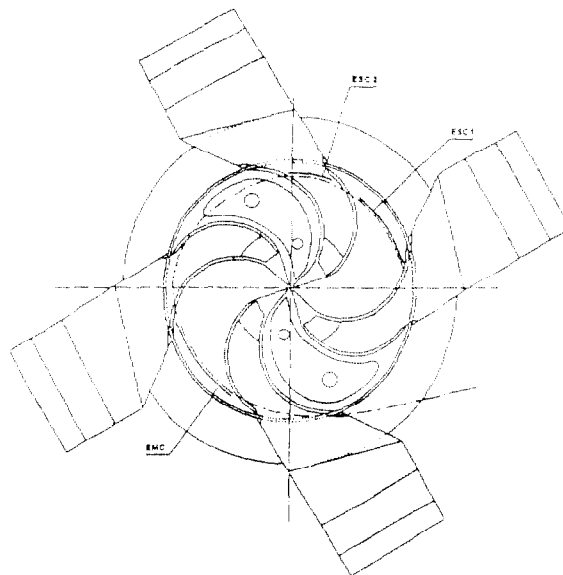


Fig. 1 Lay-out of the separated sector superconducting cyclotron for EULIMA

In the realm of superconducting cyclotrons, it was natural to compare the separated sector machine to a more classical design with a completely closed yoke. Several of these machines (MSU, Calk River, Milan, AGOR) have been completed, and their construction and operational experience is of great value for all similar projects. A four sector, four dee-in-valley design was analyzed, and its basic parameters (BSC) given in Table 1. The advantage of this approach is basically a slightly more compact design producing lower fringing fields in the

vicinity of the machine. However, due to the closed valleys, a very high spiral has to be applied, limiting the RF frequency. Consequently, the apparent machine compactness has to be paid for by a four dee system, substantially reducing the space in the machine interior. Furthermore, a split coil (or a two coil) excitation (also originating from the box-type yoke), complicates the design of the cryostat. These properties of the box-type solution persist in the case of the carbon machine.

Table 1 Main Parameters of the SC Solutions for EULIMA

	SSC1	SSC2	BSC
Particle frequency (MHz)	17.4	18.0	20.5
Energy of z/A=0.5 beam (MeV/n)	430	340	440
Number of magnet sectors	4	4	4
Sector angular width (deg)	35	35	40
Average sector spiral (deg/m)	35	35	50
Coil internal radius (m)	2.31	2.12	1.90
Coil external radius (m)	2.61	2.42	2.05
Coil current density (A/cm <sup>2</sup> )	2850	2500	3440
Number of RF cavities	2	2	4
RF frequency (MHz)	69.6	72.0	82.0
RF harmonic number	4	4	4
RF peak voltage	200	200	100

Synchrotron

Following similar ideas of other light-ion radiotherapy facilities, we have also considered a synchrotron solution for EULIMA. The natural advantage of a synchrotron is its easy energy variations covering, in our case, the interval from as low as 100 MeV/n, for superficial treatments, to 450 MeV/n, corresponding to the magnetic rigidity of 6.8 Tm. This interval is very similar to LEAR at CERN, and several technical concepts that have been installed in this machine could be exploited. The circumference of the EULIMA synchrotron is estimated at about 60 m (cf Fig. 2), and the machine could be designed in a form of a ring or a racetrack, depending on the site conditions and the design of insertion devices. Eight bending magnets of  $B_{max}=1.2$  T and  $\dot{B}_{max}=2.5$  T/s with 16 quadrupoles with  $G=10$  T/m seem to be quite adequate for the lattice arrangement. The accelerating section will consist of one (or, eventually two) 10 kV ferrite loaded RF cavities. The vacuum is conceived to be reasonably low,  $10^{-9}$  Torr, requiring UHV techniques but no in situ baking out seems necessary.

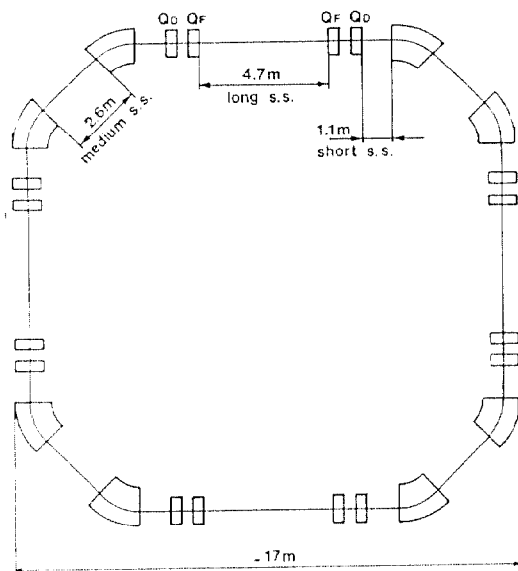


Fig. 2 An arrangement of EULIMA synchrotron lattice

A classical injection scheme has been considered, with a ECR ion source feeding the RFQ (or alternatively, a linac) with a repetition rate of 1 Hz, giving a total  $10^{14}$  pps in a useful pulse of 100  $\mu$ s at the exit. The extraction time in the range of 10 ms to few minutes (average spill length of 400 ms), gives, for example, ten slices of ten pulses each (and a mean dose per pulse of  $10^9$ ), with possible adjustment of individual slice energy, supplying a total dose of  $10^{11}$ .

This basic design could be refined to include better monitoring of the extracted beam, and beam storage and cooling facility with a higher repetition rate injector. Hence, modulation of the beam intensity and programming of dose across the irradiation volume, as well as storage of radioactive beams could become possible.

The Mechanical Studies

One of the important issues of the EULIMA superconducting cyclotron feasibility study is the achievement of the mechanical stability of the magnet structure, as it should serve as a mechanical support for the vacuum chamber, the RF cavities and the extraction devices. To achieve the necessary stability, and having in mind that the machine should be installed in a hospital-based facility, we have chosen the solution of a passive structure as it is more appropriate for this kind of environment.

Taking into account the magnet symmetries, a model which covers only one eighth of the machine has been defined as shown in Fig. 3. Since the magnetic force, which is estimated on the basis of the TOSCA model of the magnet to be 7.8 MN, is much greater than the atmospheric pressure, for the purpose of an easier description of the ANSYS model, the cover of the vacuum chamber, which is conceived as a large cylinder covered by a disk that traverses the poles, has been suppressed in the valleys. The finite element model uses 3-D 20-node isoparametric solid with 3 degrees of freedom per node ( $u_x, u_y, u_z$ ), and contains 1266 elements and around 7000 nodes. The model supposes that the magnet sectors are built as single massive pieces, which is certainly not a realistic assumption. However, since the horizontal yoke contributes most to the rigidity of the magnetic circuit, the model should be fairly correct in determining the behavior of the structure. Several calculations have been made on the basis of various boundary conditions. The main results of the calculations for the <sup>16</sup>O (SSC1) and <sup>12</sup>C (SSC2) machines are summarized in Table 2.

The deflections which occur in these stand-alone structures during energizing of the magnet lead to a reduction of the total accelerating gap of about 10 % (5 mm) in the central region of both machines. These displacements are large and may influence the stability of the cyclotron operating parameters. However, due to large magnetic forces and inevitable manufacturing errors of parallelism and adjustment, it will be very difficult to reduce the deflection of the poles below 1-1.5 mm. Hence, if this proves necessary, the pole face displacement during magnet energizing will be compensated by magnet shims, to be fabricated after initial magnetic field measurements.

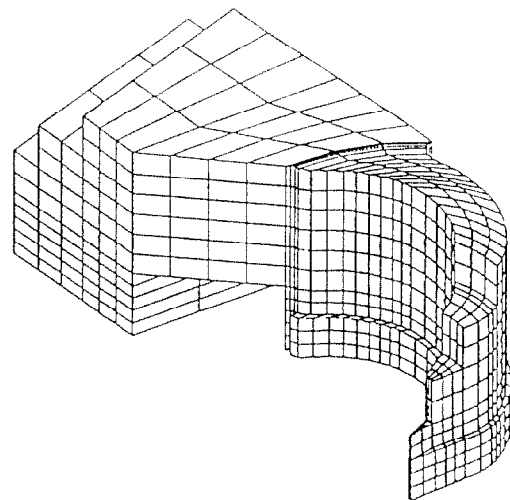


Fig.3 Finite element model of the EULIMA magnet



Table 2 Comparison of the mechanical structures of the superconducting separated cyclotron designs

	SSC1	SSC2
Outer dimension (m)	9.2	8.5
Pole radius (m)	2.1	1.9
Soft iron total mass (tons)	680	570
Magnetic force per pole (MN)	7.90	7.00
Vacuum chamber reaction (MN)	7.10	6.70
Max. deflection (mm)	-2.9	-2.3
Ave. Von Mises stress ( $\text{kg/mm}^2$ )	1.2	1.2
Max. Von Mises stress ( $\text{kg/mm}^2$ )	18	21

A very important point concerning the mechanical design is that the behavior of the magnet must be reproducible in order to recover properly the operating conditions of the machine. However, as seen from Table 2, a stress concentration occurring near the contact between the horizontal yoke and the vacuum chamber cylinder reaches the Von Mises equivalent stress value greater than  $18 \text{ kg/mm}^2$ , which is unacceptably high for soft iron and stainless steel. This stress concentration should be eliminated from the structure. As a consequence, a thick iron disk has been added on top of the magnet in order to reduce the torsion effect due to the spiral shape of the pole. This solution reduces the displacements to 1.7 mm, but since the torsion due to pole spiral is compensated only in the region close to the machine axis, the stress concentration around the contact between the horizontal yoke and the vacuum chamber cylinder still persists. Further reduction of the stress concentration from the structure will be attempted by designing a horizontal yoke with a spiral shape slightly different from that of the pole.

#### Beam extraction studies

The beam extraction system has been studied for both separated sector cyclotron designs. A preliminary layout, consisting of two electrostatic deflectors and one electromagnetic channel, as shown in Fig. 1, was studied and its main parameters listed in Table 3.

The design constraints for the hill and valley deflectors are quite different, and two types of deflectors are envisaged. As the clearance under the hill is narrow (50 mm), several technical details of this deflector need to be optimized. In particular, the shape of the cathode, design of the septum and of a reliable HV connection and supporting system have been considered. The gap between the septum and the cathode (5 mm) is dictated by optical requirements, while the length of the housing (70 mm) is given by the distance between the deflector and the vacuum chamber.

Tests with similar deflectors [6] have shown that a reduction of the deflector performances may be expected due to the modifications induced in the discharge mechanism by the presence of the magnetic field. Since a maximum electric field of 150 kV/cm for the valley deflector and 100 kV/cm for the hill deflector is required, maximum voltages of 75 kV and 50 kV, respectively, are implied for a 5 mm wide gap between the two electrodes. These figures are not too large in comparison with the known high voltage capabilities of the electrodes, but they are likely to be difficult to achieve in a machine with small clearances and a very high axial magnetic field. In order to minimize the electric field on the HV electrode, the effects of different geometries are under investigation.

In order to minimize extraction losses, the electrostatic septum must be as thin as possible. For this reason it has been proposed to construct the first septum of the valley deflector as a curtain of wires or strips. Each wire (or strip) is stretched by a spring, which retracts should the wire break. The technology for the wire septum is well known and it could be made very thin. In its construction the usually materials will be employed. However, in order to avoid outgassing, we propose to use ceramic cables for HV connections instead of the usual polyethylene.

Table 3 Main Extraction Parameters for the SSC1 and SSC2 Machines

	SSC1	SSC2
Extraction energy (MeV/n)	427.5	339.0
Extraction radius (m)	2.006	1.811
Emittance ( $\pi \text{ mm mrad}$ )	0.14	0.16
<u>Electrostatic deflector 1</u>		
Position: valley (deg)	0	0
Length (deg)	45	40
Electric field (kV/cm)	150	150
Gap (mm)	5	5
Orbit separation		
entrance (mm)	-	-
exit (mm)	11	10
<u>Electrostatic deflector 2</u>		
Position: Hill (deg)	54	50
Length (deg)	35	35
Electric field (kV/cm)	100	100
Gap (mm)	5	5
Orbit separation		
entrance (mm)	15	14
exit (mm)	56	42
<u>Electromagnetic deflector</u>		
Position: Valley (deg)	-	180
Length (deg)	-	45
Orbit separation		
entrance (mm)	-	30
exit (mm)	-	52
Magnetic field (T)	-	0.35

#### Conclusions

The feasibility study of the EULIMA accelerator performed in the past two years concentrated on several important issues of biomedical and physical basis of the project. It has been shown that a superconducting separated sector cyclotron, while fulfilling the basic requirements for the reference oxygen beam energy of 400 MeV/n and extracted beam intensity of  $10^{12}$  pps, can lead to a compact, cost-effective and overall technically feasible design. Nevertheless, other technical solutions have been considered and their relative merits evaluated.

#### References

- [1] Proc. EULIMA Workshop on the Potential Value of Light Ion Beam Therapy, (Centre Antoine Lacassagne, Nice, Nov. 1988), EUR-12165 EN
- [2] F. Farley and C. Carli, Beam Delivery System for EULIMA, Proc. EPAC, (Nice, June 1990)
- [3] N. Fietier and C. Bieth, Model Measurements and Preliminary Design of the RF Cavities for the EULIMA Cyclotron, Proc. EPAC, (Nice, June 1990)
- [4] P. Mandrillon et al., Proc. IEEE Part. Acc. Conference, Chicago, March 1989, in press, Proc. 12 Int. Conf. on Cyclotrons and their Applications, (Berlin, May 1989)
- [5] R. Ostojic and P. Mandrillon, On the Transverse Particle Stability in Highly Spiraled Magnetic Structures, NIM **A288**(1990)339-342; Proc. EPAC, (Nice, June 1990)
- [6] F. Brozzi, C. De Martinis, A. Ferrari, The Electrostatic Deflectors for the Milan Superconducting Cyclotron, Proc. 12th Int. Conf. on Cyclotron and their Applications, Berlin, May 1989)

## RADIOACTIVE ION BEAMS : RESULTS AND PERSPECTIVES FOR LIGHT ION THERAPY AND DIAGNOSTIC PURPOSES

G. Berger, M. Bouvy, Th. Daras, E. Kaerts, M. Loiselet, G. Ryckewaert

Université Catholique de Louvain, Centre de Recherches du Cyclotron ,  
Chemin du Cyclotron, 2,  
B-1348 Louvain-la-Neuve, Belgium

**Abstract :** An alternative method for the production of intense medium energy beams of radioactive isotopes has been developed by the Centre de Recherches du Cyclotron at Louvain-la-Neuve. Instead of using high velocity secondary beams coming out of a target bombarded by medium energy (up to 400 MeV/a.m.u.) ions, it uses an intense, low energy, light ion beam which is sent on a suitable target to selectively produce the desired isotopes. After extraction and purification, the gas going out of the target is ionized in a high efficiency source for subsequent acceleration to the required energy. The method has already been successfully applied for the production of  $^{13}\text{N}^{1+}$  beams. The simplicity and relatively low cost of such scheme allows the use of positron emitters like  $^{11}\text{C}$ ,  $^{13}\text{N}$ ,  $^{15}\text{O}$ ,  $^{18}\text{F}$  and  $^{19}\text{Ne}$  for eventual treatment of locally advanced tumours, as well as for the on-line diagnostic of the irradiated zone with a PET camera. The different production and acceleration schemes are reviewed and their implications in the EULIMA project are discussed.

### Introduction

The treatment of cancer with energetic light ions requires a precise localization of the Bragg peak in the tumour volume. Following the method developed at Lawrence Berkeley Laboratory, this can be verified by using a beam of radioactive positron emitting ions like  $^{19}\text{Ne}^{11}$ . In this case, the detection of the 511 keV annihilation gamma-rays by a positron emission tomography scanner (PET) allows a precise determination of the beam range<sup>[2]</sup>. Although these radioactive ions are only used for diagnostic purposes before the treatment with stable  $^{20}\text{Ne}$  ions, an irradiation with the same radioactive beam would avoid frequent beam changes and offers the possibility to check the range during the treatment. A possible way to produce high intensity radioactive beams, is to use the nuclear fragmentation of high energy nuclei after interaction with a target. This method has been analysed in detail by A. Bimbot<sup>[3]</sup>. In this paper, we discuss the possibilities to use an alternative method to accelerate radioactive ions and their implications in the EULIMA project.

### Production of high energy radioactive beams

The classical way to produce radioactive beams is to bombard a target with a high intensity ( $\sim 10^{11}$  pps) and high energy (400 MeV/u) beam. The fragmentation products are then separated from the primary stable beam and, after magnetic purification of the secondary beam coming out of the target, could be used for the treatment. This way, an  $^{15}\text{O}$  beam of  $2 \cdot 10^8$  pps is expected with a primary beam of  $10^{11}$  pps<sup>[3]</sup>.

The approach followed in Louvain-la-Neuve, uses two accelerators coupled by an on-line ion source. The first accelerator is a small industrial cyclotron which is used to produce a large amount of radioactive atoms by a suitable reaction. They are extracted from the target by a carrier gas and ionized by an Electron Cyclotron Resonance (ECR) source. A second cyclotron brings

these radioactive ions to the desired energy. With this scheme,  $1.5 \cdot 10^8$  atoms of  $^{13}\text{N}^{1+}$  have already been accelerated to 8.5 MeV<sup>[4,5]</sup>. The same method could be used in the EULIMA project, if an intensity of the order of  $10^7$  to  $10^8$  pps of fully stripped ions at 400 MeV/u can be obtained. With this intensity, the treatment dose ( $10^{10}$  atoms) would require an irradiation time of a few minutes.

### Ion choice and targetry problems

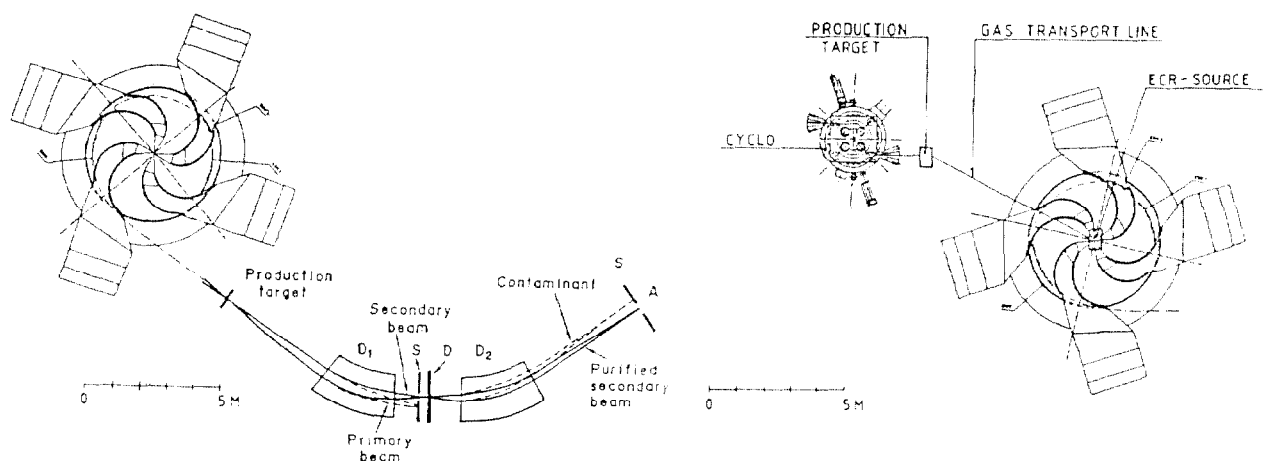
The suitable ions for light ion therapy are in the mass range between carbon and neon, so positron emitters like  $^{11}\text{C}$ ,  $^{13}\text{N}$ ,  $^{15}\text{O}$ ,  $^{18}\text{F}$ ,  $^{19}\text{Ne}$  could be used for the treatment. As shown in table 1, these elements can be produced by (p,n) or (d,n) reactions in dedicated targets, with a beam energy between 15 MeV and 30 MeV. These beams can be accelerated by compact cyclotrons up to 500  $\mu\text{A}$ <sup>[6]</sup>. The target must display the following properties : the ability to dissipate up to 15 kW of beam power, a high extraction efficiency for the release of the radioactive atoms produced inside the target material, a short term activity induced by the beam around the target and finally a low cost and a high reliability. A graphite target meets all these requirements for the production of  $^{13}\text{N}$ . It avoids problems of using high pressure nitrogen gas targets or enriched  $\text{H}_2^{18}\text{O}$  liquid targets, which are needed for the production of  $^{15}\text{O}$  and  $^{18}\text{F}$  respectively. Moreover, as the activity produced in the target has a short lifetime ( $< 1$  h), the activation problem of the target material is kept to a minimum. A compact shielding for the low energy neutrons produced by the reaction is sufficient around the target. With a natural graphite target,  $^{13}\text{N}$  can be produced by a (d,n) reaction with a production yield of  $0.96 \cdot 10^{-3}$   $^{13}\text{N}$  atoms per deuteron at 20 MeV, i.e. with 300  $\mu\text{A}$ ,  $1.8 \cdot 10^{12}$   $^{13}\text{N}$  atoms are produced in the target<sup>[7]</sup>. The yield for the (p,n) reaction on  $^{13}\text{C}$  is slightly higher ( $1.19 \cdot 10^{-3}$   $^{13}\text{N}$  atoms per proton at 20 MeV) but requires an enriched  $^{13}\text{C}$  graphite target like it is presently used in the Radioactive Ion Beam project (RIB) in Louvain-la-Neuve<sup>[8]</sup>.

Table 1 : Production of radioactive isotopes for light ion therapy with protons or deuterons [7] [11].

Isotope	Half-life	Reaction	Yield (20 MeV)	Target material
$^{11}\text{C}$	20 min	$^{11}\text{B}^*(\text{p},\text{n})^{11}\text{C}$	$\sim 2 \cdot 10^{-3}$	$\cdot \text{B}_2\text{O}_3$
		$^{14}\text{N}(\text{p},\alpha)^{11}\text{C}$	$\sim 1.8 \cdot 10^{-3}$	$\text{N}_2$
		$^{10}\text{B}^*(\text{d},\text{n})^{11}\text{C}$	$< 0.1 \cdot 10^{-3}$	$\text{B}_2\text{O}_3$
$^{13}\text{N}$	10 min	$^{13}\text{C}^*(\text{p},\text{n})^{13}\text{N}$	$1.19 \cdot 10^{-3}$	$^{13}\text{C}$
		$^{12}\text{C}(\text{d},\text{n})^{13}\text{N}$	$0.96 \cdot 10^{-3}$	C
$^{15}\text{O}$	2 min	$^{15}\text{N}^*(\text{p},\text{n})^{15}\text{O}$	$1.2 \cdot 10^{-3}$	$^{15}\text{N}_2$
		$^{14}\text{N}(\text{d},\text{n})^{15}\text{O}$	$< 0.1 \cdot 10^{-3}$	$^{14}\text{N}_2$
$^{18}\text{F}$	109 min	$^{18}\text{O}^*(\text{p},\text{n})^{18}\text{F}$	$2.4 \cdot 10^{-3}$	$\text{H}_2\text{O}^{18}$
		$^{20}\text{Ne}(\text{d},\alpha)^{18}\text{F}$	$1.1 \cdot 10^{-3}$	Ne
$^{19}\text{Ne}$	17 s	$^{19}\text{F}(\text{p},\text{n})^{19}\text{Ne}$	$0.7 \cdot 10^{-3}$	(LiF)

\*Enriched target

Figure : Schematic layout of the two possible schemes for the production of high energy radioactive beams. In the first one (left), the radioactive ions are produced at high energy by nuclear fragmentation, and the contaminants are eliminated by magnetic spectrometers and an energy degrader (drawing extracted from A. Bimbot ref. [3]). In the second one (right), the radioactive atoms are produced in a thick target and are accelerated after ionization in an on-line ECR source.



#### On-line ionization source

The  $^{13}\text{N}$  activity can be extracted from the graphite target as  $^{13}\text{N}$ - $^{14}\text{N}$  molecules by a small nitrogen gas flow ( $\sim 0.1 \text{ cm}^3$  per hour). An extraction efficiency of 50 % has already been achieved<sup>[8]</sup>. The molecules are sent to an on-line ECR source with a high ionization efficiency. The present ECR source used in Louvain-la-Neuve for the RIB project has achieved an ionization efficiency of 15 % for the  $1+$  charge state and 1 % for  $\text{N}^{4+}$ . It is a single stage ECR source working at 6 GHz and is designed to have its highest ionization efficiency for  $\text{N}^{1+}$ . Its performance has been described in detail elsewhere<sup>[9]</sup>. The stable and reliable operation of this type of source allows its use for a medical machine. In order to have a high ionization efficiency for  $\text{N}^{7+}$ , an ECR source working at 14 GHz or 16 GHz should be constructed. With the actual performance of these sources, an ionization efficiency in the order of  $5 \cdot 10^{-4}$  to  $1 \cdot 10^{-3}$  is expected for  $\text{N}^{7+}$ <sup>[10]</sup>. With these values, an intensity of  $5 \cdot 10^8$  to  $1 \cdot 10^9$  ions per second could be produced and transported for injection in the main accelerator. Lower charge states like  $^{13}\text{N}^{4+}$  could be injected in a preaccelerator and stripped to  $^{13}\text{N}^{7+}$  before injecting in the main machine, but a direct production of  $^{13}\text{N}^{7+}$  after the ECR source reduces the complexity without losing too much intensity.

#### Implication for the EULIMA project

Due to its low duty factor, a synchrotron is excluded for the acceleration of radioactive ions produced at low energy, unless a new device like an ions trap is used to store the ions before injection. However, owing to its 100 % duty factor, a cyclotron, like proposed in the EULIMA project, will accelerate these elements with high efficiency. Taking 10 % of acceleration efficiency, an intensity of  $5 \cdot 10^7$  to  $1 \cdot 10^8$  pps at 400 MeV per nucleon seems to be technically feasible. With these intensities, an irradiation of three minutes would be enough to give a treatment dose of  $10^{10}$  atoms (table 2).

Table 2 : Expected intensity of radioactive  $^{13}\text{N}$  at the different stages of the production process.

20 MeV deuteron	300 $\mu\text{A}$
Yield $\text{N}(^{13}\text{N})/\text{N}(\text{d})$	$0.96 \cdot 10^{-3}$
Extraction efficiency	50 %
Ionization efficiency $^{13}\text{N}^{7+}$	$0.5 \cdot 10^{-3} \dots 1 \cdot 10^{-3}$
Acceleration efficiency	10 %
Accelerated intensity	$5 \cdot 10^7 \dots 1 \cdot 10^8$ pps
Treatment time for $10^{10}$ particles	2 ... 3 min.

Finally this scheme can be compared with the intensities which are produced by the nuclear fragmentation scheme ( $2 \cdot 10^8$  pps for a primary beam of  $10^{11}$  pps) but it avoids the possible problems related to the activity produced around the fragmentation target. The schematic layout shown in the figure gives an idea of the relative sizes of both approaches. Shielding requirements in the case of a low energy production cyclotron are far less than in the case when nuclear fragmentation is used. Moreover, the very high intrinsic analysing power of a cyclotron like EULIMA will yield a pure beam without any contamination.

#### Conclusion

We have proposed an alternative scheme to accelerate radioactive ions. It requires a 20 MeV deuteron cyclotron to produce  $^{13}\text{N}$  in a natural graphite target, and a high efficiency ECR source to produce  $^{13}\text{N}^{7+}$ . Intensities of the order of  $5 \cdot 10^7$  to  $1 \cdot 10^8$  pps can be expected at the output of the EULIMA cyclotron. With such facility, the treatment of tumours, and the precise localization of the ions range, will be possible without any beam change.

## References

- [1] J.R. Castro *et al.*, "Heavy charged particle therapy at LBL" in Proceedings of the EULIMA Workshop, edited by P. Chauvel and A. Wambersie, 1988, pp. 219-232.
- [2] A. Chatterjee and J. Llacer, "Applications of radioactive beams in diagnostic studies" in Proceedings of The First International Conference on Radioactive Nuclear Beam, edited by W.D. Myers, J.M. Nitschke and E.B. Norman, World Scientific, 1990, pp. 403-413.
- [3] A. Bimbot, "Production of 400 MeV/u radioactive ion beams for therapy purposes" in Proceedings of the EULIMA Workshop, edited by P. Chauvel and A. Wambersie, 1988, pp. 443-468.
- [4] D. Darquennes *et al.*, "Radioactive Ion Beams at Louvain-la-Neuve : production, acceleration and uses" in Proceedings of The First International Conference on Radioactive Nuclear Beam, cfr. [2], pp. 3-12.
- [5] P. Decroock *et al.*, "Production of an intense  $^{13}\text{N}$  radioactive ion beam" in Proceedings of this conference.
- [6] J.L. Bol *et al.*, "Operational experience with 500  $\mu\text{A}$  H-isotope production cyclotron, CYCLONE 30", in Proceedings of the EPAC Conference, Rome 1988, edited by S. Tazzari, World Scientific, pp. 1488-1490.
- [7] Sindano Wa Kitwanga, "Production of  $^{13}\text{N}$  radioactive nuclei from  $^{13}\text{C}(p,n)$  or  $^{16}\text{O}(p,\alpha)$  reactions", Phys. Rev. C40, 1989, pp. 35 and Ph.D. thesis (unpublished).
- [8] M. Arnould *et al.*, "Target development for a radioactive ion beam", Nucl. Instr. Meth. A282 (1989) pp. 99-101.
- [9] P. Decroock *et al.*, "An electron cyclotron resonance ion source for efficient production of radioactive nuclear beams" in Proceedings of The First International Conference on Radioactive Nuclear Beam, see ref. [2], pp. 597-602 and Rev. Sci. Instrum. 67, 1990, pp. 279-281.
- [10] R. Geller *et al.*, "Upgrading of the multiply charged heavy ion source mini-mafios", Nucl. Instr. Meth. A243 (1986) pp. 244-254.
- [11] B.W. Wieland, R.R. Highfill, "Proton accelerator targets for the production of  $^{11}\text{C}$ ,  $^{13}\text{N}$ ,  $^{15}\text{O}$  and  $^{18}\text{F}$ ", IEEE NS-26, 1979, pp. 1713-1717.

**ROUND TABLE ON EULIMA**  
(Transcribed from a video recording)

Chairman : Dr Larson  
 Panel Members : J. Castro  
 P. Chauvel  
 F. Farley  
 P. Mandrillon  
 J.P. Meulders  
 G. Ryckewaert  
 A. Wambersie

A. WAMBERSIE

Fig 1 illustrates the need for high LET therapy combined with excellent physical selectivity [1].

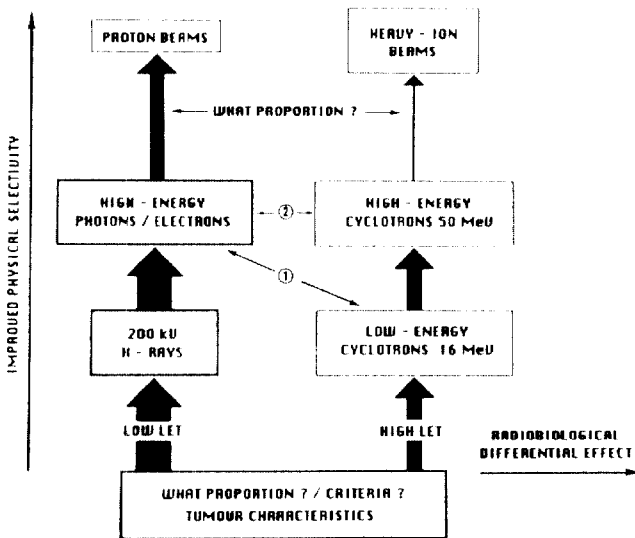


Fig 1 : Overview of radiation therapy

Improving physical selectivity is a benefit ; if one irradiates more of the tumour, and less of the surrounding tissue, there is obviously always a gain.

When we replaced 200 KeV X-rays by high energy photons, the number of locally controlled tumours was improved by a factor of 2-3 . We can go further in this direction with protons. The clinical results show that protons bring a benefit for some tumours, notably small tumours dose to critical structures. We can go further in this direction by treating the majority of patients with protons.

Next consider the biological evidence that replacing low LET radiation by high LET radiation brings an increase in the differential effect on the tumour relative to healthy tissue. The evidence is that this is beneficial in about 10 % of cases. This is a question of tumour response, low LET versus high LET, a separate factor from the physical selectivity.

Ideally we need to combine both effects, that is get the highest possible physical selectivity and also high LET. The light ions give good physical selectivity combined with high LET. As 10 % of patients can benefit from high LET, we can see how many would benefit from EULIMA.

[1] A. Wambersie in this proceedings.

P. MANDRILLON

The feasibility studies which are in progress will include four parts :

1- Accelerator : it is necessary to design a prototype accelerator capable of offering the necessary flexibility for an acceptable price. The aim of this study is to evaluate options based on a superconducting cyclotron or a synchrotron. [2]

2- Beam delivery system : two systems are feasible for delivering the dose in the tumour volume : either a raster scanning or a spot scanning (pixel scanning). The particularities of these systems are shortly described below by F. Farley.

3- A social economic study which aims at determining under which conditions EULIMA could catalyse a rapid increase of the technological level of cancer radiotherapy in Europe and for what kind of price per patient.

4- An experimental programme has been set up in order to establish the radiobiological properties (RBE-LET) of several light ions (Carbon, Oxygen and Neon) at various parts of the Bragg curve. These studies will be carried out by Dr G. Kraft at GSI. Additional experimental studies to reexamine some physical data, in particular fragmentation behind the Bragg peak, will be carried out using the LEAR machine at CERN.

[2] P. Mandrillon in this proceedings.

F. I.M. FARLEY : Beam delivery

We heard from Pedroni that the proton beam spreads to  $\pm 15$  mm at the end of the range. In contrast the ion beam is localized to about  $\pm 1.5$  mm laterally at the end of the range and 5 mm in depth. This allows the tumour volume to be treated precisely by scanning in three dimensions - see fig 1 - which shows a typical treatment plan. By adjusting the

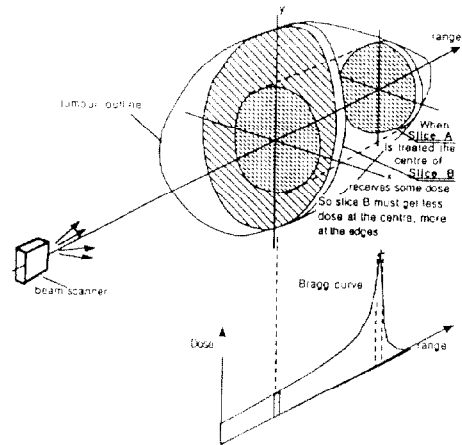


Fig 1 3D Conformal Therapy

range, the bragg curve is placed successively at various depths. Each depth slice is scanned over the tumour cross-section at that depth; note that when distal slice A is treated, the centre of central slice B will receive some dose. This must be compensated when slice B is treated, by giving more dose at the edges than at the centre. Therefore in general each slice requires a carefully computed non-uniform dose.

Pixel scanning

The favoured method of scanning laterally is to treat a series of points on a triangular mesh of spacing  $p$ , with a Gaussian spot of standard deviation  $\sigma$ .

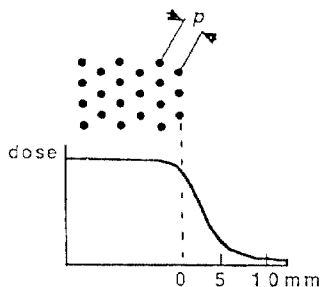


Fig. 2 Pixel Scanning

If  $\sigma > 0.5 p$  the dose is uniform to 1.2 %. The edge definition depends on  $\sigma$  and is shown, in Fig 2 for  $\sigma = 2.5 \text{ mm}$ ,  $p = 5 \text{ mm}$ . This is good enough to delineate a cross-section of arbitrary shape by choosing which pixels to treat. The procedure would be as follows : beam off-move spot to pixel-beam on until desired dose is reached-repeat for next pixel.

We see the following advantages for the pixel scan

- flexible shape in each plane
- each pixel is dosed separately giving flexible dose distribution
- no collimators
- no beam when spot is moving
- no error from magnet rise time or transient oscillations
- no error from beam intensity fluctuations
- conceptually simple computer control
- good security

An essential technical prerequisite is a means of switching the beam on and off. With a cyclotron this can be done at low energy in the injection line, because the particles only spend 60  $\mu\text{s}$  inside the machine and the beam loading is negligible. However with a synchrotron using resonant ejection to get a long burst it takes several milliseconds to cut the beam ; therefore a fast beam switch needs to be included in the transport system, and this is expensive.

The time available per pixel is determined by the desired maximum treatment time (5 min), the number of pixels ( $10^4$  for a one litre tumour), and the number of times one scans the tumour in each session (say 10). This gives 3 ms per pixel, to include spot settling time, on/off switching and treatment.

#### Scanning in depth

is achieved by varying the particle energy, for example to sweep from 5 to 20 cm depth in tissue the energy per nucleon must vary from 140-340 MeV/n (carbon beam) or 170-420 MeV/n (oxygen beam). With a synchrotron there is no difficulty in varying the extraction energy. A cyclotron however has a fixed extraction energy, so it will be necessary to reduce the energy by passing the beam through a slab of matter (called the degrader) of variable thickness. However the degrader has several undesirable effects which must be analyzed :

- a) increase of the beam phase space by multiple scattering
- b) increase of the momentum spread by energy straggling
- c) fragmentation of the incoming particle, giving lighter ions of roughly the same velocity with a longer range in the patient.

Our analysis of multiple scattering shows how to optimize the beam at the degrader [3]. The best material is diamond, the next best boron carbide. With a carbon ion beam slowing down from 20 cm to 5 cm range an output phase space of 5  $\pi \text{ mm. mrad}$  in each plane would collect 40 % of the beam.

For a proton cyclotron for identical conditions the phase space after the degrader will be about 16 times worse in each plane ! [Note : detailed calculations carried out after the conference show that this factor is 13.1 compared to oxygen and 22.5 compared to neon].

Thus the light ion accelerator offers major advantages ; but of course it is more expensive.

[3] For more detail see F.J.M. Farley and C. Carli, "Eulima Beam Delivery" in this proceedings.

## Discussion

Crawford Why is the ion beam more expensive than protons?

Farley One needs more energy per nucleon to get the necessary range, so this means higher rigidity, bigger magnets a larger accelerator.

Lefevre Could one use a two stage degrader, one upstream and one closer to the patient?

Farley If the degrader is close to the patient then the fragments will go into him. Most of these will be separated out by the bends if the degrader is close to the machine. I see no advantage in splitting the degrader.

Larson That is an advantage of carbon-12, it gives fewer fragments than oxygen or neon.

Farley I agree entirely. There is less fragmentation with carbon and the quality of treatment may be practically the same, and it is easier to build the machine. So it might be the right compromise.

Larson It would be from my point of view, this is rather apparent. It would need very strong arguments to change this a priori opinion from my side, but I may be biased.

Mandrillon For the machine design the choice of particle is very important. Range is proportional to  $A/Z^2$  so more energy is needed for heavier ions. I would be interested to hear the opinion of Dr. Castro on the choice between carbon, oxygen and neon.

Castro I think everybody knows, we have been discussing this question since the mid 1970's. I remember similar discussions before we started to use neon ions. There was never a clear resolution, and I do not think we have that now.

We selected neon because we were more concerned at that point, perhaps erroneously, about hypoxia, about having higher LET, having higher oxygen gain factors or lower OER for neon as compared to carbon. At this point in time I am not so sure that is the important consideration, in fact I don't think it is ; so I tend to think that may be carbon is a better beam, but in fact we don't know, at least from a clinical standpoint we don't know, and we really need to study that.

Pedroni The 15 mm spread for protons is correct at the end of the range of 29 cm. If you take a smaller range it will scale down linearly. At 20 cm it will be about 10 mm. It is true that heavy ion beams will be smaller. When you come to scanning, I would be scared about getting a uniform dose distribution from the overlapping of the spots. If you make the spot very small it is very difficult to construct a homogeneous dose distribution, so did you think about this problem of the overlapping of very small beams ?

Farley I did a calculation with a triangular mesh, varying the standard deviation of the spot relative to the pixel spacing. You can get any amount of variation you like. The result is surprisingly good. If  $\sigma = 0.5 p$  we already have uniformity to 1 %. It is just a question of matching the two.

Pedroni But what if the target is moving ?

Farley I quite agree. With any scanning system this is a problem. That is why we propose to scan the whole tumour ten times in each session, and if we are lucky the errors due to movement will average out.

What I would prefer to do is to synchronize the treatment with the breathing, and maybe with the heart beat also. The cyclotron has 1000 times more intensity than you need, so you can choose the treatment time to be in the right phase of the heart and the breathing. It is difficult to do, a technical challenge, but in principle one could do that.

The ideal thing is to have some detector which actually detects where the tumour is. If the surgeons could implant a piece of metal we could follow its movement with X-rays, and only treat when it is in a certain position. But otherwise you could synchronize with the pulse and the breathing.

These are technical possibilities with the cyclotron. I think not so much with the synchrotron, where the intensity is much less and you cannot turn it on and off quickly. Again this is something to discuss.

Larson This question should be actually asked after a presentation of the scientific and social aims of this facility. I would like to hear points of view on neon versus carbon. In the changing world of radiotherapy are ions an important ingredient, compared with improvements in our ability to tailor the dose to small tumours with less margin around the tumour? For radioactive nuclei, is carbon-11 or neon-19 better? A carbon machine might allow a gantry, which might not be possible with neon. Is carbon/proton comparison an issue? Should we use any spare money for this? Can we have views on these scientific questions?

Wambersie If we can shape the beam according to the target volume, it is always an advantage. But there must be a safety margin which contains normal tissue, which inevitably will be irradiated at the same level as the tumour. Therefore we need some improvement in the differential effect, which points to high LET instead of low LET.

Ryckewaert There are quite a lot of candidate designs. The machine must be capable of being constructed in series; optimized for reliability and cost effectiveness. So we should try to define as well as possible what ion and what rigidity is needed. In principle we need biological and clinical tests to specify the machine parameters.

Chauvel The choices for the Project Management Group will be a compromise between many factors, and we must bear in mind that the project should be duplicated. However it does not need to treat every case. It would be reasonable for the prototype to be able to treat 90-95% of the indications for light ions.

Castro May I comment on what was said about shaping the target volume. It is absolutely right that one will have to treat some normal tissue. Asking the surgeons, as we did early on, to outline the tumour proved in our experience to be horribly inferior to MRI and CT scans. In fact the surgeon is not at fault; he just cannot tell you the boundaries as well as the incredibly better scanning by CT and now MRI. Nevertheless, even with wonderful MRI you will have a doubt as to what is microscopic tumour and what is normal tissue. So one of the challenges for EULIMA is to look at how well we can shape and conform the high dose area, because I know André will agree with me, that the volume that receives high dose is critical. We all know from long experience that diminishing the volume which gets a high dose gives a lower incidence of severe late reactions.

So one major question for EULIMA, a question we are also trying to study, is to see if the high LET beams carbon, oxygen and neon can be safely used without serious late effects. In Berkeley we have just begun to really get data on this. We started as usual with patients with very advanced lesions; not many of them lived very long. And now we are beginning to have 3, 4, 5, 6 year survivors treated with neon, and we have some chance now to observe late effects. So that would be one challenge, to look at the optimal dose conformation and correlate that with late effects. The other challenge is to begin some biological studies to try to understand better why it is that some tumours in some patients respond to high LET. What are the biological factors, the growth parameters, is there something inherent in certain types of tumour? To begin as soon as possible with that type of study, preferably on biopsy tissue from patients treated with carbon, oxygen, neon, and correlate that with the outcome. That is another slow process, unfortunately all of this is very slow.

The third challenge is to make a comparison between protons and whatever ion one selects. That is something we have tried to do, but I think it is very difficult unless you have several centres so that you can accumulate enough patients.

Larson I would very much support a comparative study between low LET and high LET particles. For example the modification of radiation damage is certainly easier with low LET particles. I think we should bring the whole radiotherapeutic panorama of chemical and biological factors into this comparison. Maybe the EFTA countries should build a proton machine for comparison, and then we can start making a full comparison between the two.

Chauvel EULIMA can also accelerate molecular hydrogen.

Mandrilion It depends on the strategy for the machine. If it is financed it must treat a large number of patients. I wonder if it can cover many types of ion as well.

Larson It is a waste to use a light ion machine for proton therapy.

Castro I would like to add a critical note. I think in some patients (children for example, and others) you will want to use protons. Sending them to another centre introduces logistical difficulties. I personally would like to see a machine able to provide protons and one type of ion. I would urge you not to do what we have done at Berkeley. We have treated with He, C, Ne, Si, and Ar. That was a mistake because we could not learn very much from those few patients treated with C, Si and Ar. It is best to select one ion, and try to accumulate enough patients to really learn about it. But I think you need protons for comparison.

Larson It is a waste to use this wonderful machine for proton therapy. It would be better to build a small machine for proton therapy alongside for comparative studies.

Castro A proton machine for clinical work would not be small. You still need a range of 25 cm.

Farley Of course EULIMA would have all the scanning equipment that could also be used for protons. I would like to ask Dr. Castro, would you settle for helium? It is rather easier to use helium in the machine than protons. Or is that already too much of an ion?

Castro I think they are comparable from a clinical standpoint. So I think you could accept helium. But there is a small content of high LET in helium, so I would be concerned about late effects in children. Therefore I would prefer protons, but helium would be acceptable, and does have some advantages.

Larson The relevant question for society is whether protons are better than light ions. Therefore I would rather compare with protons.

Farley Just looking at this technically. Suppose that we build a carbon EULIMA, 340 MeV per nucleon. The  $H_2^+$  ion will also be 340 MeV per nucleon, each proton would have 340 MeV, and there would be two of them. Now the range of these would be very large, and you would have to do a lot of degrading to get that down to treat your little boy. I have explained that when you degrade a proton beam the phase space gets much worse than in the case of the ion. Now we are degrading from 340 MeV; we would need to look at that. Of course you can always select: throw away 99% of the protons, and select a beam with suitable momentum and phase space. We would still have plenty of intensity. That is the sort of thing you would have to do. It is a bit messy, but one could arrange to do that.

Castro It is worth a lot of thought. I would agree with Professor Larson that protons would be the preferable contrasting beam to carbon ions, if you can do it.

Wambersie I think we all agree that the comparison must be made with equally good physical selectivity. If you make the comparison between different centres, you are also comparing the skill and competence of different medical teams, the delineation of the limits of the tumour and so on.

Castro We have a collaborative trial going on, in which a proton group in Boston and ourselves are combining. By means of a close interaction in the treatment planning, dose distribution and immobilization techniques, I think we have achieved a satisfactory conformation to the protocol requirements. It is a small community, so I think we can manage the interactions reasonably well.

Chauvel It is a matter of organisation, and exchanges between the facilities.

Pedroni What about the value of using a gantry with protons, as one does with X-rays?

Castro Clearly someone from Boston would say a gantry was required. We feel less strongly at Berkeley. There is no question that a gantry is preferred. But with a combination of a vertical and a horizontal beam you can get very close; my guess is that 85-90% of the time you would be comparable to a gantry system. That is my experience at Berkeley.

Farley If you are using a gantry with X-rays there is little problem over the range or direction, and the gantry can turn continuously. With protons one might need an inclined compensator for each angle of entry, and a different scanning programme. It is not as simple as a gantry with X-rays. I can see why Dr. Castro says that vertical and horizontal only may be an optimum choice.

Larson With protons you would probably have a different fractionation scheme than with ions. You need to compare the whole arsenal of proton therapy with ion therapy. It is no good just selecting one parameter.

Castro We treat patients seated in a vertical position from several angles, but we do not scan continuously. For each angle there is a range compensator. A combination of a vertical and horizontal beam may avoid the need to treat in a seated vertical position.

Larson It would be unwise to draw any conclusions. The questions raised will no doubt be considered by the Project Management Group. We have not covered the question of carbon-11 versus neon-19.

Farley Carbon-11 has a life of 20 mn which is too long, but one can use carbon-10.

Mandrilion Oxygen-15 would be easier.

In conclusion Professor Larson thanked all the participants for their views.

## EUROPEAN STRATEGY FOR RESEARCH ON CANCER THERAPY

A. VERMORKEN

CEC - DG XII - 200 Rue de la Loi  
1049 Bruxelles, BelgiqueAbstract

Future cancer management will continue to involve surgery, radiotherapy, chemotherapy and immunotherapy working together in a more important fashion than ever before. Local approaches such as surgery and radiotherapy will be needed to get rid of as much as possible of the macroscopically visible tumour tissue so as to leave a minimal tumour burden. In this way the effect of the systemic treatments available can be maximized. As a consequence, more effective methods of local control and of systemic treatments are required in order to achieve rapid improvement in overall survival. It is estimated that selectivity of radiotherapy can be further improved using light ion therapy and boron neutron capture therapy, with direct consequences for the survival rate of cancer patients in the immediate future.

Introduction

One out of every four Europeans will suffer some type of cancer during their lifetime. If nothing is done, this proportion will become one out of every three by the year 2000. The major goal of the "Europe against Cancer Programme" is to diminish the number of cancer casualties compared to the above-mentioned trend, by at least 15 % by the year 2000 and by considerably more in the following decade.

The "Europe against Cancer Programme" covers four subjects :

- 1- Cancer prevention
- 2- Information of the public
- 3- Training of the health professions
- 4- Cancer research

These subjects should lead to prevention of significant numbers of cancer cases and to more effective treatments. It is for these reasons that the European Cancer Experts have defined their strategy for research on cancer therapy up to the year 2000.

The designation "cancer" does not refer to a uniform disease. On the contrary, it is a collective term which covers a large number of different tumours arising from many different tissues in various stages of development. In view of this diversity, it cannot be expected that all malignant tumours can be influenced or cured by any one therapeutic procedure. A fundamental difficulty of many therapeutic approaches is the fact that the tumour cell develops from a normal cell and hence there are few differences from normal tissue which can be used as a basis for a therapeutic attack. It is this lack of specificity which limits most existing therapeutic approaches, and research in most fields is therefore directed towards increasing this specificity.

There are at present various approaches to cancer treatment :

- Surgical removal of the tumour tissue,
- Radiotherapy,
- Chemotherapy,
- Immunotherapy.

1) Surgery

Surgery, usually applied to relatively limited tumours, is at present the most general successful mode of cancer treatment. About half of all cancer patients have a survival exceeding five years. Half of these may be attributed to surgery alone, and half either to a combination of surgery and radiotherapy or chemotherapy or to either of these latter treatment modalities alone, \* (see Table 1A).

Surgery is quite specific since it removes mainly diseased tissue ; its applicability is, however, normally limited to tumours which have not yet metastasized. For that reason, research in the field of early diagnosis is important and it therefore forms the strategic approach described in chapter I : Research on early detection and diagnosis (see I in Table 1). The techniques of surgery have already reached a very

high level and they can be combined with other treatment modalities. Progress in this field could result in further improvement in functional and cosmetic outcome. Improvement of surgery is therefore part of the strategic approach described in chapter II : "Research on improvement of local treatment" (see II in Table 1).

2) Radiotherapy

Radiotherapy is the most widely used form of cancer treatment, being given to two out of every three patients. Approximately one quarter of cured cancer patients owe their five-year survival to radiotherapy alone, and another eight are cured by combined treatment with surgery and/or chemotherapy. Radiotherapy is therefore involved in almost half of curative cancer treatment\* (see Table 1A). Moreover, radiotherapy is involved in the palliative treatment of many other patients.

Although in principle radiation is not selective for a cancer cell, the selective destruction of a tumour is achieved to some extent by the fact that

- considerable efforts are made to concentrate the dose in the tumour tissue and so spare the surrounding normal tissue as much as possible,
- some tumour cells are more radiosensitive than normal cells,
- the reparability of malignant tissues is thought to be less efficient than that of normal tissues.

There are now new approaches which appear promising for further increases in selectivity of radiotherapy. They are described in chapter II : "Research on improvement of local treatments".

3) Chemotherapy

Chemotherapy has been employed mostly when tumour metastases are already present. Up to now, however, noteworthy successes have been limited predominantly to haematopoietic malignancies, malignancies of embryonal origin (e.g. testicular tumours) and paediatric malignancies. At the present time, unfortunately these only make up approximately 4 % of total tumour incidence, although in about two thirds of these cases cure is indeed achieved. The early adjuvant use of chemotherapy with surgery and/or radiotherapy in the more common cancers (e.g. breast carcinoma) is encouraging, but in all other situations chemotherapy serves mainly as palliation.

4) Immunotherapy

Active immunotherapy by vaccination with tumour cell extracts has been successful in experimental systems and recently some success has been reported in humans. There are now some preliminary indications, that progress along these same lines is to be expected in the future. As an example, the histo-compatibility antigens hold a key position in cellular interactions with the immune system. In animal models reintroduction of missing histo-compatibility antigens (neo-antigens) into tumour cells renders these cells more sensitive to immune rejection processes. It has also been shown that introduction of new transplantation antigens by in vitro mutagenesis induces a response against the tumour cells. Both approaches may become extremely useful in cancer treatment, they will however only be effective against relatively small numbers of cells and they will thus need to be used in conjunction with other anticancer modalities such as surgery, radiotherapy and chemotherapy.

Research on improvement of chemotherapy and immunotherapy is described in chapter III : Research on improvement of systemic treatments (see III in Table 1).



## Strategic approaches for research on cancer therapy

### I-Research on early detection and diagnosis

Several observations clearly indicate that screening can reduce the incidence and mortality from both cervical cancer and breast cancer. yet several problems remain to be solved :

#### A-Methodological problems

For example :

- evaluation of the best techniques for mammography,
- investigation on the possibilities of computerized image analysis for the reading of mammograms,
- investigation on the possibilities of computerized image analysis for the reading of cervical smears.

#### B-Social problems

One of the main difficulties of screening programmes is the insufficient compliance of women. Moreover, for cervical cancer, it has been observed in several countries that women belonging to the highest risk group are those with the lowest compliance.

In addition to research necessary for allowing implementation of screening based on existing methods like those for breast and cervical cancer, research is also necessary for methods that are now under investigation for other types of cancer such as colorectal cancers, prostatic cancers and malignant melanoma.

### II-Research on improvement of local treatments

#### A-Improvement of results of existing local treatments

Surgery, usually applied to relatively limited tumours is at present the most successful mode of cancer treatment. It should be kept in mind that the high success for surgery is in part due to the fact that skin cancer falls into this category. Progress in surgery could lead to improvement of both the functional and the cosmetic outcomes of operations. Examples are :

- limb-sparing procedures,
- breast-sparing operations,
- less need for colostomy,
- the many surgical advances in the head and neck region.

For that reason, radiotherapy forms one of the most important treatment modalities today. It is estimated that selectivity of radiotherapy can be further improved with direct consequences for the survival rate of cancer patients in the immediate future. Radiotherapy will undoubtedly gain more than surgery or chemotherapy and immunotherapy from a supranational research dimension.

#### a) Development of optimum treatment protocols

Clinical treatment research remains important, especially for new treatments, since optimum protocols for combination with other treatment modalities have to be developed.

#### b) Investigation of resources required to assure high quality treatment all over Europe and harmonization of treatment quality

It is obvious that both human and other resources like those for equipment are not uniformly distributed over Europe. Moreover, there is a difference in quality of treatment in specialized cancer centres and peripheral hospitals. It is necessary that an inventory is made of the resources required to allow high quality treatment throughout Europe. As soon as an inventory of resources required is available a socio-economic study aiming at determining obstacles in implementing high quality treatment all over Europe has to be performed and the results made available as soon as possible to the national authorities of the Member States.

### B- Development of new local treatments

Although in radiotherapy one generally aims at minimizing the effect of the dose on normal tissue, that effect is still a limiting factor for the total dose which can be given to the tumour. A further increase in the dose would be of significant importance since the relation between tumour response and the radiation dose is very steep at the end - even small further increases in the dose would have significant effects on the likelihood of tumour control.

The ideal situation in radiotherapy is for a large amount of energy to be deposited in the tumour volume and none outside in the surrounding healthy tissue. This means in principle no sideways spreading out of the beam, and a very well defined distribution of the energy in depth. Another crucial factor is that about 20 % of tumours are radioresistant, i.e. they do not respond to treatment with photons or electrons ; they are, however, sensitive to beams which deposit their energy in microscopically localized packets (high energy deposition), a process which increases the probability of giving a lethal dose to every cell (e. g. beams of light ions) ; this is part of strategic approach no II as described in Table 1.

Existing treatment with photons electrons, neutrons and protons all have their own shortcomings :

- Photons, even with megavolt energies, suffer from sideways spreading and the in-depth dose distribution is not selective because of an exponential decrease in energy deposition.
- Electrons have a better in-depth selectivity but suffer from considerable sideways spreading, and as a consequence they are not suitable for deeply seated tumours.
- Neutrons are more effective for treatment of radioresistant tumours because of high energy deposition, but they suffer from the same problems of exponential decrease as photons.
- Protons have good ballistic accuracy but are not more effective than photons or electrons for radioresistant tumours.

Two new approaches appear very promising for a further increase in selectivity of radiotherapy :

#### a) Radiotherapy with ions of light atoms (light ions)

Beams of light ions such as those of carbon, oxygen and neon travel in virtually straight lines with negligible sideways spreading and they deposit a large fraction of their energy at the end of their range. This allows a well-defined distribution of the dose in depth better even than that of protons. In addition, because of their intense local ionization, light ions could be effective against radioresistant tumours.

Excellent results with light ion therapy have been obtained for some types of tumours at Berkeley, California, and some European cancer patients have already been treated there. In Japan a full-time facility for medical use is now being built in order to treat about one thousand cancer patients a year.

#### b) Boron Neutron Capture Therapy (B.N.C.T.)

For various reasons, some boron compounds may accumulate in some tumours, and particularly in brain tumours where a reduction in the tumour blood-brain barrier encourages their selectivity. Upon irradiation with neutrons the boron atoms capture the neutrons and give rise to alpha and lithium particles. These have a high energy and their track is less than a fraction of a millimeter in tissue, so that they do not leave the tumour. It is estimated that in this way, with the same dose to surrounding normal tissue, the dose to the tumour can be increased by about one third.

The first clinical trials in Japan indicate that this treatment could be beneficial for treatment of certain brain tumours such as gliomas, and trials for other tumour types are being initiated.

### III- Research on improvement of systemic treatments

#### A- Research on maximization of effects of systemic treatments by eliminating a maximum of visible tumour tissue.

The potentially great precision of treatment with light ions and BNCT allows eradication of slow growing metastases. (This is the case for e.g. with some breast carcinomas, some colorectal carcinomas, some large cell bone metastases, some sarcomas, kidney tumours and adenoid cystic carcinomas). This approach will lead to a maximization of the effect of both existing and new systemic treatments since high precision radiotherapy would allow the elimination of as much as possible of the macroscopically visible tumour burden. The results recently obtained with adjuvant therapy for breast cancer support this approach and do indeed demonstrate that presently existing systemic treatments have a significant effect on cure provided that most of the macroscopically visible tumour tissue has been eradicated.

#### B- Research on targeting of systemic treatments

Chemotherapy has for the moment a limited value for most forms of cancer. One of the reasons therefore is the limited dose that can be given before the side effects become unacceptable and life threatening. For the future, targeting of cytostatic agents with either monoclonal antibodies or drug carriers may improve the selectiveness of chemotherapy. Another avenue for research is the combination with biological response modifiers which can be used to protect critical normal tissues (hemopoietic growth factors or inhibitors and factors to enhance effects on the tumour).

Conventional chemotherapy can be improved by increasing the dose and protecting the patient's bone marrow by either autologous transplantation with cryo-preserved autologous marrow or treatment with growth factors acting on bone marrow precursor cells (colony stimulating factor).

#### C- Research on biological response modification including immunotherapy

Research in the field of immunotherapy has concentrated on four approaches :

- A non specific immunotherapy, using BCG and corynebacterium parvum, has not been successful in humans. A recent approach is the use of cytokines, products of white blood cells, which stimulate the activity and growth of immune cells in a non-specific fashion. These substances include the interferons, interleukins and tumour necrosis factor. The interferons have in addition a cytotoxic effect on the expression of antigens in a pure form through recombinant DNA techniques.

- Adoptive immunotherapy consists of transfusion of autologous lymphocytes. Recently this technique was combined with the application of interleukin-2, both in vivo and in vitro, to maximally stimulate the effector immune cells. This method has been moderately successful in the treatment of melanoma and renal cell cancer.

- Passive immunotherapy consists of the injection of antibodies (usually monoclonal antibodies) directed against the tumour. This method had some effects in the treatment of melanoma, colon cancer and cancer of the pancreas.

- Active immunotherapy by vaccination with tumour cells or cell extracts has been successful in experimental systems and only recently some success has been reported in humans. There are now some preliminary indications, however, that progress along this same line is to be expected in the future. However, this approach will only be effective against relatively small numbers of cells and thus it will need to be used in conjunction with other anticancer modalities such as surgery, radiotherapy and chemotherapy.

A new variation on active immunotherapy is the vaccination with so-called anti-idiotypes, which are antibodies raised against monoclonal antibodies directed towards tumour antigens and therefore immunological mirrors of these antigens.

Recent biological findings, including agents inducing differentiation in cancer cells, as well as growth factors, receptors, and mechanisms of signal transduction may also find a place in cancer therapy.

### Fundamental research

Even if the "Europe against Cancer" programme has set up a year 2000 target, its overall aim is to improve the treatment possibilities even if they are not expected to be reality before the year 2000, the programme target year. In the fundamental area, which by nature, cannot set up itself a target year to get results, the European Community, has nevertheless a specific contribution to add to existing national efforts.

In many areas unique expertise is present in the European Community, but it suffers from a number of weaknesses among which are : small-scale operations without much collaboration and coordination, shortage of means especially in terms of postdoctoral research positions, but also of sophisticated equipment and working budgets.

#### Conclusion

Radiotherapy is the most widely used form of cancer treatment at the moment. Two new approaches : light ion treatment and boron neutron capture therapy appear promising vis-à-vis further increases in selectivity in radiotherapy. Accelerators will play a key role in their design. For boron neutron capture therapy an alternative exists : neutron sources emerging from nuclear power plants. If results of clinical trials are promising, hospital based, high intensity accelerators will have to be developed. For light ion treatment the design of a high energy accelerator is a prerequisite. In both the USA and Japan facilities for light ion treatment are either at design stage, under construction or in part-time use.

The Commission of the European Communities considers that it is necessary to design a prototype accelerator which will be capable of offering the necessary flexibility for the lowest possible price but yet allowing industrial production after an experimental phase. For that reason, the synchrotron option is to be compared which that of a superconducting cyclotron.

Table 1 A [1]

Situation now in Cancer Treatment



Treatment used	Primary tumour	Metastasized tumour	
- surgery alone	22 %		
- radiotherapy alone	12 %		
- both combined	6 %		
- all combinations including chemotherapy		5 %	
Patients curable now	40 %	5 %	45 %
Strategic approach (see table below)			
No cure available	18 %	37 %	55 %

Table 1 B

Strategy

Problem	Remedy
I Late diagnosis	screening
II a) Poor treatment	Quality control
b) tumours with difficult localization	protons light ions and BNCT
c) tumours currently radioresistant	Light ions and BNCT
III conventional treatments not effective	Improved local treatments combined with improved systemic treatments.

#### Reference

- [1] De Vita V.T. (1983) Progress in Cancer Management, Cancer 51, 2401-2409.